

AD-779 060

FUNDAMENTALS OF EMP DATA MANAGEMENT
AND PROCESSING

Robert L. Hutchins, et al

Braddock, Dunn and McDonald, Incorporated

Prepared for:

Defense Nuclear Agency

13 March 1974

DISTRIBUTED BY:

NTIS

National Technical Information Service
U. S. DEPARTMENT OF COMMERCE
5285 Port Royal Road, Springfield Va. 22151

UNCLASSIFIED

SECURITY CLASSIFICATION OF THIS PAGE (When Data Entered)

REPORT DOCUMENTATION PAGE		READ INSTRUCTIONS BEFORE COMPLETING FORM
1. REPORT NUMBER 3179F	2. GOVT ACCESSION NO.	3. RECIPIENT'S CATALOG NUMBER AD- 779 060
4. TITLE (and Subtitle) FUNDAMENTALS OF EMP DATA MANAGEMENT AND PROCESSING		5. TYPE OF REPORT & PERIOD COVERED Final
		6. PERFORMING ORG. REPORT NUMBER BDM/A-19-73-TR-T1
7. AUTHOR(s) Dr. R. L. Hutchins, J. W. Dyche		8. CONTRACT OR GRANT NUMBER(s) DASA 01-71-C-0036
9. PERFORMING ORGANIZATION NAME AND ADDRESS Braddock Dunn & McDonald, Inc. 1st Natl. Bank Bldg., 5301 Central Avenue, NE. Albuquerque, New Mexico 87108		10. PROGRAM ELEMENT, PROJECT, TASK AREA & WORK UNIT NUMBERS Subtask L37CAXYX970-04
11. CONTROLLING OFFICE NAME AND ADDRESS Director Defense Nuclear Agency Washington, D.C. 20305		12. REPORT DATE 13 March 1974
		13. NUMBER OF PAGES 414
14. MONITORING AGENCY NAME & ADDRESS (if different from Controlling Office)		15. SECURITY CLASS. (of this report) UNCLASSIFIED
		15a. DECLASSIFICATION/DOWNGRADING SCHEDULE
16. DISTRIBUTION STATEMENT (of this Report) Approved for public release; distribution unlimited.		
17. DISTRIBUTION STATEMENT (of the abstract entered in Block 20, if different from Report)		
18. SUPPLEMENTARY NOTES		
19. KEY WORDS (Continue on reverse side if necessary and identify by block number) Reproduced by NATIONAL TECHNICAL INFORMATION SERVICE U S Department of Commerce Springfield VA 22151		
20. ABSTRACT (Continue on reverse side if necessary and identify by block number) This document presents a thorough but general treatment of the subject of EMP test data management and processing techniques for pulse simulator EMP test data. The subject matter is divided into two general areas: (1) the planning, implementation and operation of a test data system, and (2) test data processing and analysis techniques. The Advanced Research EMP Simulator (ARES), under Management of the Defense Nuclear Agency (DNA), is used as a model for much of the material presented.		

DD FORM 1473
1 JAN 73

EDITION OF 1 NOV 65 IS OBSOLETE

UNCLASSIFIED

SECURITY CLASSIFICATION OF THIS PAGE (When Data Entered)

I

UNCLASSIFIED

SECURITY CLASSIFICATION OF THIS PAGE(When Data Entered)

20. ABSTRACT (Continued).

The treatment of test data processing and analysis covers the many techniques which are currently used in both preparing and assessing EMP test data. The Fourier transform tends to be a very important tool in data assessment and has, therefore, been given particular emphasis in this treatment.

II

UNCLASSIFIED

SECURITY CLASSIFICATION OF THIS PAGE(When Data Entered)

PREFACE

This document has been prepared under contract DASA 01-71-C-0036 for the Defense Nuclear Agency by Braddock, Dunn and McDonald, Inc., Albuquerque Operations in accordance with Work Order 179024. The Handbook contains a comprehensive treatment of the subject of the EMP Data system and data reduction technology. The ARES Site Project Officer is Major B. Sanderson (USAF), Air Force Weapons Laboratory. The ARES Project Officer is Major W. Youngblade (USA) Headquarters, Defense Nuclear Agency.

Major contributors to this document are: James W. Dyche, Dr. Robert L. Hutchins, Jeffrey L. Cooke, Willie M. Servis, and Marilyn R. Lauck.

TABLE OF CONTENTS

<u>Section</u>		<u>Page</u>
	PREFACE	1
1	INTRODUCTION	9
	1.1 HANDBOOK SCOPE	9
	1.2 RELATIONSHIP OF THE DATA SYSTEM TO THE OVERALL EMP TEST PROGRAM, AN OVERVIEW	10
	1.2.1 Data Analysis Function	11
	1.2.2 Data System	12
	1.2.3 Data Management	12
	1.2.4 Data Reduction	14
	1.3 PLANNING AND ITS IMPORTANCE	15
	1.3.1 Who Must Be Involved in Planning and Why	17
	1.3.2 Planning Areas	19
	1.4 SYSTEM SOFTWARE REQUIREMENTS	24
	1.5 SYSTEM OPERATIONAL PROCEDURES	25
	1.6 SYSTEM FACILITY REQUIREMENTS	26
	1.7 SYSTEM OPERATING PERSONNEL	28
	1.8 INFLUENCE OF DATA QUALITY ON DATA SYSTEM FUNCTIONS	30
	1.8.1 Input Data Quality	30
	1.8.2 Internal and Output Data Quality	31
	1.9 GLOSSARY OF TERMS	32
2	THE DATA SYSTEM AND DATA MANAGEMENT	33
	2.1 INTRODUCTION	33
	2.2 THE GENERAL DATA SYSTEM MODEL	35
	2.2.1 Users - The External Environment	35
	2.2.2 Interface	35
	2.2.3 The Internal Environment	37
	2.3 DATA SYSTEM INPUTS AND OUTPUTS	37
	2.3.1 Typical Data System Inputs	38
	2.3.2 Typical Data System Outputs	43
	2.3.3 The Processing Request	45

TABLE OF CONTENTS (Continued)

<u>Section</u>	<u>Page</u>
2.4 DATA SYSTEM PROCESSING AND CONTROL REQUIREMENTS	51
2.4.1 The EMP Test Data Bank	52
2.4.2 Processing Cycles	56
2.5 PROCESSING HARDWARE SUBSYSTEM	82
2.5.1 The Microfilm Subsystem	82
2.5.2 Digitizing Subsystem	90
2.5.3 Digitizer Control	107
2.5.4 Computer Subsystem	121
3 DATA REDUCTION TECHNIQUES	127
3.1 INTRODUCTION	127
3.1.1 The EMP Problem	127
3.1.2 The Frequency Domain Approach	129
3.1.3 Frequency Domain Analysis for Transient Time Domain Data	132
3.1.4 Section Review	134
3.2 PREPROCESSING TECHNIQUES	136
3.2.1 Digitization	137
3.2.2 Data Scaling	153
3.2.3 Time Tying	159
3.3 BASIC TRANSFORM THEORY	167
3.3.1 Introduction	167
3.3.2 Definitions	169
3.3.3 Interpretation of the Integral Pair	171
3.3.4 Waveform Modification	181
3.3.5 Simple Transforms	188
3.3.6 Plotting Aids	195
3.3.7 Special Functions	219
3.3.8 Product of Two Functions	231
3.3.9 Transform Theory Summary	244
3.3.10 Laplace Transforms	247
3.3.11 Examples	251

TABLE OF CONTENTS (Continued)

<u>Section</u>	<u>Page</u>
3.4 SAMPLED FOURIER TRANSFORMS	282
3.4.1 Introduction	282
3.4.2 Sampling Functions	284
3.4.3 Comb and Rep	291
3.4.4 The Fourier Series Transform	295
3.4.5 The Time Sampled Fourier Transform (TSFT)	307
3.4.6 Discrete Fourier Transform	318
3.5 IMPLEMENTING TRANSFORMS FOR DATA ANALYSIS	330
3.5.1 Introduction	330
3.5.2 Data Flow Analysis	331
3.5.3 Transform Methodology	336
3.5.4 Truncation Errors	363
3.5.5 Numerical Integration	377
3.5.6 Transfer Function Estimation	392
REFERENCES	401

LIST OF ILLUSTRATIONS

<u>Figure</u>		<u>Page</u>
1-1	Relationship of Data Management and Processing Functions to Overall EMP Test Program	13
1-2	Flow Diagram Illustrating Interrelationship of Data System Planning Areas	20
2-1	General Data System Model	36
2-2	ARES Request Form for Data System Input and Special Output Requests	48
2-3	ARES Request Form for Standard Output Requests	49
2-4	Data System Processing Cycle for Processing Polaroid Photograph Input Data into EMP Test Data Bank	58
2-5	Log-In Logbook Index	59
2-6	Response Photograph as Indexed and Recorded on Microfilm	62
2-7	Environmental Photographs as Indexed and Recorded on Microfilm	63
2-8	Calibration Photographs as Indexed and Recorded on Microfilm	65
2-9	Data System Processing Cycle for Processing Characterization Data Lists into EMP Test Data Bank	70
2-10	Data System Processing Cycle for Retrieval and Display of Characterization Data	73
2-11	Sort Output-Card Image	74
2-12	Sort Output-Matrix	75
2-13	Data Cycle as used for Data Processing	78
2-14	Recordak Micro-File Machine	85
2-15	ITEK 335 Transflo Processor	86
2-16	ITEK 303 Contact Printer	88
2-17	Bell and Howell Micro-Data Printer	89
2-18	Basic Graphical Digitizer Elements and Their Interconnection	93
2-19	Quantization Grid for Graphical Digitizer	96
2-20	Result of Digitizing the Waveform of Figure 2-19	97

LIST OF ILLUSTRATIONS (Continued)

<u>Figure</u>		<u>Page</u>
2-21	Model of Ideal Analog-to-Digital Conversion Process ($n = 3$)	99
2-22	Effect of Offset Error on the Analog-to-Digital Conversion Process	99
2-23	Effect of Gain Error on the Analog-to-Digital Conversion Process	100
2-24	Effect of Linearity Error on the Analog-to-Digital Conversion Process	100
2-25	Photographic Problems	103
2-26	Bendix Datagrid Manual Digitizer System	111
2-27	Telereadex Type 29E Graphic Digitizer	115
2-28	Programmable Film Reader Mod-3	118
2-29	Block Diagram of the Sandia Image Digitizer	119
3-1	Block Diagram of Typical EMP Test Signal Recording System	154
3-2	Complete Response Waveform Recorded at 500 ns/Division	161
3-3	First 1/5th of the Complete Waveform Recorded at 100 ns/ Division	161
3-4	Double Exponential Waveform	198
3-5	Normalization Factor, N , for Double Exponential	199
3-6	Transform Magnitude and Phase for a Double Exponential	201
3-7	Relative Variation of the Transform Magnitude with Risetime and Falltime of a Double Exponential	204
3-8	Q Versus Damping Rate for a Damped Sinusoid	210
3-9	Normalization Factor, N , for a Damped Sinusoid	212
3-10	Transform Magnitude and Phase for a Damped Sinusoid	213
3-11	Data Flow Analysis	333
3-12	Time Domain Function Used for Sampling Study - $f(t)$	352
3-13	Transform of $f(t)$, $\bar{F}(\omega)$, When $f(t)$ is Sampled 4 Times Per Cycle	352
3-14	Transform of $f(t)$, $\bar{F}(\omega)$, When $f(t)$ is Sampled 8 Times Per Cycle	353

LIST OF ILLUSTRATIONS (Concluded)

<u>Figure</u>		<u>Page</u>
3-15	Transform of $f(t)$, $\bar{F}(\omega)$, With Random Time Sampling Averaging 8 Samples Per Cycle	353
3-16	Inverse Fourier Transform of a Damped Sinusoid With an Additional Phase Shift - $\phi(f) = 2\pi fT$	358
3-17	Fourier Transforms for Ideal $g(t)$ and Amplitude Truncated $g(t)$	371
3-18	Fourier Transforms for Ideal $g(t)$ and Slope Discontinuous $g(t)$	372
3-19	Illustration of Time Window Technique for Truncation Error Reduction Using Window Shape (1)	378
3-20	Illustration of Time Window Technique for Truncation Error Reduction Using Window Shape (3)	379
3-21	Integral of Typical Derivative Waveforms with Ramp and dc Offset Errors	383
3-22	Fourier Transform of Derivative of Double Exponential Waveform with Ramp and dc Offset Errors	385
3-23	Fourier Transform of Derivative of Damped Sinusoid Waveform with Ramp and dc Offset Errors	386
3-24	Integral of Typical Analytic Derivative Waveforms with Ramp and dc Offset Errors Using Total Area Correction Technique	388
3-25	Integral of Typical Experimental Derivative Waveform with Ramp and dc Offset Errors With and Without Use of Total Area Correction Technique	389
3-26	Fourier Transform of Typical Experimental Derivative Waveform with Ramp and dc Offset Errors	393
3-27	Integral of Typical Experimental Derivative Waveform with Ramp and dc Offset Errors Using Fourier Transform Techniques with Low Frequencies Filtered Out	394
3-28	Unfiltered and Filtered Transfer Function Estimates Illustrating Noise Contamination Problems and Fixes	399

LIST OF TABLES

<u>Table</u>		<u>Page</u>
3-1	Relative Differences Between Actual Asymptotic Values of $-20 \log 10 \sqrt{1 + (\omega/\omega_0)^2} \text{ (dB)}$	203
3-2	Phase Variation of the Term $(1 + j\omega/\omega_0)^{-1}$	205
3-3	Relative Frequency Where $ G(\omega) $ Attains Specified Relative Magnitudes	216
3-4	Relative Frequency Where $\phi \{G(\omega)\}$ Attains Specified Values	216
3-5	Comparison of Running Time of the Fit and the FFT	362

SECTION 1

INTRODUCTION

1.1 HANDBOOK SCOPE

The scope of the EMP Data Handbook is threefold, designed to:

- (1) Present a practical guide to the planning, design, and operation of the EMP test data system.
- (2) Present a tutorial and practical guide to the use of commonly used EMP test data reduction tools and techniques.
- (3) Illustrate the importance of the test data management and reduction functions as the interface between the test system (simulator) and the data analyst.

The Handbook uses the Advanced Research EMP Simulator (ARES)^{*} data management and processing system as a model for most of the subject matter covered. However, many subject areas are generalized to broaden the applicability of the Handbook.

This introduction is the first of three sections of the Handbook. The remainder of the introductory section covers general aspects of data

^{*}ARES is located at Kirtland AFB, New Mexico and is under the management of the Defense Nuclear Agency (DNA).

management and processing systems which are important to their design and operation. These include:

- (1) Relationship of the data system to the overall test program, an overview.
- (2) Factors which must be considered in planning for a data system and the importance of these factors.
- (3) The influence of data quality on the successful performance of the management and processing functions.

The final topic in Section 1 is a glossary of terms used in the Handbook.

Sections 2 and 3 present a detailed discussion of the subjects of the data system and data processing respectively. (In presenting the various subjects of Sections 2 and 3, a familiarity with certain topics is assumed on the part of the reader. References are liberally used throughout these two sections to assist the user in gaining this familiarity, if necessary.)

1.2. RELATIONSHIP OF THE DATA SYSTEM TO THE OVERALL EMP TEST PROGRAM, AN OVERVIEW

Most EMP test programs can be broken down into three main functions:

- (1) Generation of test data.
- (2) Management and processing of test data.
- (3) Analysis of test data.

The generation of test data is the responsibility of the test system, including the simulator and associated personnel. Such generation executes the EMP test plan and records the various tested system responses. (These response recordings are most often Polaroid oscillographs; here called raw test data.) The test system is also responsible for maintaining the simulator operation including test volume field mapping, test sensor calibration and recording instrumentation calibration. Each of these activities also results in data (again Polaroid oscillographs) which will be termed simulator calibration data.

1.2.1 Data Analysis Function

The data analysis function, using test data, includes all activities associated with the vulnerability assessment of the tested system. This assessment normally takes place throughout the test program and requires the use of test data in various forms ranging from raw test data to transfer function estimates of various tested system components or subsystems. Data assessment most often begins with the characterization of raw test data. In this process, gross tested system response characteristics are measured from the test response photographs, such as peak-to-peak response currents and predominant frequencies.

It seems fairly evident that most EMP test programs result in a large volume of test data and this volume of test data is further expanded through the requests of the data analysts that the raw test data be converted into forms better suited for assessment purposes. This conversion process is typically termed "data processing." Note that the term "data reduction" is sometimes used for this function. Data processing, however, is a more encompassing term and will be used throughout the Handbook.

1.2.2 Data System

The function which is responsible for handling and processing this large volume of data is typically called the data system or data mill. It has two main responsibilities:

- (1) Management of the test data.
- (2) Processing of test data.

Then, in effect, the data system acts as an interface between the test system and the data analyst, and as a service organization to both. This relationship is shown in its simplest form in Figure 1-1. In Figure 1-1 it is shown that the data management function really provides the interfaces while the data processing function is an internal function within the data system and interfaces to the "outside world" only through the data management function.

1.2.3 Data Management

Data management is perhaps a new term to use for this data system function but it is the one that most accurately describes it. The sheer volume of raw test data involved, the processing of data required before the data analyst can use it, and timeliness with which this processing must take place, require a system which can "manage data."

The essential parts of data management are:

- (1) The control of data in process in the data system.
- (2) Maintenance of the total EMP test data bank.
- (3) Quality control.

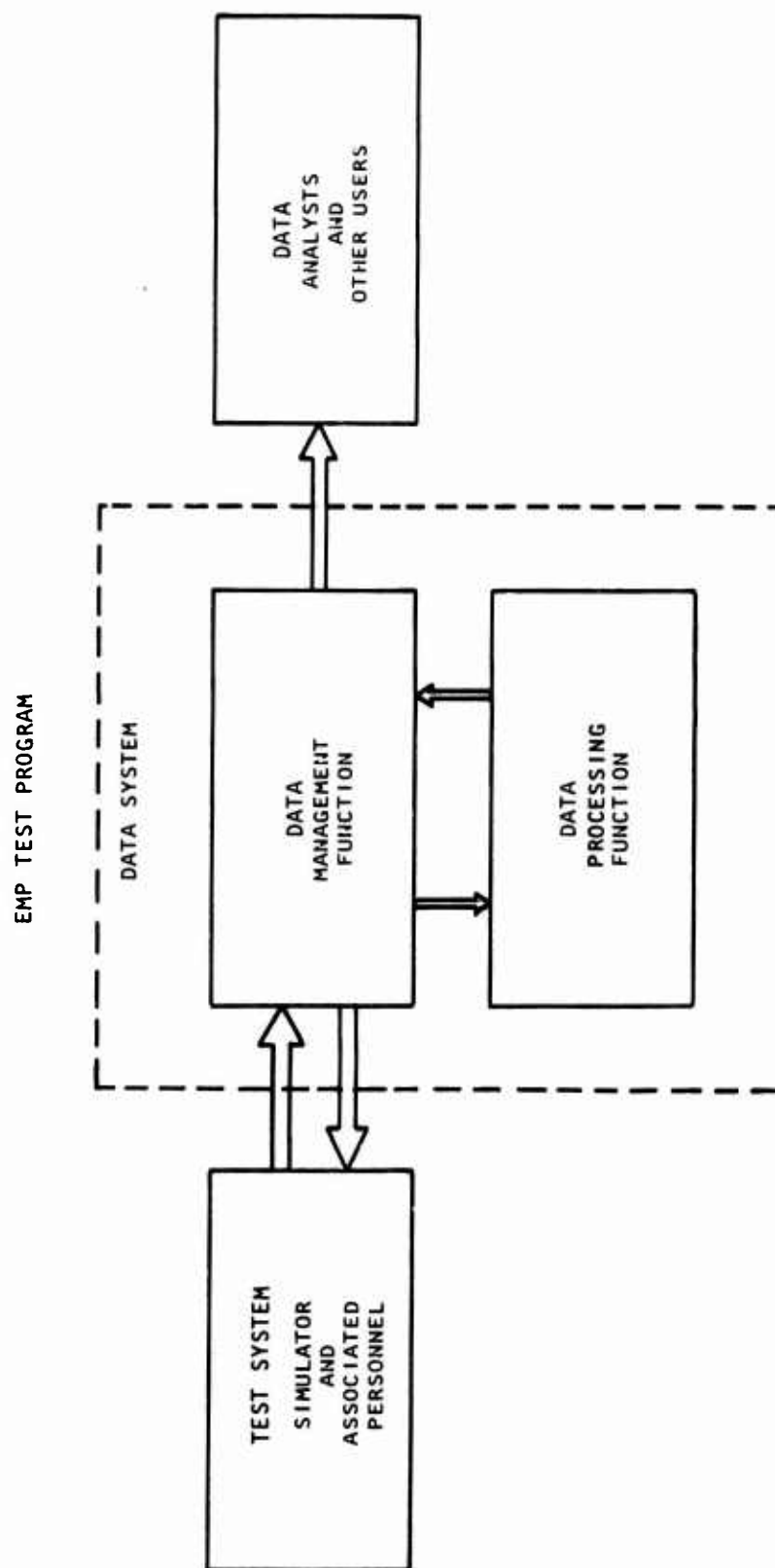


Figure 1-1. Relationship of Data Management and Processing Functions to Overall EMP Test Program

Control is considered an essential part in the sense that large quantities and various types of data are in process within the data system at any one time. Because of scheduling requirements or priorities set by users (the test system and/or data analysts), a considerable amount of control must be used with the data system to assure best results.

Data are the most obvious product of the EMP test program, and they must be in an easily accessible and usable form to be of maximum use to the overall program. This requires a comprehensive data bank into which data can be easily and efficiently entered (in all its various forms) and from which it can be retrieved easily as required.

Finally, because both the test system and the data analysts need the data system for all data handling and processing, the data system must include a working quality system. This must be done both in the sense of controlling the data that are input to the system, and also in continued control as the data are processed.

1.2.4 Data Reduction

The second major function of the data system, data processing is shown in Figure 1-1 as off-line from the main flow path through the system. It is depicted this way because data processing is normally performed on only a limited amount of the total test data set generated. The main data processing services performed in the data system include:

- (1) Digitization
- (2) Characterization
- (3) Data Conversions (Fourier transforms, transfer function estimation, etc.)

Note that it is common for characterization to be performed on all test data generated. Also, in the case of ARES, the characterization process is carried out in the test system rather than the data system and only the resulting data are entered into the data system for storage in the data bank. The reason behind this arrangement is that characterization should be carried out by the persons responsible for planning the tests and assessing test results. There is, however, no reason why the characterization process cannot be done within the data system if operation personnel are properly trained. (For example, this is the case on the B-52 vulnerability assessment program being carried out at the Kirtland AFB Vertically Polarized Dipole (VPD) as part of the Aeronautical System Vulnerability assessment program.)

In any event, data processing of all types can be looked upon as a function performed on request from either the test system or data analysts.

1.3 PLANNING AND ITS IMPORTANCE

The total task of putting a data system into operation can be broken down into four basic subtasks:

- Planning
- Design
- Implementation
- Operation

The success of the design, implementation, and operation subtasks is directly proportional to proper planning. Therefore, the importance of planning cannot be over-emphasized as the first step in the total process.

This is as true for the planned revamping of an existing data system in preparation for a new test program, as it is for initial data system design.

Before discussing how a planning exercise should be carried out and the factors which must be considered during the exercise, it will be helpful to outline some of the problems that poor planning can cause. Major problems include:

- (1) System hardware not available at the beginning of the test program. Possible causes: long lead time hardware items not identified and not ordered as soon as possible.
- (2) System inability to handle data load. Possible causes: improperly predicted load, improperly sized staff, inadequately trained staff, or improperly designed instrumentation system.
- (3) System inability to meet user requested turnaround time. Possible causes: Improperly sized staff, improper evaluation of instrumentation capabilities, or improperly designed operational procedures.
- (4) Generation of poor quality data. Possible causes: poorly designed quality control procedures, poor input data quality from the test system, improperly trained staff, or improperly designed hardware system.
- (5) Poor quality of processed data output. Possible causes: lack of understanding in the use of data processing techniques, or poor input data quality.

(6) Inflexibility in performing data reduction functions.

Possible causes: improperly designed computational hardware and software.

The foregoing list covers problems that occur both in attempting to bring a data system "on the air" and in its day-to-day operation. It is understood that any new or modified system of this type must be "debugged" when it is put into operation; therefore, smooth operation cannot be expected immediately. However, if the first six months of a one-year test program are spent debugging the data system, then the remaining six months are often spent playing "catch-up" and the data system can become the nemesis of the test program.

1.3.1 Who Must Be Involved in Planning and Why

There are several persons associated with the overall EMP test program who must become involved in the data system planning exercise. The following list represents those persons who were involved in the ARES planning exercise. Other test programs may be organized in a different manner. However, this list indicates the management level and responsibilities which should be represented.

1.3.1.1 The Test Director

The Test Director has the complete picture of how the intended test program is to be conducted, its schedule, and how the test schedule affects the scheduling requirements of all components of the test program, including the data system. He is in the best position to determine the general objectives and requirements for the data system.

1.3.1.2 The Facility Director

The Facility Director is responsible for the day-to-day operation of the test facility. He is, therefore, responsible for facility security requirements, regulations, and other applicable procedures. He is also responsible for coordinating any construction or installations which must take place.

1.3.1.3 The Data System Supervisor

The Data System Supervisor is responsible for the design, implementation, and operation of the data system. His role in the planning exercise is, therefore, obvious.

1.3.1.4 The Data Coordinator

The Data Coordinator is responsible to act as the interface between the various interested contractors and the data system. He is, therefore, responsible for understanding the contractor's requirements which affect the data system and for putting these requirements into the planning process.

1.3.1.5 Air Force Representatives

There are a number of Air Force representatives who may become involved in various areas of planning. These include procurement of advice on procuring GFE, base computational facilities representative to advise on the use of site computer facilities, and instrumentation personnel familiar with equipment to be used in the data system, (e.g., mini-computers, microfilm equipment, and digitizers).

These individuals should coordinate through a series of meetings to establish the requirements for the data system. The planning areas which must be discussed in these meetings are covered in the next subsection.

1.3.2 Planning Areas

The areas which are important to the design, implementation, and operation of the data system are covered below. A flow diagram is provided (Figure 1-2) to illustrate how the various areas interrelate and the order in which they must be considered in the planning exercise.

1.3.2.1 System Input/Output (I/O) Requirements

System I/O requirements begin with which data mediums will flow into the data system and which mediums will be required from the system.

In the case of ARES, there are two primary input mediums, the Polaroid photographs (raw data) and the characterization parameters derived from each photograph. These input data, of course, come from the test system. The data output mediums, in the case of ARES, include computer listings or printouts, plots, punch cards, and digital magnetic tape. These outputs are generated when dictated by the data processing requirements set by data analysts working with the test program. However, test engineers can also dictate output requirements, based on their needs for the processing of simulator calibration data.

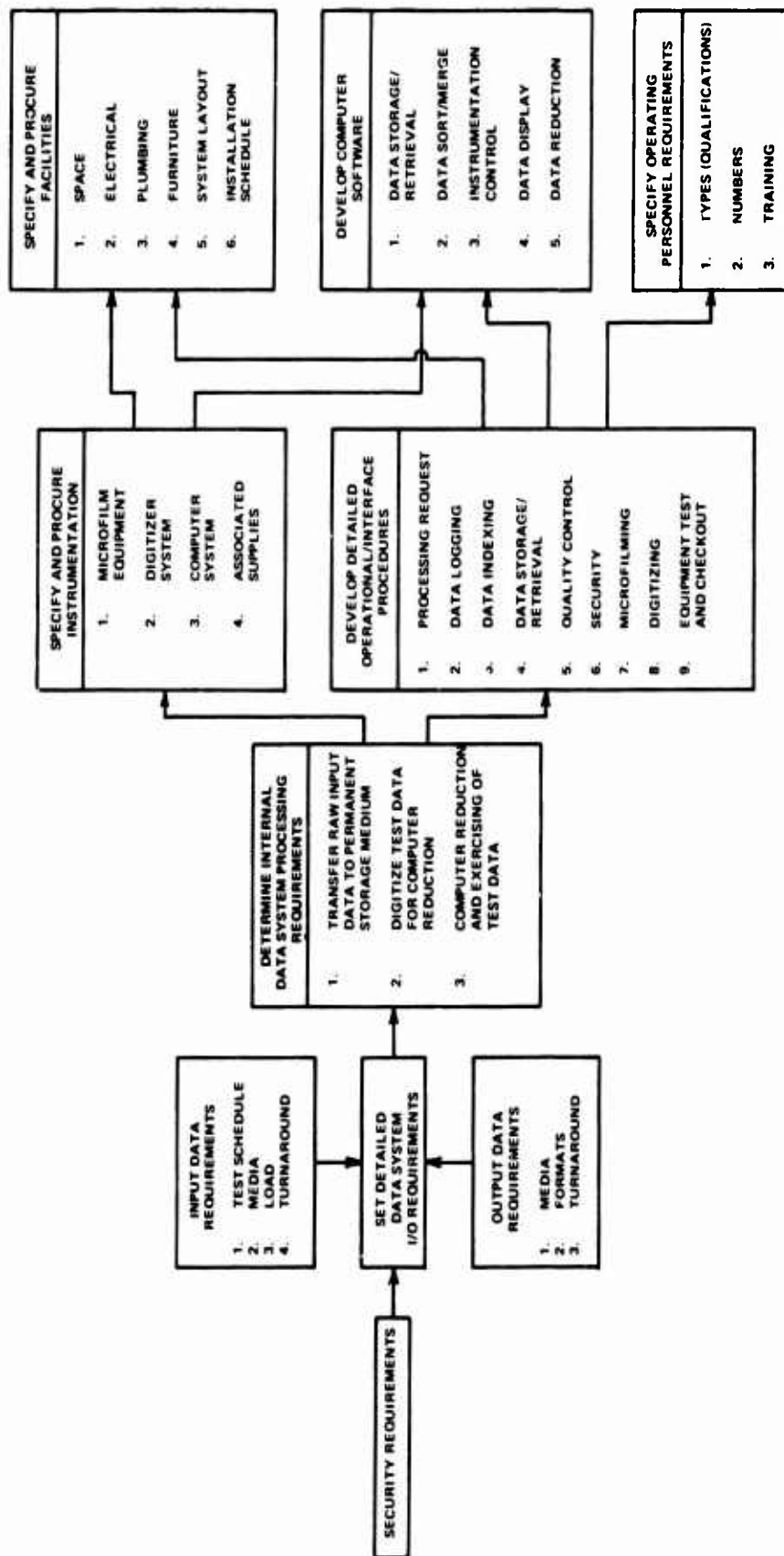


Figure 1-2. Flow Diagram Illustrating Interrelationship of Data System Planning Areas

1.3.2.2 System I/O Load Level and Turnaround Requirements

The overall test schedule for the EMP test will specify the timing for each test to be run, the number of test shots to be fired, and the number of photographs generated per shot. This information can be used to determine both the average and peak raw test data flow rates into the data system. It may also be important in planning for an increased data system staff for known work load peaks.

Turnaround time required for processing data through the data system is a function of how the processed data are to be used in test planning. For example, it may be deemed necessary to have Fourier transforms or transfer function estimates back from the data system within a turnaround time of one to three hours after test photographs are submitted to the data system. As another example, it may be satisfactory for characterization data to be entered into the data bank with turnaround time as much as 24 to 72 hours after submission to the data system.

Output load requirements can be assumed to be much lower than input load requirements. This is because most of the test data flow into the data system and are stored in the data bank. The data that flow out are in reduced form and are a small fraction of the total data quantity.

1.3.2.3 System Processing Requirements

There are several basic processing capabilities which a data system can be expected to do. These fall into three basic categories: (1) entry of data into the data bank, (2) retrieval of data from the data bank, and (3) performing various processing functions. The processing method used is dependent on the form in which the data enter the data system, the forms in which the data are stored in the data bank, the forms in which data are displayed upon retrieval from the data bank, and the

types of data processing required. For example, most input data are in the form of Polaroid photographs, but may be most conveniently stored in the data bank on microfilm. Therefore, microfilm processing would be required. Characterization data may be put into the data bank in the form of written or typed lists of parameters, but would be stored in the data bank on digital magnetic tape. Therefore, a means of processing new characterization data for storage on tape would be required. As one final example, the generation of a Fourier transform from a photographic time waveform would require several processing steps. The first processing step would normally be digitization of the oscillograph trace. However, it may be desirable to enlarge the waveform by microfilm enlargement in order to achieve better resolution in the digitizing process. After digitization, the data must be processed through a digital computer to generate the Fourier transform and display the results in graphic format. The intermediate steps in the processing are dependent on the specific on-site data processing capabilities.

1.3.2.4 System Equipment Requirements

Once requirements (1) through (3) are established, equipment to perform the various processing requirements can be specified and procured. Since certain types of processing will require several pieces of equipment, the equipment must be selected for interface compatibility where necessary. For example, it may be desirable to feed the output of a digitizer onto digital magnetic tape which can be transferred directly to a digital computer for further processing. Thus, an interface system must be used between the digitizer and tape drive which can accept digitizer output format, convert to a computer compatible format, and write data onto tape in the computer compatible format. Such an interface system may be a mini-computer (which is the case at ARES).

There are three main data processing subsystems:

- (1) The microfilm processing subsystem.
- (2) The digitizer subsystem.
- (3) The computer subsystem.

The microfilm subsystem will normally include both recording and reader/printer capability. It must be selected for ease of use and quality of end product. For example, if microfilm is used to produce photographic enlargements for digitizing and an enlargement is of low quality, then the digitization results will suffer.

The digitizer subsystem must be able to handle the specified data load at the specified level of accuracy and resolution. There are many digitizer alternatives to choose from, ranging from completely manual to completely automatic systems. Each has advantages and disadvantages, and a trade-off analysis is required in order to make a proper selection.

The required computer subsystem is dependent on such factors as what computer facilities are remotely accessible from the data system, what turnaround time can be expected from remote facilities, and what types of data processing and instrumentation control must be performed on-site. As an example, the ARES data system has a NOVA 1200 mini-computer which is used to control a digitizer and to process characterization data for recording on digital magnetic tape. It is not used to run data processing algorithms such as Fourier transforms because of its limited configuration (however, it could be so used with proper hardware expansion). Therefore, all software codes used in data processing are run on the Kirtland AFB CDC 6600 computer system which is accessible through a remote job entry terminal

located within the data system. Factors which must be considered in selecting a data system computational capability include availability of off-site computers, software processing requirements (core memory, bulk storage, plotting, etc.), turnaround time, interfaces with other processing equipment, and cost.

One factor which is paramount in the processing equipment planning is the ordering of long lead time items as early as possible. The lead time between ordering and delivery for most equipment of the types discussed above is 60 to 120 days.

1.4 SYSTEM SOFTWARE REQUIREMENTS

There are several computer software programs used in a data system depending on the data processing requirements. The following is a representative list of the software developed at ARES to support the data system:

- (1) NOVA 1200 program to control the digitizer, format the digitizer output, and record on digital magnetic tape.
- (2) NOVA 1200 program to accept characterization data via teletype, format it, and record on digital magnetic tape.
- (3) CDC 6600 program to update the master characterization data tape from daily characterization tapes.
- (4) CDC 6600 program to sort characterization data based on characterization parameter specification. Master characterization data tape used as the input data base.

- (5) CDC 6600 program to generate Fourier transforms using linear Fourier transform algorithm.
- (6) CDC 6600 program to generate Fourier transforms using Fast Fourier Transform algorithm.

It is evident that the software requirements can be considerable and require understanding in a number of software disciplines. For example, writing the software to control the digitizer required understanding the use of software drivers for peripheral hardware systems. Developing sort software required understanding of large machine sort/merge codes and, in addition, a complete understanding of user requirements so that output data are displayed in the most usable format. Development of Fourier transform codes required understanding of the various limitations of computer implemented Fourier analysis techniques.

Development and debugging of the necessary software must also be considered a long lead time item, taking anywhere from one to three months for a new data system.

1.5 SYSTEM OPERATIONAL PROCEDURES

In order for data to move smoothly through the data system and to maintain a consistently high level of quality control, a comprehensive set of operating procedures must be developed. These procedures must include the methodology for:

- (1) Entering data into the data system (including who interfaces with whom, what additional information must accompany the raw data, how it is logged into the system, and initial quality control inspection).

- (2) Entering data into the data bank (including indexing items of data, microfilming, storage, and quality control).
- (3) Retrieving data from the data bank (including request forms specifying data needed and any additional processing required, copying, and quality control).
- (4) Carrying out data processing requests (including request forms specifying processing required, equipment operating procedures, software usage procedures, classification level of data, and output format procedures).
- (5) Classified data control (including processing classified data on computer facilities, storage of classified data, and coding schemes for declassification of data).

1.6 SYSTEM FACILITY REQUIREMENTS

It is most convenient to house the complete data system in a single building. This allows the processing system (equipment and personnel stations) to be laid out in such a fashion that smooth coordination can be maintained between each processing step. In the case of ARES¹, this has been done in a single 12- by 65-foot trailer. In planning a facility, these are the factors which must be considered:

- (1) Floor space sufficient to house all data processing equipment, supporting equipment, and operating personnel stations.
- (2) Supporting equipment such as general office equipment (desks, tables, chairs, typewriters, duplicating machines, etc.).

- (3) Data storage equipment such as file cabinets for Hollerith cards, microfilm reels, digital magnetic tape, notebooks, etc.
- (4) Classified containers.
- (5) Heat and air-conditioning (a driving factor in air-conditioning is the instrumentation BTU output).
- (6) Plumbing including lab facilities for microfilm work, toilet facilities, and drinking fountains.
- (7) Electrical: Sufficient service must be planned to meet instrumentation and equipment needs, and electrical outlet layout so that service is convenient to all instrumentation and equipment stations. Proper grounding must also be considered.
- (8) Shielding and Decoupling: If the data facility is located close to the EMP simulator, significant field levels will occur inside the facility. Also, impulse noise can feed through on electrical powerlines. These types of noise, which can cause equipment malfunctions, have been experienced at ARES and resulted in interruptions in the operation of various data processing systems. The noise and EMP radiation problems were reduced significantly by properly filtering powerlines and by electrically shielding the data facility. This is an extremely important problem and it may prove impossible to use certain equipment close to an EMP simulator. EMP field levels should be monitored before a data facility location is selected.

1.7 SYSTEM OPERATING PERSONNEL

Personnel requirements can be broken down into job type and number. The types are, of course, determined by the activities to be carried out in the data system; the number is determined by both activities and overall expected processing load. Here is a list of the normal type of personnel and their capabilities associated with a data system:

- (1) Data System Supervisor: must have full knowledge of all activities associated with EMP data management and data processing.
- (2) Data Librarian: must be able to design and maintain the EMP data bank including all data storage and retrieval methods.
- (3) Microfilm Operator: must be able to operate microfilm recording, duplication and printing equipment. May also be required to perform equipment maintenance.
- (4) Keypunch Operator.
- (5) Digitizer Operator: must be able to produce consistently high quality digitizations within the limits of the raw test data provided. Requires high level of patience, sharp eyes, and good manual dexterity.
- (6) Computer Programmer: must understand computer and software systems used. Preferably, has been responsible for the development of procurement of all software.

- (7) Computer Operator: must be able to set up and execute day-to-day software programs used in the data system. This requires the use of on-site or off-site computer facilities or both.

It is desirable to have a given individual do more than one of the jobs outlined above. This is desirable from the standpoint that a number of the jobs will not require one person's full time attention, and it is desirable from the standpoint of cross training of people as backups to assure that one key job is not dependent on one person. There are three key positions of responsibility in the data system: the Supervisor, the Data Librarian, and the Programmer. The Supervisor's responsibilities are obvious, but it should be noted that it is useful for him to have programming experience as backup in that position. The Librarian's position is crucial because he or she should be the designer of the data bank and responsible for data quality control. The Programmer position is crucial because of the importance of software to overall data system operation. In addition, the Programmer should be the designer of the software system. All other jobs can be done by data clerks who can be cross trained in microfilming, digitizing, key punching, computer operation, and general data handling or processing.

This philosophy worked efficiently in the ARES² data system. As an example of personnel level requirements, the ARES data system used a two shift operation to process an input data load of approximately 300 Polaroid photographs per day plus accompanying characterization lists, and an output load of approximately 25 digitizations per day as well as associated computer processing of the resulting data. The first shift operation consisted of a supervisor, a data librarian, and three data clerks; the second shift, a supervisor, a programmer, and a data clerk.

1.8 INFLUENCE OF DATA QUALITY ON DATA SYSTEM FUNCTIONS

This subsection is provided to alert the reader to possible problems which can arise if consistent data quality standards are not established. These standards must be designed for data flowing into the system, being processed within the system, and flowing out of the system. The burden of meeting and maintaining input data standards, for the most part, falls on the test system where the data are generated and initially recorded. Meeting standards for processing within the data system as well as for data output from the data system is the responsibility of the data system itself. However, the responsibility for setting the standards, to a large extent, rests with the users, the test system, and data analysts, with the approval of the test conductor.

1.8.1 Input Data Quality

Input data quality must be maintained in two areas; the quality of the raw test data and the quality of supporting data which accompany the raw test data. Assuming raw test data to be Polaroid photographs, the quality of these data can be maintained only through proper maintenance and use of recording instrumentation. Technicians must be trained to operate an oscilloscope for the "best" recording conditions in terms of oscilloscope focusing, scope intensity, amplitude dynamic range, sweep speed, and graticule lighting. Poor quality photographs degrade any data processing using the photographs.

Supporting data which accompany the photographs include test conditions, such as oscilloscope settings, plus any peculiar test conditions which may affect the photographs. These data are usually recorded on the back of the photographs and/or forms designed for this purpose. Consistency in recording these data must be maintained, otherwise, there will be interpretation problems by the data personnel.

1.8.2 Internal and Output Data Quality

The data system must create and maintain high standards of data quality throughout its operation. If input data quality meets the standards, there is no reason or excuse for output data quality to fall below established standards. This can be assured through a well planned quality control system with check points at all key points in the processing cycle.

Setting up and maintaining these standards is often easier said than done because vague measures of quality must be used in some cases. Two good examples of this are in the microfilm copying of Polaroid photographs and the digitization process. Both processes require operator judgment as to whether the best end product is being generated. This requires an extensive program for training operator personnel for their full appreciation of the variables involved.

Data users must get involved in the procedures for processing data under certain conditions. For example, how a photograph should be digitized when the waveform is blurred or truncated. The users must have a full appreciation of the effects of such photograph quality on data processing results (e.g., a Fourier transform or transfer function estimate).

1.9 GLOSSARY OF TERMS

- (1) Data System - Service organization responsible for the processing and control of all test data generated on an EMP test program.
- (2) Data Management Function - First of the two major data system functions. Responsible for the control and maintenance of the EMP test data bank. Controls data being processed by Data System.
- (3) Data Processing Function - Second of the two major data system functions. Responsible for providing data processing services to meet user needs.
- (4) Test System - Organization conducting test and providing raw data to Data System.
- (5) Data Analysts - Any persons associated with the EMP test program who use test data for vulnerability assessment.
- (6) Characterization - The process of measuring and recording gross test waveform characteristics such as peak-to-peak current, and primary and secondary frequency components.
- (7) Digitization - The process of converting an analog signal or waveform into an ordered set of digital X-Y pairs.

SECTION 2

THE DATA SYSTEM AND DATA MANAGEMENT

2.1 INTRODUCTION

EMP test programs typically generate large quantities of test data which are used during and following the test program for the vulnerability assessment of the system tested. There is a definite requirement to organize the test data so that they are readily accessible during the vulnerability assessment and, in many instances, to process the data into forms more useful to the assessment than in their raw form. The system responsible for these control and processing requirements is the Data System or, as it is often called, "the Data Mill."

In Section 1, the test program was broken into three elements:

- (1) The test system which generates the test data.
- (2) The data system which controls and processes the data.
- (3) The data analysts who use the data in vulnerability assessment.

In addition, the relationship between these three elements was shown in Figure 1-1 as the data system performing the interface between the test system and the data analysts. This concept can be expanded by defining the data system as a service organization designed to satisfy the data requirements of both the test system and the data analysts. As such a service organization, the data system accepts newly generated test data from the test system and processes it into the EMP test data bank (permanent storage) and processes data out of the data bank for use by the data analysts. This concept is modified only slightly to include the possibility of data being processed out of the data bank for use by the test system (e.g., simulator calibration data).

A second way of viewing the data system is on a functional basis; as performing two basic functions:

(1) Data Management

(2) Data Processing

The concept of data management, then, is almost synonymous with the term data system. It can be said that all data flowing into or out of the data system are controlled by the data management function, whereas only limited quantities of the incoming or outgoing data are processed by the data processing function. (The subordinate role of the data reduction function is also illustrated in Figure 1-1.) This relationship can be stated in another way by saying that all control of test data within the Data System and most of the data processing requirements are the responsibility of data management whereas only a limited number of the data processing requirements are the responsibility of the data processing function.

In the remainder of this section it will be shown how a data system is organized and how it operates from the functional standpoint. This will be done by presenting a simple model of the data system which will be built upon in the course of discussion. The elements of the model are either data control (management) or data processing in nature. Each of these elements will be discussed in terms of how it functions individually and how it fits into the data system.

2.2 THE GENERAL DATA SYSTEM MODEL

2.2.1 Users - The External Environment

The generalized model shown in Figure 2-1 will be used in describing the various data system control and processing elements, and their interrelationships. It will be noted first that the external environment is shown as the data system "user" who either submits data to the system for processing or retrieves processed data from the system. In either case, these actions are started by a formal request to the system.

2.2.2 Interface

The interface between the external environment and internal environment requires that there must be formal procedures for starting processing action within the data system. As will be shown in later discussions, the formality of the interface itself assures that data flowing into or out of the system are properly quality controlled and recorded in permanent logs. This action insures:

- (1) The quality of the data flowing into the data system, placing the responsibility for this quality on the submitter (Test System).
- (2) The quality of all data flowing out of the data system, placing the responsibility for this quality on both the user and the data system. Responsibility is placed on the user from the standpoint of the completeness of his request for processing action and on the data system for the quality of the processed data passed to the user. The user must be aware of the capabilities and limitations of the data processing system and must fit his requests within these.

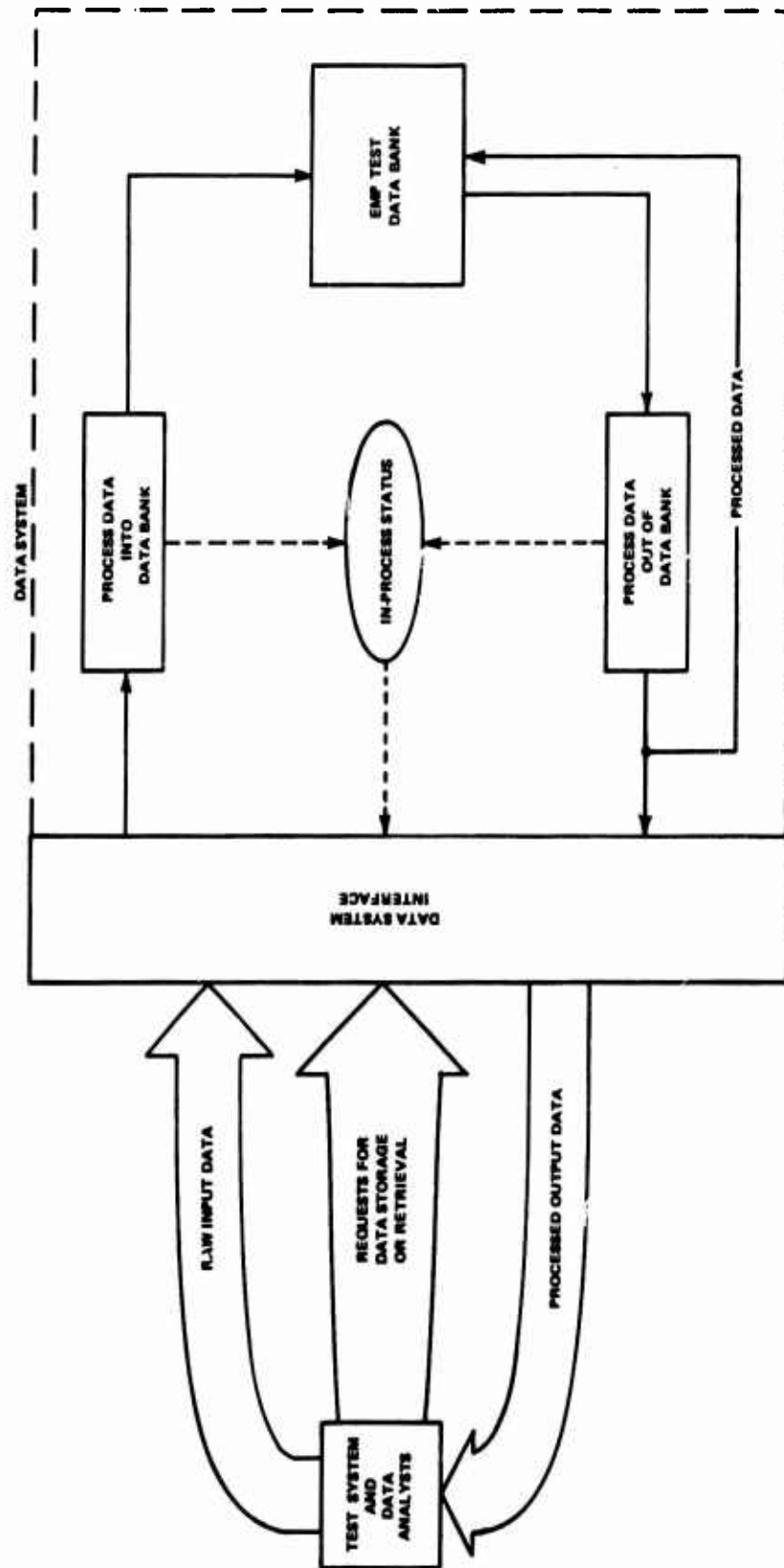


Figure 2-1. General Data System Model

In addition, the interface acts as a buffer zone where special problems can be resolved (such as turnaround time requirements, changes in projected test schedules, or requests for special processing action, and changes to reduction procedures or programs).

It should be noted that the control action of data processing which takes place at the interface is a major data management subfunction.

2.2.3 The Internal Environment

Inside the data system, three types of action take place: (1) processing data into the data bank, (2) processing data out of the data bank, and (3) maintenance of the processing system (software and hardware). In either case, the processing involved will take on many different forms depending on the medium of the input data, the medium in which the data are stored, and the medium of the output data. It should be noted, in the case of processing data out of the data bank, that the results of processing, besides being passed to the user, are often stored in the data bank as a permanent record of this action. Thus, the processed results are available to other users at future dates on an immediate basis.

In addition to the function of data processing, there is the function of data control. The control function allows the data system supervision to determine the status of any "job" in process within the system. Thus, the Supervisor can determine if schedules are being met within his operation and, if need be, to report the status of a given job to the user.

2.3 DATA SYSTEM INPUTS AND OUTPUTS

Before discussing the details of how data are processed through the system, how data are stored, and how control is exercised over the system, details of system inputs and outputs must be established. The types or

mediums of system input/output (I/O) described are typical for a data system supporting a pulse simulator such as ARES.

The concept of the "request" as a formal way of initiating the storage or retrieval of data from the data bank was introduced in the discussion above and is shown schematically in Figure 2-1. It would seem logical to address the request as the first topic under I/O because all I/O is accompanied by a formal request. However, the description of the request is more easily made with a knowledge of typical I/O. Therefore, the request will be covered last.

2.3.1 Typical Data System Inputs

The most typical data system input data for pulse simulators are Polaroid photographs of waveforms. There are two categories of such photographs:

- Test Response Photographs.
- Simulator Calibration Photographs.

2.3.1.1 Test Response Photographs

Test response photographs which make up the bulk of the photographic data, are typically generated on a test/shot/channel basis. That is, a test program is broken down into a number of individual tests, during which a number of test shots are made where one shot is equivalent to pulsing the test object one time. During each test shot, a number of oscilloscope channels of test responses (transient waveforms) are recorded on Polaroid photographs. In the case of recent ARES tests, there were 20 oscilloscopes (10 channels with two scopes per channel) for recording response data and it was typical for as many as 20 test shots to be made during a given test setup (specific sensor placement). The average number of shots per day was between eight and 10. Thus, the number of response photographs generated averaged between 160 and 200 per day.

Where a test ranged from five to 20 shots, the response photographs were usually submitted to the data system as packages on a test or multitest basis. Therefore, the number of response photographs in a package of data submitted to the data system ranged from 200 to 1000. The rate of input of response photographs to the data system is, of course, peculiar to the test program being conducted and the EMP simulator system used. However, the important factor that came out of the ARES experience was that the rate of response photograph input to the data system did not fluctuate much during the test program. There was a gradual build-up to a broad peak level and then a fairly abrupt decrease as the program ended.

It is interesting to note at this point that individual tests can be numbered sequentially. Thus, test, shot, and channel numbers can conveniently be used as a natural identifier or index to identify test photographs. This number sequence was written on the back of all ARES photographs by the test system personnel.¹

2.3.1.2 Calibration Photographs

There are two common types of calibration or simulator checkout photographs generated for pulse simulators:

- Simulation Environment Photographs
- Instrumentation Calibration Photographs

Environment photographs are generated on a continuing basis to assure that the test volume environment is within specifications. In the case of ARES, four recording channels (in addition to the 20 response channels) were available for recording environmental data. An average of two such environment waveforms were photographed for each shot, bringing the average total number of photographs generated during a test shot to 22. These environment photographs were packaged separately from the response photographs but

were submitted to the data system simultaneously. As in the case of response photographs, certain supporting information needs to be included with the environment photographs to identify them and indicate the test and instrumentation conditions under which they are recorded. The identification information is written on the back of the photographs. The identifier used is normally the test/shot/channel number. Supporting test and instrumentation information is written on a form prepared for this purpose and is keyed to the test/shot/channel number. In the case of ARES³, such forms were called "run Sheets," and were not attached to the photographs.

Instrumentation calibration photographs are taken periodically to assure that the instrumentation system from the test sensor through the recording oscilloscope camera is functioning properly. Thus, the volume of such photographs is dependent on how often the test system considers these tests necessary. Several categories of such tests were run at ARES including:

- Frequency Sweep to Check Instrumentation
Frequency Response
- Noise Check
- Linearity Check
- Calibration Pulse Check

These calibration tests are not generally tied to a given test and shot, but are a specific test of a channel at a certain time and date. Thus, the test, shot, and channel identifier scheme will not suffice. An appropriate identifier scheme to be written on the back of each calibration photograph would include:

- Channel Number
- Date
- Time
- Test Type (as listed above)

2.3.1.3 Characterization Parameter Lists

It is very common in pulse testing to make measurements of key response waveform (photograph) parameters and to assemble these along with other test parameters which identify the photographs and the test conditions under which it was generated. This process is termed characterization, and the listing of parameters is termed a characterization data list or simply characterization data.

For ARES⁴, the process of characterization was carried out by the test system with the parameter lists passed to the data system for processing into the data bank. This characterization process could, however, be performed by the data system. The basic input data to the characterization process are the response photograph plus the additional supporting data which identify the test and test conditions. Thus, if the characterization is done within the data system, these supporting data would have to accompany the response photograph into the system.

The following parameter list is that used to characterize each response photograph at ARES during the MINUTEMAN II/III test program. Some of these parameters are self explanatory; others are not and may be peculiar to the particular test for which the list was designed. Therefore, no explanation will be given for any of the parameters. Those parameters

measured from the response photograph are indicated with an asterisk. The remaining parameters are test and test condition identifiers which would have to be supplied by the test system if the characterization process took place in the data system. Note the inclusion of test, shot, and channel numbers in the list.

- Test Series (MINUTEMAN II or III)
- Test Number
- Shot Number
- Date of Test
- Test Configuration Number
- Environment Level
- Risetime of Pulse^{*}
- Channel Number
- Sweep Speed
- Location Number of Sensor
- Location I.D. Number
- Probe Impedance
- + Calibration Divisions^{*}

- + Signal Divisions*
- - Calibration Divisions*
- - Signal Divisions*
- Verification Number*
- Primary Frequency*
- Secondary Frequency*
- Loop
- Plume/Chaff
- Active/Detector
- Braid/No Braid
- Close/Open/Base
- Closure/Opening

2.3.2 Typical Data System Outputs

Typical data system outputs which are requested by the user include:

- (1) Copies of Polaroid photographs.
- (2) Digitizations of Polaroid photographs.

(3) Computer reduction of digitized data.

(4) Sorts of characterization data sets.

2.3.2.1 Photograph Copies

There are two common methods for passing copies of photographs back to the user. Both assume that the photograph data are stored in the data bank on microfilm. The first method is copies of the microfilm itself. For example, complete microfilm copies of all photographs generated on the MINUTEMAN II/III test program at ARES were made for several interested contractors on the program. The second method of photograph copies are hard copy prints (8-1/2 x 11 inches) made from the microfilm. Microfilm printers are available for this purpose.

2.3.2.2 Digitization Data

Digitization is the process of converting analog graphical waveform data into numerical data for computer input. Digitization of photographic data is often done as an intermediate step for further data reduction done internal to the data system. However, the data analyst is often interested in performing his own computer analysis with digitized waveforms used as input data. The medium in which the digitized data set is passed back to the user depends on the digitizing system used in the data system. Punched cards or digital magnetic tape are common mediums compatible with most computer systems. Both of these mediums are available from the ARES Data System.

2.3.2.3 Computer Reduction Output

It is typical for a data system to have a computer software package⁵ for performing various data processing functions on digitized data.

Examples are Fourier transform generation, waveform integration, transfer function estimation, and waveform unfolding (removal of instrumentation transfer characteristics). The outputs from these computer operations are computer printouts and plots of graphic results. Many computer facilities have both hard copy and microfilm plotting capability.

2.3.2.4 Characterization Data Sorts

Characterization parameter sets are often used by the data analyst to search out special trends in the test response data. This searching process is typically done by sorting parameter sets based on key parameter specifications. These sorts are done with a computer⁶ and the output is a computer printout which results in either a standard or user specified special format.

The mediums of output data typically required of a data system are:

- Microfilm
- Microfilm Hard Copies
- Punched Cards
- Magnetic Tape
- Computer Printout
- Computer Plots

2.3.3 The Processing Request

The data system processing request is simply a form which is submitted by the user to initiate entry of data into the data bank,

request its retrieval, and/or any other processing within the capability of the data system. In the case of entering data into the data bank, the request form accompanies the raw test data as it enters the data system. The form must contain sufficient pertinent information so that the data system knows what data it is receiving and what to do with it. This information, which must be supplied by the user, should include:

- (1) Submitter (user's name).
- (2) Submission date.
- (3) Type of photograph (response, environment, and/or calibration).
- (4) Number of photographs of each kind.
- (5) Test number to which photographs belong.
- (6) Any peculiarities about the data.
- (7) Any special processing instructions.

From the discussions in Paragraph 2.3.1, it is obvious that there were only two basic forms of data system input data during the ARES MINUTEMAN II/III tests; photographs and characterization parameter lists. Throughout the test program, both forms of data were processed into the data bank in a consistent manner. Therefore, the instructions for processing the data into the data bank were repetitious and, for the most part, implicitly understood by both the users and the ARES Data System and did not have to be entered on the request form. Only deviations from the norm, such as peculiarities in the data (e.g., photographs missing) or special processing instructions, if any, were entered on the request form.

There are basically two types of requests for retrieving data from the data bank; standard and special. For standard requests, the instructions for processing required are implicitly understood by the user and the data system. Thus, the request form used to initiate a standard processing request need contain only the following information:

- Submitter
- Submission Date
- Processing Requirement
- Data Bank Items to be Processed

In the case of special processing requests, very explicit instructions must be given by the user. For example, ARES special processing requests usually involved the data system's developing new computer software in order to process or display results in a nonstandard manner.

ARES used two request forms during the MINUTEMAN II/III test program as shown in Figures 2-2 and 2-3. The first form was used to initiate all input requests and special output requests. The second form was used to initiate all standard output requests. Both forms have a space for the date and the submitter's name. The first form has a space for the number of photographs submitted. This number told the data system how much data they were receiving in the package and gave them a quality control check number (i.e., they were able to count the number of photographs in order to determine if the count coincided with the stated number).

DATA SYSTEM INPUT, COVER SHEET FOR
(Submit to Data Support Team - Shift Supervisor)

Date _____

Submitter _____

Number of pictures submitted _____

FOR DATA SUPPORT USE ONLY:

Received _____ (Time)

Control # _____

Entered in request log by _____

Characterized _____, _____

Keypunched/verified _____

Microfilmed _____ Thru _____

Library (Film & Cards) _____

Shift Supervisor _____

INSTRUCTIONS:

Figure 2-2. ARES Request Form for Data System
Input and Special Output Requests

DATA REDUCTION REQUEST SHEET

Requester _____		Priority <input type="checkbox"/>	
Date _____		1 = Routine, 2 = As soon as practicable, 3 = Immediate	
Analysis Required		Required	Plot Format
Time Domain (Scaled)	<input type="checkbox"/>	<input type="checkbox"/>	<input type="checkbox"/>
Fourier Transform	<input type="checkbox"/>	<input type="checkbox"/>	<input type="checkbox"/>
Transfer Function	<input type="checkbox"/>	<input type="checkbox"/>	<input type="checkbox"/>
Amplitude	<input type="checkbox"/>	<input type="checkbox"/>	<input type="checkbox"/>
Phase	<input type="checkbox"/>	<input type="checkbox"/>	<input type="checkbox"/>
Other (See Remarks)		<input type="checkbox"/>	<input type="checkbox"/>
Plot Format	X	Y	
	Log	Log	A
	Log	Lin	B
	Lin	Log	C
	Lin	Lin	D
Photo Listing			
I.D.#	Swp. Spd.	Probe Z	Atten.
1.			
2.			
3.			
4.			
5.			
6.			
7.			
8.			
9.			
10.			

Number of Photographs <input type="checkbox"/>	
Required Form of Output	<input type="checkbox"/>
Microfilm Plot	<input type="checkbox"/>
CalComp Plot	<input type="checkbox"/>
Mag Tape List	<input type="checkbox"/>
Cards List	<input type="checkbox"/>
Line Printer	<input type="checkbox"/>
X-Y Plot	<input type="checkbox"/>
X-Y Listing	<input type="checkbox"/>
Remarks _____	
BDM Internal Use Only	
Rec'd _____ (Time)	Shift Supervisor _____
Control # _____	
Entered in log by _____	
Digitized _____	
Characterized _____	
Keypunched/Verified _____	
Library _____	
Completed _____ (Time)	

Figure 2-3. ARES Request Form for Standard Output Requests

Additional information needed was filled in the space marked "Instructions." Examples of instructions are:

"Environment Pictures for 373-2 through 401-1."

This means environmental photographs from test 373, shot 2 through test 401, shot 1.

"Response Pictures for 845-1 through 875-10."

The same meaning is attached to this statement as for the environment photographs. However, for response photographs, normally a characterization parameter list accompanied each response photograph.

"Response Pictures Missing for 856-7 and 856-9"

This means, shots 7 and 9 were not made for test 856.

When the form shown in Figure 2-2 was used to initiate a special output request, the blank for number of photographs submitted was, of course, left empty, and all information was supplied in the "Instructions" area. Always included in the instructions were test/shot/channel numbers for the data to be used (i.e., the common index for most data stored in the data bank was the test/shot/channel number).

The form shown in Figure 2-3 was used for standard output requests. The form has a number of standard data reduction functions listed under "Analysis Required," and a number of output and display options which could be checked. Also, there is a space to list the photographs to be used in the processing, plus some pertinent parameters (sweep speed, etc.) which might have been needed during the processing.

It should be noted that both forms contain a space titled "BDM Internal Use Only" or "For Data Support Use Only." These forms accompanied the data being processed through the data system and were used in the control procedures used internal to the data system. This control use is covered in detail in Paragraph 2.4.

2.4 DATA SYSTEM PROCESSING AND CONTROL REQUIREMENTS

The ground work has now been laid to discuss the internal workings of the data system. The actions which take place will be looked at as either "processing" data into the data bank or "processing" data out of the data bank as suggested in the model (Figure 2-1). The term "processing" as used here denotes various sequential processing steps which the data must go through in order to prepare them for data bank storage or for the user. This series of steps will be termed a processing cycle.

Several such cycles can be defined for a data system designed to satisfy the data requirements of a pulse simulator (transient waveform data). The number of cycles involved depends on the number of different forms of data input to the data system, how the data are to be stored in the data bank, and the requirements for output data. The individual processing steps in each cycle are also dependent on these factors. In any case, the processing steps are directed toward changing the medium or format of the test data into a more efficient or usable form, and are, for the most part, hardware oriented.

In addition to the processing steps which take place in a cycle, there are a number of control steps which take place. There are three categories of control which are commonly used:

- Data Bank Control
- Data In-Process Control
- Quality Control

Data bank control functions are basically library oriented. They involve using a well-defined data logging and indexing system that allows assessment of the contents of the data bank at any time. This is very important from the standpoint of retrieving data from the data bank.

In-process control of data involves procedures for checking the in-process status of any request submitted to the data system. The procedures allow the data system supervisor to know if schedules are being met and if his operation is running smoothly in general. It also allows the supervisor to report the status of a request back to the user if necessary. This may be important if the user has requested an other-than-normal schedule or processing procedure to be used by the data system.

Quality control procedures are used throughout each processing cycle to assure the quality standards of data entering the data system, entering the data bank, and leaving the data system.

Since the steps which take place in a processing cycle are dependent on the input to the cycle and its data output, it will be instructive to consider how data are typically stored in the data bank. Once these are defined, the particular processing and control steps which take place in definable cycles can be discussed. The cycles selected for discussion are ones patterned after those used in the ARES Data System.¹ This is also true for the discussion of the data bank which follows.

2.4.1 The EMP Test Data Bank

The EMP test data bank is a collection of various types of test information generated during a test program. In fact, it should

contain all test information generated during the test program so that a complete data record of the test is permanently recorded and controlled. The mediums used in storing data in the data bank are normally selected for ease and utility of future retrieval as well as for convenience (as in the case of data reduction results being stored in the data bank as well as being passed on to the user) (see Figure 2-1). In this case, the medium passed to the user is also the medium stored.

Common data bank storage media are:

- Microfilm
- Digital Magnetic Tape
- Punched Cards
- Punched Paper Tape
- Computer Printout
- Computer Plots
- Forms
- Index Logs

2.4.1.1 Microfilm

Microfilm is a compact and convenient medium for storage of photographs. As many as 1500 photographs can be recorded on a single reel of microfilm. Microfilm can be rapidly scanned with a scanner to inspect and select data for further processing. It can be easily duplicated so that records of test data can be passed out to

multiple users (usually contractors associated with the test program) as well as be stored in the data bank. Hard copies of any recorded frame can also be made with a hard copier capability. Besides being used for the storage of photographs, microfilm is commonly used to record computer graphic output of high quality. During the ARES MINUTEMAN II/III test program, the ARES Data System recorded more than 90,000 Polaroid photographs on microfilm and made 12 copies of all microfilm for distribution to users. In addition, approximately 6,000 computer reductions were performed on response photographs which resulted in six or more microfilm plots each. Based on the volume of data for this program, the utility of microfilm as a storage medium is obvious.

2.4.1.2 Digital Magnetic Tape

Digital magnetic tape is also a compact medium of data storage and especially convenient for numerical data which are to be subsequently exercised by a computer (e.g., characterization data). Magnetic tape is susceptible to possible degradation (e.g., data accidentally being overwritten by the computer). Therefore, some method should be used to assure that such degradation does not take place (e.g., a backup tape of permanently stored data).

2.4.1.3 Punched Cards/Punched Paper Tape

Either punched cards or punched paper tape provides a convenient means of storing limited quantities of numerical data used

in subsequent computer processing. This is especially true if the user may request a limited set of these stored data for his own use as computer input. For example, the results from digitizing a limited number of waveforms are more conveniently passed to the user as punched cards than as magnetic tape and most likely more convenient for the user since his program probably exists as a card deck.

2.4.1.4 Computer Output

Usually the computer output will be stored as part of the data bank since much of the data reduction done by data systems is computer based. The common computer output mediums are printouts and plots, although punched cards and magnetic tape can also be outputs. Plots are typically generated in one of three ways: (1) microfilm (as covered in Paragraph 2.4.1.1), (2) digital plotter (e.g., CalComp), and (3) line printer. Binders are commonly available for storing printout and digital plots.

2.4.1.5 Forms

The use of request forms has already been discussed in Paragraph 2.3. Other forms may be used which aid the various processing cycles. These forms are valuable records of user input to the system and internal actions taken within the system. They, therefore, must be stored, preferably in permanent binders.

2.4.1.6 Index Logs

The data bank is, in effect, a library system containing a variety of data mediums. Any library system must have an indexing system which allows access to the data. In the data system data bank, this is accomplished through the use of written logs which

indicate what has come into the data system for processing and what is stored in the data bank. All such logs should be included as part of the data bank. Two log forms are common: notebooks and computer printout listings. Accepted library practices should be followed in selecting an indexing system.

2.4.1.7 Others

Obvious additional candidates for storage are the Polaroid photographs and characterization parameter lists which enter the data system as raw data.

2.4.2 Processing Cycles

Four processing cycles are discussed below. These four are the cycles which were used at ARES during the MINUTEMAN II/III test program. They are considered very typical of the processing cycles which would be found in any data system handling pulse simulator data (transient EMP waveforms).

In discussing the cycles, each definable processing or control procedure will be identified. Those procedures of major importance which need extensive explanation will be covered in more detail in Paragraph 2.5 and in Section 3, which cover data processing techniques.

The four processing cycles to be covered are:

- (1) Processing Polaroid photographs data into the data bank.
- (2) Processing characterization parameter data lists into the data bank.

(3) Retrieval and display of characterization parameter data.

(4) Retrieval, processing, and display of photograph data.

2.4.2.1 Processing Polaroid Photographs

The processing cycle for Polaroid photographs is shown in Figure 2-4. The incoming data or input to the cycle is a request form previously filled in by the user* (test system) and a package of photographs. The supporting data are written on the back of each photograph (see Paragraph 2.3 covering data system I/O). The first step in the processing cycle is to log the work unit into the system. This is done by making a copy of the request form and entering this copy in a log-in notebook. Recall (Paragraph 2.3) that the request form contains all pertinent information about the input data. It, therefore, acts as an ideal entry in a log-in notebook.

In addition to entering the request form in the log book, a sequential internal data system control number is assigned to the work unit. This number is taken from the log-in notebook "index." Certain summary information about the incoming work unit is also filled in the index as shown in Figure 2-5. This information includes submission date, submitter's name, a very brief description of the job, and the number of photographs in the work unit (if applicable). Thus, the index is merely a summary in the log of the request forms and allows a quick check of submissions to the data system. The assigned control number, a simple, internal identifier of work units in process, is used for internal control purposes.

*The concept of a Data Coordinator was introduced in Section 1. At ARES, the Data Coordinator was the individual who acted for all users as liaison to the data system. He, therefore, submits all requests.

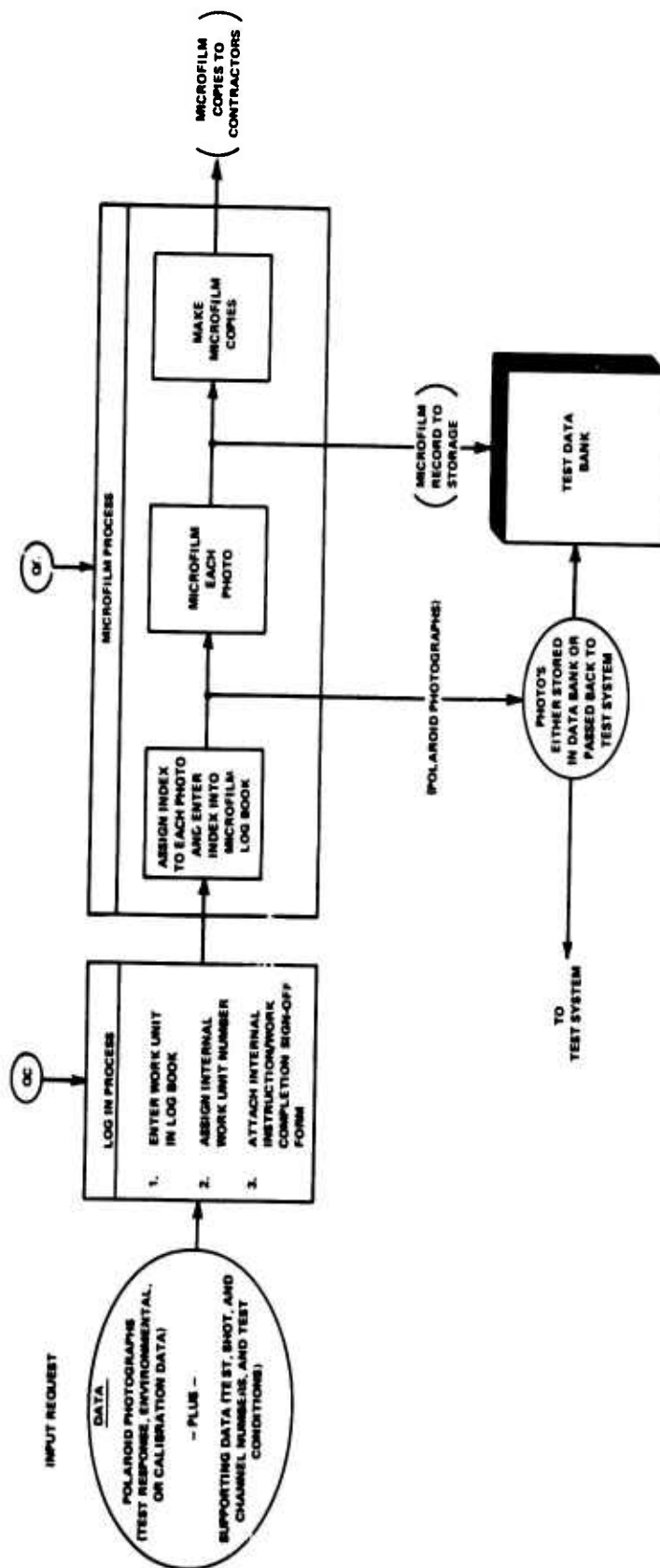


Figure 2-4. Data System Processing Cycle for Processing Polaroid Photograph Input Data into EMP Test Data Bank

[illegible]

Figure 2-5. Log-in Logbook Index

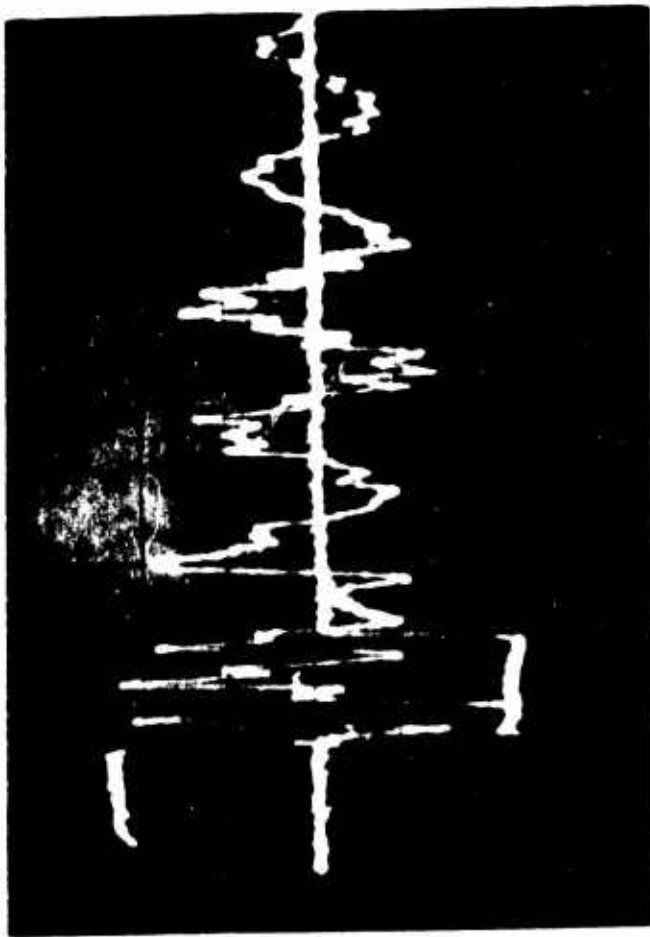
Referring to the example request form of Figure 2-2, it is seen that an area of the form has been reserved for "Data Support Use Only." This form accompanies the work unit through the processing cycle as a control mechanism (i.e., a sign-off form to indicate that given steps in the cycle have been completed). Thus, the first point of "sign-off" will be the log-in step. The steps taken at the log-in process before sign-off can be summarized as follows:

- (1) Write the date and time the work unit (request) is received on the request form. Also, assign the next free work unit control number from the log book index to the request form.
- (2) Copy the request form and enter the copy in the log book as a permanent record of that request.
- (3) Quality control the work unit by counting the number of photographs to assure the count coincides with the number entered on the request form by the test system, inspecting the back of each photograph to assure that proper supporting information is written there, and inspecting the instructions on the request form to assure that they are understood and consistent with the data submitted.
- (4) Sign off the request form for the log-in process as completed.
- (5) Attach the request form to the work unit and pass on to the next processing step.

The next processing step is the microfilming of all photographs as shown in Figure 2-4. This step typically involves indexing each photograph, recording the indexed photograph on microfilm, and making extra copies of the microfilm.


The index procedure used for the three categories of photographs (response, environment, and calibration) may differ depending on how the photographs are normally identified and what supporting information goes along with the photograph concerning conditions under which the photograph was generated. For example at ARES⁷ the three categories of photographs were handled in this way:

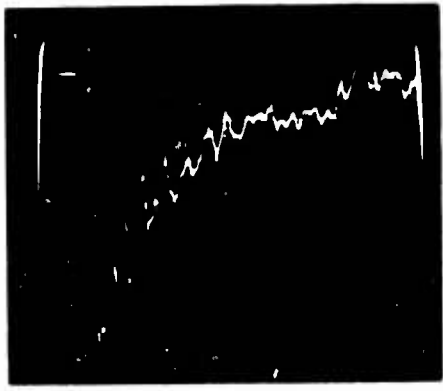
- (1) Response photographs were indexed with a test/shot/channel number label placed on the photograph at the time it was "shot" onto the microfilm as shown in Figure 2-6. No additional supporting information was added to the index because all necessary supporting data were part of the characterization data list available in the data bank through the test/shot/channel number. All response photographs were put on microfilm reels labeled with the letter "R" denoting "response." A sequential number was also used in the label, (i.e., R-1, R-2, and so on).
- (2) Environmental photographs were indexed with a test/shot/channel number but supporting information was also included as shown in Figure 2-7. Thus all pertinent information associated with the photograph was recorded on microfilm along with the photograph. A special form called a photomount was developed for this purpose. The information



6520504A
0330464

Figure 2-6. Response Photograph as Indexed
and Recorded on Microfilm

		100MV	
		ATTENUATION	
		10NS	
		-2.25 MV	
		RISE TIME	
		10.5	
		PROBE TYPE	
		MGL 5A	
		POWER DIVIDER	
		874	
		SCOPE TYPE	
		454	
		TIME	
		0920	
COMMENTS			
TITLE		DATE 7-23-71	
RUN NO. 11	SHOT NO. 1	MONITOR PT.	
CONFIG.	CHANNEL 1A		

		20MV	
		ATTENUATION	
		100NS	
		-2.25 MV	
		RISE TIME	
		10.5	
		PROBE TYPE	
		HSD 1A	
		POWER DIVIDER	
		874	
		SCOPE TYPE	
		454	
		TIME	
		0920	
COMMENTS			
TITLE		DATE 7-23-71	
RUN NO. 11	SHOT NO. 1	MONITOR PT.	
CONFIG.	CHANNEL 39		

E0101183

Figure 2-7. Environmental Photographs as Indexed and Recorded on Microfilm

needed to fill in the photomount was obtained from a "run sheet" which accompanied environmental photographs into the data system. Environmental photographs were put on microfilm reels labeled with the letter "E," (i.e., E-1, E-2, etc.).

- (3) Calibration photographs were treated in a manner similar to the environmental photographs with all supporting information included in the indexing scheme as shown in Figure 2-8. The main identifier in the index is the date and type of calibration. The photomount concept was also used in micro-filming calibration photographs. Microfilm reels were labeled with the letter "C" (i.e., C-1, C-2, etc.).

The handwritten microfilm log book is kept so that the information on microfilm can be retrieved. The indexing scheme used in the written log should be based on cross referencing the microfilm reel number (R-5, C-15, E-2, etc.) and the reel frame number^{*} to the photograph index, (i.e., test/shot/channel number for response and environmental photographs, and date and calibration type for calibration photographs). Thus one section of the log could be filled out as:

<u>REEL</u>	<u>FRAME</u>	<u>PHOTO INDEX</u> (TEST/SHOT/CHANNEL)
E-15	431	73/6/1
E-15	432	73/6/2
⋮	⋮	⋮

* A reel of 16 mm microfilm typically has 1500 to 1600 frames or individual pictures on it. These frames can be thought of as numbered sequentially for the purposes of finding information on a given reel.

LINEARITY CHECK

Level:

Channel:

Vertical: 100 mv/div

Horizontal: 20 ns/div

Date:

Time:

Notes:



C010745

(a)

CALIBRATION PULSE & RAMP

Level:

Channel: 4

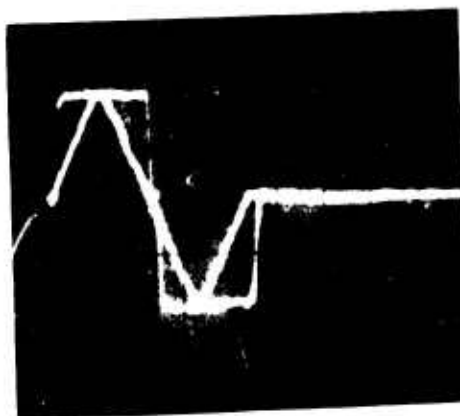
Vertical: 50 mv/div

Horizontal: 100 ns/div

Date: 9/8/71

Time:

Notes:



C010443

(b)

Figure 2-8. Calibration Photographs as Indexed and Recorded on Microfilm

<u>REEL</u>	<u>FRAME</u>	<u>PHOTO INDEX</u>
E-15	436	73/6/6
R-54	1103	73/6/1
R-54		73/6/2
⋮	⋮	⋮
R-54	1142	73/6/40
E-15	437	73/7/1
⋮	⋮	⋮
C-4	139	11/13/72-NOISE*

As shown, both the reel and frame numbers run sequentially and act as the key indices.

A second section could be filled in with the photograph index or identifier as the key index. Response and environmental photographs use the same identifier, thus they could be entered as follows:

<u>TEST/SHOT/CHANNEL</u>	<u>RESPONSE</u>		<u>ENVIRONMENTAL</u>	
	<u>REEL</u>	<u>FRAME</u>	<u>REEL</u>	<u>FRAME</u>
73/6/1	R-54	1103	E-15	431
73/6/2	R-54	1104	E-15	432
⋮	⋮	⋮	⋮	⋮
73/6/6	R-54	1108	E-15	436
73/6/7	R-54	1109	E-15	437
⋮	⋮	⋮	⋮	⋮
73/6/40	R-54	1142	E-15	470
73/7/1	R-54	1143	E-15	471
73/7/2	R-54	1144	E-15	472
⋮	⋮	⋮	⋮	⋮

* Note: This is a calibration photograph entry. Therefore, its index is the date and calibration test type.

<u>TEST/SHOT/CHANNEL</u>	<u>RESPONSE</u>		<u>ENVIRONMENTAL</u>	
	<u>REEL</u>	<u>FRAME</u>	<u>REEL</u>	<u>FRAME</u>
73/7/6	R-54	1148	E-15	442
73/7/7	R-54	1149		
.	.			
.	.			
73/7/40	R-54	1182		

Calibration photographs cannot be included in this indexing scheme because they do not use a test/shot/channel number as a key identifier. However, they can be indexed in a similar way as follows:

	<u>TYPE</u> [*]	<u>REEL</u>	<u>FRAME</u>
7/3/72	FS	C-1	773
7/3/72	N	C-1	774
.	.	.	
.	.	.	
7/15/72	LC	C-1	942
7/15/72	FS	C-1	943
.	.	.	.
.	.	.	.
9/28/72	N	C-2	13

The last step in the microfilm process is to make copies of the microfilm as required by the user. Copies are usually made of a total microfilm reel rather than partial reel. Therefore, copying is not a continuing process but only occurs when one or more reels are full.

A continuing procedure which must take place throughout the microfilming process is quality control. In a data system, quality control factors considered are completeness, consistency, and quality of the results of each processing step. Thus the quality control checks which are exercised during the microfilming process include:

* Note that "type" denotes type of calibration photograph (i.e., Frequency Sweep (FS), Noise Check (N), etc.).

- (1) Check for ambiguities or inaccuracies in supporting data written on the back of photographs or run sheets.
- (2) Visual checks to make certain that microfilm image quality is consistent with photograph image quality.
- (3) Inspection of microfilm indexing to assure that all supporting information is correct. If inaccuracies are found, the photograph should be reshot with the corrected supporting information and spliced into the microfilm reel.
- (4) Check the microfilm copies for image quality.
- (5) Randomly check microfilm log book with microfilm reels to see if log indexing data match reel indexing data on a frame by frame basis.

The final actions which take place in the photograph processing cycles are:

- (1) Sign off the request form (Figure 2-2) to indicate microfilming is complete.
- (2) Pass the request sheet to the data system supervisor or his assignee so that the input log book can be up-dated to show the job as complete.
- (3) Store photographs in data bank.

2.4.2.2 The Characterization Data Cycle

Characterization data lists are input to the data system to be processed into the data bank. The processing cycle to do so is shown in Figure 2-9. The output (the output data medium) of the cycle is assumed to be digital magnetic tape. This assumption is based on the assumed use of characterization data by the user or data analyst. The data analyst is typically interested in sorting and organizing the characterization parameter sets for particular trends in the data. This sorting and organizing is best done by a digital computer and because of the volume of data involved* the input data are best stored on magnetic tape.

As explained earlier, a characterization data set (or parameter list) is generated for each response photograph and they normally are part of a total data package input to the data system (photographs plus parameter lists). Except for the fact that the total package arrives under the same request form, the parameter lists can be treated as a separate input.

The first step in the processing cycle is to log the request into the data system and perform the first quality control check on the data package. The logging in procedure is exactly the same as that given for the photographic input data. A copy of the request form is entered in the log book, an internal control number is assigned, and the original request form is attached to the package of parameter lists.

The quality control exercised at log-in consists of counting the number of parameter lists submitted to see if the count

*The ARES MINUTEMAN II/III Test Program ended up with some 80,000 characterization data sets, each with 31 numerical parameters.

coincides with that given on the request form and scanning the data in each list to determine if each list is complete.

The next step in the cycle of Figure 2-9 is to transfer the parameter lists to digital magnetic tape format. Two methods are shown for doing so (teletype or punch card input) and are dependent on what type of computer facilities are available to the data system. Using a teletype requires an on-site computer which is equipped with a teletype and a tape drive. Using punched cards requires either an on-site or off-site computer equipped with a card reader and tape drive. The tape created from the new parameter lists can be termed an "update tape." When creating an update tape, it is typical to make each parameter set a separate "record" on the update tape.

The final step in the process is to add the newly recorded data to a master tape containing all previous parameter sets, which is the data bank for characterization data. However, before doing so, the new data should be quality controlled to assure that no mistakes were made in the translation process. This can be done by listing the update tape contents and comparing the listing with the parameter lists, or by listing the punched cards (if they are used) and making the same comparison. If errors are found, one must have a means of correcting the update tape. If punched cards are used, one can simply change the incorrect cards and then generate the update tape. When cards are not used (i.e., the teletype method is used) cards could be generated (punched) from the update tape, corrections made, and a new update tape made.

Adding the update tape contents to the master tape is simply a tape-to-tape transfer operation requiring a computer equipped with at least two tape drives and the appropriate software to do so. It is a definite advantage to have two master tapes available with one acting as a back-up in case the primary tape is destroyed.

2.4.2.3 Characterization Data Retrieval/Display Processing Cycle

Characterization data sets are used by the data analyst to search for meaningful trends in test data. This search is typically done on a digital computer using a data SORT/MERGE routine to select various characterization data sets, with the selection based on key parameter specifications. The selected data are then displayed in a manner which allows easy interpretation by the data analyst.

The processing cycle to retrieve and display characterization data is shown in Figure 2-10. The cycle is started by a request from the user which must specify:

- (1) Which characterization data sets are to be included in the retrieval process (SORT/MERGE).
- (2) On which data set parameters the retrieval is to be based.
- (3) How the retrieved results are to be displayed.

The data input to the cycle is the master characterization data tape (discussed in Paragraph 2.4.2.2) plus instructions to set up the sort program and data output format. These instructions are usually submitted via punched cards. The output formats for displaying results normally consist of standard formats and special formats. ARES used two standard output formats: the card image and matrix shown in Figures 2-11 and 2-12 respectively. The software to produce either of these was written as part of the SORT/MERGE routine and the selection of either was made in the instruction cards at the user's option. The software for any special display format was generated by the data system to user specifications.

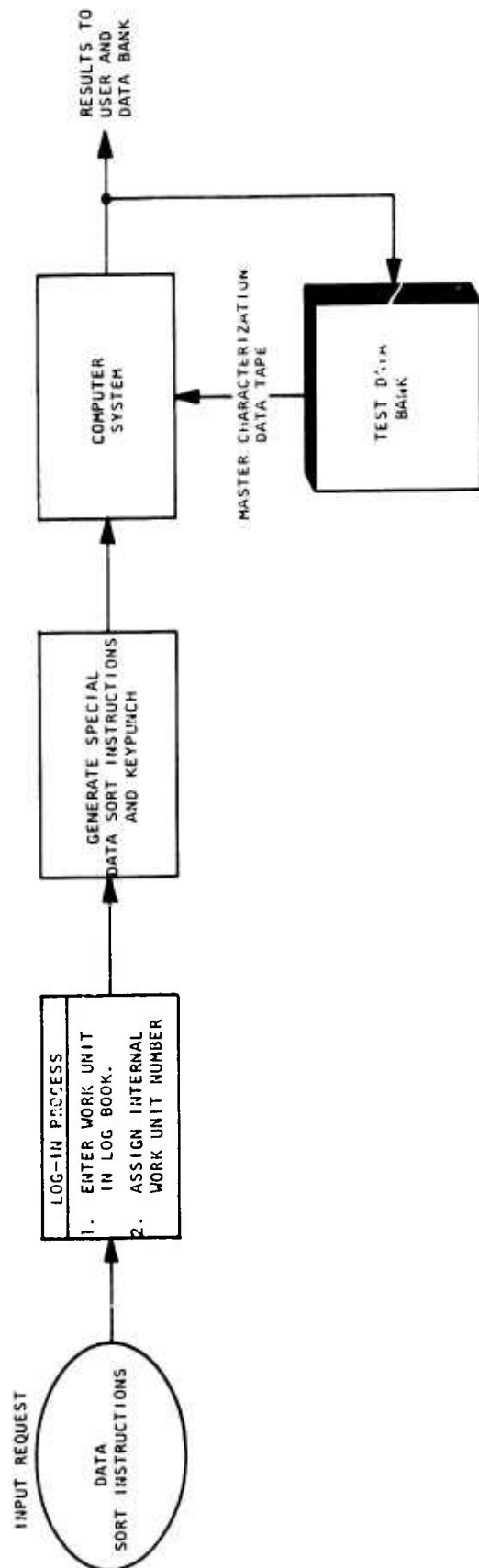


Figure 2-10. Data System Processing Cycle for Retrieval and Display of Characterization Data

A large computer system^{*} is normally required for sorting the characterization data sets. This is because large systems are equipped with the necessary random access and bulk storage peripheral devices (disk and tape units) used in data sorting, and have available "canned" SORT/MERGE software packages which can be integrated into a total software package accepting sort and displaying instructions, performing the sort, and displaying the results.

The log-in procedure for this processing cycle amounts to the user submitting a request form with the information listed above (i.e., data sets to be included in the sort by test/shot/channel number, parameters to sort on, and display requirements). The request form should be copied and the copy entered in the log book as a permanent record. An internal control number is also assigned to the request form as discussed in Paragraph 2.4.2.1. If the request calls for a special display format, the details of the requirement should be reviewed by a data system programmer to assure that they are clearly understood.

At this point, the request is passed on to a programmer so that required sort and display instruction punch cards can be generated. Once this is done, the instruction cards are submitted to the computer system to perform the sort and display. The displayed results are then quality checked to assure that they meet the request instructions. They are then passed to the user. Copies of the results can be retained as data base records. However, characterization data sorts are usually specialized enough, in terms of the particular data sets involved, that there is a low probability that a request for the same sort conditions would be called for again.

* Examples of computer systems typically equipped to perform SORT/MERGE operations are CDC 3000 or 6000 series machines or IBM 360 or 370 series machines.

2.4.2.4 Data Reduction Processing Cycle

The term "data processing" is used in the Handbook to denote a number of computer implemented techniques for transforming raw test data into forms more suitable to assessment. Assessment activities are carried on by both the test system and data analysts. The test system is primarily interested in the proper operation of the simulator and associated instrumentation so the raw data of interest here are environmental and calibration photographs. The data analyst is primarily interested in assessment of the tested system and uses the response photograph as his raw data. In either case, the data processing or transformation techniques typically include waveform integration, Fourier transforms, or transfer function estimation.

The data input to the data processing cycle is the Polaroid photograph. Since the data processing techniques require the use of a computer, the photograph data must be converted to a computer readable format. This is done by the process of digitization (see Paragraph 2.5.2 for a detailed discussion of photograph digitization). Once digitized, the test data are fed to the computer system as input to the appropriate data processing technique and results are displayed as required.

The processing cycle is shown in Figure 2-13. Action in the cycle is initiated by a request from the user. The first step in the cycle is the logging in of the request by the data system. The request is not normally accompanied by test data since all photographic data reside in the test data bank on microfilm. Therefore, the request form must specify:

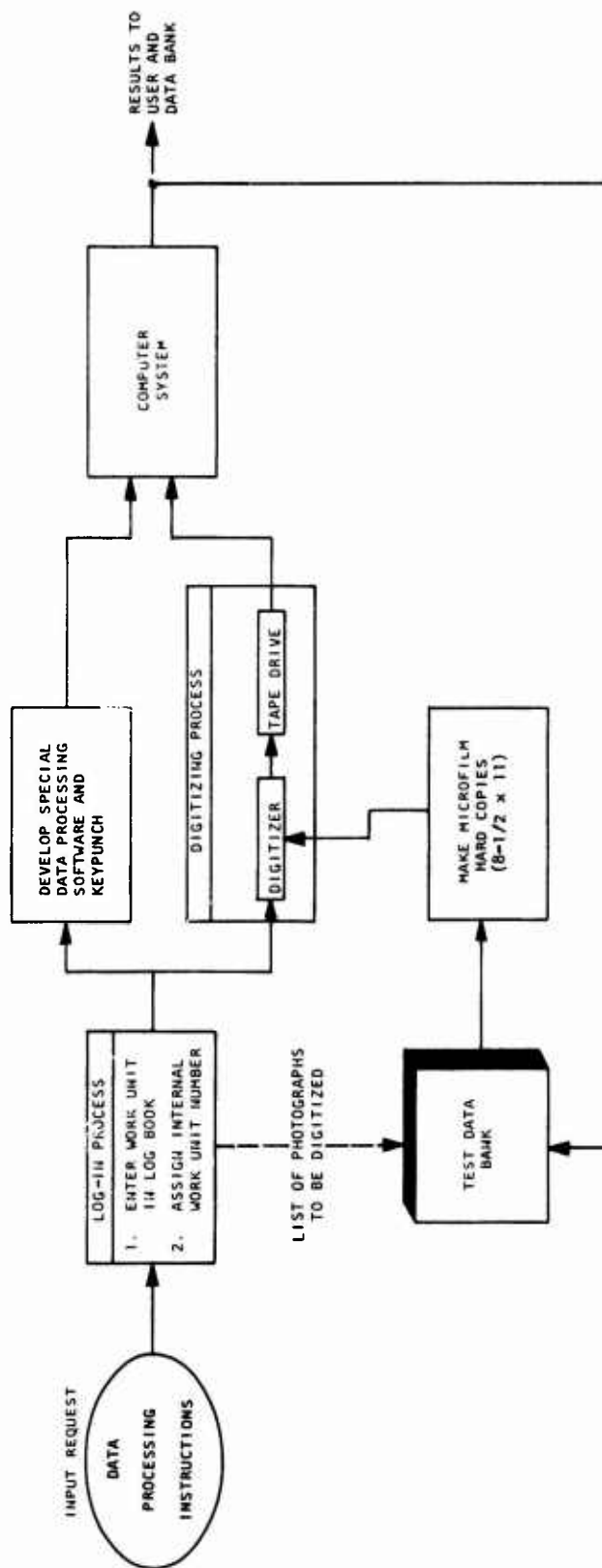


Figure 2-13. Data Cycle as used for Data Processing

- (1) What photographs are to be processed.
- (2) What data processing action is to be taken.
- (3) Any special computer software which must be generated to perform the data processing.
- (4) Any special instructions (e.g., the way in which digitization is to be carried out).

The log in procedure consists of copying the request form, assigning an internal control number to the request, entering the copy in the log book, and passing the request on to the next processing step (digitization). If the request calls for special software development, the request should be reviewed by a data system programmer at the time of log in so that a clear agreement of what is to be done is reached by the data system and submitter (user).

Usually a number of standard or "canned" data reduction techniques are available to the data system. Therefore, a request form, such as that shown in Figure 2-3, is convenient. The form does not have space for any special instructions so that all processing operations must be implicitly understood by both the user and the data system. If special instructions are required, the form of Figure 2-2 can be used alone or to supplement the form of Figure 2-3.

Following log in, processing can take two parallel paths, photograph digitization and software generation. Digitization is necessary in every case; software generation is necessary in only those cases where instructions so indicate and, presumably, these cases are limited.

The digitization process begins with location of the photographs of interest on microfilm and the generation of hard copies of the microfilm waveforms to be used in digitizing. As indicated in Paragraph

2.4.2.1, when photographs are recorded on microfilm, an eye legible index is also recorded. Thus, the photographs of interest are first located by identifying the microfilm reel containing the photograph (this is conveniently done via the microfilm log book), then scanning the reel with a microfilm scanner to visually locate the photographs. The scanner should be equipped with a hard copy printer, so that as a photograph is located, a hard copy is made. Note that there is a definite advantage to using the microfilm hard copies in digitizing as opposed to the photograph itself. The hard copy is typically 8-1/2 x 11 inches in size, whereas the Polaroid photograph has approximate dimensions of 3 x 4 inches. Thus, the waveform is enlarged more than two times which allows better resolution in digitizing.

As indicated above, the results of digitizing are a sample data representation of the photograph waveform in a computer readable medium. The medium will normally be either punched cards or digital magnetic tape.

Any software development which is done in parallel with the digitization process needs little explanation except to say that the programmer responsible for generating special data processing computer routines must have a thorough understanding of the subject of time series analysis. In particular, he must have an appreciation of transient waveform analysis, the effects of sampling on such waveforms, how to use various numerical algorithms available for exercising the sampled data, and the effects of noise contamination on computed results. This type of understanding suggests the data system programmer should have an engineering, physics, or applied mathematics background with a good understanding of EMP test data assessment techniques.

Following digitization and software generation (if necessary), the data are submitted to the computer system for processing. Which data processing code is used determines the type of computer required to perform the codes. Typical codes include:

- (1) Preprocessing program to scale digitized data and perhaps time via multiple waveforms.
- (2) Linear Fourier transform algorithm.
- (3) Fast Fourier transform algorithm.
- (4) Transfer function estimation algorithm.
- (5) Window integration routine.
- (6) Data display routines for plotting results.

Most of the codes listed above can be done on a computer equipped with 30K or more words of core memory. For convenience, the computer should be equipped with one or more magnetic tape drives, a card reader, a line printer, and a plotter.

Since most scientific software is written in FORTRAN, the computer system should be able to compile FORTRAN source code. The execution time for processing software depends on two factors: the computer and the efficiency of the FORTRAN compiler. Large machines like a CDC 6600 are specifically designed for "number crunching" computations which is characteristic of many data processing codes. This is basically due to the per instruction execution time and the basic computer word length (60 bits for the CDC 6600). Large scientific computers also generate very efficient machine codes from their FORTRAN compilers.

As the size of the computer is reduced (in terms of basic computer word length in bits), the execution time for a given code generally increases, often by an order of magnitude or more.

The final step in computer data processing is the display of results. Results are typically displayed as plots or as computer printouts. When plots are made, it is important to assure that

the plot axis labeling and scale are correct for the variables plotted. To do so, one must understand the units of the data input to the processing code and how units are changed by the processing codes.

2.5 PROCESSING HARDWARE SUBSYSTEM

The four test data processing cycles commonly found in EMP data systems were discussed in Paragraph 2.4. Three major hardware subsystems were outlined in those discussions: the microfilm subsystem, the digitizer subsystem, and the computer subsystem. These three subsystems are covered in more detail here to better understand their required design and operation. Because digitizers are probably the least understood of the three categories of hardware (that is, as they are used in processing EMP test data), the greatest emphasis is put on these systems.

2.5.1 The Microfilm Subsystem

2.5.1.1 Equipment Requirements

Under the assumption that both the microfilm copies and hard copy prints of microfilmed test data are required from the data system, there are four basic pieces of microfilming equipment required:

- Microfilm Camera
- Film Developer System
- Film Copier
- Scanner/Hard Copy Printer

As indicated in earlier subsections, the average daily microfilming load may be as high as 300 Polaroid photographs, with occasional peaks of 600 or more. Thus, the microfilm camera must be convenient and reliable to use with features such as easy focusing and an automatic exposure meter to assure proper light level.

Film developing can be done by hand in a dark room or in an automatic system. Normally, the automatic developer systems are completely self contained, having one-pass systems which can operate in complete daylight and which require minimum handling of chemicals. An automatic system with such features is a definite requirement, especially when large quantities of microfilm must be processed.

Also, a film copier system is needed to make microfilm copies for distribution to parties who need a permanent record of test data collected. The only requirement on such a system is that it produce copies with least degradation in information content.

The basic requirement on the hard copy system is that it produce high quality reproduction of the microfilm information. The information is, of course, test waveforms and the hard copies are required as the waveform images for the digitizing process. Therefore, the quality of the digitized data is proportional to the quality of the microfilm hard copy. There are two basic types of hard copy processes: dry and wet. Both process types were thoroughly evaluated when the ARES Data System was being developed and it was found that all dry processes produce prints of unacceptable quality. Therefore, a wet process system is a definite requirement.

2.5.1.2 Example Microfilm Equipment

A brief description of the microfilm equipment used at ARES is given as examples of some equipment that meets data system requirements.

2.5.1.2.1 Recordak Micro-File Machine¹²

The Recordak Micro-File machine is designed for making permanent microfilm (16 mm) of documents up to 26-1/4 inches by

36-3/4 inches. The microfilm records are normally made on 100-foot rolls of 16 mm film (see Figure 2-14).

All controls are integrated in the machine and the lens system provides automatic focusing at all reductions. Each selected reduction ratio is indicated to the operator. The film unit is raised or lowered by a wheel on the front of the machine.

The photoelectric exposure meter determines the required light intensity and, being in a fixed position, the meter does not have to be swung over the document to determine proper exposure. A split-field range finder allows the operator to easily adjust the copy level for depth of field focus.

The model MRD-2 has a photo reduction range of from 5:1 to 21:1.

2.5.1.2.2 ITEK 335 Transflow Processor¹³

The Transflow Microfilm Processor provides an automatic film processor and features straight-through processing, daylight loading, premixed chemicals, and simultaneous processing of multiple film rolls and widths.

The straight-through film channel passes through three stages; processing, washing, and drying. Any point in the film transport may be reached in a matter of seconds by raising the three top hoods and lifting out the tank covers (see Figure 2-15).

The processor is designed for complete daylight operation. Film is processed under ordinary room light. No prethreading is required. Film is started by attaching it to a 36-inch opaque leader which is then fed into the feed rollers of the processor.

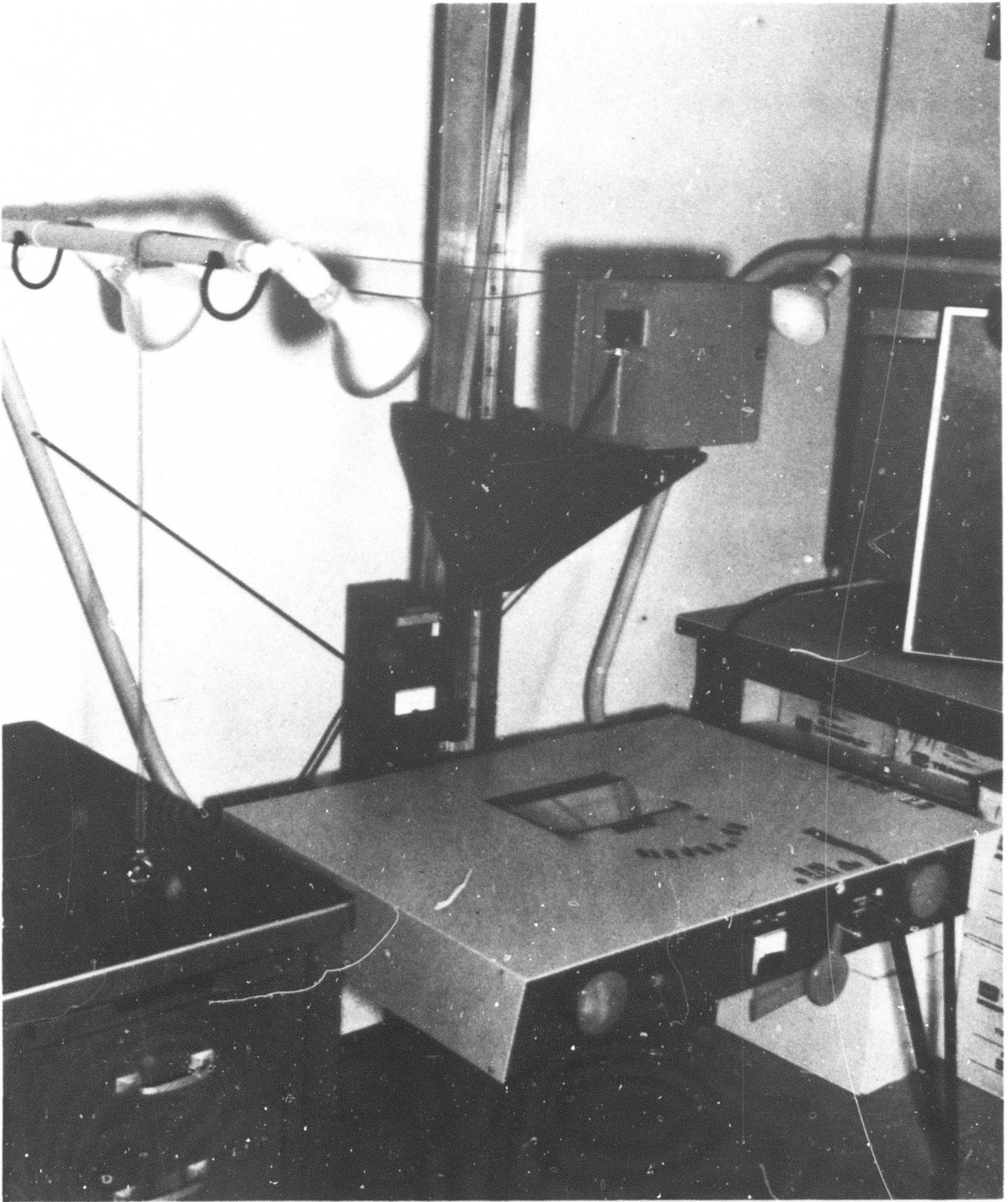


Figure 2-14. Recordak Micro-File Machine

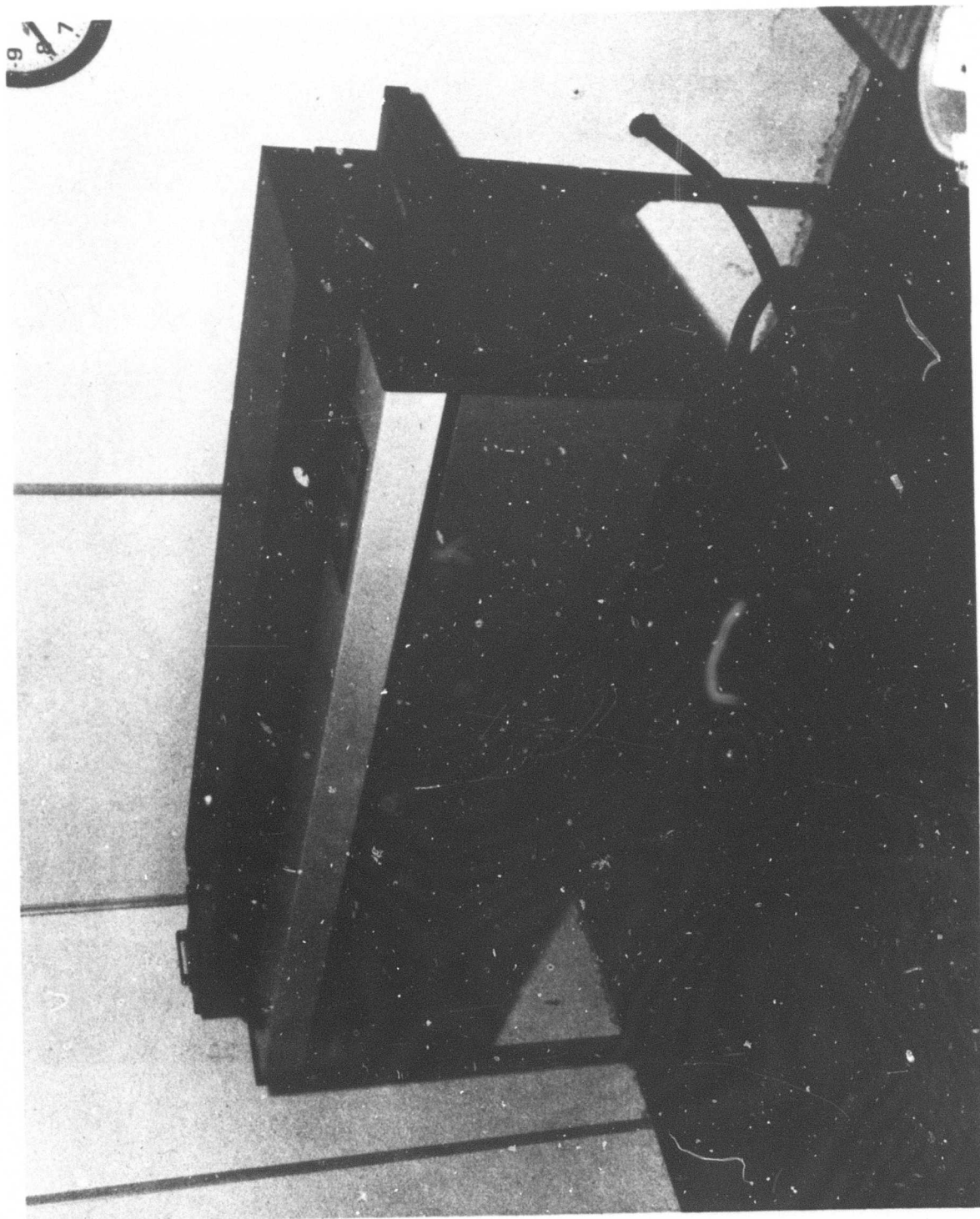


Figure 2-15. ITEK 335 Transflo Processor

Eleven pairs of rollers pass the film through the processor in a straight line to the delivery rollers and the take-up section. Here the leader is removed and the film wound on the take-up spool.

The basic units include a film input magazine; developer, fixer and wash applicators; dryers, and take-up spools. Each section of the processor has two sets of rollers that feed the film through in a straight line. In support of the main film track are the supply tanks, drains, thermometers, and control units.

2.5.1.2.3 ITEK 303 Contact Printer¹⁴

The ITEK 303 contact printer will make contact copies of microfilm, including 16 mm, 35 mm, and 70 mm film. At ARES, 16 mm film is standard. Figure 2-16 shows the four spindles for holding the negative film to be printed, take-up reel after printing, the positive roll of film to be printed, and its take-up spindle.

2.5.1.2.4 Bell & Howell Micro-Data Printer¹⁵

The Bell & Howell Micro-Data Printer is used to make positive prints of microfilmed data. This machine has controls for varying the print size, as well as the contrast of the prints. Other controls provide for variable speed control of the film, image rotation to allow any desired rotation of image axes, focus control, and a scan control to provide movement of the image on the screen in either a horizontal or vertical direction. Figure 2-17 shows a photograph of controls and film mounting.

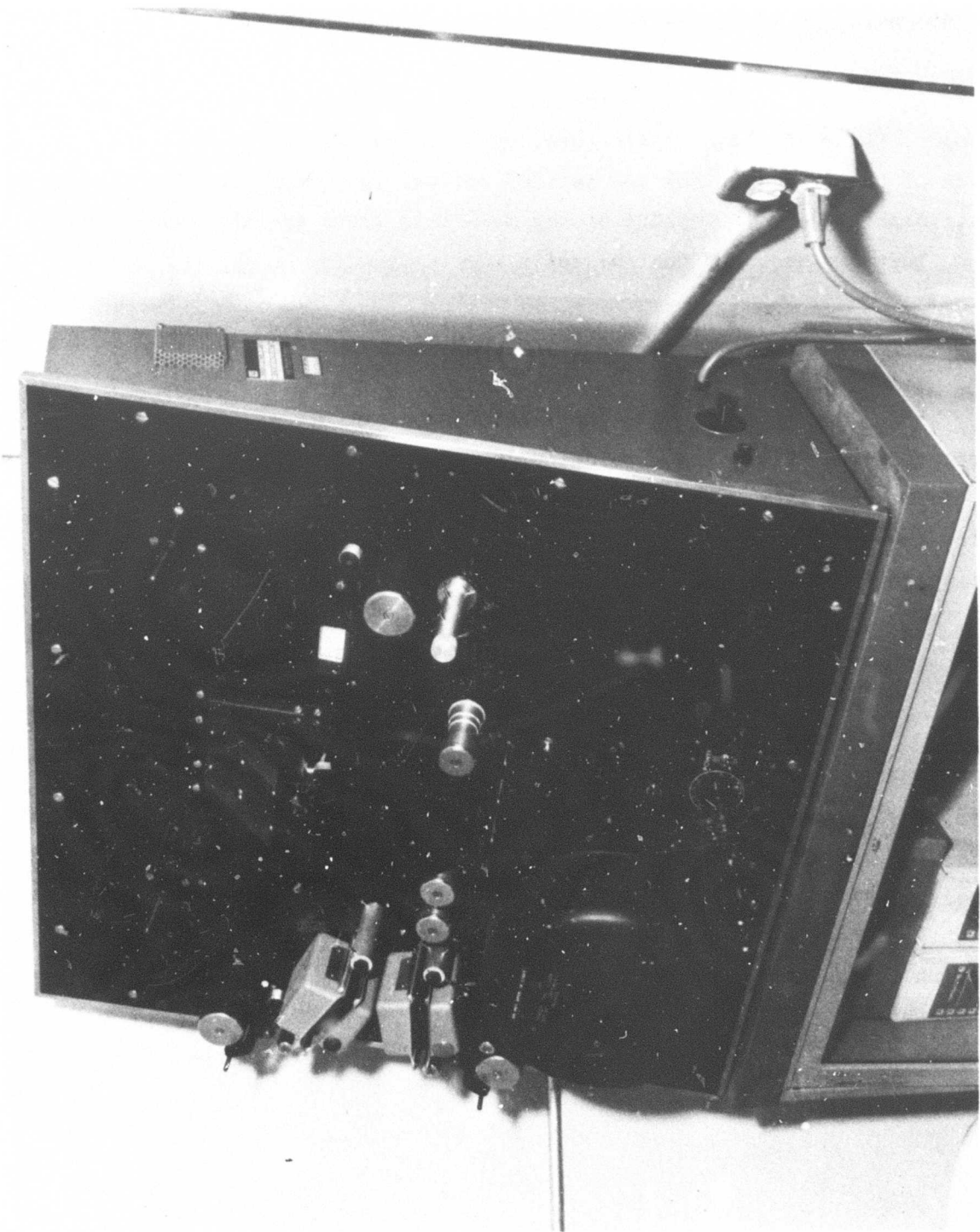


Figure 2-16. ITEK 303 Contact Printer

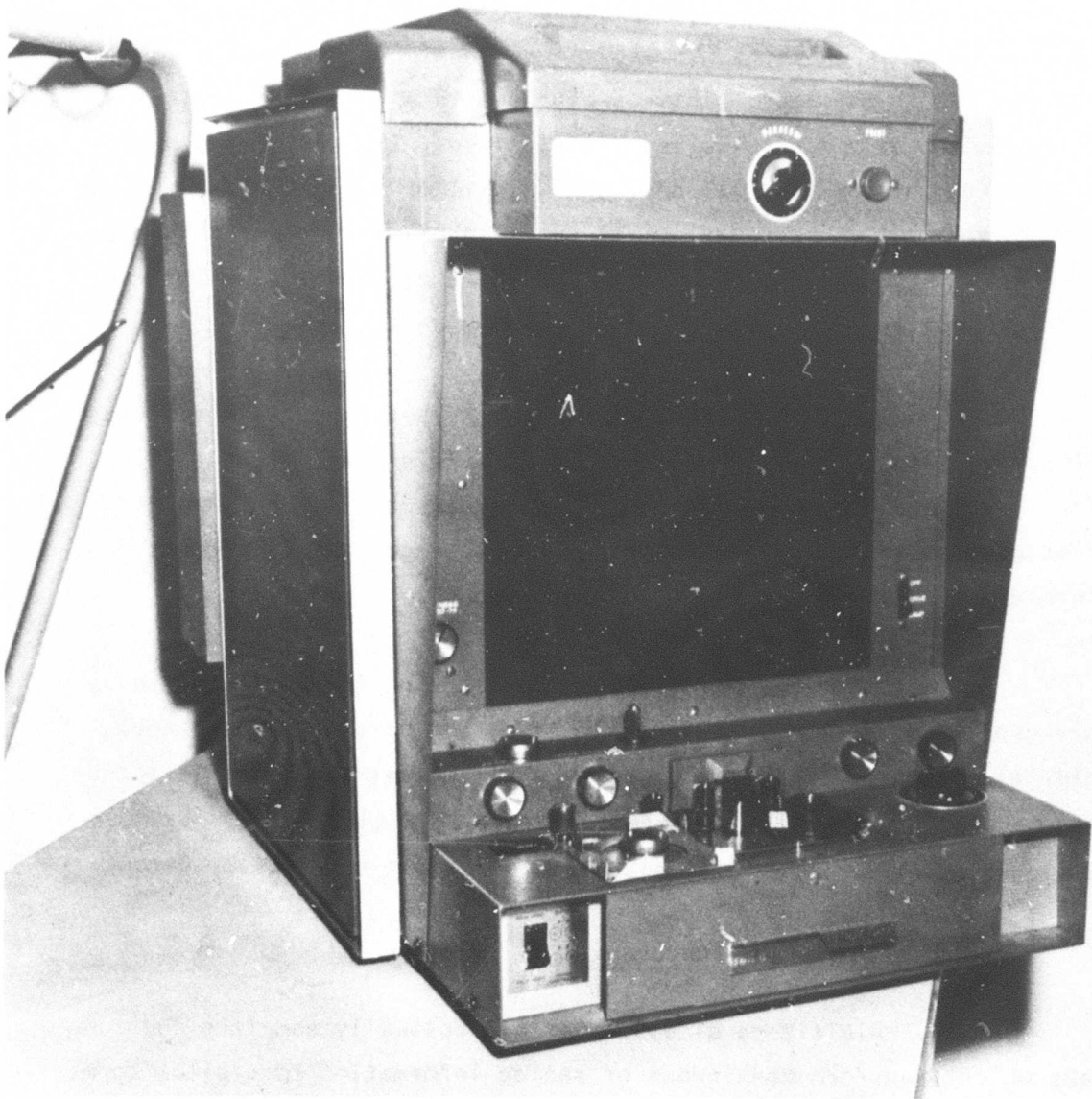


Figure 2-17. Bell and Howell Micro-Data Printer

2.5.2 Digitizing Subsystem

2.5.2.1 Introduction

Digital computer processing of EMP test data requires that the test data be conveyed from continuous analog test signals to a form usable by a digital computer. This usable form is a series of digital words and the conversion process is called digitization. The conversion process can take place in real-time in which case the "digitizer" operates directly on test sensor voltages or currents; or it can take place in other than real-time which requires that the test signals be recorded on an intermediate medium such as a storage oscilloscope or a photograph.

Because of signal bandwidth requirements, and because real-time analog to digital converters with a sufficiently high sampling rate have yet to be perfected (i.e., sampling rates of 2×10^8 samples/second or greater are normally required), the storage of test signals on an intermediate medium is the most common approach.

Since the intermediate recording medium technique is commonly used (that medium most commonly being the Polaroid photograph), the material presented in this subsection will concentrate on digitizers for the conversion of graphical photograph data to digital data. Examples of digitizers of other types will also be covered but to a lesser extent.

2.5.2.2 Digitizer Fundamental^{9,10}

Digitizers of all types are basically samplers and encoders which transform continuous or analog information to digital form. The analog information of interest for this discussion is a graphical representation of an EMP time waveform. The graphical medium can be a Polaroid photograph, microfilm copy of the Polaroid, or enlargement made from either.

In the transformation or conversion process, it is necessary to sample and transform selected locations, (x_i, y_i) , on the spatial waveform into pairs of digital words (Z_{x_i}, Z_{y_i}) . Since the measurement of x-y coordinate locations must be made with respect to some reference location or distance (x_R, y_R) , one can define:

$$Z_{x_i} = \frac{x_i}{x_R} \quad (\text{Eq. 2-1})$$

$$Z_{y_i} = \frac{y_i}{y_R}$$

In these two equations, Z_{x_i} and Z_{y_i} are taken to be the closest digital approximation to x_i/x_R and y_i/y_R respectively.

If x_R and y_R are assumed to be "full scale" distances, then both Z_x and Z_y can be implicitly represented as fractional binary numbers of the form

$$Z = a_1 2^{-1} + a_2 2^{-2} + \dots + a_n 2^{-n} \quad (\text{Eq. 2-2})$$

in which the a_i are 0 or 1. It should be clear that Z is always less than unity since $x_i \leq x_R$ and $y_i \leq y_R$.

The $a_1 2^{-1}$ term represent the bits in the digital word. The $a_1 2^{-1}$ term is called the most significant bit (MSB) and has a value of $1/2$ (2^{-1}). The $a_n 2^{-n}$ term is called the least significant bit (LSB) and has a value of $1/2^n$. The value of the binary word is obtained by adding up the value of all terms which have a non-zero coefficient ($a_i = 1$). The value of the digital word when all coefficients equal 1 is $1 - 2^{-n}$ or normalized full scale less one LSB.

This particular binary representation or code is called "natural binary." There are many other codes used in digitizers, all of which are variations of natural binary and are usually chosen for convenience in application or in interfacing with other systems. Examples include binary coded decimal (BCD), bipolar, offset binary, one's complement, and two's complement.

2.5.2.3 System Operational Requirements

There are a number of factors which are fundamentally important to digitizer performance and selection such as resolution, accuracy, basic operational mode (manual or automatic), and control. Before discussing these, it will be valuable to develop a simple model of graphic digitizers to use in subsequent discussions.

All graphic digitizers can be looked upon as having four basic elements (see Figure 2-18):

- (1) Reference Plane
- (2) Pointer or Cursor
- (3) Analog-to-Digital Converter
- (4) Control Unit

The reference plane acts as the working surface on which the graphical or spatial waveform to be digitized is placed. The pointer is used to locate the point on the waveform to be digitized. The reference plane/pointer normally acts in an emitter/sensor relationship so that the position of the pointer on the reference plane can be sensed. There are many electronic and electromechanical schemes used to form this relationship but all produce essentially equivalent results.

REFERENCE PLANE
AND
POINTER

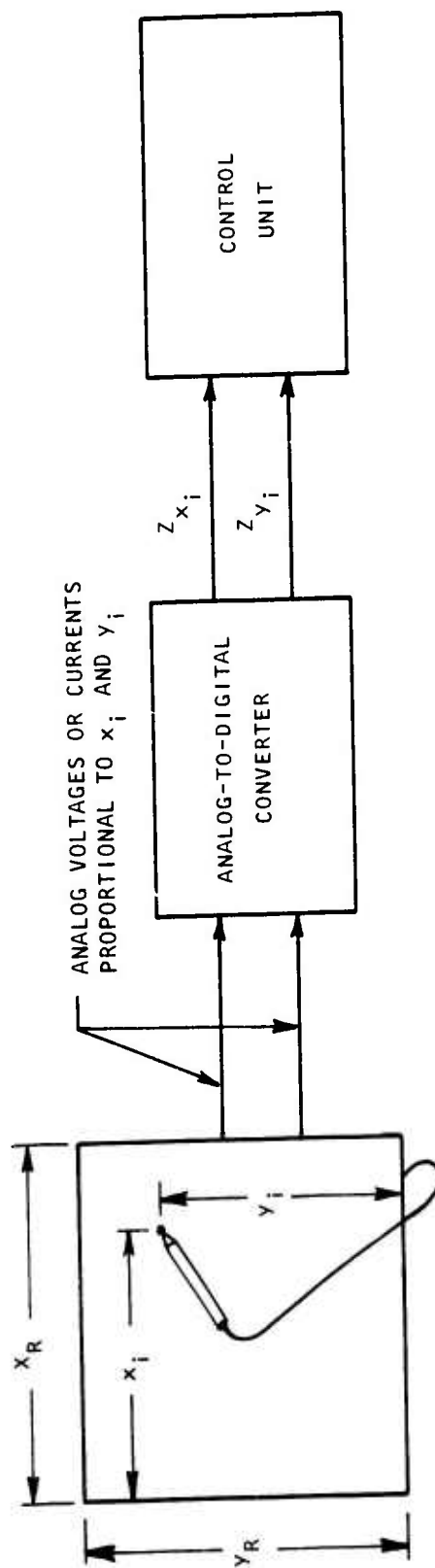


Figure 2-18. Basic Graphical Digitizer Elements and Their Interconnection

For most digitizers, the emitter/sensor system produces analog voltages or currents proportional to the position of the pointer on the reference plane. The voltages or currents are then fed to an analog-to-digital converter to produce Z_x and Z_y , the digital outputs.

The control unit basically serves the purpose of buffering, formatting, and storing the digital outputs from the analog-to-digital converter. It can serve a number of additional functions important to digitizing EMP waveforms (see the discussion in the paragraph on control).

2.5.2.3.1 Resolution

The first operational factor of fundamental importance is digitizer resolution. For graphical digitizers, the resolution is determined by the usable dimensions of the reference plane (x_R and y_R) and the number of bits in the digital words, Z_x and Z_y . (Note that the number of bits (n) is assumed in these discussions to be the same for both words although this is not always the case.) A digital word with n bits has 2^n unique states (e.g., for $n = 3$, there are 2^3 or 8 unique states). Then, the number of uniquely definable locations, N , in either orthogonal dimension (x or y) of the reference plane is given by:

$$N_x = \frac{x_R}{2^n} \quad (\text{Eq. 2-3})$$

and

$$N_y = \frac{y_R}{2^n} \quad (\text{Eq. 2-4})$$

Assuming the digitizer to be linear, these uniquely definable locations are equally spaced across the surface of the reference plane.

As seen in Figure 2-18, resolution governs the quantization error in Z_x and Z_y . The dots represent the uniquely definable locations on the reference plane. As the pointer is moved along the continuous waveform, the analog-to-digital conversion logic selects that location which the pointer is closest to, with transitions theoretically made halfway between any two adjacent points. The result of digitizing the waveform in Figure 2-19 with the resolution indicated is illustrated in Figure 2-20.

In actual fact, the resolution for most commercially available graphical digitizers is sufficient so that the quantization error is more than acceptable for digitizing photographic data. Available resolution is typically between 0.01 and 0.001 inches. Considering the dimensions of a Polaroid waveform, one can visualize that the resulting digitized waveform will be very close to the pattern traced during digitizing. Note that this does not imply the digitized waveform is necessarily equivalent to the actual waveform, but only to the pattern traced. The equivalence of these two waveforms (actual and digitized) is a function of operator ability and photograph quality in the case of a manual system, or of photograph quality and system complexity in the case of an automatic scanning system.

2.5.2.3.2 Accuracy^{9,10}

Accuracy (conversely error) is the measure of closeness between the actual and theoretical digitizer outputs. Referring to the simple discrete grid model of Figure 2-19, when the pointer or cursor is closest to grid point (x_k, y_k) , then the digitizer outputs should be Z_{x_k} and Z_{y_k} . This may not be the case for reasons of poor design or digitizer operation outside the specified environmental limits (e.g., temperature, humidity, and dust). The types of error which may occur include:

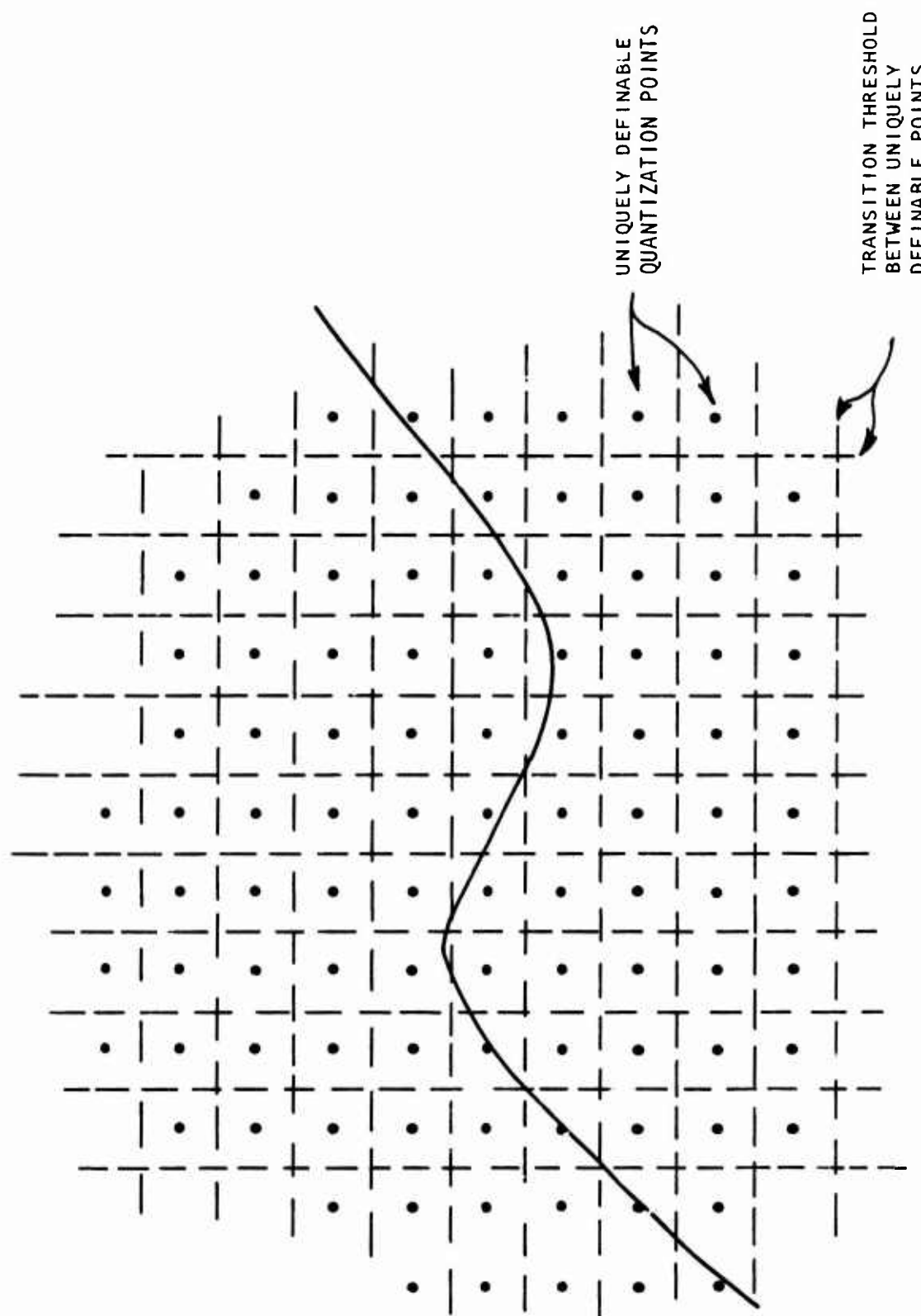


Figure 2-19. Quantization Grid for Graphical Digitizer

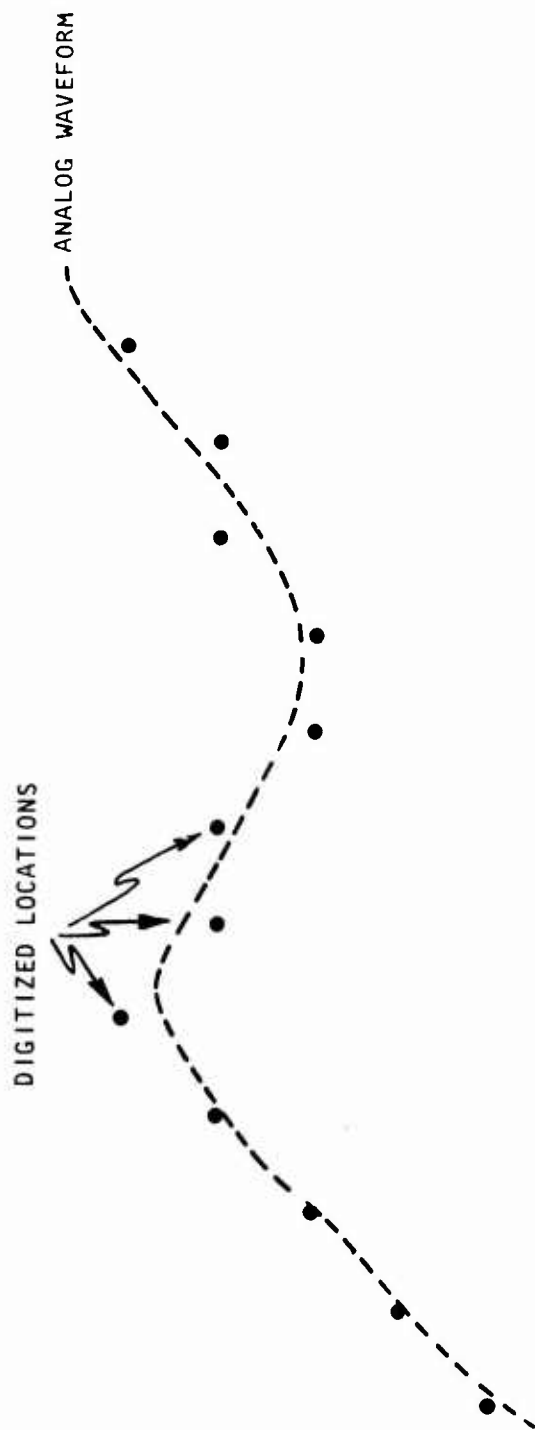


Figure 2-20. Result of Digitizing the Waveform of Figure 2-19

- Quantization Error
- Offset or Bias Error
- Scale Factor Error
- Linearity Error

To discuss the effects of these errors, the simple analog-to-digital conversion model of Figure 2-21 will be used. The model, as shown, is a graphical representation of the ideal conversion process. The abscissa represents the analog input normalized to full scale. The ordinate represents the resulting digitized output. Note that a digital word of length 3 is assumed giving eight unique quantization levels. Note also that the transition in the ideal case is assumed to take place midway between quantization levels. The numerical value of the digital word as well as its bit values are given along the ordinate.

Figure 2-21 clearly illustrates the effects of quantization error alluded to in the discussion on resolution. Any analog input value between $9/16$ and $11/16$ of full scale will be converted to a digital value of $5/8$ (code of 101).

Figure 2-22 illustrates the second type of error, offset or bias. The error is strictly analog in nature and occurs either in the process of sensing the location of the pointer on the reference plane or in the analog-to-digital converter. The offset shown would cause all digital outputs to be low in value by $3/16$ of FS. The offset could, of course, be such that all readings would be high by some value.

The third error type, scale factor or gain error, is illustrated in Figure 2-23. Here the analog-to-digital conversion process is linear but transitions no longer take place at the ideal transition thresholds. For example, the lower conversion threshold for full

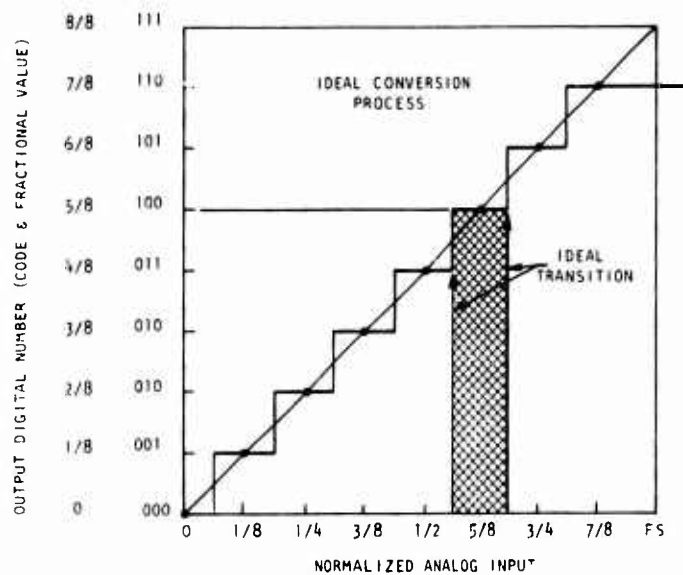


Figure 2-21. Model of Ideal Analog-to-Digital Conversion Process ($n = 3$)

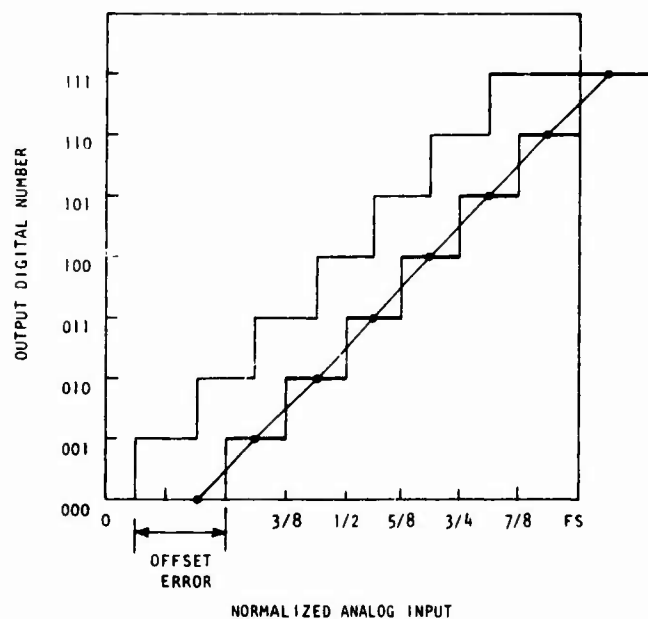


Figure 2-22. Effect of Offset Error on the Analog-to-Digital Conversion Process

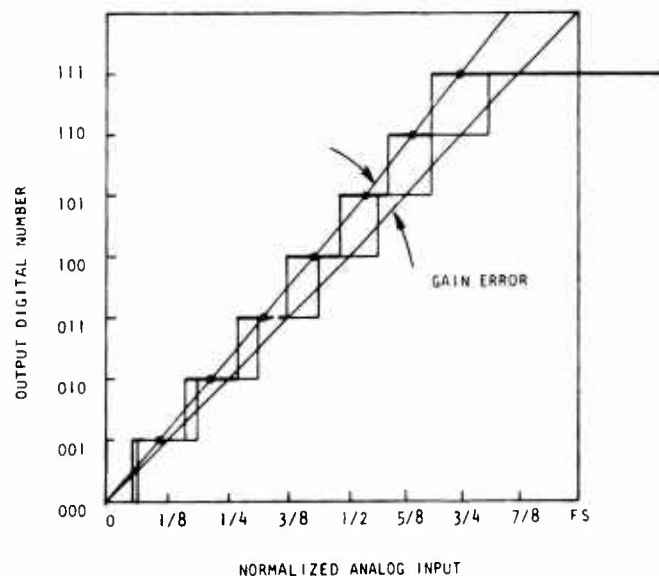


Figure 2-23. Effect of Gain Error on the Analog-to-Digital Conversion Process

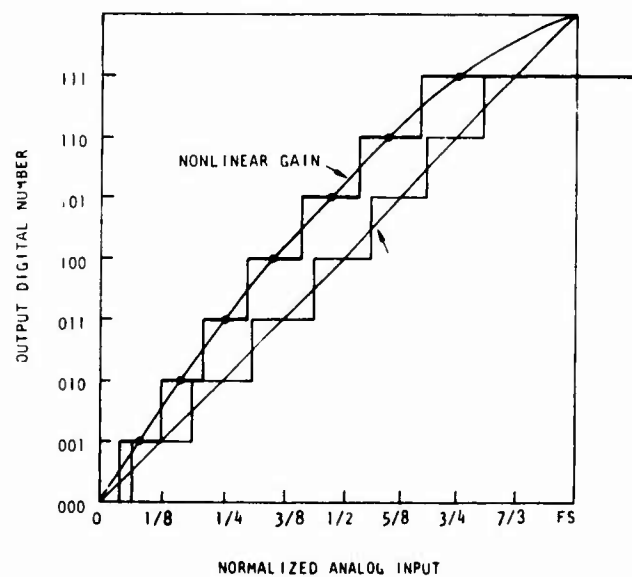


Figure 2-24. Effect of Linearity Error on the Analog-to-Digital Conversion Process

scale digital ($Z = 111$) is located at $3/4$ FS rather than $7/8$ FS as it should be. This is also an analog type error which takes place prior to the conversion process.

The final error type discussed is linearity error, shown in Figure 2-24. An arbitrary nonlinear gain curve has been drawn to illustrate its effects. The gain relationship can, in fact, be any relationship that distorts the conversion in a nonlinear way.

As in the case of resolution, most commercially available digitizers should have the above discussed error problems worked out so that the digitizer operates with an acceptable overall accuracy. An acceptable accuracy is one on the order of the stated resolution. For example, if the resolution is given as 0.001 inch, then an acceptable accuracy would be ± 0.005 inch or less. This means that a distance measured from any point in the reference plane to any other point in the reference plane can be in error by as much as ± 0.005 inch. However, the stated accuracy is usually an "expected maximum error" in the statistical sense, which means that ± 0.005 inch is a maximum error where the expected error is zero.

2.5.2.3.3 Basic Operational Mode

Graphical digitizers currently in use for EMP test data reduction can be divided into three categories:

- Manual
- Semiautomatic
- Automatic

Manual systems, as the name implies, are manually operated, requiring an operator to move the pointer from waveform location to location during

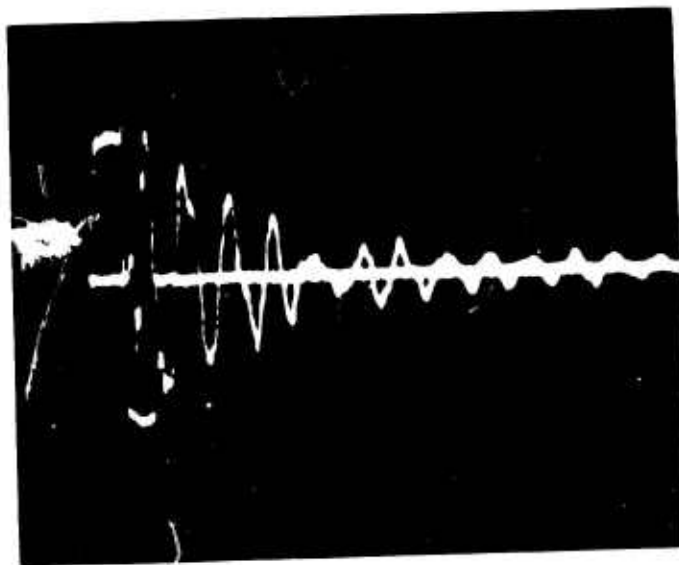
digitizing. The chief advantage of the manual systems lies in the operator's ability to overcome certain photograph quality problems with which a semiautomatic or automatic digitizer may have problems. These photographic quality problems are partly due to the inherent complexity of EMP test data, and partly due to human error or instrumentation problems during the recording process. Examples of such photograph problems are illustrated in Figures 2-25a through 2-25f. These six test photographs were generated at ARES and are considered typical of the types of test data digitized by data system.

The first example (Figure 2-25a) illustrates a near ideal waveform for digitizing. The photograph has good contrast and the waveform has good frequency resolution (i.e., the waveform is sufficiently spread out so that all portions are clearly defined).

The second example (Figure 2-25b) illustrates a test waveform in which at least two resonant frequencies appear, one much higher in frequency relative to the other. Thus the high frequency information as recorded has very poor resolution and is almost impossible to digitize accurately.

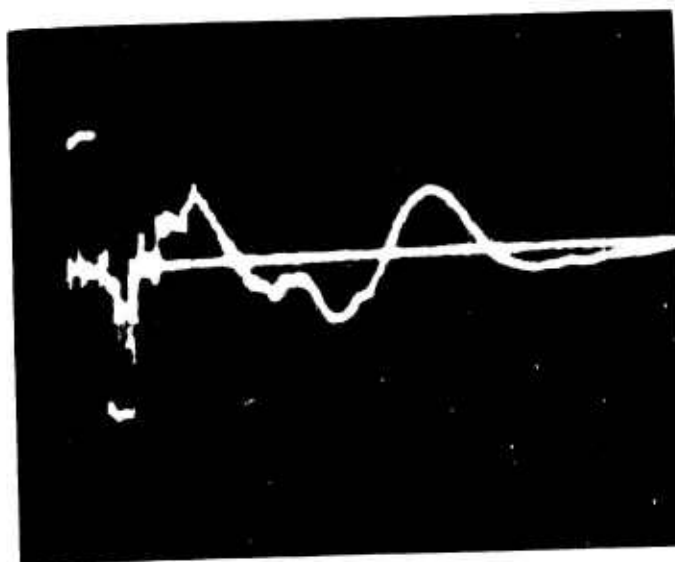
The third example (Figure 2-25c) is very similar to the second, except that the high frequency information persists for the total duration of the recorded waveform. Again the frequency definition is very poor which would make digitizing very difficult. The photograph also has poorer contrast than the first two examples.

The fourth example (Figure 2-25d) illustrates the problem of portions of the waveform completely disappearing due to oscilloscope writing speed (waveform slope and amplitude). As in the third example, high frequency information persists for most of the waveform duration.



4861111B

(a)



4850305B

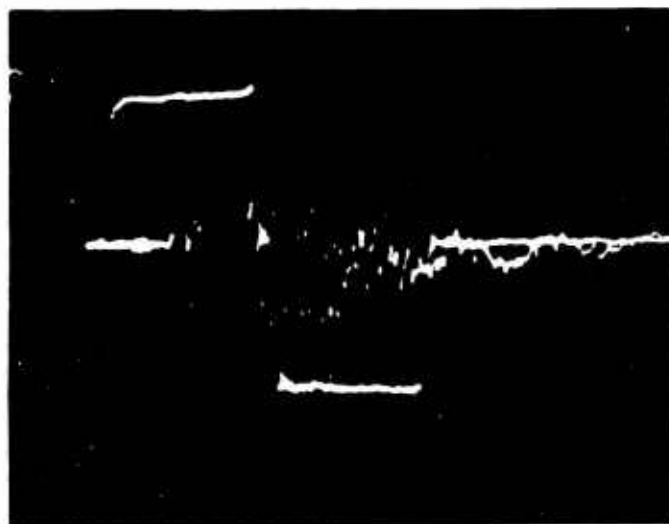
(b)

Figure 2-25. Photographic Problems



4510305B

(c)



4870611A

(d)

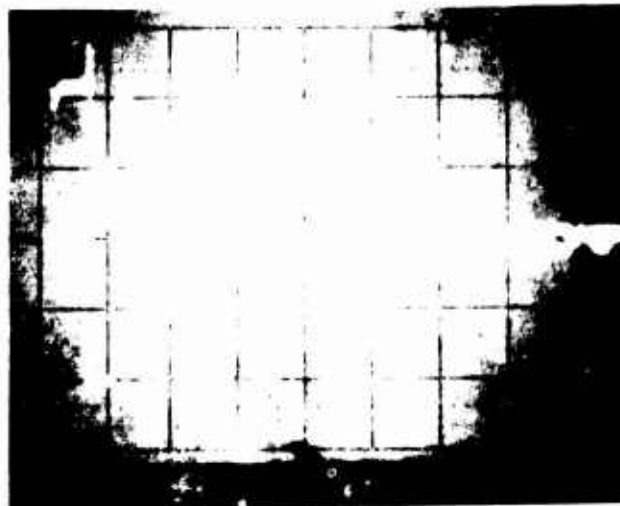
Figure 2-25. Photographic Problems (Continued)

The fifth example (Figure 2-25e) illustrates poor photograph contrast most likely due to improper setting of the graticule lighting on the oscilloscope.

The final example (Figure 2-25f) illustrates the problem of baseline drift in which the waveform appears to be biased from its true baseline. This is most likely due to oscilloscope malfunction. There is virtually no way to correct for this type of error because of the inherent distortion to the waveform.

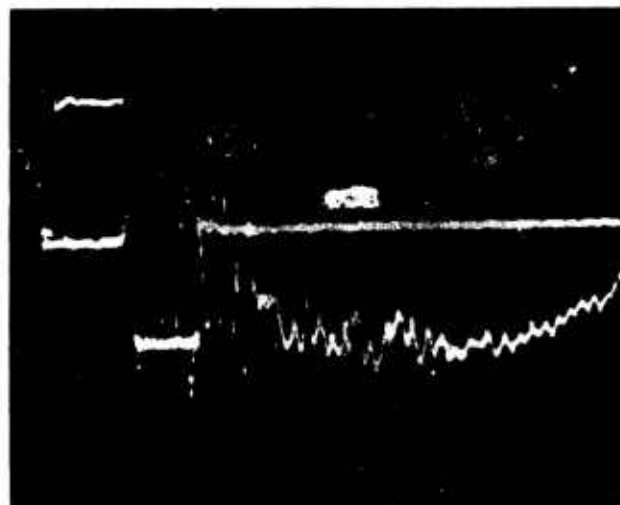
As implied at the outset of this discussion, a properly trained operator can overcome many of these poor quality problems. This is certainly true in many cases where the waveforms are complex with poor frequency resolution. It is also true where contrast is poor within certain limits. In these cases the operator can guess at and "fill in" missing or hard to distinguish waveform data. This procedure, of course, runs the risk of adding waveform features during digitizing which do not exist. Finally the major disadvantage of manual systems is: (1) they are slow (one to three minutes to digitize a single waveform), and (2) the operator can become disinterested and do a poor job over long periods of time.

Semiautomatic digitizers normally operate on a light scanning principle in which the grey level (density) of a photograph (in this case its negative) is sensed and, based on sensed level, the waveform is located and conversions are made. In this case the light beam acts as the pointer and precision position fixing of the light beam during scanning acts as the reference plane. The scanning process is automatic and very fast, normally allowing a complete waveform to be digitized in well under one second. These systems are configured so that the operator can interact in the scanning process and manually digitize "difficult" portions of the waveform. These waveform portions are



4500203B

(e)



0231500

(f)

Figure 2-25. Photographic Problems (Concluded)

difficult in the sense that there is insufficient photograph contrast or frequency resolution for the automatic scanning system to accurately locate the waveform.

Automatic digitizer systems are essentially equivalent to semiautomatic except that there are limited or no means for operator interaction. Thus waveform problems as discussed above cannot be easily overcome.

2.5.3 Digitizer Control

There are several control-oriented functions which are mandatory for digitizers used in EMP data reduction, and certain additional functions which are desirable but optional. The discussions here are again directed toward manual digitizer systems rather than semiautomatic or automatic systems mainly because manual systems are predominantly used in EMP data reduction due to the test data quality problem as outlined in the previous subsection.

The control functions which are considered mandatory are:

- (1) Means of initiating single point digitizations.
- (2) Means of indicating that a digitizing sequence is completed.
- (3) Means of storing output digital data which are compatible with the computer system which will use the data.
- (4) Means of labeling digitized data sets.

There are two typically used modes of digitizing EMP waveform data: point-by-point and continuous or evenly spaced in X. Point-by-point

is the more commonly used mode for which the operator selects points to be digitized along the waveform, using waveform characteristics (slope and curvature) as selection criteria. This produces a set of digitized points in which the X-axis values increase ($Z_{x_i} > Z_{x_{(i-1)}}$) but are not evenly spaced (nonconstant ΔX). To operate this mode, the operator must be able to initiate a conversion after selection of each point. Many commercially available digitizers come equipped with a button on the pointer (cursor) or foot pedal for this purpose.

In order that no extraneous data points are taken after the end of the waveform is reached, a means of "turning off" the digitizer and ending the digitized data set is required. Again, this function is normally provided by a push button on the pointer.

The output digitized data must obviously be stored on some medium compatible with the computer system in which it will be used. There are three common mediums for this purpose, digital magnetic tape, punch paper tape, and punch cards. Most commercial graphic digitizers are available with interface options to interface with one or more of these storage media.

Labeling digitized data sets is necessary for identification when the sets are used as input data for data reduction computer programs. Labeling requires that a means of entering the label into the storage system must be provided. A teletype or other keyboard device satisfies this purpose, along with an appropriate interface to the storage system.

Control functions which are desirable but not mandatory (i.e., these functions if necessary can be performed by a digital computer subsequent to the digitizing operation) include:

- (1) Establishment of a waveform origin with all subsequent digitized points referenced to the origin location.
- (2) Reformatting of data.
- (3) Digitizing in a continuous mode with data points selectively retained based on a constant ΔX criteria.
- (4) Quality control.

Establishing an origin is a matter of selecting an origin location, storing the Z_x and Z_y value for this location, and subtracting these values from the Z_x and Z_y value for all subsequent data points. This is a feature provided in some commercial digitizers. If not, it can be accomplished as a preprocessing step by a digital computer.

Reformatting of data is often necessary to put it into the required form for use by the digital computer. This reformatting can often be accomplished by the interface system which interfaces the digitizer to the storage system. If not, it can also be accomplished as a preprocessing step by a digital computer.

Controlling the digitizer to generate constant ΔX data requires a fairly sophisticated level of control. The constant ΔX selection process can be done subsequent to digitizing by a digital computer, but that means a large number of data points must be recorded at the time of digitizing with the appropriate constant ΔX points selected from this large data set. Depending on the resolution of the digitizer and the speed at which the operator traces the waveform, the rate at which data must be stored by the storage system may be beyond its limit. For these reasons, the selection process is best accomplished in real-time by the digitizer control system.

The final optional control function, quality control, basically amounts to the capability for making various reasonableness checks on the digitized data to assure that the resulting data set is not in error. Certain errors can be corrected by subsequent computer processing, but others that cannot be corrected may render the data set useless.

The approach which the ARES data system has taken to control its digitizer system is to interface a commercial digitizer system, with very limited control features, to a mini-computer. The mini-computer, because of its programmability, is able to provide all optional control functions for maximum digitizer flexibility.

2.5.3.1 Example Digitizer Systems

Several examples of digitizer systems presently in use for EMP data reduction or which show promise for future application are described in this subsection. The examples cover both graphical digitizers (manual and automatic) and direct digitizers.

2.5.3.1.1 The Bendix Datagrid^{TM 11}

The Datagrid very closely matches the graphical digitizer model discussed in Paragraph 2.5.2.3 covering System Operational Considerations and is the digitizer presently in use at ARES. As seen in Figure 2-26, the system consists of a digitizing surface (reference plane), cursor (pointer) with control buttons and a rack-mounted unit containing the analog-to-digital conversion electronics and certain control functions. In the case of ARES, the digital outputs from the conversion unit are fed to a mini-computer which completes the necessary control requirements.

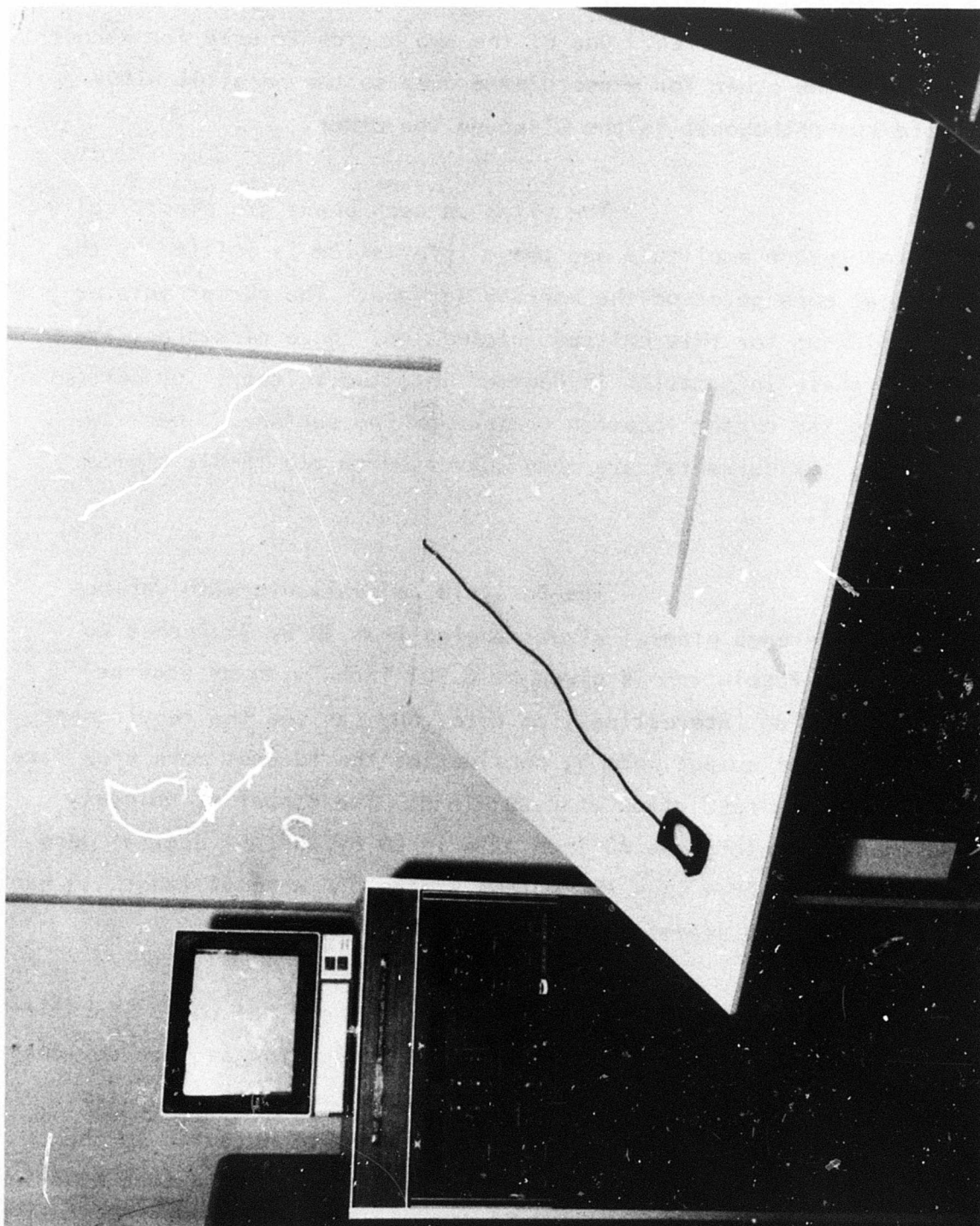


Figure 2-26. Bendix Datagrid Manual Digitizer System

The detailed operating principles for the Datagrid are kept proprietary by Bendix. However, in general, the reference plane contains two large printed circuit boards located just under the working surface. Each printed circuit board is etched to form a series of closely spaced parallel wires. One of the two boards is used for x-coordinate data and the other for y-coordinate data so the parallel wires of one board run orthogonal to the wires on the other.

The wires on each board are electrically driven so that unique amplitude and phase information is emitted by the wire network at each point on the working surface. The cursor acts as a receiver or pick-up for this emitted information. Once picked up, the amplitude and phase information is decoded into two voltages (or currents) proportional to the cursor location on the working surface. These two analog voltages (or currents) are then converted to two 16-bit digital words (Z_x and Z_y).

The Datagrid is available with various working area (reference planes) sizes ranging from 30 by 36 inches to 42 by 60 inches. Resolution is given as 0.001 inch, with an accuracy of 0.005 inch. As an interesting side note, one can see the requirement for a 16-bit digital output word by considering the largest work area size of 60 inches and the resolution of 0.001 inch. The number of uniquely definable locations along the 60-inch axis is 60×10^3 . A digital word of length 16 has 2^{16} or $\sim 64 \times 10^3$ unique states. A word of length 15 has only $\sim 32 \times 10^3$ unique states. Thus 16 bits are required.

There are numerous control options available for the Datagrid which include interfaces to several storage devices (card punch, paper tape punch, and magnetic tape), zero set (establish origin), and continuous curve tracing with constant ΔX output. In the case of ARES, the decision was made to interface the Datagrid to a NOVA

1200 mini-computer, allowing the NOVA 1200 to provide the necessary control functions. The control software written for the NOVA 1200 includes:

- (1) Accept digitizer outputs, format for compatibility with CDC 6600 data reduction codes, and write onto digital magnetic tape in a CDC 6600 readable format.
- (2) Accept identification label via the teletype and append to digitized data set.
- (3) Implement constant ΔX algorithm for continuous waveform tracing.
- (4) Automatically check for time regression (i.e., Z_{X_i} must be greater than $Z_{X_{i-1}}$).

Besides the control functions provided by the NOVA 1200, the Datagrid through cursor push-buttons can establish an origin anywhere on the digitizing surface, initiate a conversion, indicate the completion of a digitizing sequence, and delete an incorrect data point.

2.5.3.1.2 The Universal Telereader¹²

The Telecomputing Corporation Universal Telereader (Type 17A-1) is a manually operated film reader capable of digitizing hard copy material such as Polaroid photographs. Measurement of waveform coordinates is accomplished by positioning a horizontal and a

vertical cross hair to be coincident at the coordinate. To assist the operator and to achieve better resolution, the pattern being digitized is projected onto a frosted glass screen with an enlargement of 2.15X using a 65 mm lens system or 3.45X using a 38 mm lens system. The system has a resolution of 0.0006 inch using the 65 mm lens system and 0.00035 using the 35 mm lens system.

The operator positions the cross hairs with two independent control knobs, one for the horizontal cross hair and one for the vertical cross hair. The angular position of these knobs is sensed and converted to appropriate digital outputs.

A telereader is presently in use at the AFWL Computational Services Division, Photo Reduction Section. This particular system is interfaced to a card punch as the method for storing output data.

2.5.3.1.3 The Telereadex¹³

The Data Instruments Telereadex (Model 29E-17) is a manually operated film reader designed to digitize graphical patterns recorded on microfilm (see Figure 2-27). Images from the microfilm are projected onto a 28 by 28 working surface using a lens/mirror system. Various lens sizes (50 mm, 105 mm, 190 mm, and 360 mm) are available for varying amounts of image enlargement. Digitizing is achieved by positioning a set of cross hairs over the point of interest on the working surface and actuating the digitizer. Positioning is accomplished by two independent control knobs, one for the horizontal cross hair and the other for the vertical cross hair.

The system has a resolution of 0.0028 inch on the working surface. This translates into a resolution of 0.0016 mm for

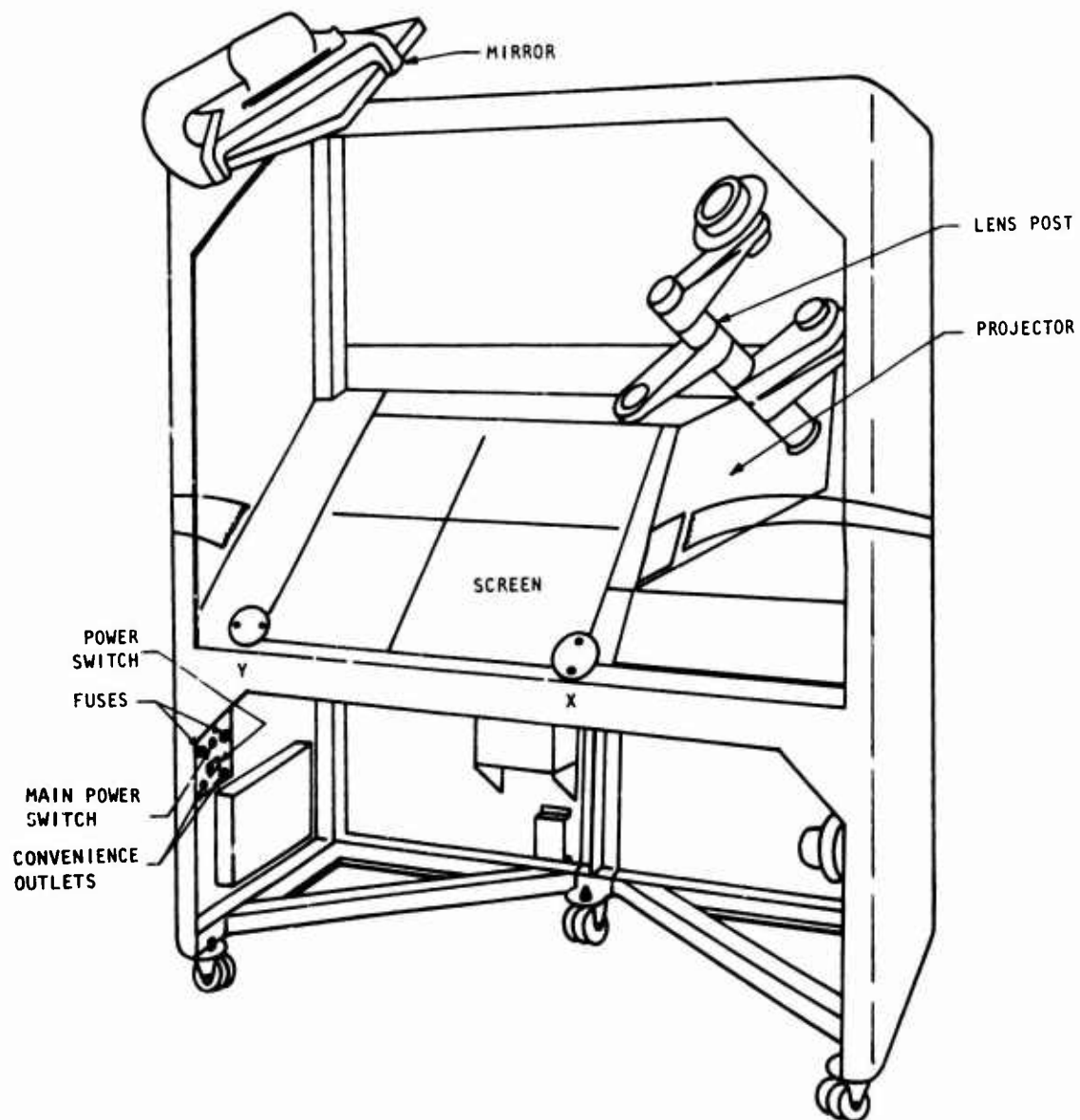


Figure 2-27 Telereadex Type 29E Graphic Digitizer

the 50 mm lens system at the microfilm plane, 0.0037 mm for the 105 mm lens system, etc.

The Telereadex is presently in use at the AFWL Computational Services Division, Photo Reduction Section. This particular system is interfaced to both a digital magnetic tape system and a card punch system as storage devices for output data.

2.5.3.1.4 The Hewlett-Packard 9864 Digitizer¹⁴

The Hewlett-Packard 9864 Digitizer is a manual digitizer system consisting of a digitizer and an HP 9810, 9820, or 9830 calculator. The digitizer is supplied by Bendix to Hewlett-Packard, and therefore, has the same operating principles as the Bendix Datagrid digitizer described in Paragraph 2.5.3.1. The HP 9820 calculator gives a very versatile digitizer system since a number of fairly sophisticated algorithms can be implemented to exercise the digitized data.

The working area of the digitizer is 17 by 17 inches. Its resolution is given as 0.01 inch, with an accuracy ± 0.001 inch in the temperature range of 15°C to 30°C.

The AFWL Vertically Polarized Dipole Data System presently uses an HP 9864 digitizer system for Polaroid photograph transient EMP data reduction. The system consists of the digitizer, calculator, plotter, and cassette tape drive. The system is capable of implementing a linear Fourier transform algorithm as part of its data reduction capability. Since the digitizer comes from Hewlett-Packard as a system, all software required to make maximum use of the system as a graphical digitizer is included as part of the package. Note also that additional peripheral devices can be interfaced to the HP 9864 such as a teletype or paper tape punch, so that data can be transferred to another computer system.

2.5.3.1.5 The Automatic Image Digitizer¹⁵

The Automatic Image Digitizer is a highly sophisticated semiautomatic graphical digitizer system operated by the AFWL Computational Services Division, Photo Reduction Section (see Figure 2-28). The hard copy medium for the system is microfilm. As seen in Figure 2-28, the system uses a complex light scanning scheme to measure microfilm grey level or density.

The system basically consists of a programmable light source for scanning the film, a density measuring system, a film transport system, and signal processor and logic unit. The signal processor/logic unit consists of a PDP-7 digital computer, a graphic CRT display, teletype, and digital magnetic tape drives.

The system is interactive in that the operator can manually digitize selected portions of the waveform via the CRT display terminal. The operator can also edit portions of a digitized data act via the CRT display terminal. In the automatic scan mode, the system can digitize a complete waveform in approximately 30 seconds. Depending on the amount of manual operator interaction, a typical good quality EMP transient waveform takes from one to four minutes to digitize.

2.5.3.1.6 The Sandia Image Digitizer¹⁶

The Sandia Image Digitizer (SID) is a semi-automatic graphic digitizer developed by Sandia Corporation for the purpose of digitizing black and white graphic pictures (see Figure 2-29). The system is built around a television camera which scans the black and white image and converts the camera output to digital information proportional to the black/white scale of the scanned image (i.e., the system discriminates only two grey levels, either black or white).

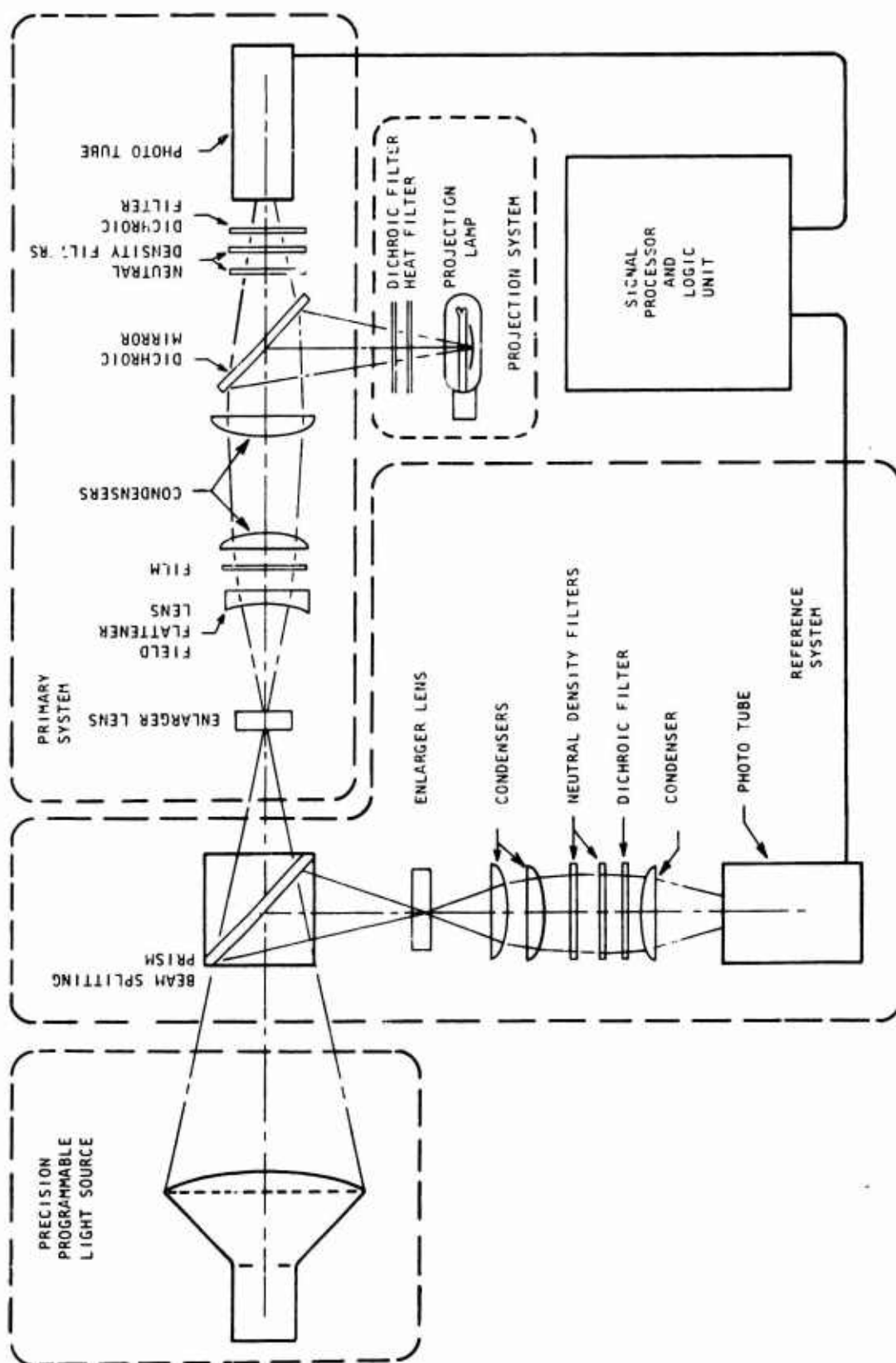


Figure 2-28. Programmable Film Reader Mod-3

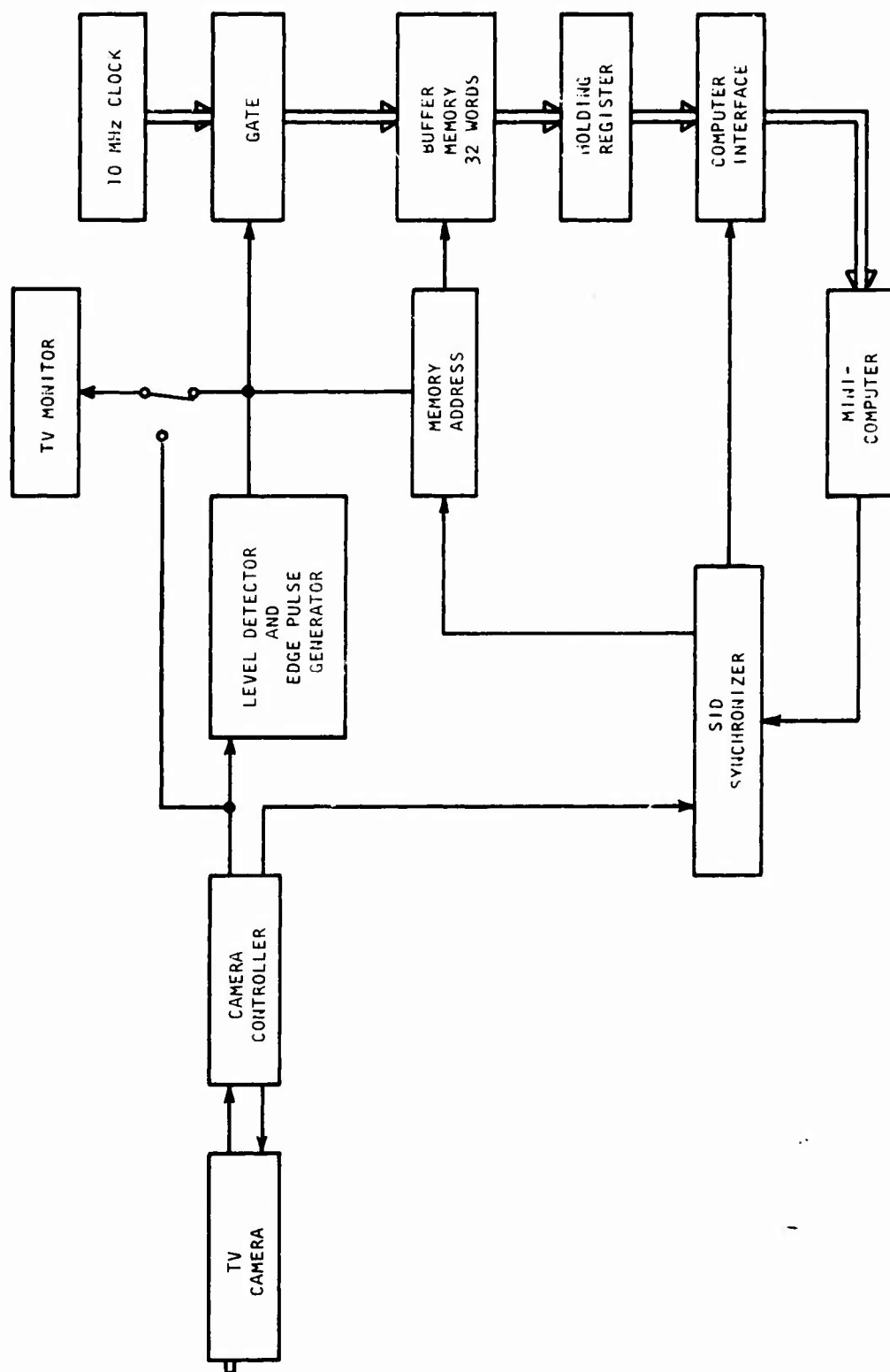


Figure Kb. Block Diagram

Figure 2-29. Block Diagram of the Sandia Image Digitizer

Regardless of picture size, all pictures are laid out in a 500 by 500 point matrix if the aspect ratio is 1:1. Thus, system resolution is a function of picture size. The digitizing speed ranges from 66 to 133 milliseconds depending on picture complexity. There is a TV monitor associated with the system which is used in setting up the picture for digitizing (i.e., defining boundaries). The total digitizing time per picture is then the sum of the setup time and automatic scan time.

The control system for the digitizer is a PDP-8 mini-computer. The computer allows considerable flexibility in exercising the digitized data with additional data reduction or analysis software algorithms.

2.5.3.1.7 Biomation Model 8100 Transient Recorder¹⁷

The Model 8100 Transient Recorder is a direct analog-to-digital converter system. Thus, test data are digitized in real-time. The system sampling rate is variable from one sample every 10 seconds to one sample every 10 nanoseconds. At the high sampling rate, the system is claimed to have a frequency response of dc to 25 MHz.

The amplitude resolution is $1/256$ of full scale input voltage, (i.e., an 8-bit digital output word is used). Total storage capacity for digital output is 2000 words. At maximum sampling rate, this corresponds to total data taking duration of 20 μ sec.

The direct digitizing technique has the distinct advantage of operating directly on the probe voltage, thus eliminating the intermediate storage of data on Polaroid photographs and the associated data quality problems. At present, the major disadvantage is the sampling rate. It is generally accepted that recorded transient EMP data should be recorded up to 100 MHz or greater. This would imply sampling intervals of 5 nanoseconds or less.

2.5.4 Computer Subsystem

2.5.4.1 Computer Requirements

In the discussions on processing cycles, a computer was indicated as being used in:

- (1) Adding a new characterization data set to a master data tape.
- (2) Retrieving and displaying characterization data.
- (3) Executing various data reduction codes.

The updating of the master characterization tape is a simple card-to-tape or tape-to-tape data transfer operation and requires a computer system with a card reader and tape drive or two tape drives. Any computer system down to a mini-computer^{*} will satisfy this requirement.

The retrieval and display of characterization data on the other hand has much more demanding requirements. The retrieval operation is essentially a SORT/MERGE operation and is most efficiently performed on a computer system equipped with large scale, random access, mass storage devices (disks). Large scale computer systems are usually so equipped and often have general purpose SORT/MERGE codes written for them which will satisfy characterization data retrieval requirements.

The computer requirements for executing data reduction codes depend on several factors such as:

- (1) Core required.
- (2) Execution time relative to computer execution

^{*} Mini-computers are typically defined as stored program computers with a basic word length of 16 bits or less.

(3) Accuracy required in results.

(4) Input/output requirements.

A recent study¹⁸ of ARES computer requirements for data reduction concluded that a properly configured mini-computer could have handled the majority of the data reduction codes used during the MINUTEMAN II/III test program. If the mini-computer is looked upon as the lower bound in required computing capability for executing data reduction software, here is how the mini-computer must be configured:

- (1) Central processing unit with 32K words of main memory.
- (2) A disk - 256K word or more storage capacity.
- (3) A card reader - 100 to 300 cards/minute.
- (4) A line printer - 200 to 500 lines/minute.
- (5) A keyboard terminal - teletype or equivalent.
- (6) A digital plotter - 0.001 to 0.01 inch resolution.
- (7) Floating point hardware.
- (8) An industry standard tape drive.

The need for 32K words of core memory is based on the fact that most EMP data reduction software routines can be written within 32K words. If one finds that this is not so in his case, a number of popular

mini-computers can have their memories expanded beyond 32K words. It should be noted that in the case of mini-computers, core memory is a very cheap commodity relative to other computer system costs.

The disk is a necessity so the computer can be run under a disk operating system (DOS), much like the monitor systems in large computers. The specified disk size (in words stored) would allow a reasonable number of programs and data sets to reside on a disk at any one time.

The card reader, line printer and terminal device are all necessary input/output peripherals and the operating speeds given tend to reflect what is available commercially.

The plotter is very much a necessity because so much of the data reduction output is required in the form of plots. The resolution range given is readily obtainable in available plotters.

The floating point hardware is required to decrease the execution time of floating point operations, which are commonly involved in scientific software. For example, a floating point multiplication can be executed 10 to 20 times faster using the special hardware, than if executed by software. Thus, the floating point hardware will assure minimum program execution times.

Finally, the tape drive is specified as a convenient means of communicating with other computer systems and a means of storing mass data. For example, the master characterization data tape could be updated on the mini-computer system, with the tape carried to a large scale computer for SORT/MERGE operations.

As part of the above mentioned ARES computer study, a linear Fourier transform code was bench marked on a CDC 6600 and a popular mini-computer, to test execution accuracy. The results of the bench mark showed that the mini-computer generated more than acceptable accuracy in its results.

There is one possible additional use for a computer in the data system and that is as a controller for the digitizer. This, of course, depends on what type of digitizer is used. However, if a computer is so used, a mini-computer would more than satisfy the requirement.

To summarize the data system computer requirements, all but the sort/merge capability can be satisfied by a mini-computer. Again, the emphasis on the mini-computer is to set a lower bound on required capability. The choice of how the computer system is configured depends on such factors as:

- (1) Whether off-site computer facilities are available to the data system.
- (2) The proximity of these facilities to the data system.
- (3) If the off-site facility is configured to satisfy the majority of the data system needs.
- (4) If the off-site facility is sufficiently loaded (or overloaded) so it cannot provide the required turnaround time.

2.5.4.2 Computer Subsystem Alternatives

There are basically three alternatives for meeting the data system computer requirements in terms of hardware subsystems:

- (1) Use off-site computer facilities and hand carry all input and output to and from the computer.
- (2) Use off-site computer facilities, but with a remote job entry terminal* on-site which allows the computer to be accessed directly from the data system.
- (3) Have all necessary computer capability on-site with the exception of the sort/merge capability.

Alternative (1) has the obvious disadvantage that a great deal of time would be wasted commuting between the data system and computer facility to submit jobs and pick up results. It may satisfy a small test program where a limited amount of test data are generated, but certainly not a large test program.

Alternative (2) would eliminate much of the commuting problem. However, it leaves the data system completely dependent on a remote computer facility. If the computer facility can meet capability (e.g., plotting) and turnaround requirements, then it is a very good alternative. If not, then the whole EMP test program could suffer.

*An example of a remote job entry terminal is the 200 User terminal used at ARES to access the CDC-6600 computer system at Kirtland AFB.

The final alternative essentially makes the data system independent of any other computer system. This may be a necessity in the case where a suitable off-site computer facility is not available or in the case where testing is being conducted at a remote site and it is desirable to have all necessary capability at the test site for rapid assessment of test data.

This third alternative is certainly the most convenient from the standpoint of operating the data system. Assuming that a mini-computer system were used, the disk operating systems presently available for mini-computers can operate in a multiprocessing environment. This means that several tasks can, in effect, be going on in parallel. Thus, the mini-computer could be accepting new characterization data sets via the teletype or card reader, formatting the data and storing it on tape. At the same time, it could control the digitizer, buffer in the digitized data, and store completed data sets on a disk for data reduction. And it could simultaneously be executing a data reduction code such as a Fourier transform algorithm and plot the results. The reason this type of operation can be performed on a time effective basis is because at least two of the above operations (processing characterization data and controlling the digitizer) leave the computer CPU idle for long periods of time. Thus, the CPU can be shared among multiple tasks.

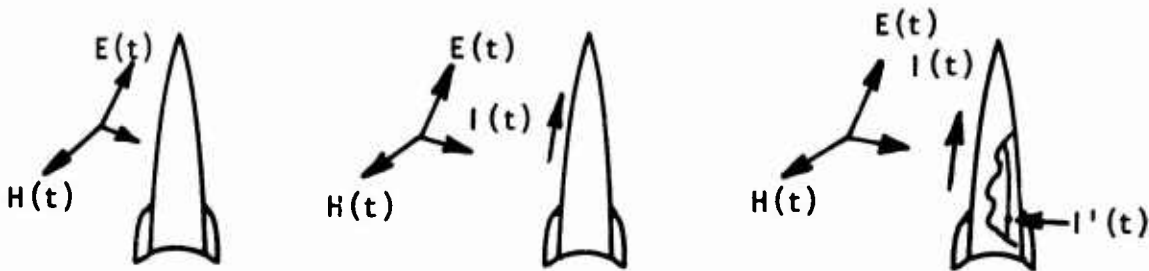
SECTION 3

DATA REDUCTION TECHNIQUES

3.1 INTRODUCTION

3.1.1 The EMP Problem

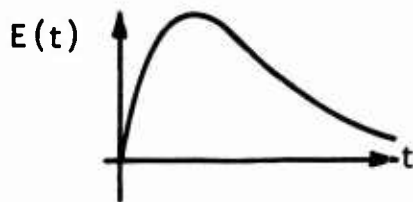
The EMP threat and most simulated EMP tests consist of exposing some system to a transient electromagnetic field which induces transient currents ($I(t)$) on the metallic skin of the system and on its internal wiring. One of the primary experiments in an EMP test program consists of measuring the transient induced currents ($I'(t)$) on internal wiring in the vicinity of critical subsystems in order to determine the subsystems' susceptibility to the EMP threat.



The objective of most EMP test programs is to find some relationship between the exciting fields (i.e., $E(t)$) and the resulting current at some critical locations (i.e., $I'(t)$). This objective has

three motivations. One is to minimize the resources required to conduct a comprehensive test. If the relation between $E(t)$ and $I'(t)$ can be found, it is possible that the physical system under evaluation can be replaced by a mathematical model. The second motivation is that an understanding of the relationship between $E(t)$ and $I'(t)$ can allow a theoretical assessment of the system's susceptibility to those electromagnetic environments that cannot be simulated properly. The third motivation is that an understanding of the relationship between the exciting fields ($E(t)$) and the induced response ($I'(t)$) at a given location would lead to sufficient understanding to identify the electromagnetic coupling mechanisms. An understanding of the details of the coupling mechanisms is a prerequisite for modifying the system to reduce or eliminate these unwanted induced signals.

Unfortunately, the relationship between the transient EMP fields and the induced current response is seldom made evident by inspecting the time domain data.

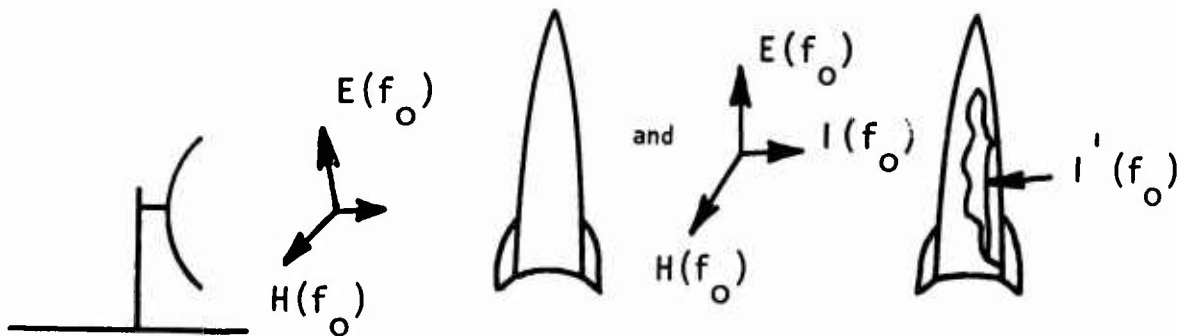


The difficulty in relating the excitation to the induced response is that the two are related by an integral and/or differential equation whose form(s), as well as scaling parameter(s), must be determined before the relationship can be established. Therefore, a more efficient

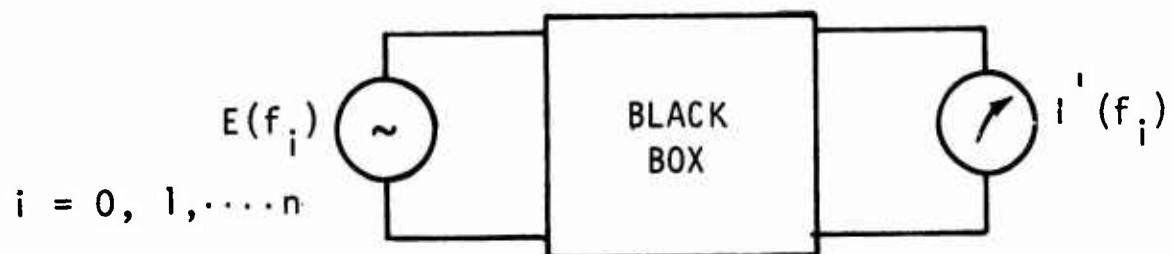
procedure than using time domain experimental data to relate the excitation to the response is required to achieve maximum knowledge possible from expensive EMP test programs. This procedure is available through the use of frequency domain analysis techniques.

3.1.2 The Frequency Domain Approach

The most straightforward approach to obtaining frequency domain coupling relationships is through continuous wave (CW) testing. Assume that the system is illuminated by electromagnetic fields that are oscillating at a single frequency (CW),



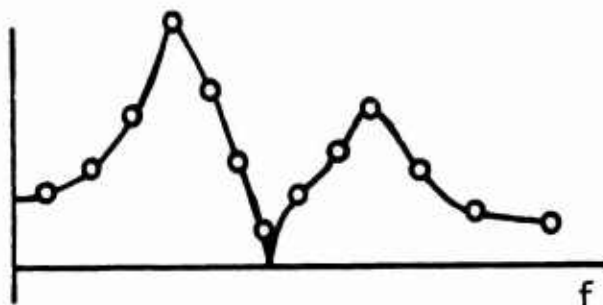
and the induced current at some monitor point, $I'(f_o)$, is measured. Symbolically, this experiment can be represented as a generator driving a "black box" while its response is measured at a specified pair of terminals.



If one changes the oscillating frequency of the generator and measures the amplitude of the current, $|i'(f_i)|$, and its phase, $\phi[i'(f_i)]$, relative to the generator at each change, the relationship between excitation and response ($H(f_i)$) can be obtained as a function of frequency.

$$|H(f_i)| = \left| \frac{i'(f_i)}{E(f_i)} \right|$$

$i = 0, 1, \dots, n$



In many cases, this relationship, $H(f_i)$, is relatively simple compared to that in the time domain case because it is still governed by the basic integral/differential equations. However, in the frequency domain it is possible to reduce the equations for $H(f_i)$ to the ratio of two polynomials in frequency

$$H(f_i) = \frac{a_0 + a_1 f_i + \dots + a_m f_i^m}{b_0 + b_1 f_i + \dots + b_n f_i^n} \quad (\text{Eq. 3-1})$$

For a system that is linear and small compared to the wavelength of the exciting fields, this reduction to polynomial form is always possible. Systems that are linear and large compared to the wavelength of the excitation can usually be approximated to any desired degree of accuracy by this ratio of two polynomials in frequency form. The advantage of this polynomial form in the frequency domain is that the relationship between the excitation and the response is expressed in terms of an algebraic function rather than the integral/differential equations required in the time domain formulation. Obviously an algebraic form offers relative ease of analysis. An additional advantage of formulating the excitation/response problem in the frequency domain is the existence of considerable experience and published results on the subject that are not available for the transient time domain formulation.

3.1.3 Frequency Domain Analysis for Transient Time Domain Data

The previous subsection has indicated that the determination of the excitation/response relationship can be simplified considerably if the analysis is done in the frequency domain rather than the time domain. Unfortunately, the EMP threat and most EMP testing have transient time domain electromagnetic field excitations and induced responses. Therefore, some relationship for transforming between data in the time and frequency domains is required so the experimentally measured excitation and response in the time domain can be converted to a frequency domain form where the subsequent analysis is simplified. Such a relationship is available and is known as the Fourier Integral Transform (FIT).

The remaining portions of this section will deal largely with the theory and application of the FIT and its related formulations. But before proceeding further, the fundamental prerequisites for the use of the FIT or any time/frequency transform procedure must be emphasized. If these prerequisites do not apply, then the analysis must be conducted in the time domain; however, the available time domain analysis techniques are beyond the scope of this discussion.

The first and most important prerequisite for the use of any time/frequency domain transform is that the excitation/response relationship must be linear. Simply stated, the response of the system must be proportional to the amplitude of the input. If

$$I_1 \sim E_1 \quad (\text{Eq. 3-2})$$

then

$$I_2 = A I_1 \sim E_2 = A E_1 \quad (\text{Eq. 3-3})$$

where A is an arbitrary constant. Linearity must apply for both CW frequency domain and transient time domain excitations.

Another aspect of the linearity prerequisite is superposition. Superposition means that the response given the simultaneous application of two excitations must equal the sum of the responses if the excitations were applied separately. An example where superposition does not apply is when the response is proportional to the square of the input. Then

$$I_1 = E_1^2$$

$$I_2 = E_2^2$$

$$I_1 = I_2 \neq (E_1 + E_2)^2$$

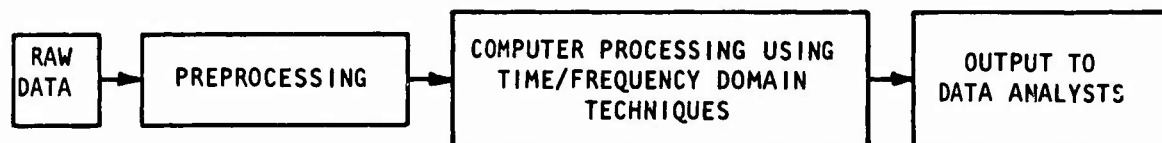
Because of this linearity requirement, one must be aware of which coupling relationships tend to be linear and which do not. The coupling of electromagnetic energy from the EMP environment to the metallic skin and internal wiring of a system is generally linear. Important exceptions are: (1) when arcing or voltage breakdown occurs in the system, (2) when the conductivity of the atmosphere surrounding or internal to the system is a function of the EMP fields, and (3) when the coupling is due to electromagnetic fields diffusing through a ferromagnetic shield. Also, the transfer of energy from internal wiring to critical subsystems is generally nonlinear. However, the purpose of system level EMP tests is to experimentally determine the amount and type of electromagnetic coupling at various points in the system. It is generally assumed that the nonlinear loads (subsystems) absorbing energy have a minor effect on the nature of coupling onto cable bundles, etc. Therefore, frequency/time domain techniques are generally applicable for the study of coupling where nonlinear coupling effects are considered minor. The techniques are not applicable when studying the deposition of coupled energy into critical subsystems with active elements because of severe nonlinear effects.

The second prerequisite for use of frequency/time domain transform techniques presented in the following subsections, is that the relationship between the excitation and the response cannot be a function of the time when the excitation is applied. This prerequisite requires some interpretation for EMP test conditions. If the excitation/response relationship changes when the system is in a different state (i.e., power on versus power off), then frequency/time domain transform techniques can be used only if each state is studied separately. The techniques do not apply if the system is changing states during excitation. For example, the time when the system and its associated environment are changing states is when the system is immersed in an atmosphere with a time varying conductivity. In such a case, the analysis must be conducted entirely in the time domain.

3.1.4 Section Review

The remaining parts of this section present the frequency/time domain techniques applicable to EMP test data reduction in preparation for assessment. The order of presentation will follow the logical procession of data from the field to the finished product.

A discussion of preprocessing techniques is first. The data generally come from the field in the form of analog traces on Polaroid photographs. These data must undergo several operations before any transform techniques are applied with the aid of a digital computer. This preprocessing includes analog-to-digital conversion, scaling, and combining of related time domain records.



Thus, several preprocessing techniques will be discussed as a prerequisite to presenting the theory and practical use of transform techniques.

The discussion of the time/frequency domain techniques begins with a thorough discussion of the theory of the FIT applicable to EMP data reduction. This material is presented because most of the errors occurring in the computer processing of EMP data occur because the analyst has only a partial understanding of the applicable theory of the FIT. Next, related transform techniques such as the Fourier Series Transform (FST) and the Discrete Fourier Transform (DFT), which are commonly used in EMP data reduction, are discussed. Finally, a subsection explaining the practical application of the various time and frequency domain techniques is presented. This subsection includes a description of the limitations of the techniques as well as the various types of errors that commonly occur in the use of these techniques. This subsection is particularly pertinent since it covers certain classes of errors which can contaminate test data, how these errors affect the results of transform techniques, and how the effects of these errors can be minimized. The errors include the noise that typically contaminates waveform data during digitizing and the truncation of waveforms which occurs when the waveforms are recorded on oscillographs.

3.2 PREPROCESSING TECHNIQUES

It is generally assumed throughout the handbook that test waveform data are initially recorded as Polaroid oscillographs and that the data reduction techniques (as described later in this section) are implemented on a digital computer. There are certain preparatory steps which must be taken to ready test data for input to data reduction routines.

At a minimum, the raw test data must be converted from the oscillograph or analog form to a computer readable form. This is accomplished through the digitization process.

The coordinate data generated through digitizing must have certain scale factors applied before they are used as input data. The scaling operation converts the waveform data to the value (and units) of the physical observable as originally sensed. Some of the scaling data are generated during digitizing, while others are derived from recording instrumentation parameters. Scaling is performed as a digital computer operation.

A final preprocessing technique which is used in data reduction is time tying. In this technique, two or more waveforms of the same physical observable (recorded at different time bases) are tied together to form a more complete waveform. Again, this is a digital computer implemented technique.

The following paragraphs cover each of these preprocessing techniques in detail.

3.2.1 Digitization

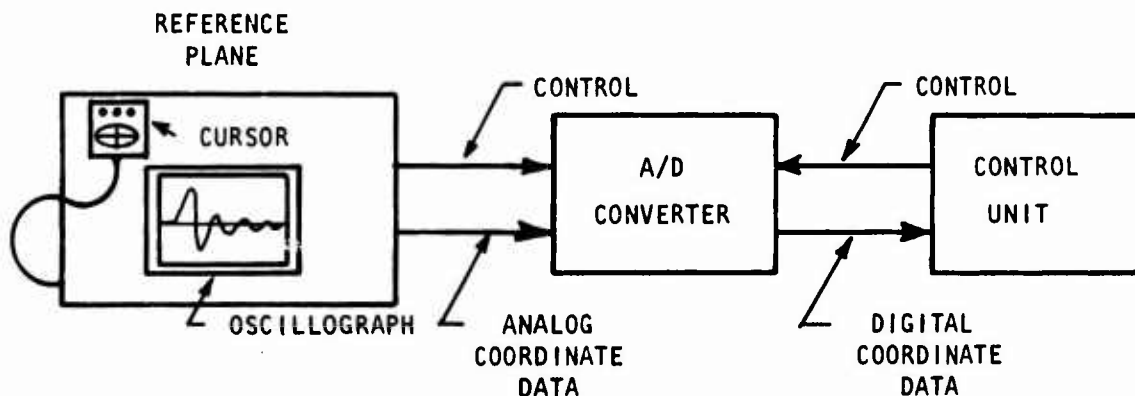
The subject of digitization technology is presented in some detail in Paragraph 2.5.2 from basically a hardware standpoint. The material presented in this paragraph is directed toward operational procedures in the use of manual digitizers for preparing oscillographs as data reduction input. Two subject areas are discussed:

- (1) Setting up digitizer and calibrating the oscillograph.
- (2) The procedures followed in digitizing the waveform.

Before starting these discussions, however, it is useful to summarize the manual digitizer model presented in Paragraph 2.5.2.3.

3.2.1.1 Manual Digitizer Model

The manual graphic digitizer has four principal components: (1) a reference plane which acts as a working surface, (2) a pointer or cursor for selecting points on waveforms to be digitized, (3) an analog-to-digital converter, and (4) a control unit.



The reference plane/cursor act in an emitter/sensor arrangement which allows the position of the cursor on the reference plane to be measured as two electrical signals x_i and y_i , the coordinates of the cursor. These analog signals are fed to the A/D converter where they are converted into digital words, Z_{x_i} and Z_{y_i} .

The cursor is a free moving device which is manipulated by the operator to locate points on the oscillograph for digitizing. The cursor is assumed to be equipped with three control buttons which control signals to the A/D converter. The first button allows an origin to be established at any desired point on the reference plane. The second button initiates an A/D conversion once a desired point is located. The third button signals that the end of a waveform has been reached and digitizing is to terminate.

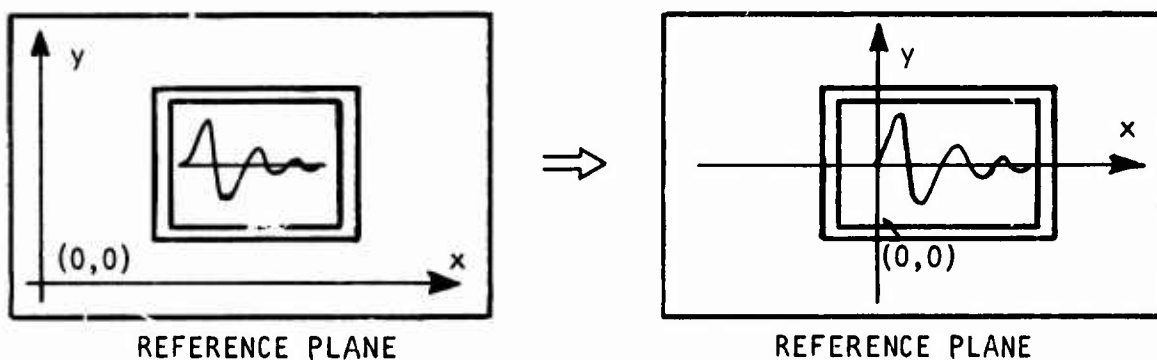
The function of the A/D converter is self explanatory. The function of the control unit is to buffer, reformat, and store the digital data. It can also control the A/D converter so that evenly spaced (constant Δx) data can be obtained if desired. The control unit is also assumed to be able to accept alphanumeric data from a keyboard device such as a teletype. Note that this manual digitizer model closely resembles the Bendix Datagrid System¹⁹ used in the ARES Data System. Even so, the setup and digitizing procedures covered in the following paragraphs hold for any manual digitizer.

3.2.1.2 Digitizer Setup

The purpose of the digitizing process is to convert a test variable, such as current, $I(t)$, voltage, $V(t)$, or magnetic field strength, $B(t)$, which is in oscillograph form to digital data. Whereas the test variable has units of amperes/second, volts/second, etc., the oscillograph has units of length, which the digitizer measures, usually

in inches. Thus, scaling data must be derived from the oscillograph which allows the measured waveform coordinate pairs (x_i, y_i) to be scaled to the correct test variable units.

The first digitizer setup procedure simply involves establishing an origin on the reference plane. The digitizer normally assumes its origin at the lower left-hand corner of the reference plane. However, it is desirable to have the origin at the origin of the oscillograph waveform.



An origin transformation is accomplished by simply selecting the desired origin point on the reference plane and subtracting its coordinate values from all subsequent digitized coordinate pairs.

$$x'_i = x_i - x_o$$

$$y'_i = y_i - y_o$$

(Eq. 3-4)

where:

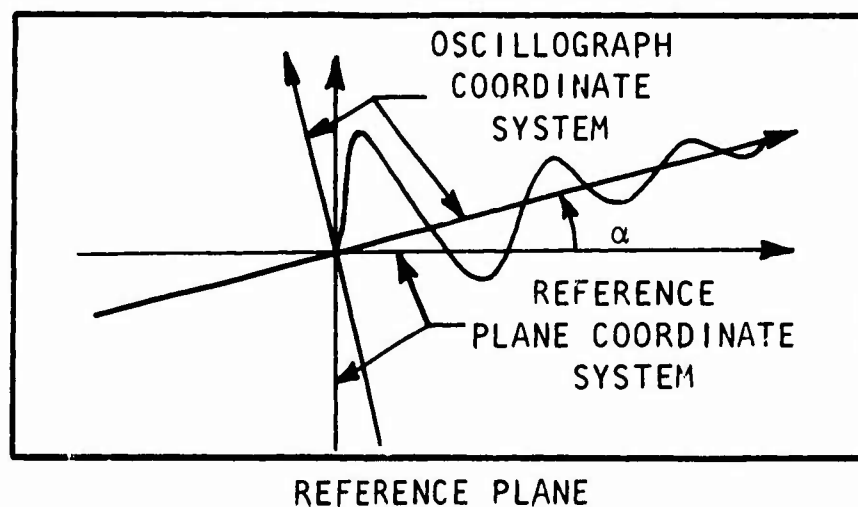
(x_i, y_i) = coordinates measured relative
to the reference plane origin

(x_o, y_o) = coordinate of the desired
origin

(x'_i, y'_i) = position of (x_i, y_i)
relation to (x_o, y_o)

Many digitizers do this transformation as an internal operation, with resulting digitized data referenced to the desired origin. (Recall the origin set button on the cursor in the digitizer model.) If the transformation is not done internal to the digitizer, x_o and y_o must be stored as part of the total data set with subtraction performed as a preprocessing operation as indicated in Equation 3-4.

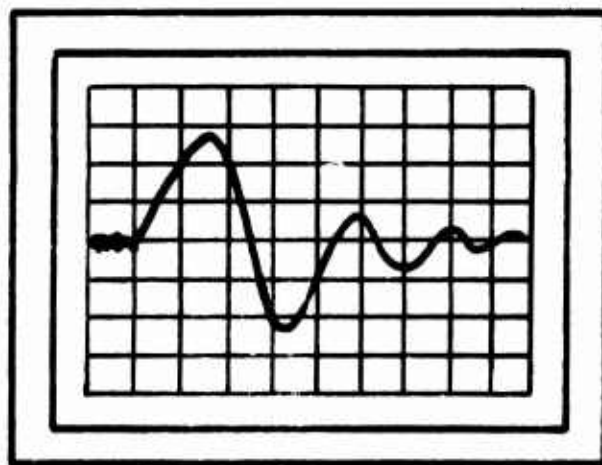
Next, data must be taken which allow any rotation in the oscillograph coordinate system relative to the reference plane coordinate system to be corrected.



If the angle α between the two coordinate systems can be determined, then digitized coordinate pairs (x_i, y_i) can be rotated through α degrees by the following transformation:

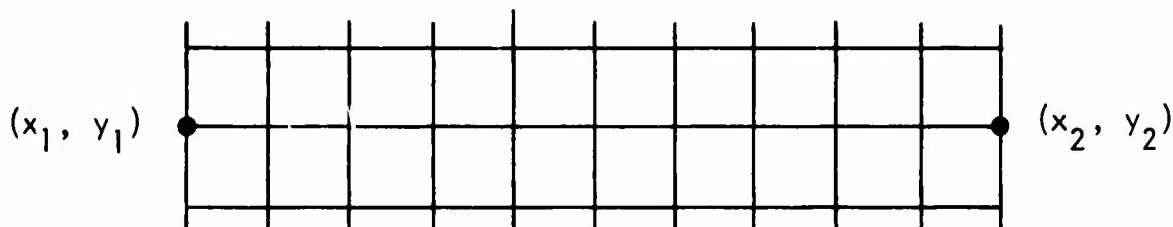
$$\begin{bmatrix} x'_i \\ y'_i \end{bmatrix} = \begin{bmatrix} \cos \alpha & \sin \alpha \\ -\sin \alpha & \cos \alpha \end{bmatrix} \begin{bmatrix} x_i \\ y_i \end{bmatrix} \quad (\text{Eq. 3-5})$$

The angle α can be derived as follows: It is assumed that the recording oscilloscope graticule image is superimposed on the waveform oscillograph.



OSCILLOGRAPH

This graticule is the coordinate system for the oscilloscope. Measure the coordinates of any two constant y points on the graticule.

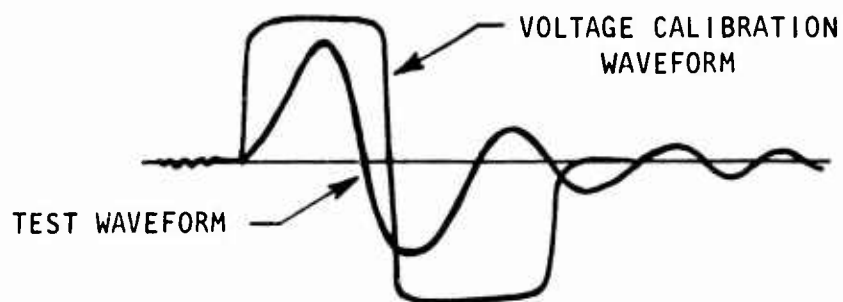


These two points are on a given horizontal graticule line and α is determined as

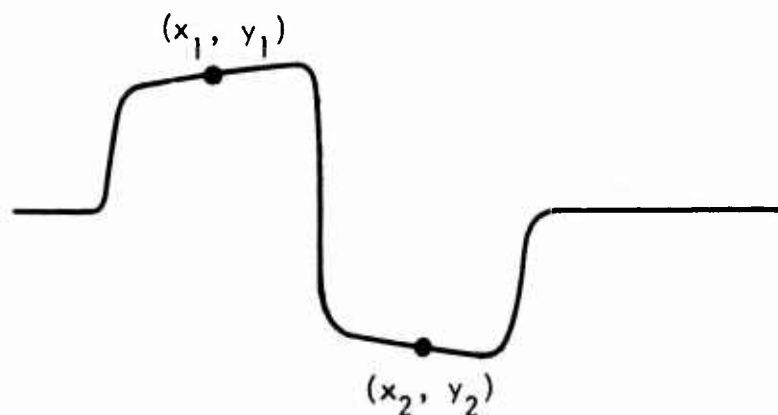
$$\alpha = \tan^{-1} \left(\frac{Z_{y2} - Z_{y1}}{Z_{x2} - Z_{x1}} \right) \quad (\text{Eq. 3-6})$$

Note that the two coordinates should be taken at opposite ends of the graticule image, since small errors in measuring these two points are amplified as the points move closer together.

The next data taken are used to scale the Z_{y_i} data to the proper test variable units. It is common to superimpose a rectangular waveform of known peak-to-peak amplitude in volts on the test waveform at the time of recording.



If this combined waveform is measured at its upper and lower values, then a scale factor in units of volts/inch can be derived from the data points.



Since the peak-to-peak voltage, V_{pp} is assumed known, the desired scale factor is derived as

$$SF_V = V_{pp} / (z_{y_1} - z_{y_2}) \quad (\text{Eq. 3-7})$$

where:

SF_V = the desired vertical
scale factor in volts/inch

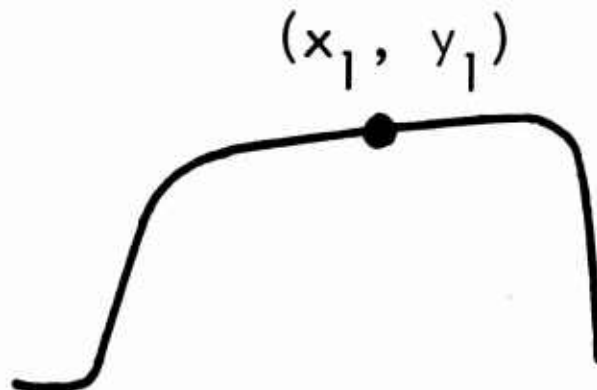
V_{pp} = the peak-to-peak waveform
voltage known a priori

Z_{y_1} and Z_{y_2} = digital values of y_1 and y_2 in
units of inches.

Thus, any subsequent y_i coordinate, measured in inches, can be converted to volts by

$$Z'_{y_i} = Z_{y_i} \times SF_V \text{ (inch x volts/inch)} \quad (\text{Eq. 3-8})$$

Note that the rectangular waveform may not be of constant amplitude at its supposedly constant amplitude positive and negative excursions, but may exhibit a rapid rise and then a slow rise to a peak value.



Thus, there must be an agreement between the data system (digitizer operator), the test system, and the data analysts as to where this

waveform is to be sampled. In the case of ARES, the agreed upon point was approximately half-way along slow rising portions of the waveform.

If a voltage calibration pulse is not superimposed on the oscillograph waveform, then the vertical scale factor must be derived from both oscillograph measurements and oscilloscope setup data; namely, the vertical input amplifier gain setting normally given in volts/centimeter. The distance between any two contiguous horizontal graticule lines on the oscillograph is one centimeter relative to the oscillograph (i.e., if the oscillograph is enlarged for digitizing, then the distance is larger than one centimeter but still one centimeter relative to all information recorded on the oscillograph). Thus, digitizing these two points gives the data necessary to calculate a parameter with units of inches/centimeter. The oscilloscope vertical amplifier gain in volts/centimeter can then be entered through the keyboard terminal as part of the data set. The vertical scale factor is computed as

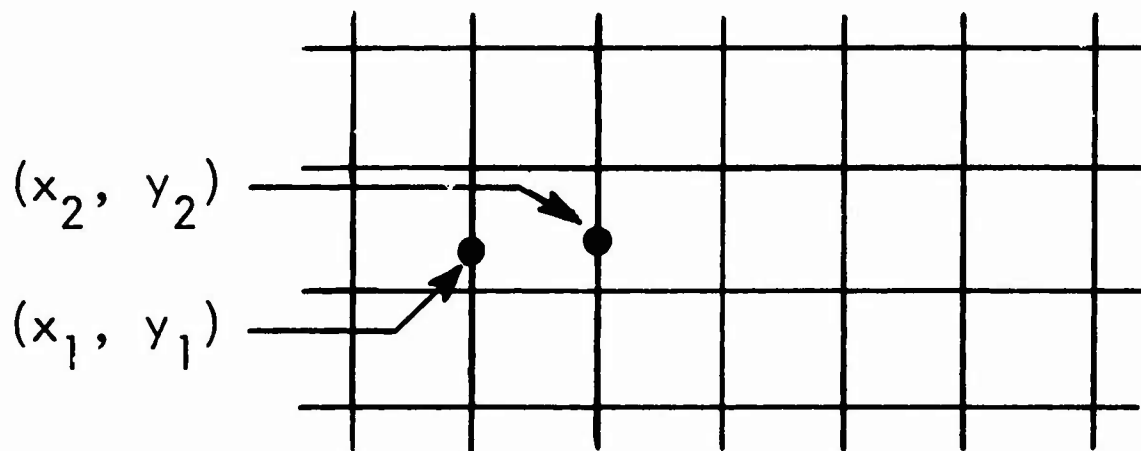
$$SF_V = G_{VA} / (Z_{Y_1} - Z_{Y_2}) \text{ volts / inch} \quad (\text{Eq. 3-9})$$

where

G_{VA} = the oscilloscope vertical amplifier
gain in volts/centimeter

$(Z_{Y_1} - Z_{Y_2})$ = the scale parameter in inches/centimeter
relative to the oscillograph

The final setup data taken are for computing the horizontal or time-axis scale factor SF_H . This procedure is equivalent to that discussed above except that the distance is measured between two contiguous vertical instead of horizontal graticule lines.



These two measurements are used to compute a parameter with units of inches/centimeter

$$P = Z_{x_1} - Z_{x_2} \quad (\text{Eq. 3-10})$$

The sweep rate of the oscilloscope is read from the oscilloscope in centimeters/second and is entered into the data set via the keyboard terminal.

Then SF_H can be computed by

$$SF_H = SR \times P \text{ inches/second} \quad (\text{Eq. 3-11})$$

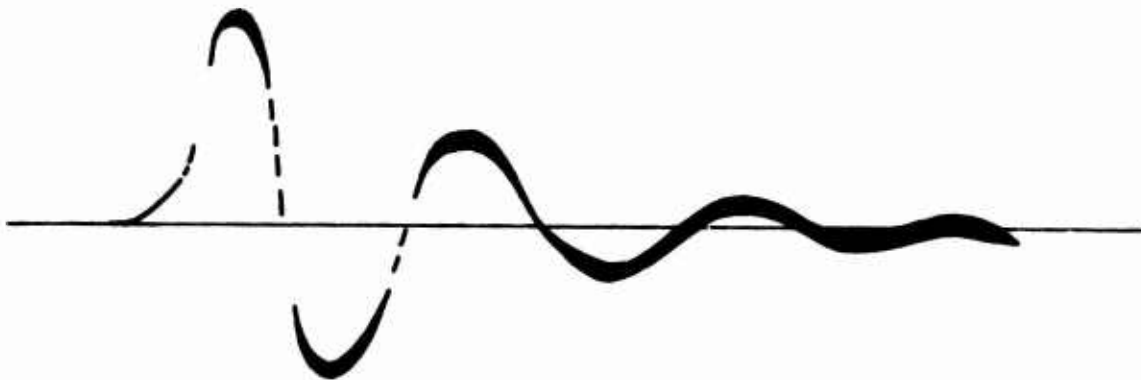
where:

SR = oscilloscope sweep rate in
centimeters/second

3.2.1.3 Waveform Digitizing

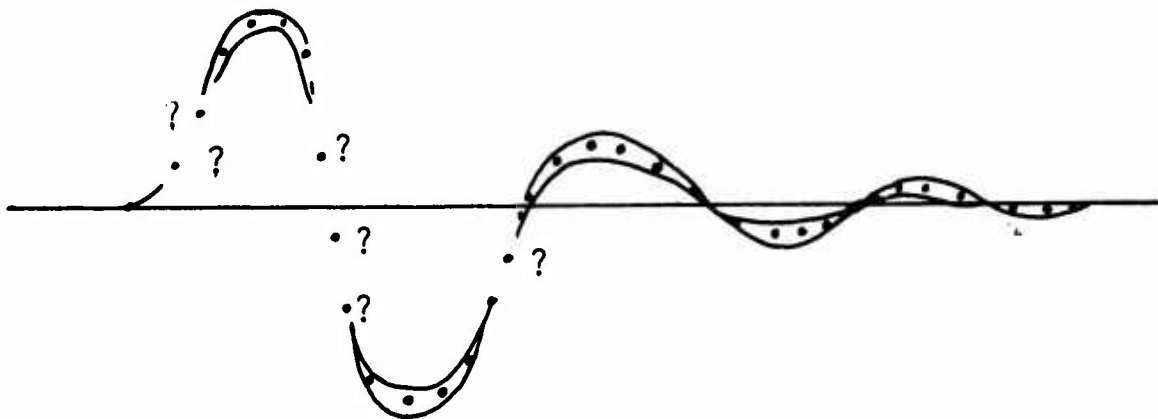
The material contained in this discussion pertains to some of the practices which should be considered in digitizing oscillograph data. The discussion can be started by stating that the use of a manual digitizer involves an operator for all phases of the digitizing process and, therefore, one must assume a considerable amount of value judgment on the operator's part. EMP transient waveforms are typically complex and often of poor quality (see Figures 2-24a through 2-24f).^{*} Therefore, the operator must be well trained and have an appreciation of the problems which can result from poorly digitized data if reasonably consistent and high quality results are to be obtained.

Typically, the oscillographs are made at very high oscilloscope writing rates (e.g., five to 10 cm/ns) where the oscilloscope trace tends to fade out (i.e., a high waveform slope typically appears at the beginning of the waveform with the trace becoming relatively thick as the writing rate slows down).



^{*} Data quality is often sacrificed for quantity in large system test programs.

Thus, the operator is faced with guessing at the location of the waveform where no data exist and at the location of the waveform when it is so thick there is a loss of resolution. When the waveform is very complex (i.e., multiple resonant frequencies) the problem is compounded. The typical procedure is for the operator to guess as best he can at where the trace would have been in places where it has dropped out and to digitize points in the center of the waveform in portions where the trace is thick.



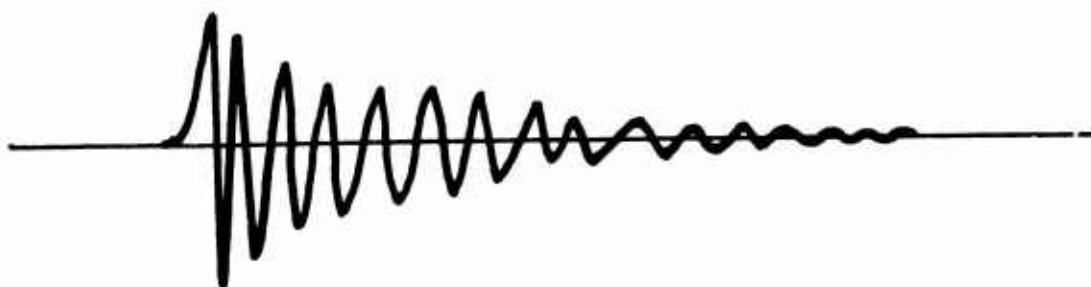
Since the cursor which the operator uses to select the points he digitizes normally leaves no marking of where he has been (i.e., what points on the waveform have been digitized) he is apt to "bounce around" as he moves along the waveform. This bouncing around basically amounts to adding some type of random noise pattern to the digitized data set. The actual nature of this noise distribution has been studied by a number of interested parties [31], [32], [33]. The important point here is that the noise is known to contaminate data reduction results; especially Fourier transforms and transfer function estimates.

There are two possible solutions for minimizing this problem, neither of which are known to have been tested at this point in time. The first solution would have the data analyst for whom a given

oscillograph is being digitized, trace over the oscillograph waveform with a pin to fill in missing portions and define his interpretation of the center of thick portions of the trace. The operator would then digitize the data analyst's traced waveform. This puts the responsibility of what the waveform is to actually look like on the analyst who is best qualified to make that judgment. This procedure would be time consuming and thus be limited to selected oscillographs.

The second procedure would be to equip the digitizer with a writing stylus as a cursor if possible. The basic design of some manual digitizers will not allow this (e.g., the Telereadex Digitizer) but others such as the Bendix Datagrid can be so equipped. The operator could then leave a permanent record of where he had last digitized. This procedure would allow him to smooth out the waveform which he traces as he digitizes. It would also leave a permanent record of "what was digitized" for the data analyst to inspect if he suspects problems in the data set he is using in his analysis.

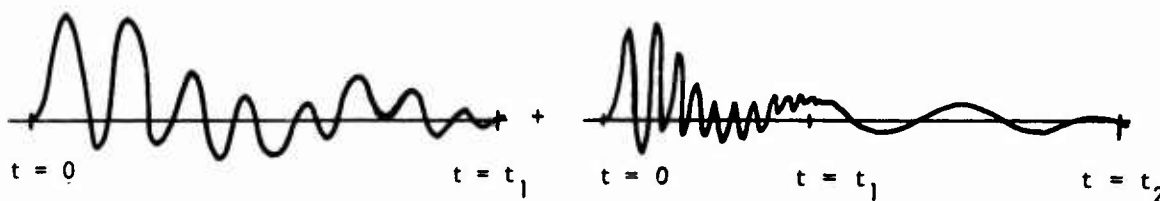
A second difficult problem which the digitizer operator faces is digitizing a waveform recorded at a relatively low sweep rate so that there are many "cycles" of data in the waveform.



With a dense oscillating waveform as sketched above, the natural tendency is to sample the signal at the peaks, since finer resolution is difficult or impossible to achieve. Thus, this waveform is sampled twice each cycle. Then a user would hope that a Fourier transform of these digitized data would yield good spectrum data in the vicinity of the resonant frequency. However, the Nyquist sampling criteria (see Paragraph 3.4.5.2 for a detailed discussion) state that the highest independent and potentially valid frequency component corresponds to an oscillation that is sampled twice each cycle. Furthermore, if the unsampled waveform has frequency components higher than the Nyquist frequency, then these components will be irretrievably mixed with components at frequencies less than the Nyquist frequency. This mixing is called aliasing. Therefore, the region of the transform in the vicinity of the resonant frequency, the region of greatest interest, will be in error. This error is compounded by the fact that the transform of the random digitizing error discussed above sometimes peaks near the Nyquist frequency. Therefore, the waveform must be sampled at a higher rate. A higher sampling rate would move the Nyquist frequency above the resonant frequency of the waveform shown in the sketch and reduce the amount of aliasing. Furthermore, the peak in the contribution due to random errors, when present, would be moved away from the region of greatest interest.

It is generally accepted that the sampling rate must yield a Nyquist frequency three to five times the highest frequency of interest. In the previous example, the rate would correspond to sampling six to ten times per cycle. However, this brings us back to the problem originally stated. When the waveform has a high density of data, the digitizer operator cannot hope to obtain the required number of samples per cycle. In fact, as is often the case, there is only enough oscillograph resolution to obtain two or three samples per cycle. There is only one known solution to this problem and that is time tying of waveforms. The waveform portion containing most of the high frequency information in response data typically occurs in the early part of the response and damps

out within the first 10 to 25 percent of the total response. Therefore, this high frequency portion can be recorded at a high enough sweep rate to "expand" the waveform for digitizing from $t = 0$ to $t = t_1$. Then a slower sweep oscillograph of the same response can be digitized from $t = t_1$ to $t = t_2$, where t_2 is essentially where the total response dies out.



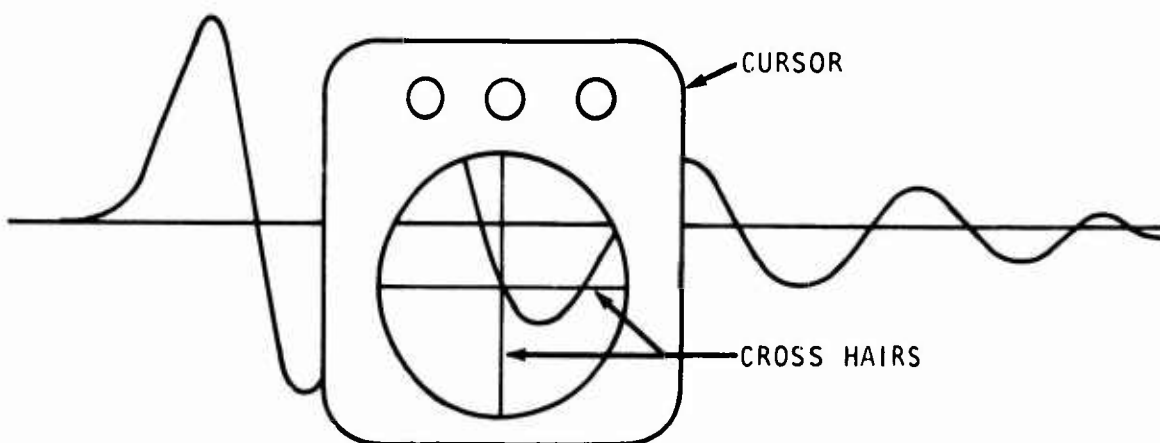
The subject of time tying of transient waveforms and some of the problems associated with the technique are discussed in more detail in Paragraph 3.2.3.

The material presented so far covers some of the considerations and problems associated with generating nonevenly spaced digital data (i.e., nonconstant Δx). There are data reduction algorithms such as the Fast Fourier Transform (FFT) algorithm which require constant Δx data as input. The procedure for obtaining such data is to trace the waveform with the cursor in a continuous manner and let the control unit select coordinate pairs which are constant in Δx .^{*} This assumes first that the A/D converter can operate on a continuous basis (i.e., sample the position of the cursor and convert the samples at a high enough rate that the desired Δx can be obtained). And second, the control unit has the capability to inspect the incoming coordinate pairs (z_{x_i}, z_{y_i}) and

^{*}Equally spaced (constant Δx) data can be obtained by interpolation of non-constant Δx data. However, this procedure is rarely used due to the loss in computer efficiency and the uncertainty in the effects of interpolation errors.

make selections on a constant Δx basis. Both of these criteria are met in the ARES digitizer system. There is a waveform tracing rate at which the operator can get ahead of the conversion rate of the A/D converter, but for the ARES system the rate is so high there is no problem.

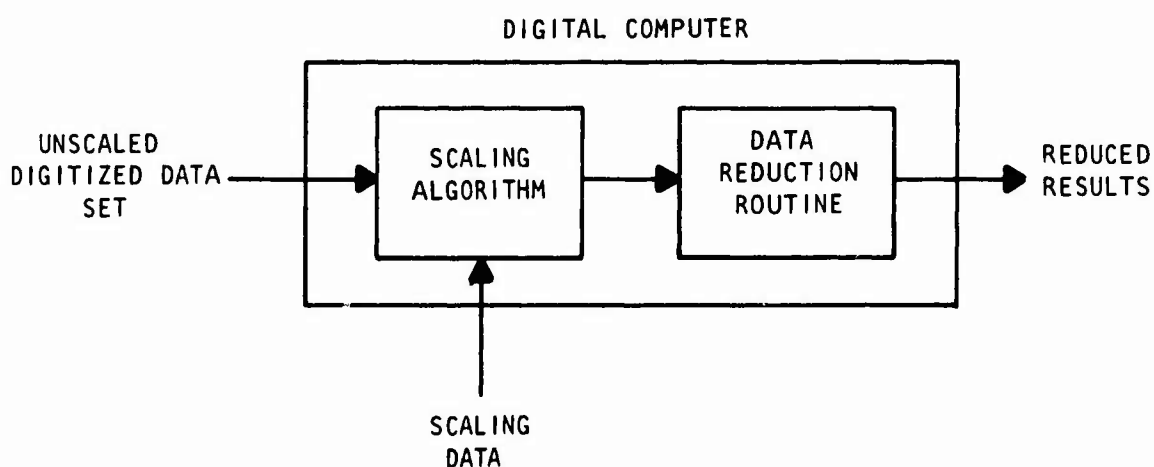
The basic problem which the operator faces in performing the procedure is maintaining a tracing which closely matches the actual oscillograph waveform. If the digitizer is equipped with a bomb-sight type cursor, the operator must keep a set of cross hairs centered on the waveform as he moves the cursor along the curve.



This tracing procedure may be made more reliable if a writing type stylus were used as a cursor. This type of cursor would allow the operator to trace the waveform, leaving a permanent record of the waveform actually digitized. The writing or pen stylus is also a more natural instrument for tracing since it has a pen point.

3.2.2 Data Scaling

Before a digitized data set is used as input to a data reduction routine, it must be scaled to the proper units. This scaling operation is done by a digital computer algorithm specifically designed to perform appropriate scaling computations.



In the previous paragraph (3.2.1), those scaling data measured during the digitizing operation were discussed. These data accompany the digitized waveform data as part of the total unscaled data set. There is, however, additional scaling data which must be fed to the scaling algorithm. The need for these data results from the way in which oscillograph data are recorded. This is illustrated in Figure 3-1 which is a simple block diagram representation of the instrumentation system for sensing and recording test variables. The physical observable is the electromagnetic variable being sensed. Typical variables of interest are:

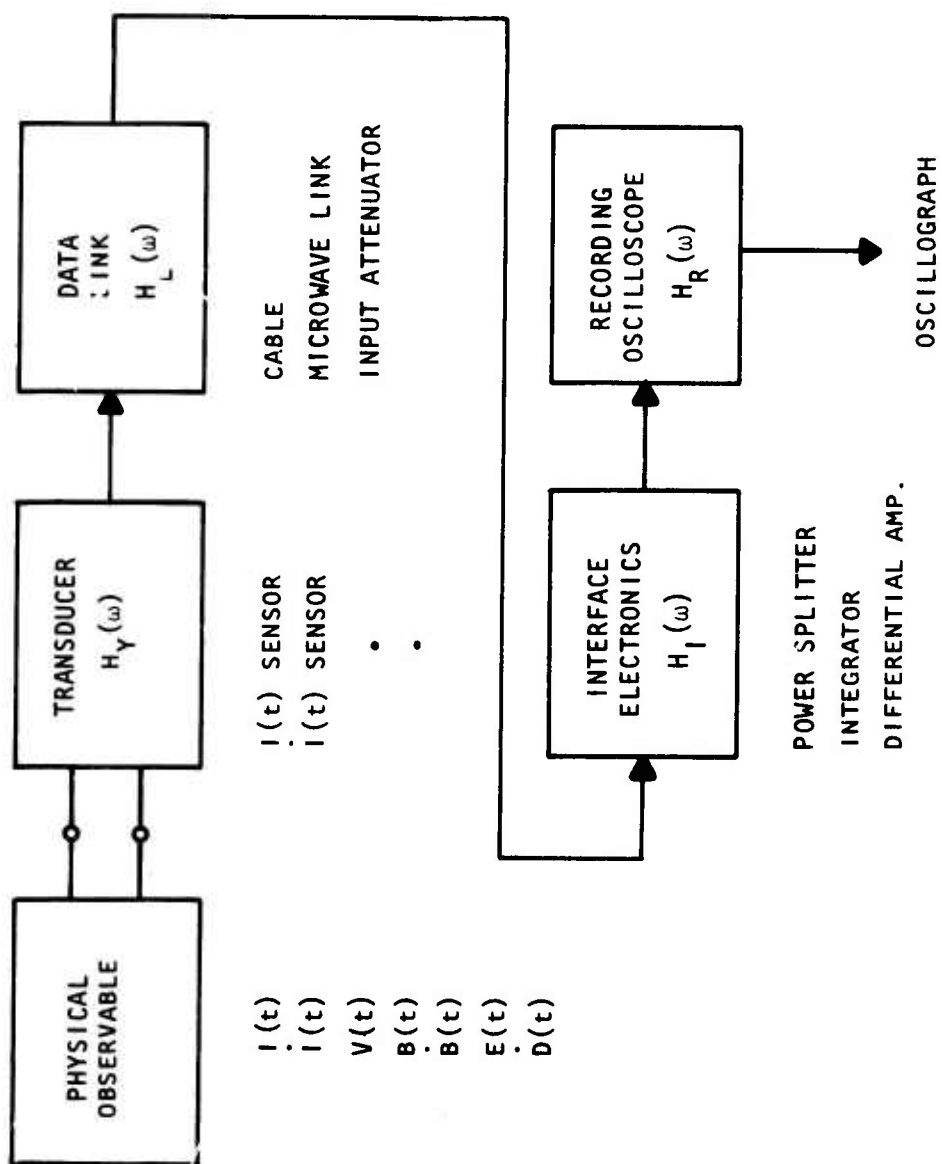


Figure 3-1. Block Diagram of Typical EMP Test Signal Recording System

- Current, $I(t)$
- Time Rate of Change of Current, $\dot{I}(t)$
- Voltage, $V(t)$
- Magnetic Flux Density, $B(t)$
- Time Rate of Change of $B(t)$, $\dot{B}(t)$
- Electric Field Intensity, $E(t)$
- Time Rate of Change of Electric Flux Density, $\dot{D}(t)$.

The transducer or test probe is the device specifically designed to sense the variable (physical observable) of interest and to output a voltage proportional to the sensed variable. Thus, there is a transfer characteristic or function, $H_T(\omega)$, associated with the transducer. If the physical observable is voltage, then the transducer transfer function has units of volts/volt or simple gain (or attenuations) if the observable occurs. If the observable is current, the transfer function has units of impedance in ohms.

$$V_T(\omega) = H_T(\omega) I_O(\omega) \quad (\text{Eq. 3-12})$$

where:

$V_T(\omega)$ = the frequency domain representation of
transducer output voltage

$H_T(\omega)$ = transducer transfer function

$I_O(\omega)$ = the frequency domain representation of
the physical observable (current)

The data link is either a cable or microwave transmission system for transmitting the test variables to the recording instrumentation. A microwave system used at ARES for current probes has an overall link gain of 28 dB and a cable link used for field probe data which has a link gain of unity. It is often necessary to insert an attenuator at the microwave link input so that the input signal does not over drive the system. The data link transfer function ($H_L(\omega)$) is simply a gain (units of volts/volt) over some usable frequency band, with a value equal to the algebraic sum of the link gain and attenuator gain.

The interface electronics are used to interface the data link to the recording oscilloscope. The interface is often a power splitter, which divides the signal so that it can be recorded on two oscilloscope channels. This represents an input to output voltage gain of -6 dB. An integrator may also be used as part of the interface when an observable such as $\dot{B}(t)$ is sensed but it is desired to record $B(t)$. Passive integrators which cause signal attenuation are typically used. (Attenuation is variable with frequency.) Thus, the interface electronics transfer function ($H_I(\omega)$) acts to attenuate the output of the data link and has units of volts/volt. This is more complex when an integrator is used.

Finally, the oscilloscope input amplifier can be used for either amplification or attenuation. Therefore, its transfer function ($H_R(\omega)$) also has units of volts/volt.

A simple example will illustrate how the digitization scaling data and recording instrumentation scaling data must be applied to a digitized data set to generate a proper input data set for data processing routines. First, assume that the physical observable is induced current at some point in the test object and that the recording instrumentation system consists of a current transducer, microwave data link with input attenuator, interface electronics consisting of a power splitter, and a recording oscilloscope with input amplifier set at unity gain. Also assume that the oscilloscope superimposes a voltage calibration pulse on all waveforms of 20 millivolts peak-to-peak.

The first step in the calibration procedure is to subtract the origin coordinates Z_{x_0} and Z_{y_0} from all other digitized coordinates if this has not been done in the digitizer. Next, the rotation angle α is computed as indicated in Equation 3-6 and applied to all coordinate pairs as indicated in Equation 3-5. Then, the vertical and horizontal scale factors, SF_V and SF_H are computed as shown in Equations 3-7 and 3-11. These scale factors are applied to the digitized coordinates as

$$Z'_{x_i} = SF_H \times Z_{x_i} \quad (\text{Eq. 3-13})$$

$$Z'_{y_i} = SF_V \times Z_{y_i} \quad (\text{Eq. 3-14})$$

where:

Z'_{x_i} = scaled x- (or time) axis coordinates in
units of seconds

Z'_{y_i} = scaled y-axis coordinates in units of
millivolts

Z_{x_i} = unscaled or digitizing x-axis coordinates
in units of inches

Z_{y_i} = unscaled or digitizing y-axis coordinates
in units of inches.

The time-axis coordinates Z'_{x_i} are properly scaled at this point. Note that Z'_{x_i} are indicated as having units of seconds. This is because SF_H is assumed to have units of seconds/inch. Z'_{x_i} could as easily carry units of microseconds or nanoseconds depending on how SF_H is computed (see Paragraph 3.2.1.2). Z'_{x_i} at this point are scaled to their value in millivolts as recorded on the oscilloscope. It remains yet to scale them to the values of the physical observable which, in this case, is current.

To do so, note first that all of the instrumentation transfer functions are simple gains or attenuations that are assumed constant over their usable bandwidth, and all but one, the transducer transfer function, have units of volts/volt or are essentially unitless. Second, note that some of the gain factors involved in the transfer functions are constants (data link gain, power splitter attenuation, and oscilloscope amplifier gain) and others are variable (transducer transfer impedance and data link input attenuator). The fixed gain (or attenuation) factors can be lumped into a single scaling constant, G . The variable scale factors, transducer impedance, Z_T , and data link attenuator, A , can be treated as separate parameters. Final amplitude scaling can be computed as,

$$Z'_{y_i} = \frac{Z'_{y_i} \times G \times A}{Z_T} \text{ milliamps} \quad (\text{Eq. 3-15})$$

where:

Z'_{y_i} = properly scaled physical observable -
induced current - in milliamps

Z'_{y_i} = y-axis variable scaled to recording
oscilloscope voltage level in millivolts

G = fixed instrumentation gain

A = variable attenuator gain

Z_T = transducer transfer impedance in ohms

Note that if instrumentation gains are read in dB, then G and A must be calculated as

$$A = \log_{10}^{-1} \left(\frac{\text{attenuator setting in dB}}{20} \right) \quad (\text{Eq. 3-16})$$

and

$$G = \log_{10}^{-1} \left(\frac{\text{sum of the fixed gain values in dB}}{20} \right) \quad (\text{Eq. 3-17})$$

As indicated in earlier discussions, the interface electronics may contain an integrator in order to generate the desired physical observable when its derivative is sensed. Passive RC integrators are typically used for this purpose. For the typical transient waveforms seen in EMP testing (double exponential and damped sinusoids), the passive integrator introduces both attenuation (variable with frequency) and errors depending on waveform characteristics and integrator design parameters. This subject is treated in considerable detail in Reference 20.

3.2.3 Time Tying

3.2.3.1 Introduction

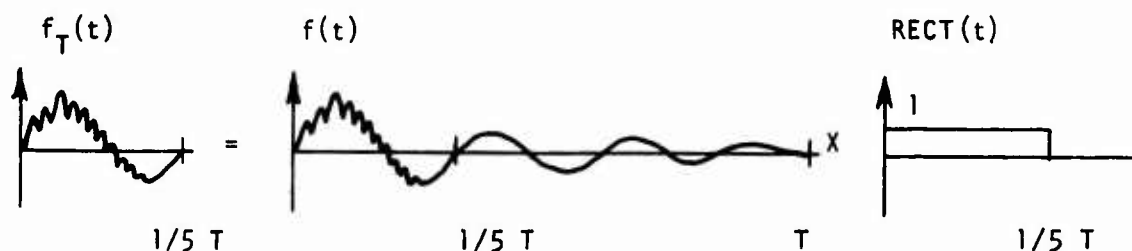
The electromagnetic response of a test object to EMP pulse (as opposed to CW) testing is generally of the form,

$$f(t) = \sum_{i=1}^m A_i e^{-\alpha_i t} + \sum_{j=1}^n B_j e^{-\gamma_j t} \sin(\beta_j t + \phi_j) \quad (\text{Eq. 3-18})$$

A typical response will be characterized by two or more resonant frequencies or damped sinusoids, with one of the resonant frequencies much higher than the others (five to 10 times) and with the high frequency response damping out early in the total response (first five to 20 percent). Thus, a typical response may look like the response waveform shown in Figure 3-2. This response has resonances at 1, 5, and 25 MHz.

If one were to attempt to digitize the waveform of Figure 3-2, it is obvious that it would be extremely difficult to digitize the early part of the waveform because of the "density" (or poor spatial resolution) of the information. The way around this dilemma is to expand the early portion of the waveform, as shown in Figure 3-3, so that the desired spatial resolution is obtained. However, in doing so, only $1/5$ of the total response waveform is represented in Figure 3-3, or the waveform has been truncated after $1/5$ of its total extent. If the truncated waveform were used as the input data to a data reduction routine (such as a Fourier transform), a considerable amount of distortion or error could occur in the transform results.

The nature of the error in the Fourier transform can be conveniently analyzed by noting that the truncated function ($f_T(t)$) is equal to the complete function ($f(t)$) multiplied by a rectangular wave of unit amplitude which starts at $t = 0$ and terminates at $t = 1/5 T$, where the length of $f(t)$ is T .



As shown in Paragraph 3.3 (which covers Fourier transform fundamentals) when two time functions are multiplied in the time domain, their respective Fourier transforms are convolved in the frequency domain. The rectangular

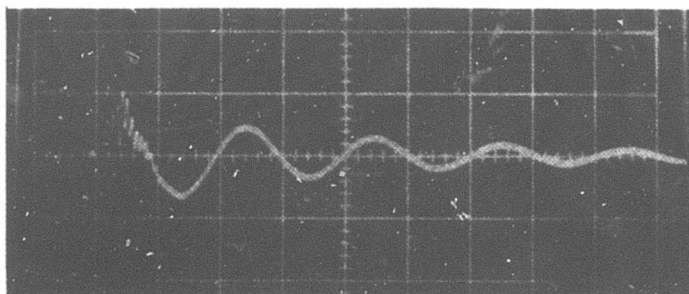


Figure 3-2. Complete Response Waveform
Recorded at 500 ns/Division

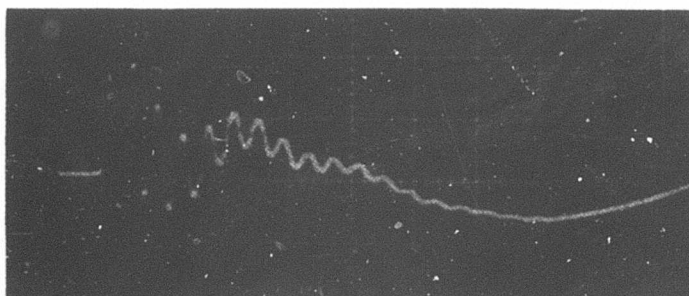


Figure 3-3. First 1/5th of the Complete
Waveform Recorded at 100 ns/
Division

time function $\text{Rect}(t)$ has as its Fourier transform the Sinc function where

$$\text{Sinc}(\omega T) = \frac{\sin(\omega T)}{\omega T}$$

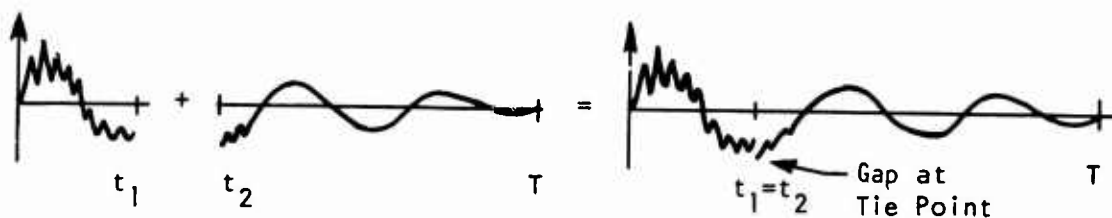
Thus whenever a time function is truncated, its Fourier transform is convolved with a Sinc function.

The solution to this problem is through time tying. In using this technique, the waveform of Figure 3-3 would be digitized to represent the response from $t = 0$ to $t = 1/5 T$. Then the waveform of Figure 3-2 would be digitized from $t = 1/5 T$ to $t = T$ to complete the digitized data set. These two data sets are then combined to obtain a digitized data set for the total waveform.

3.2.3.2 Implementation Problem Areas

There are several problems involved in the implementation of time tying. The first, and perhaps most severe, is how to find the "tie" point. The expanded (fast sweep) waveform is digitized from $t = 0$ to $t = t_1$ and the slow sweep waveform is digitized from $t = t_2$ to $t = T$, where again $t = T$ is the end of the recorded response. The end objective of whatever method is used to find the tie point is to have $t_2 = t_1$.

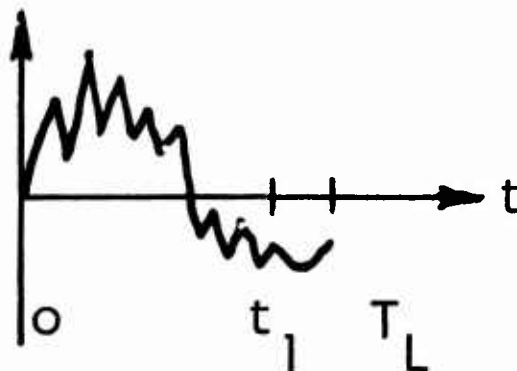
A second problem arises when the two recording oscilloscopes do not have the same vertical gain even though they are set the same. This results when the oscilloscopes are out of alignment. When this occurs, the two waveforms will not have the same amplitude value at the tie point which results in a discontinuity in the resulting waveform.



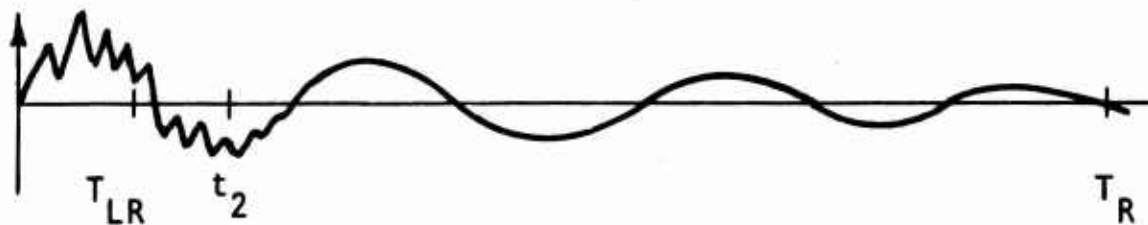
The final problem area which must be considered is in digitizing the waveforms. As will be discussed in subsequent paragraphs, cross correlation or least square error techniques are typically used in searching for the proper tie point. To use these techniques, there must be a common Δx (Δt) between sample points for each waveform. This means that either a digitizer which can take constant Δx data is used or point-by-point data are taken and then an interpolation routine is used to generate the constant Δx data sets. If the Δx for the two waveform segments is not the same, one should at least be an integral multiple of the other to facilitate tie point searching methods.

3.2.3.3 Methods for Finding the Tie Point²¹

Methods generally involve searching for the strongest similarity in the shape of the two waveforms in the vicinity of the proposed tie point. This means that the two waveforms must have some overlap about the proposed tie point. To facilitate the following analysis, let the two waveforms be designated the left waveform (fast sweep) and the right waveform (slow sweep). Let the left waveform be defined from $t = 0$ to $t = T_L$ and let a proposed tie point be selected at a value of $t < T_L$, say $t = t_1$.



Some criteria must be developed for selecting t_1 (e.g., $t_1 = 0.9 T_L$). Next, let the right waveform be defined from $t = T_{LR}$ to $t = T_R$ where $T_{LR} < t_1$. Also pick a point $t = t_2$ so that $t_2 \approx t_1$. Doing so gives an approximate location for starting the search for the tie point.

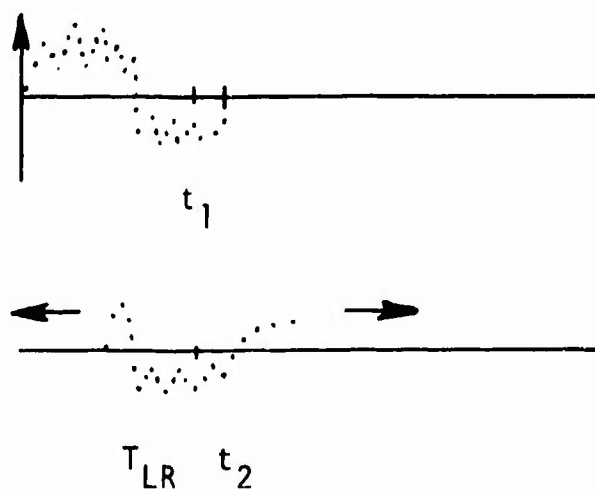


One may be tempted to make $T_{LR} = 0$ or the beginning of the right waveform. However, referring to Figure 3-3, it can be seen that this would require digitizing the high frequency data which begin at $t = 0$. Making $T_{LR} = 500$ ns on the scale of Figure 3-3 would be more realistic since this is a point at which there is sufficient waveform resolution for digitizing.

Based on the above definitions, the overlap between the two digitized data sets is from T_{LR} to T_L assuming the data sets are aligned at $t_1 = t_2$. What is desired now is a measure of closeness between the overlapping portions of the two waveforms. When the measure is maximized, presumably the waveforms are in the correct position and the tie can be made. There are at least three such measures available.

- (1) The cross correlation index.
- (2) The least squares error.
- (3) The absolute value of error.

In using any of these techniques, one can assume that the left waveform is fixed and the right waveform has slid to the left or right about $t = t_1$ in search of the maximum.



When the two data sets are aligned at $t_1 = t_2$, there will be m common data points between the two data sets in the interval of overlap (T_{LR} to T_L). However, as the right waveform is slid to the left, m increases and to the right m decreases. It is convenient to base the measure of closeness on a fixed number of points as the waveform is slid left and right. Therefore, one can pick n data points ($n < m$) centered on t_1 and base the measure always on these n points. This, of course, assumes that a maximum will be found before a position is reached such that the number of overlapping points is less than n when sliding the waveform to the right.

3.2.3.4 Correcting for Amplitude Differences²²

If there is relative amplitude difference between the left and right waveforms, this can be corrected for after the time tie point has been found. To do so, one can ratio the n overlapping points in the two waveforms to find the relative point-to-point amplitude difference. These n ratios can then be averaged to develop a scale factor to apply to all data points of the appropriate waveform.

Even when a time tie point has been found, and the waveforms are scaled to the same relative amplitude, there may be a discontinuity at the tie point. That is, if the coordinates of point t_1 are (x_1, y_1) and the tie point for the right waveform is t_3 with coordinates (x_3, y_3) , then y_1 may not equal y_3 (x_3 by definition equals x_1). The problem arises as to what y value should be chosen for this coordinate point and what criteria should be used to select it. No such criteria are known to exist. However, to minimize any discontinuity at this point, an interpolation based on several data points on either side of this point would be appropriate.

3.2.3.5 Summary

Time tying of EMP test waveforms is apparently not a commonly used technique.* This might be surprising since many of the response data recorded have high frequency information at the beginning of the response waveform which damps out quickly but the total response lasts from five to 10 times as long. Therefore, the analyst is faced with using digitized data that do not well represent the waveform when a slow sweep waveform is digitized. On the other hand, if a fast sweep oscillograph is used in digitizing, he must accept truncation error. It is not so surprising then that these techniques are not widely used since there are obviously many problems involved in implementing a practical algorithm.

One of the more promising practical techniques for time tying is being pioneered at the AFWL computer division. The two digitized waveforms are displayed on a digital CRT (vector display) with light pen capability. An operator makes a time tie decision based completely on visual judgment, apparently with very acceptable results.

3.3 BASIC TRANSFORM THEORY

3.3.1 Introduction

There are a variety of transform techniques that convert data as a function of the independent variable, time, into a function proportional to the inverse of time, namely frequency. Choice of a particular transform technique depends on the nature of the data being studied, the instrumentation used to record the data, and the available data reduction capabilities. EMP experimental data are characterized as transient time domain analog types of signals that are transmitted and recorded with analog instrumentation. On the other hand, the bulk of the instrumentation calibration data are obtained experimentally as functions of frequency.

*The SEIGE MILL at AFWL is one facility which has successfully used time techniques.

These conditions imply that the optimum transform technique is the Fourier integral Transform (FIT)*. Consideration of the available data reduction hardware, computer software, and computer running economy could suggest the use of the Time Sampled Fourier Transform (TSFT), the Fourier Series Transform (FST), or the Discrete Fourier Transform (DFT)**. All these transforms are candidate techniques for use in EMP data analysis; however, the TSFT, the FST, and the DFT can be shown to be special cases of the FIT. Therefore, this subsection will be devoted to the FIT. A thorough understanding of the FIT will provide the necessary background for understanding the application and limitations of the other transforms that will be discussed in the following subsections.

The following portions of this subsection will present selected topics on the theory of the FIT that are most applicable to the reduction and analysis of EMP data. This material is not intended to duplicate that contained in several good references on the subject. Inevitably, the results of this section will not be original, however, the approach used in presenting the material will differ from the available references. The material is directed to the typical individual who is not a mathematical specialist, but is assigned to the analysis of EMP data. Emphasis will be placed on two aspects: one is the development of a set of mathematical procedures that are directly applicable to EMP data analysis; the second is acquiring skill in interpreting mathematical relations and graphical displays of data. The selection of topics is based on observations at ARES of the most useful techniques and the areas where mistakes were the most frequent.

This subsection on the FIT contains nine major topics. The first is a definition of the FIT and a discussion of when the transform exists. Next is the interpretation of the defining integral for certain

* The rationale for this statement will be developed in a later portion of this section.

** The Fast Fourier Transform (FFT) is a very efficient version of the DFT.

classes of waveforms. Skill in this interpretation is required to understand methods commonly used to compute the FIT. The third topic concerns scaling relations among transform pairs. Then the transforms of several common waveforms are developed. These simple transforms and the scaling relations permit the analysis of a large variety of waveforms. The fifth topic is a presentation of graphical methods useful for obtaining hand sketches of Fourier transforms. These forms permit a simple check on the accuracy and validity of transform calculations. The next topic is a presentation of two special functions, namely the delta and the step function. The seventh topic develops the relationship between multiplication of two functions in one domain (either time or frequency) and the corresponding convolution operation in the opposite domain. Thorough mastery of these last two topics is required to understand applications of transform theory. The next topic is a comparison of the FIT to the related Laplace transform. Finally, a series of examples is presented that illustrates the application of the material presented previously. Some of these examples are based on problems occurring at ARES.

3.3.2 Definitions

The Fourier Integral Transform, $G(\omega)$, of the function, $g(t)$, is defined as

$$G(\omega) = \int_{-\infty}^{\infty} g(t) e^{-j\omega t} dt, \quad \omega = 2\pi f \quad (\text{Eq. 3-19})$$

where ω is the angular frequency. The inverse of Equation 3-19 expressing $g(t)$ as a function of $G(\omega)$ is given by

$$g(t) = \frac{1}{2\pi} \int_{-\infty}^{\infty} G(\omega) e^{j\omega t} d\omega \quad (\text{Eq. 3-20})$$

Equations 3-19 and 3-20 are known as the FIT pair and the relationship of this pair is sometimes symbolically indicated as

$$g(t) \longleftrightarrow G(\omega) \quad (\text{Eq. 3-21})$$

The only restriction on the definition of the FIT is that the integrals must exist. The prerequisite of linearity is not required at this stage because there has been no attempt yet to relate the response to the excitation. A qualitative statement concerning the existence of the defining integrals is that if $g(t)$ corresponds to a finite energy process, the integrals exist. A mathematical statement of the above is that $g(t)$ must be absolutely integrable or

$$\int_{-\infty}^{\infty} |g(t)| dt < \infty \quad (\text{Eq. 3-22})$$

There are important exceptions where $g(t)$ is not absolutely integrable and the Fourier transform exists. These exceptions are discussed in the subsection on special functions. However, in most engineering applications, Equation 3-22 is an adequate test.

There are several comments concerning the basic definitions. One is that the usual notation will be used where upper case letters signify frequency domain functions and lower case letters signify time domain functions. Sometimes the notation, $F\{ \}$ is used

$$F\{g(t)\} = G(\omega) = \int_{-\infty}^{\infty} g(t) e^{-j\omega t} dt \quad (\text{Eq. 3-23})$$

to signify the time to frequency domain transform and, $F^{-1}\{ \}$,

$$F^{-1}\{G(\omega)\} = g(t) = \frac{1}{2\pi} \int_{-\infty}^{\infty} G(\omega) e^{j\omega t} d\omega \quad (\text{Eq. 3-24})$$

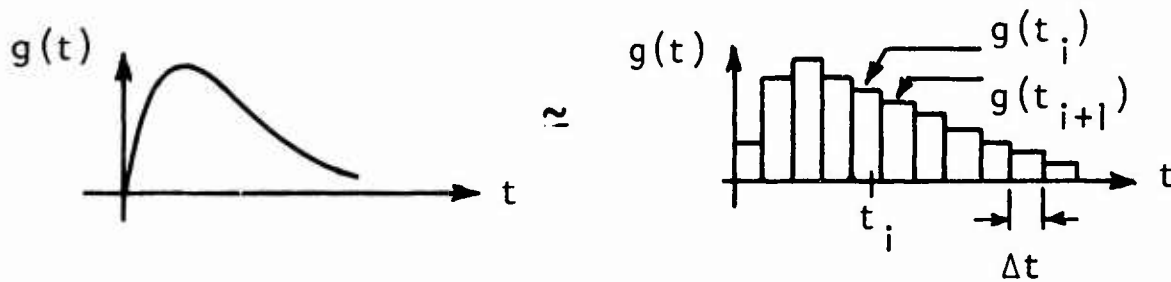
to indicate the frequency to time domain transform. A second comment is that, in general, both $g(t)$ and $G(\omega)$ can be complex. In other words, they have a real and an imaginary part. The third comment concerns the scale factor $1/(2\pi)$ and the signs of the exponents inside the integral. Other valid definitions of the FIT pair could have factors such as $1/\sqrt{2\pi}$ in front of each integral and have the signs of exponents reversed. However, the notation used in Equations 3-19 and 3-20 are the most common forms used in engineering work. The reader should be alert to other possible definitions used elsewhere.

3.3.3 Interpretation of the Integral Pair

Before considering particular examples of functions, $g(t)$, to be used in Equations 3-19 and 3-20, there are several generalizations that can be deduced from the basic form of the integrals. These include the superposition process, restrictions on the real and imaginary parts of $G(\omega)$ based on the form of $g(t)$ and the shape of $g(t)$ as a function of the form of $G(\omega)$.

3.3.3.1 Superposition

One important observation concerning the definitions of the FIT is that the transform consists of a superposition process. Consider a specific frequency, ω_0 . Then, reducing the integral to the sum of pulse approximations of the functions



you find that $G(\omega_0)$ consists of contributions from $g(t)$ at each value of time, t_i , weighted by the values of $e^{-j\omega_0 t_i}$.

$$G(\omega_0) \approx \sum_i g(t_i) e^{-j\omega_0 t_i} \Delta t \quad (\text{Eq. 3-25})$$

In this application, $e^{-j\omega_0 t_i}$ is a function of t_i only since ω_0 is fixed. In a similar manner, the value of $g(t)$ at a specific time, t_0 , consists of contributions from $G(\omega)$ at each value of ω . Thus,

$$g(t_0) \approx \frac{1}{2\pi} \sum_i G(\omega_i) e^{j\omega_i t_0 \Delta\omega} \quad (\text{Eq. 3-26})$$

3.3.3.2 Even and Odd Symmetry

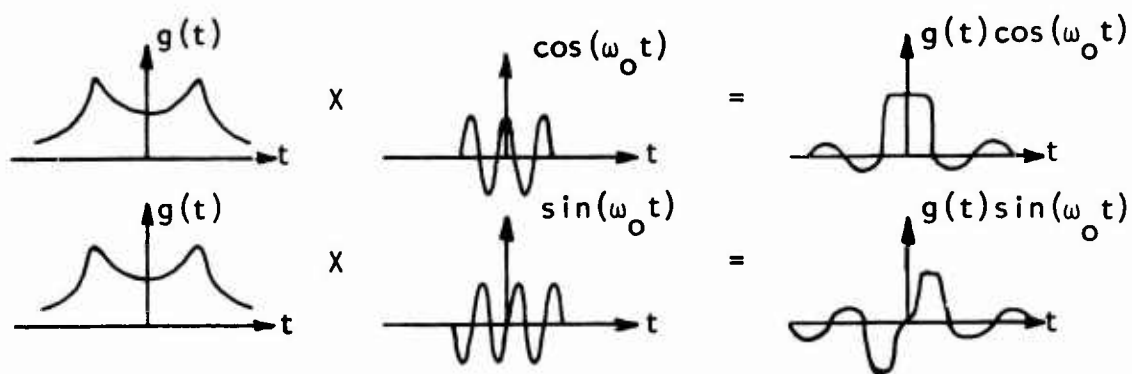
It was mentioned previously that both $g(t)$ and $G(\omega)$ can be complex in the definition of the FIT. However, any measurement of a transient time domain phenomenon is entirely real, and this restriction allows certain simplifications of the integral definitions. Noting Euler's identity

$$e^{\pm j\theta} = \cos\theta \pm j\sin\theta \quad (\text{Eq. 3-27})$$

one finds that Equation 3-19 can be written as

$$\begin{aligned} G(\omega) &= \int_{-\infty}^{\infty} g(t) \cos(\omega t) dt - j \int_{-\infty}^{\infty} g(t) \sin(\omega t) dt \\ &= R_e\{G\} + j I_m\{G\} \end{aligned} \quad (\text{Eq. 3-28})$$

where the notation R_e and I_m signify the real and imaginary parts respectively. Thus, in general, $G(\omega)$ is complex when $g(t)$ is real. Now consider the symmetry of the definitions of $R_e\{G\}$ and $I_m\{G\}$. Note that $\cos\omega t$ is an even function of t and $\sin(\omega t)$ is an odd function of t . If $g(t)$ is an even function of t ,



the contribution to the integral over the interval $(0, \infty)$ is equal to the contribution from the interval $(-\infty, 0)$ and $G(\omega)$ is real

$$G(\omega) = R_e\{G\} = 2 \int_0^{\infty} g(t) \cos(\omega t) dt, \quad g(t) \text{ even} \quad (\text{Eq. 3-29})$$

The imaginary part is identically equal to zero since the contribution to the integral from $(0, \infty)$ is equal and opposite to that from $(-\infty, 0)$. If $g(t)$ is an odd function of t , then $G(\omega)$ is imaginary.

$$G(\omega) = j I_m\{G\} = -j 2 \int_0^{\infty} g(t) \sin(\omega t) dt, \quad g(t) \text{ odd} \quad (\text{Eq. 3-30})$$

The justification is similar to that for the case when $g(t)$ is even.

Inspection of Equation 3-28 shows that $R_e\{G\}$ is an even function of ω and $I_m\{G\}$ is an odd function of ω when $g(t)$ is real. This fact can be verified by noting

$$R_e\{G(\omega)\} = \int_{-\infty}^{\infty} g(t) \cos(\omega t) dt = \int_{-\infty}^{\infty} g(t) \cos(-\omega t) dt = R_e\{G(-\omega)\} \quad (\text{Eq. 3-31})$$

and

$$I_m\{G(\omega)\} = \int_{-\infty}^{\infty} g(t) \sin(\omega t) dt = - \int_{-\infty}^{\infty} g(t) \sin(-\omega t) dt = -I_m\{G(-\omega)\}$$

The restriction that $g(t)$ is real can be used to simplify the inverse transform given by Equation 3-20. Substituting Equations 3-27 and 3-28 into Equation 3-20, one finds

$$g(t) = \frac{1}{2\pi} \int_{-\infty}^{\infty} \left[R_e\{G\} + j I_m\{G\} \right] \left[\cos(\omega t) + j \sin(\omega t) \right] d\omega \quad (\text{Eq. 3-32})$$

$$g(t) = \frac{1}{2\pi} \int_{-\infty}^{\infty} \left[R_e\{G\} \cos(\omega t) - I_m\{G\} \sin(\omega t) \right] d\omega + j \frac{1}{2\pi} \int_{-\infty}^{\infty} \left[R_e\{G\} \sin(\omega t) + I_m\{G\} \cos(\omega t) \right] d\omega$$

Note that both of the terms in the second integral of Equation 3-32 are odd since they are the product of an even and an odd function. Since the integral of an odd function over the interval $(-\infty, \infty)$ is equal to zero, the second part of Equation 3-32 is indentially equal to zero and $g(t)$ equals

$$g(t) = \frac{1}{2\pi} \int_{-\infty}^{\infty} \left[R_e\{G\} \cos(\omega t) - I_m\{G\} \sin(\omega t) \right] d\omega \quad (\text{Eq. 3-33})$$

Since both terms inside the integral of Equation 3-33 are even, $g(t)$ can be written as

$$g(t) = \frac{1}{\pi} \int_0^{\infty} \left[R_e\{G\} \cos(\omega t) - I_m\{G\} \sin(\omega t) \right] d\omega \quad (\text{Eq. 3-34})$$

3.3.3.3 Transient Signals

For a transient signal, one can define a specific starting time, t_0 , such that $g(t) \equiv 0$ for $t < t_0$. The starting time can be arbitrarily set to zero without loss of generality. Then $g(t) \equiv 0$ for $t < 0$. Using Equation 3-34 and substituting $-t$ for t , one finds

$$g(-t) = \frac{1}{\pi} \int_0^{\infty} \left[R_e\{G\} \cos(-\omega t) - I_m\{G\} \sin(-\omega t) \right] d\omega \quad (\text{Eq. 3-35})$$

$$0 = \frac{1}{\pi} \int_0^{\infty} \left[R_e\{G\} \cos(\omega t) + I_m\{G\} \sin(\omega t) \right] d\omega \quad (\text{Eq. 3-36})$$

The integral over each term in Equation 3-35 is generally not equal to zero since each term is an even function of ω . Therefore, the integral over each term must be equal in amplitude and opposite in sign such that

$$\frac{1}{\pi} \int_0^{\infty} R_e\{G\} \cos(\omega t) d\omega = - \frac{1}{\pi} \int_0^{\infty} I_m\{G\} \sin(\omega t) d\omega \quad (\text{Eq. 3-37})$$

Using this relationship, it is found that $g(t)$ reduces to

$$g(t) = \frac{2}{\pi} \int_0^{\infty} R_e\{G\} \cos(\omega t) d\omega = - \frac{2}{\pi} \int_0^{\infty} I_m\{G\} \sin(\omega t) d\omega \quad (\text{Eq. 3-38})$$

It should be noted that Equation 3-38 is not valid when $t = 0$. Referring to Equation 3-34 with t set equal to zero, one finds

$$g(0) = \frac{1}{\pi} \int_0^{\infty} R_e\{G\} d\omega \quad (\text{Eq. 3-39})$$

3.3.3.4 Negative Frequency

Inspection of Equations 3-19 and 3-20 shows that the concept of negative frequency is employed in the definition of the FIT. An interesting question is what is the physical significance of a negative frequency. The answer is that there is no physical significance whatsoever in this concept. The origin of the negative frequency concept stems from the use of $e^{+j\omega t}$. However, Equation 3-27 can be used to show that

$$\begin{aligned}\cos(\omega t) &= \frac{1}{2} \left[e^{j\omega t} + e^{-j\omega t} \right] \\ \sin(\omega t) &= \frac{1}{2j} \left[e^{j\omega t} - e^{-j\omega t} \right]\end{aligned}\quad (\text{Eq. 3-40})$$

At a fixed value of time, these real valued trigonometric functions consist of contributions from positive and negative frequencies. These trigonometric functions have physical significance since they can be measured with a physical instrument where only positive frequencies have any meaning. Indeed, inspection of Equation 3-34 shows that if $g(t)$ is real, only positive values of frequency are required. Thus, the concept of negative frequency has mathematical significance only, and it is employed to obtain the notational simplicity afforded by use of the function $e^{+j\omega t}$.

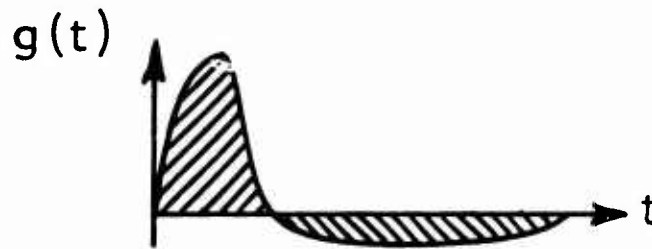
3.3.3.5 Asymptotic Values

Use of asymptotic values of $g(t)$ and $G(\omega)$ provides a means of checking the accuracy and validity of transform calculations. Two asymptotic forms are available in the previous material. They are the values of $g(t)$ and $G(\omega)$ as t and ω , respectively, approach zero. Equation 3-41 gives the value of $g(t)$ as t approaches zero from positive values of time and Equation 3-42 gives the value of $G(\omega)$ as ω approaches zero from positive values of frequency.

$$g(0^+) = \frac{1}{\pi} \int_0^{\infty} R_e \{G\} d\omega \quad (\text{Eq. 3-41})$$

$$G(0^+) = \int_0^{\infty} g(t) dt \quad (\text{Eq. 3-42})$$

Thus, the dc or zero frequency component of a transient waveform is equal to the net area under $g(t)$



Equation 3-42 has an interesting physical interpretation applicable to EMP studies. Since it is impossible for an antenna to radiate energy at zero frequency, then an antenna excited by some transient voltage source must radiate a waveform that has exactly zero net area.

The asymptotic values of $G(\omega)$ as ω approaches infinity are of considerable interest. The following development shows that the asymptotic values are dominated by the type of discontinuities in $g(t)$. Consider a waveform, $g(t)$, with a discontinuity equal to

$$\Delta g = g(t_0^+) - g(t_0^-) \quad (\text{Eq. 3-43})$$

at $t = t_0$. The symbols $g(t_0^+)$ and $g(t_0^-)$ indicate the values of $g(t)$ when t approaches t_0 from positive and negative values of time respectively. Now divide the integral defining $G(\omega)$ into two parts such that

$$G(\omega) = \int_{-\infty}^{t_0} g(t) e^{-j\omega t} dt + \int_{t_0}^{\infty} g(t) e^{-j\omega t} dt \quad (\text{Eq. 3-44})$$

Integrating Equation 3-44 by parts, one finds

$$G(\omega) = \left(\frac{-1}{j\omega}\right) \left\{ \left[g(t)e^{-j\omega t} \right]_{-\infty}^{t_0} + \left[g(t)e^{-j\omega t} \right]_{t_0}^{\infty} \right\} + \left(\frac{1}{j\omega}\right) \left\{ \int_{-\infty}^{t_0} g'(t)e^{-j\omega t} dt + \int_{t_0}^{\infty} g'(t)e^{-j\omega t} dt \right\} \quad (\text{Eq. 3-45})$$

where $g'(t)$ indicates the derivative of $g(t)$. If the second line of Equation 3-45 is integrated by parts, $G(\omega)$ equals

$$G(\omega) = \left(\frac{-1}{j\omega}\right) \left\{ \left[g(t)e^{-j\omega t} \right]_{-\infty}^{t_0} + \left[g(t)e^{-j\omega t} \right]_{t_0}^{\infty} \right\} + \left(\frac{-1}{j\omega}\right) \left(\frac{1}{j\omega}\right) \left\{ \left[g'(t)e^{-j\omega t} \right]_{-\infty}^{t_0} + \left[g'(t)e^{-j\omega t} \right]_{t_0}^{\infty} \right\} + \left(\frac{1}{j\omega}\right)^2 \left\{ \int_{-\infty}^{t_0} g''(t)e^{-j\omega t} dt + \int_{t_0}^{\infty} g''(t)e^{-j\omega t} dt \right\} \quad (\text{Eq. 3-46})$$

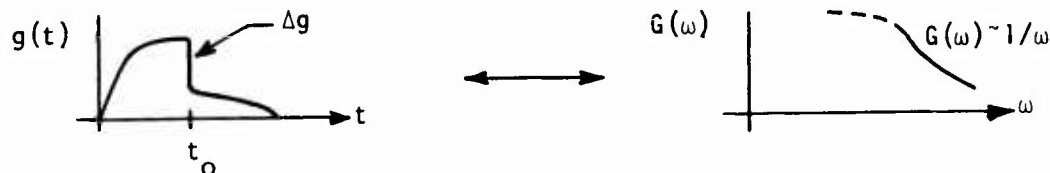
This messy equation can be simplified by noting that if $g(t)$ is a finite energy process, $g(t)$ must approach zero for large values of positive and negative time. Also note that the second and third lines of Equation 3-46 are multiplied by a $1/\omega^2$ term. Thus

$$G(\omega) = \frac{\Delta g}{(j\omega)} e^{-j\omega t_0} + o\left(\frac{1}{\omega^2}\right) \quad (\text{Eq. 3-47})$$

where $o\left(\frac{1}{\omega^2}\right)$ indicates that the terms on the second and third lines of Equation 3-46 are on the order of $1/\omega^2$. In the limit as ω approaches

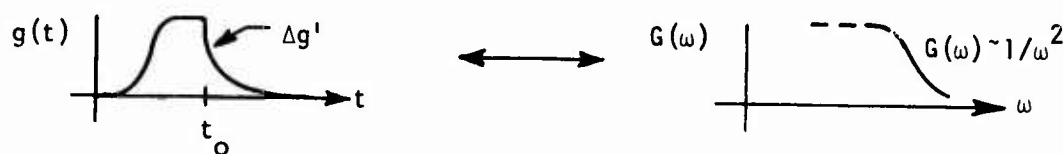
infinity, $G(\omega)$ is approximately equal to

$$G(\omega) \approx \frac{\Delta g}{(j\omega)} e^{-j\omega t_0}, \quad \omega \rightarrow \infty \quad (\text{Eq. 3-48})$$



If $g(t)$ is continuous but has a slope discontinuity equal to $\Delta g'$ at $t = t_0$, the value of $G(\omega)$ as ω approaches infinity is

$$G(\omega) \approx \frac{\Delta g'}{(j\omega)^2} e^{-j\omega t_0}, \quad \omega \rightarrow \infty \quad (\text{Eq. 3-49})$$



if $g(t)$ and its first $n-1$ derivatives are continuous but its n^{th} derivative has a discontinuity equal to $\Delta g^{(n)}$ at $t = t_0$, $G(\omega)$ approaches

$$G(\omega) \approx \frac{\Delta g^{(n)}}{(j\omega)^{n+1}} e^{-j\omega t_0}, \quad \omega \rightarrow \infty \quad (\text{Eq. 3-50})$$

Equations 3-49 and 3-50 may be verified by repeated integration by parts.

3.3.4 Waveform Modification

There are a variety of simple operations that can be performed on a waveform such as axis scaling, waveform translation in both the time and frequency domain, and differentiation. These operations result in simple modifications of the transform of the basic waveform. Knowledge of the effect of these simple operations is mandatory for one who would use transform theory with any facility. The following paragraphs develop some of the more important relations.

3.3.4.1 Similarity

Given a function $g(t)$ and its transform $G(\omega)$, suppose the variable in $G(\omega)$ is changed to t and the function $G(t)$ is plotted in the time domain. Now it is desired to find the transform of $G(t)$. The result may be obtained in the following way. First change t to $-t$ in Equation 3-20

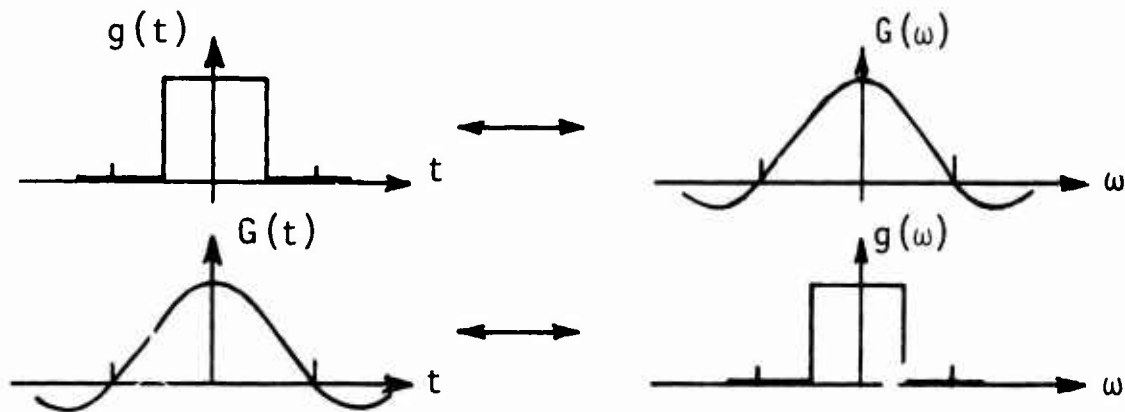
$$g(-t) = \frac{1}{2\pi} \int_{-\infty}^{\infty} G(\omega) e^{-j\omega t} d\omega \quad (\text{Eq. 3-51})$$

Now exchange the variables t and ω

$$g(-\omega) = \frac{1}{2\pi} \int_{-\infty}^{\infty} G(t) e^{-j\omega t} dt \quad (\text{Eq. 3-52})$$

If Equation 3-52 is multiplied by 2π , one finds the transform of $G(t)$ is

$$F \{ G(t) \} = \int_{-\infty}^{\infty} G(t) e^{-j\omega t} dt = 2\pi g(-\omega) \quad (\text{Eq. 3-53})$$



Thus, the transform of $G(t)$ is found by substituting $-\omega$ for t in $g(t)$ and multiplying by the factor 2π .

3.3.4.2 Axis Scaling

There are many occasions where it is desired to scale the amplitude and time axes of a waveform by a multiplicative constant and calculate the modified transform. This procedure is nearly always required when using analytic forms of Fourier transform pairs listed in standard references. Since the Fourier transform is a linear operation, scaling the time domain waveform by an arbitrary constant results in a transform scaled by the same constant. Given a transform pair $g(t) \leftrightarrow G(\omega)$, and if $g(t)$ is multiplied by an arbitrary constant, A , which can be real, imaginary, or complex, the resultant transform is

$$Ag(t) \leftrightarrow AG(\omega) \quad (\text{Eq. 3-54})$$

The effect of scaling the time axis of a waveform $g(t)$ that has a transform $G(\omega)$ may be found in the following way. Let the variable, time, be multiplied by a real positive constant such that the time domain waveform is now $g(at)$. The transform is formally defined as

$$F \{ g(at) \} = \int_{-\infty}^{\infty} g(at) e^{-j\omega t} dt \quad (\text{Eq. 3-55})$$

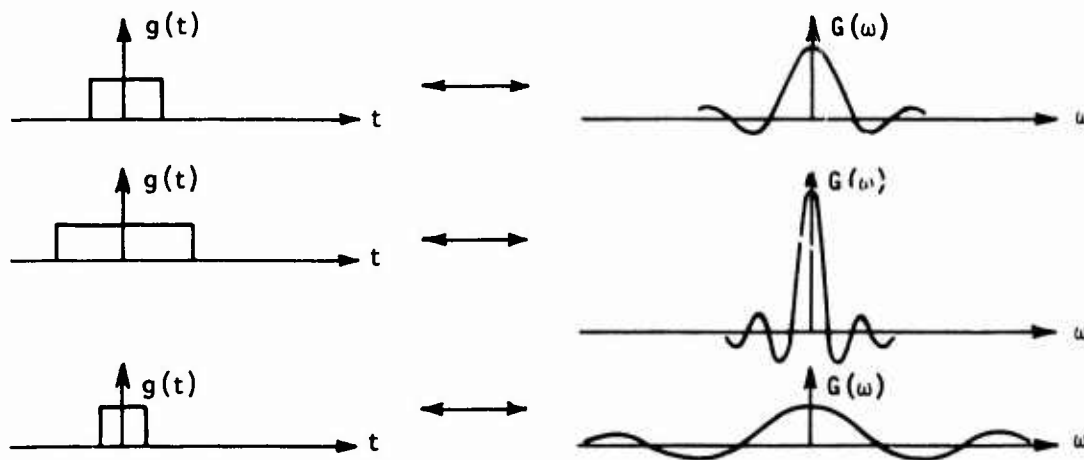
Now substitute the variable, $\tau = at$, into Equation 3-55 to yield

$$\begin{aligned} F \{ g(at) \} &= \frac{1}{a} \int_{-\infty}^{\infty} g(\tau) e^{-j\tau(\omega/a)} d\tau \quad (\text{Eq. 3-56}) \\ &= \frac{1}{a} G(\omega/a) \end{aligned}$$

If a is either positive or negative, the result is

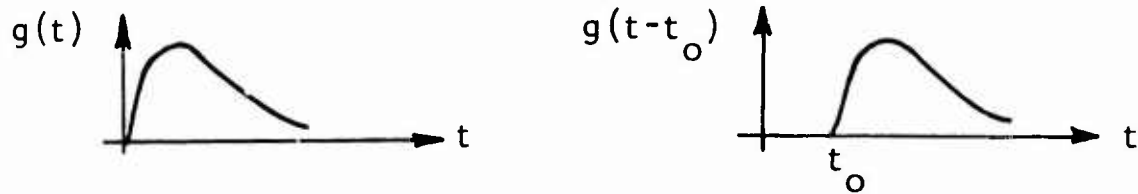
$$F \{ g(at) \} = \frac{1}{|a|} G(\omega/a) \quad (\text{Eq. 3-57})$$

Thus, if the time axis is stretched ($a < 1$), the frequency axis is compressed and the frequency domain amplitude is increased.



3.3.4.3 Time and Frequency Shifts

Shifting the origin of either $g(t)$ or $G(\omega)$ is used quite frequently/in deriving new transform pairs. The effects of such shifts on the resulting transforms is demonstrated below. Assume one has a transform pair, $g(t) \leftrightarrow G(\omega)$, and one shifts the time origin to form $g(t - t_0)$.



The transform of $g(t - t_0)$ is formally defined as

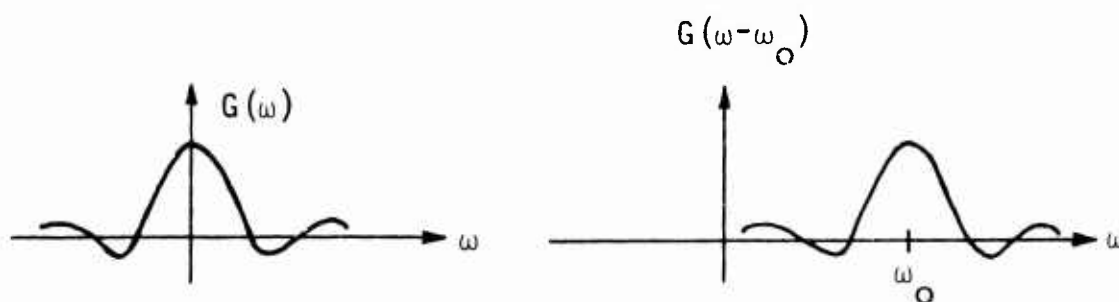
$$F \{ g(t - t_0) \} = \int_{-\infty}^{\infty} g(t - t_0) e^{-j\omega t} dt \quad (\text{Eq. 3-58})$$

If $\tau = t - t_0$ is substituted in the above equation, one finds

$$\begin{aligned} F \{ g(t - t_0) \} &= \int_{-\infty}^{\infty} g(\tau) e^{-j\omega(\tau + t_0)} d\tau \quad (\text{Eq. 3-59}) \\ &= e^{-j\omega t_0} \int_{-\infty}^{\infty} g(\tau) e^{-j\omega \tau} d\tau \\ &= e^{-j\omega t_0} G(\omega) \end{aligned}$$

Thus, a shift in the origin of a time function does not affect the magnitude of the original transform. However, a phase term proportional to frequency is added to the original phase of the transform.

The effect of a shift in the origin of $G(\omega)$ can be found in a similar manner. Assume the origin of $G(\omega)$ is shifted by an amount, ω_0 , to form $G(\omega - \omega_0)$.



The formal definition of the transform is

$$F^{-1}\{G(\omega - \omega_0)\} = \frac{1}{2\pi} \int_{-\infty}^{\infty} G(\omega - \omega_0) e^{j\omega t} d\omega \quad (\text{Eq. 3-60})$$

Substituting ω' for $\omega - \omega_0$, one finds

$$F^{-1}\{G(\omega - \omega_0)\} = \frac{1}{2\pi} \int_{-\infty}^{\infty} G(\omega') e^{j(\omega' + \omega_0)t} d\omega' \quad (\text{Eq. 3-61})$$

$$= e^{j\omega_0 t} \frac{1}{2\pi} \int_{-\infty}^{\infty} G(\omega') e^{j\omega' t} d\omega'$$

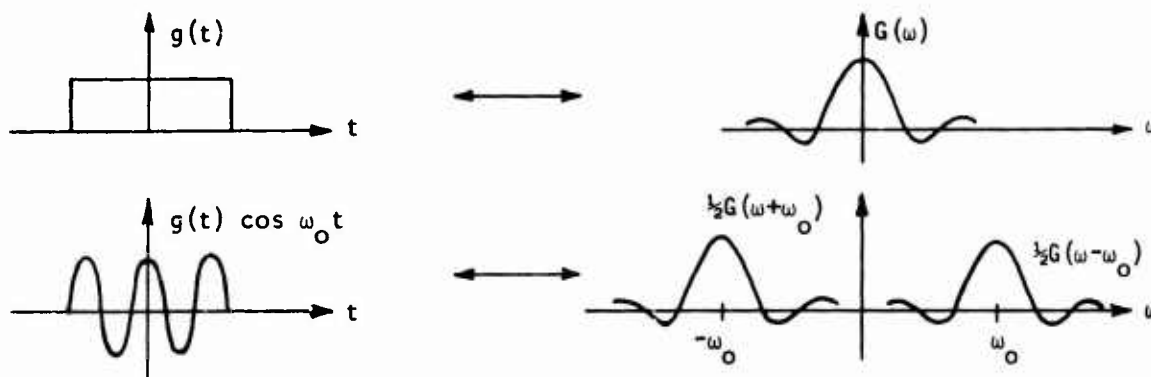
$$= e^{j\omega_0 t} g(t)$$

Thus, a shift in the origin of $G(\omega)$ by the amount ω_0 results in a time domain function equal to the original time domain function, $g(t)$, multiplied by the term $e^{j\omega_0 t}$. A practical application of these results is to find the transform of a modulated carrier wave. Noting that

$$F^{-1} \{ G(\omega + \omega_0) \} = e^{-j\omega_0 t} g(t) \quad (\text{Eq. 3-62})$$

one finds

$$F \{ g(t) \cos \omega_0 t \} = \frac{1}{2} [G(\omega + \omega_0) + G(\omega - \omega_0)] \quad (\text{Eq. 3-63})$$



3.3.4.4 Differentiation

Signals proportional to the time derivative of measured currents or electromagnetic fields are commonly produced by existing EMP test instrumentation. Therefore, the relationship between the transform of a derivative signal and the original function is required.

Direct differentiation of Equation 3-20 yields the desired results. The derivative may be taken inside the integral because t is a parameter in this case. The n^{th} derivative of Equation 3-20 yields

$$g^{(n)}(t) = \frac{1}{2\pi} \int_{-\infty}^{\infty} (j\omega)^n G(\omega) e^{j\omega t} d\omega \quad (\text{Eq. 3-64})$$

Thus, the transform pair associated with the n^{th} derivative of a time domain function is

$$g^{(n)}(t) \leftrightarrow (j\omega)^n G(\omega) \quad (\text{Eq. 3-65})$$

Although one is tempted to define the inverse process at this time, namely integration, the topic will be deferred to a later section where the necessary material can be developed.

The transform of the derivative of a frequency domain function, $G(\omega)$, is determined in a similar manner to the above. The n^{th} derivative of Equation 3-19 is

$$G^{(n)}(\omega) = \int_{-\infty}^{\infty} (-jt)^n g(t) e^{-j\omega t} dt \quad (\text{Eq. 3-66})$$

Therefore, the transform pair associated with the n^{th} derivative of a frequency domain function is

$$G^{(n)}(\omega) \leftrightarrow (-jt)^n g(t) \quad (\text{Eq. 3-67})$$

Equations 3-65 and 3-67 define the transforms of the derivatives of time and frequency domain functions assuming that they exist. Discontinuities could prevent the definition of the derivative. Furthermore, the n^{th} derivative of a function might not have a valid Fourier transform. Therefore, the derivative relations must be used with care.

3.3.5 Simple Transforms

There are several waveforms that characterize the essential features of many EMP test waveforms. Furthermore, these waveforms and their associated transforms are sufficiently simple to compute and plot that the EMP data analyst should have a thorough working knowledge of these relations. The following paragraphs develop some of the most common transform pairs.

3.3.5.1 Exponential

Consider a waveform given by

$$g(t) = e^{-\alpha t}, \quad \alpha > 0, t \geq 0 \quad (\text{Eq. 3-68})$$

Straightforward application of Equation 3-19 yields the Fourier transform of this signal

$$\begin{aligned} F \{ e^{-\alpha t} \} &= \lim_{T \rightarrow \infty} \int_0^T e^{-\alpha t} e^{-j\omega t} dt \\ &= \left(\frac{1}{\alpha + j\omega} \right) \lim_{T \rightarrow \infty} \left[1 - e^{-\alpha T} e^{-j\omega T} \right] \quad (\text{Eq. 3-69}) \\ &= \frac{1}{\alpha + j\omega} \end{aligned}$$

Thus

$$e^{-\alpha t} \leftrightarrow \frac{1}{\alpha + j\omega} \quad t \geq 0, \alpha > 0 \quad (\text{Eq. 3-70})$$

3.3.5.2 Double Exponential

A so-called double exponential signal is characteristic of the electromagnetic environment in EMP simulators such as ARES. This waveform is expressed as

$$g(t) = e^{-\alpha t} - e^{-\beta t}, \quad \beta > \alpha > 0, t \geq 0 \quad (\text{Eq. 3-71})$$

The transform of the above equation is obtained by using Equation 3-69

$$\begin{aligned} F \{ e^{-\alpha t} - e^{-\beta t} \} &= \frac{1}{\alpha + j\omega} - \frac{1}{\beta + j\omega} \\ &= \frac{\beta - \alpha}{(\alpha + j\omega)(\beta + j\omega)} \end{aligned} \quad (\text{Eq. 3-72})$$

Thus

$$e^{-\alpha t} - e^{-\beta t} \leftrightarrow \frac{\beta - \alpha}{(\alpha + j\omega)(\beta + j\omega)}, \quad \beta > \alpha > 0, t \geq 0 \quad (\text{Eq. 3-73})$$

3.3.5. Damped Sinusoid

A decaying sinusoidal oscillation is characteristic of many response signals observed on EMP tests. Assume this waveform is represented as

$$g(t) = e^{-\alpha t} \sin \beta t, \quad \beta > \alpha \geq 0; t \geq 0 \quad (\text{Eq. 3-74})$$

Then application of Equations 3-19 and 3-40 yield

$$\begin{aligned}
F \{ e^{-\alpha t} \sin \beta t \} &= \lim_{T \rightarrow \infty} \int_0^T e^{-\alpha t} \sin \beta t e^{-j\omega t} dt \\
&= \lim_{T \rightarrow \infty} \frac{1}{2j} \int_0^T \left[e^{-t(\alpha + j\omega - j\beta)} - e^{-t(\alpha + j\omega + j\beta)} \right] dt \\
&= \lim_{T \rightarrow \infty} \frac{1}{2j} \left\{ \frac{1}{\alpha + j\omega - j\beta} \left[1 - e^{-\alpha T} e^{-jT(\omega - \beta)} \right] - \right. \\
&\quad \left. \frac{1}{\alpha + j\omega + j\beta} \left[1 - e^{-\alpha T} e^{-jT(\omega + \beta)} \right] \right\} \\
&= \frac{\beta}{(\alpha + j\omega)^2 + \beta^2} \quad (\text{Eq. 3-75})
\end{aligned}$$

The Fourier transform pair is

$$e^{-\alpha t} \sin \beta t \leftrightarrow \frac{\beta}{(\alpha + j\omega)^2 + \beta^2}, \quad \beta > \alpha > 0, t \geq 0 \quad (\text{Eq. 3-76})$$

3.3.5.4 The Rect and Sinc Functions*

A very useful transform pair for application and interpretation of Fourier transform is the rectangular pulse function and its associated transform. The pulse function, $\text{Rect}_T(t)$, is defined as

$$\begin{aligned}
\text{Rect}_T(t) &= 1 \quad |t| < T/2 \\
&= 0 \quad |t| > T/2
\end{aligned} \quad (\text{Eq. 3-77})$$

* The notation Rect and Sinc was first adopted by P. M. Woodward in his book, Probability and Information Theory, With Applications to Radar, Pergamon Press, 1964.

The subscript, T, indicates the pulse has a width equal to T. The transform of $\text{Rect}_T(t)$ is obtained through use of Equation 3-19

$$\begin{aligned} F \{ \text{Rect}_T(t) \} &= \int_{-T/2}^{T/2} (1) e^{-j\omega t} dt \\ &= -\frac{1}{j\omega} \left[e^{-j\omega T/2} - e^{j\omega T/2} \right] \quad (\text{Eq. 3-78}) \\ &= T \frac{\sin(\omega T/2)}{(\omega T/2)} \end{aligned}$$

For notational simplicity, let us define the Sinc function as

$$\text{Sinc}(x) = \frac{\sin(\pi x)}{(\pi x)} \quad (\text{Eq. 3-79})$$

This function has the following properties

- (1) $\text{Sinc}(x) \rightarrow 1$ as $x \rightarrow 0$
- (2) $\text{Sinc}(x) = 0$ if $x = \pm n$, n is an integer
- (3) $\int_{-\infty}^{\infty} \text{Sinc}(x) dx = 1$
- (4) $\int_{-\infty}^{\infty} \text{Sinc}(x - m) \text{Sinc}(x - n) dx = 1$ if $m = n$
 $= 0$ if $m \neq n$

The $\text{Sinc}(x)$ function is closely related to the familiar tabulated function, $\text{Si}(x)$. $\text{Si}(x)$ is defined as

$$\text{Si}(x_0) = \int_0^{x_0} \frac{\sin(y)}{(y)} dy \quad (\text{Eq. 3-81})$$

Substituting πx for y in the above equation, one finds

$$\text{Si}(x_0)/\pi = \int_0^{x_0} \frac{\sin(\pi x)}{(\pi x)} dx \quad (\text{Eq. 3-82})$$

and

$$\text{Si}(\pi x_0)/\pi = \int_0^{x_0} \frac{\sin(\pi x)}{(\pi x)} dx = \int_0^{x_0} \text{Sinc}(x) dx \quad (\text{Eq. 3-83})$$

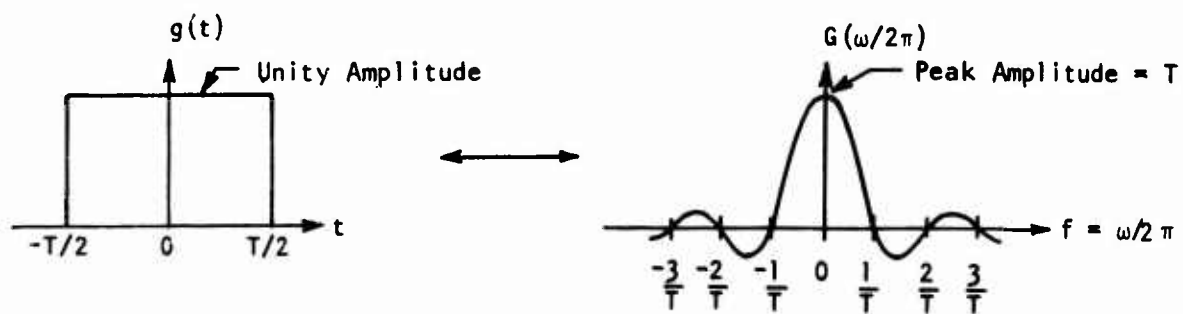
The Sinc function can be used in Equation 3-78.

Note that $\omega T/2 = \pi fT$ so that

$$\frac{\sin(\omega T/2)}{(\omega T/2)} = \text{Sinc}(fT) \quad (\text{Eq. 3-84})$$

Therefore, the Rect and the Sinc functions form a Fourier transform pair

$$\text{Rect}_T(t) \leftrightarrow T \text{Sinc}(fT) \quad (\text{Eq. 3-85})$$



Note that sketches of the Rect and Sinc functions have been used previously.

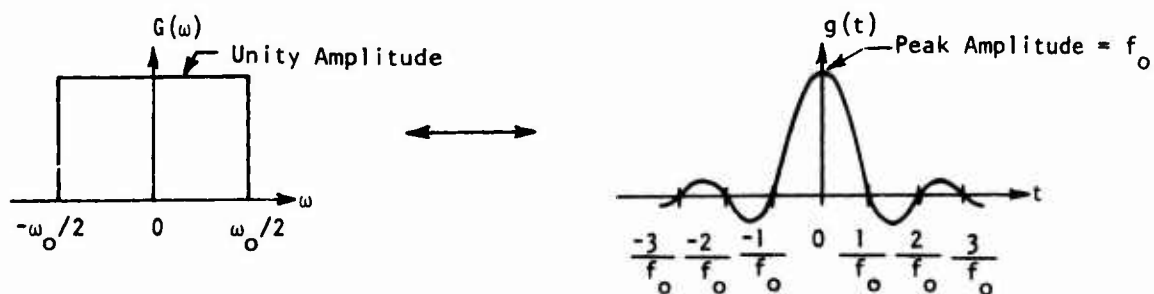
It can be shown in a similar manner, that a pulse in the frequency domain yields a Sinc function transform in the time domain.

$$F^{-1} \{ \text{Rect}_{\omega_0}(\omega) \} = \frac{1}{2\pi} \int_{-\omega_0/2}^{\omega_0/2} (1) e^{j\omega t} d\omega \quad (\text{Eq. 3-86})$$

$$= f_0 \text{Sinc}(f_0 t), \quad \omega_0 = 2\pi f_0$$

Thus

$$\text{Rect}_{\omega_0}(\omega) \leftrightarrow f_0 \text{Sinc}(f_0 t) \quad (\text{Eq. 3-87})$$



Note that the results of Equation 3-88 could have been obtained by using the similarity principal stated in Equation 3-87.

3.3.5.5 Gaussian

A Gaussian function has considerable use in all phases of analysis

$$g(t) = e^{-\alpha t^2}, \quad \alpha > 0 \quad (\text{Eq. 3-88})$$

Its transform may be obtained by use of Equation 3-19

$$\begin{aligned} F \{ e^{-\alpha t^2} \} &= \int_{-\infty}^{\infty} e^{-\alpha t^2} e^{-j\omega t} dt \\ &= \int_{-\infty}^{\infty} e^{-\alpha \left(t^2 + j\frac{\omega}{\alpha}t \right)} dt \end{aligned} \quad (\text{Eq. 3-89})$$

Noting that

$$t^2 + j\frac{\omega}{\alpha}t = \left(t + j\frac{\omega}{2\alpha} \right)^2 + \left(\frac{\omega}{2\alpha} \right)^2 \quad (\text{Eq. 3-90})$$

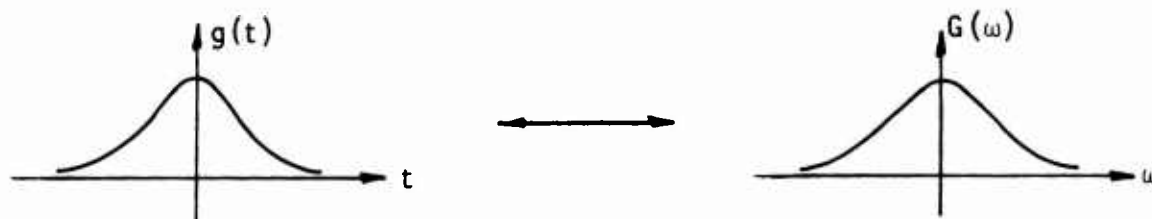
and that

$$\int_{-\infty}^{\infty} e^{-\alpha x^2} dx = \sqrt{\frac{\pi}{\alpha}} \quad (\text{Eq. 3-91})$$

one finds the Fourier transform pair is

$$e^{-\alpha t^2} \leftrightarrow \sqrt{\frac{\pi}{\alpha}} e^{-\left(\frac{\omega^2}{4\alpha} \right)} \quad (\text{Eq. 3-92})$$

Thus, the Fourier transform of a Gaussian is another Gaussian.



A particularly symmetric form of this transform pair is obtained when α is set equal to π . Then

$$e^{-\pi t^2} \leftrightarrow e^{-\frac{\omega^2}{4\pi}} = e^{-\pi f^2}, \quad \omega = 2\pi f \quad (\text{Eq. 3-93})$$

3.3.6 Plotting Aids

The double exponential and the damped sinusoid waveforms resemble a large percentage of EMP experimental data. Consequently, estimates of the transforms of the experimental data can be obtained by using the relatively simple analytic transforms of the double exponential or the damped sinusoid. Furthermore, the astute analyst will use these analytic forms to check numerical transforms of experimental data whenever possible. The following paragraphs provide some simple rules for estimating key parameters and plotting the transforms.

3.3.6.1 Double Exponential

3.3.6.1.1 Parameter Estimation

Assume one has an experimental data record that resembles a double exponential and wants to obtain an estimate of its Fourier transform. The first step is to estimate the parameters, A , α , and β , in

$$g(t) = A(e^{-\alpha t} - e^{-\beta t}), \quad \beta > \alpha > 0, t \geq 0 \quad (\text{Eq. 3-94})$$

from the experimental data. An implicit assumption made by analysts in estimating α and β is that the risetime is much smaller than the decay time. If this assumption is valid, then β and α can be determined by consideration of only the risetime and decay time, respectively, of the experimental waveform.

The parameter, α , is determined by the late-time behavior of the waveform. Inspection of Equation 3-94 shows that when $\beta \gg \alpha$, the late-time behavior is approximately given by

$$g(t) \simeq Ae^{-\alpha t}, \quad \beta \gg \alpha, t \gg 0 \quad (\text{Eq. 3-95})$$

Now define a decay time, t_D , to be the time from the beginning of the waveform to the point where the magnitude of $g(t)$ has decayed to 10 percent of its peak value. A decay time could be defined between any two easily identifiable points on the waveform. However, the definition given above is the one used most often. Using our definition of t_D and noticing that $e^{-\theta} = .1$ when $\theta = 2.3$, one finds

$$\alpha = 2.3/t_D \quad (\text{Eq. 3-96})$$

The parameter, β , is determined by the early-time behavior of the waveform. Note that for $t \ll t_D$, $e^{-\alpha t} \approx 1$, and Equation 3-73 can be approximated as

$$g(t) \approx A(1 - e^{-\beta t}), \quad \beta \gg \alpha, t \ll t_D \quad (\text{Eq. 3-97})$$

Now define the risetime, t_R , as the time difference between the two points on the initial rising portion of the waveform where the amplitude equals 10 percent and 90 percent of peak. In this case

$$\beta = 2.2/t_R \quad (\text{Eq. 3-98})$$

Note that both β and α have units of $(\text{seconds})^{-1}$. Figure 3-4 shows a double exponential with definitions of t_R and t_D indicated.

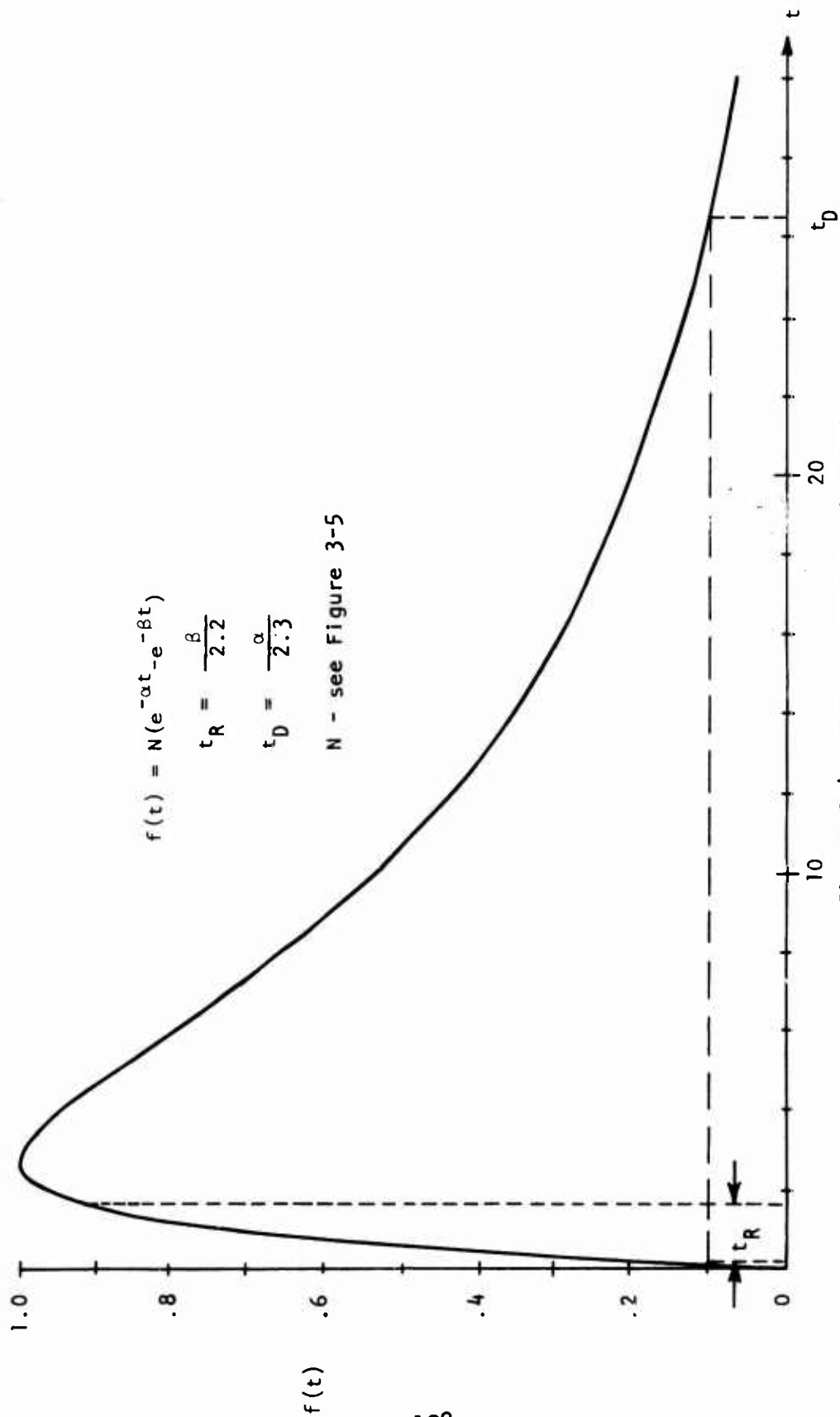
The parameter, A , cannot be determined by simply noting the peak value, P , of the experimental waveform. The reason is that the peak value of the function

$$f(t) = e^{-\alpha t} - e^{-\beta t} \quad (\text{Eq. 3-99})$$

does not, in general, equal unity. The multiplicative constant, N , required to normalize the peak value of $f(t)$ to unity is given in Figure 3-5 where N is plotted as a function of β/α . After determining N from Figure 3-5, and P from the experimental data record, one finds

$$A = PN \quad (\text{Eq. 3-100})$$

Note that A has the same units as the ordinate of the experimental data record (i.e., volts/meter, etc.).



$$f(t) = N(e^{-\alpha t} - e^{-\beta t})$$

$$t_R = \frac{\beta}{2.2}$$

$$t_D = \frac{\alpha}{2.3}$$

N - see Figure 3-5

Figure 3-4. Double Exponential Waveform

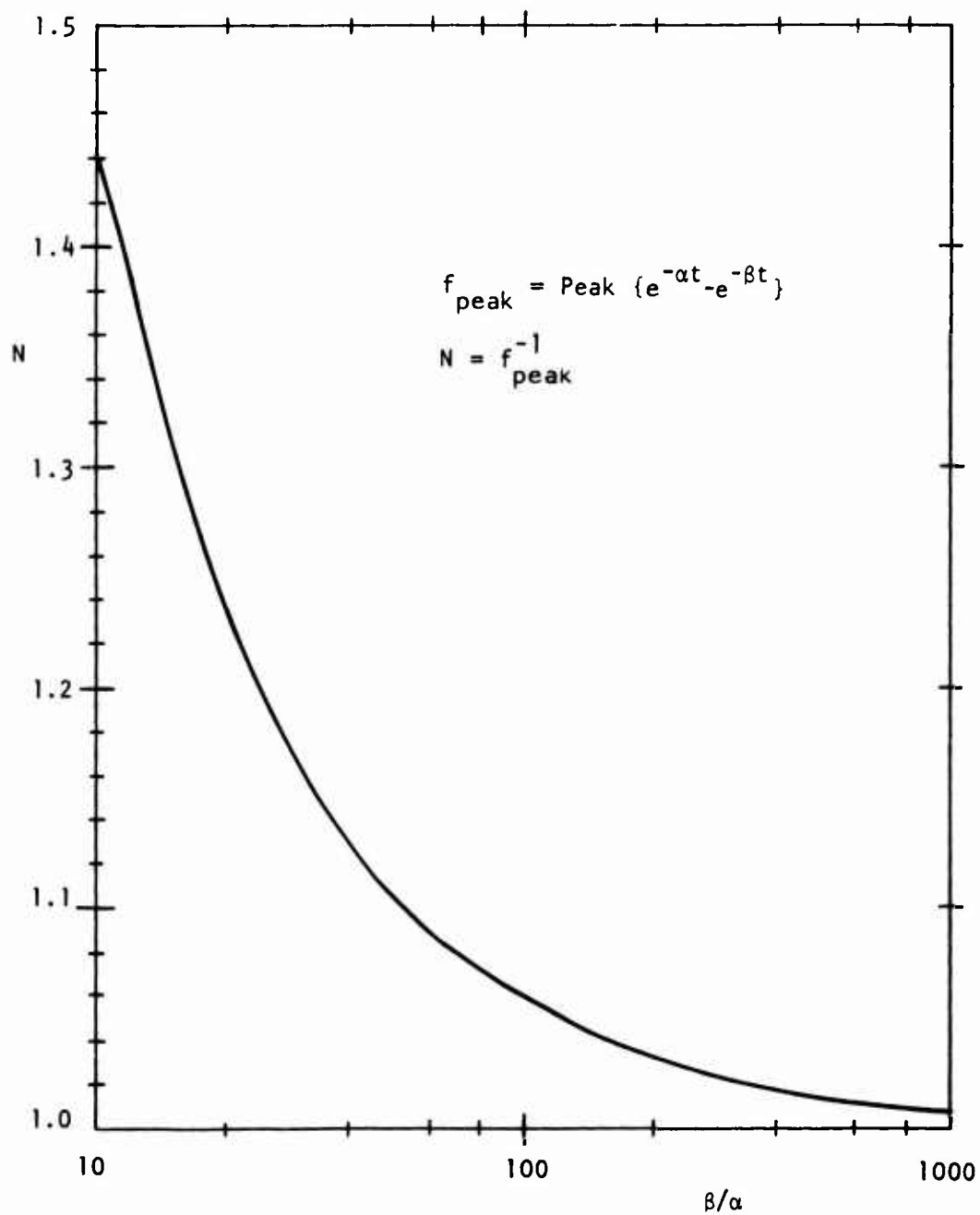


Figure 3-5. Normalization Factor, N , for Double Exponential

3.3.6.1.2 Fourier Transform

The Fourier transform of Equation 3-94, the double exponential, without the scale factor A is given by Equation 3-73. The most common way of displaying Fourier transform data is with a "log-log" plot. This type of plot has two advantages: One is that exponential or power law dependence of the transform is readily apparent, and the second is that the data can be plotted by hand rather simply.

The logarithm of the transform is best obtained if it is first written in the following form

$$G(\omega) = A \frac{\beta - \alpha}{\beta \alpha} \frac{1}{(1 + j\omega/\alpha)(1 + j\omega/\beta)} \quad (\text{Eq. 3-101})$$

Then the logarithm (base 10) of the magnitude of $G(\omega)$ is

$$\log_{10}|G(\omega)| = \log_{10}\left|A \frac{\beta - \alpha}{\beta \alpha}\right| - \log_{10}|1 + j\omega/\alpha| - \log_{10}|1 + j\omega/\beta| \quad (\text{Eq. 3-102})$$

where the vertical bars indicate the absolute value of the quantity. A plot of Equation 3-102 versus the independent variable, $\log \omega$, is shown in Figure 3-6.

Several features of this type of plot should be indicated. One is that the resultant amplitude is the sum of three factors rather than the multiplicative relationship given by Equation 3-101.

The second factor is that the amplitude factors in Equation 3-102 vary with frequency in a relatively simple manner. The first factor in Equation 3-102 is constant with frequency. The second and third factors have the form

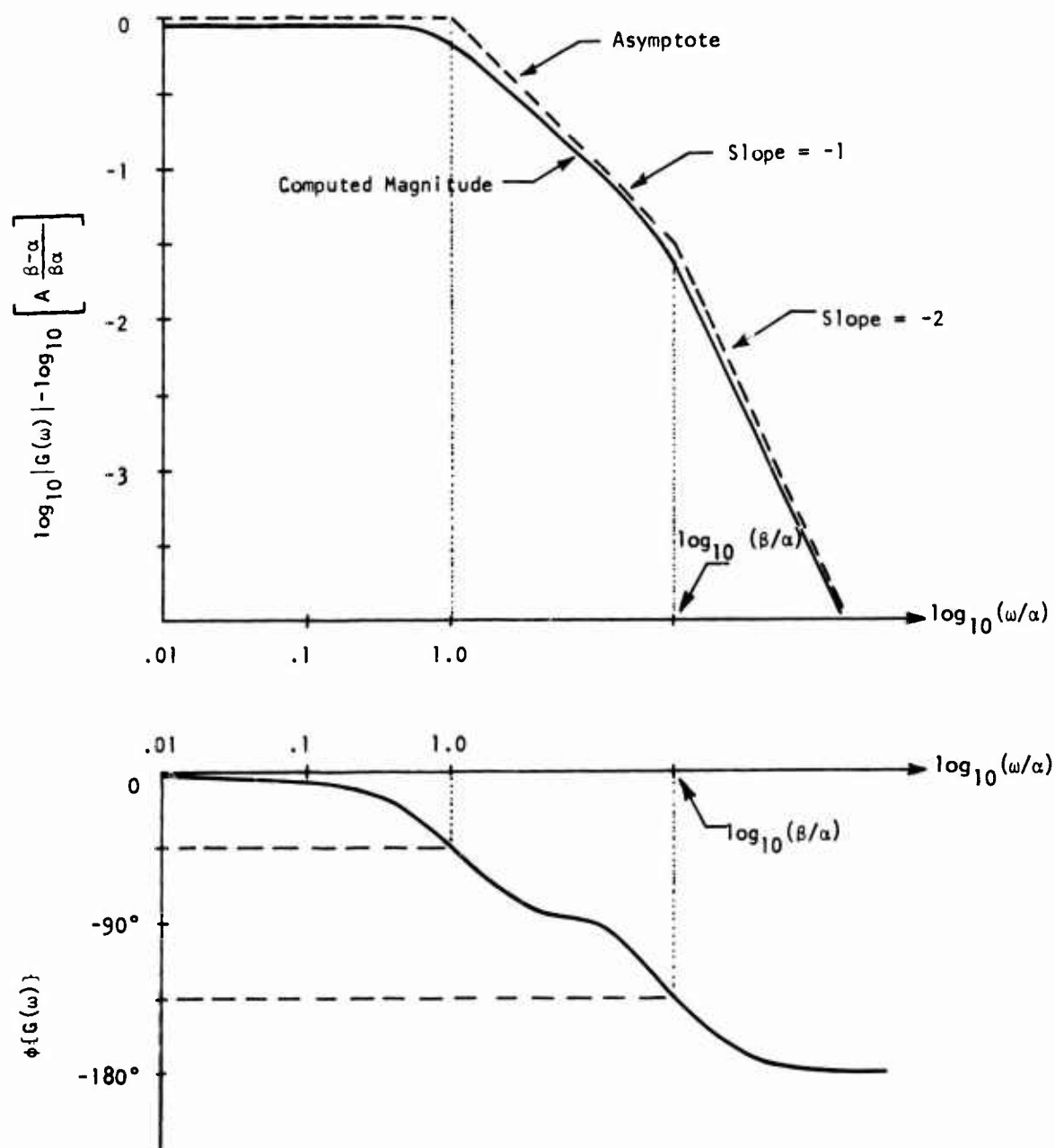


Figure 3-6. Transform Magnitude and Phase for a Double Exponential

$$F(\omega) = -\log_{10} |1 + j\omega/\omega_0| = -\log_{10} \sqrt{1 + (\omega/\omega_0)^2} \quad (\text{Eq. 3-103})$$

This equation has the asymptotic values

$$F(\omega) \approx 0 \quad \omega \ll \omega_0 \quad (\text{Eq. 3-104})$$

$$F(\omega) \approx -\log_{10}(\omega/\omega_0), \quad \omega \gg \omega_0$$

Furthermore, on a log-log plot, the slope of $F(\omega)$ is -1. This can be seen by letting $F(\omega) = y$ and $\log(\omega) = x$ such that

$$y = -x + \log \omega_0 \quad (\text{Eq. 3-105})$$

The derivative of this equation with respect to x is then equal to -1.

The third feature of this log-log plot of the transform of a double exponential is that the magnitude of the transform is well approximated by its asymptotic values. The first factor in Equation 3-102 is constant with frequency. The second factor in Equation 3-102 can be approximated as having zero magnitude with $0 \leq \omega < \alpha$. For $\omega > \alpha$, the second term will have a slope equal to -1. The third factor varies in a similar manner except the characteristic frequency, called the corner or break frequency, is β instead of α . Therefore, the magnitude of Equation 3-102 can be approximated as the sum of straight line segments. These asymptotic values of Equation 3-102 are indicated in Figure 3-6 by dotted lines.

The fourth feature of the log-log plot is that the amplitude can be expressed in common engineering units, decibels (dB), by multiplying Equation 3-102 by the factor 20. Thus, the slope of the asymptotic values of $\log_{10}|G(\omega)|$ are

$$\frac{d \left\{ \log_{10} |G(\omega)| \right\}}{d \left\{ \log(\omega) \right\}} = 0$$

$$= -20 \text{ dB/decade for } \alpha < \omega < \beta \quad (\text{Eq. 3-106})$$

$$= -40 \text{ dB/decade for } \omega > \beta$$

where the term, decade, refers to a factor of 10 in frequency. It should be noted that the asymptotic values of $\log_{10} |G(\omega)|$ are approximate and have their greatest error in the vicinity of the corner or break frequency. When using asymptotic values to approximate factors of the form, $-\log_{10} \sqrt{1 + (\omega/\omega_0)^2}$, the error (error = (true-asymptote)/true) in terms of ω/ω_0 is given by the following table:

TABLE 3-1
RELATIVE DIFFERENCE BETWEEN ACTUAL AND ASYMPTOTIC
VALUES OF $-20 \log_{10} \sqrt{1 + (\omega/\omega_0)^2}$ (dB)

Relative Frequency (ω/ω_0)	.1	.25	.50	.76	1.00	1.31	2.00	4.00	10.00
Error (Decibels)	-.04	-.26	-.97	-2.00	-3.00	-2.00	-.97	-.26	-.04

Thus, one would adjust the asymptotic magnitude values by the error terms in Table 3-1 to obtain the true magnitude. In the event that one had a transform with a term $(1 + j\omega/\alpha)$ in the numerator, the slope of the logarithmic amplitude versus logarithmic frequency would be +1 and the error terms in Table 3-1 would be positive.

The fifth and final feature of the log-log plot of the double exponential transform is that the effect of varying the risetime (β) or the decay time (α) is readily determined. The effect of these variations is shown in Figure 3-7.

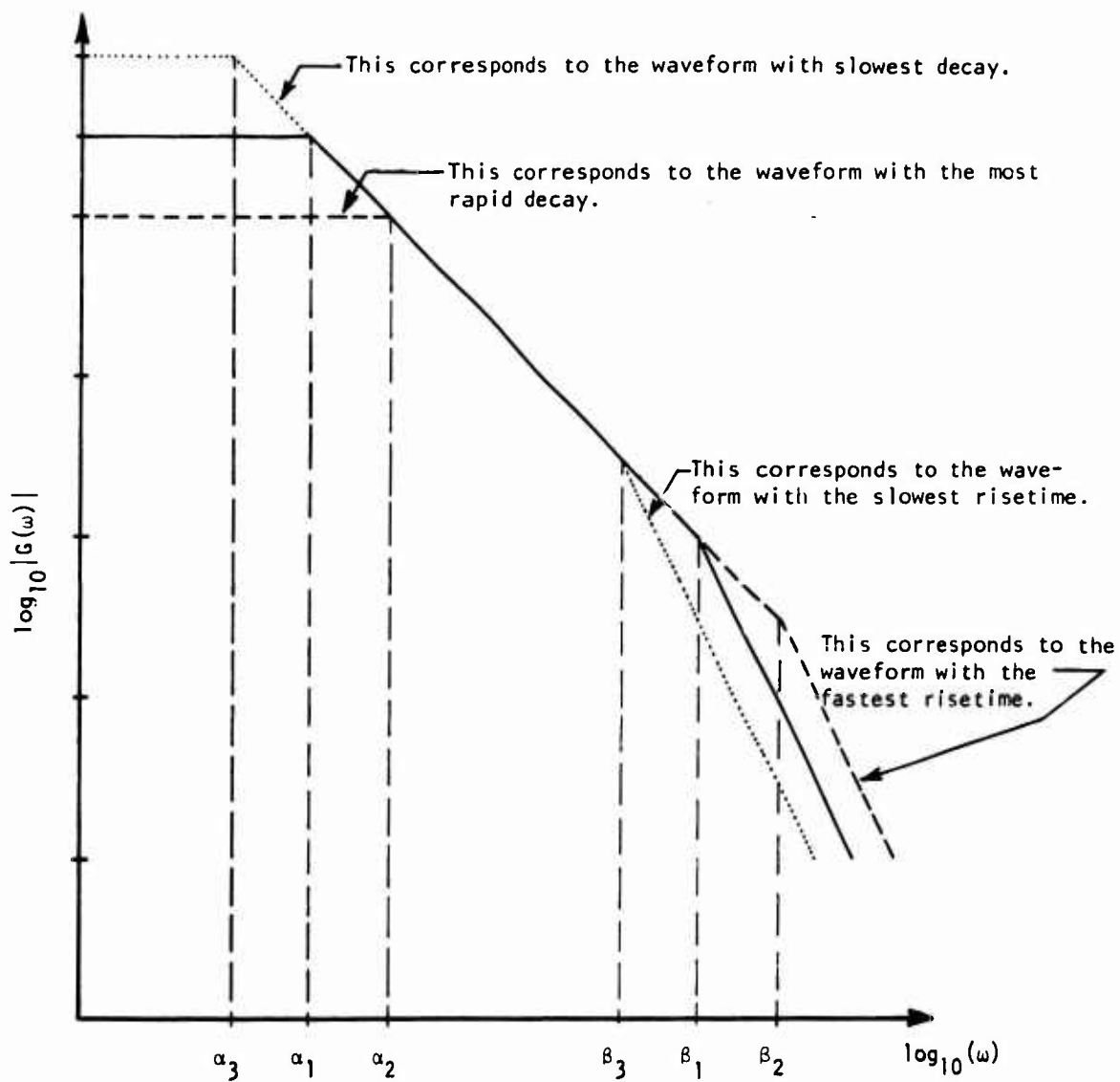


Figure 3-7. Relative Variation of the Transform Magnitude with Risetime and Faltime of a Double Exponential

It should be noted that the abscissa in a plot of $|G(\omega)|$ versus ω has units equal to those corresponding to $g(t)$ divided by radians/second. Thus, if $g(t)$ has units of volt/meter, then $|G(\omega)|$ has units of (volts/meter)/(radians/second).

A plot of the amplitude of $G(\omega)$ versus frequency provides one half of the information available about $G(\omega)$. The other half of the information is the phase of $G(\omega)$. It is customary to plot the phase (not the logarithm of the phase), versus $\log(\omega)$. The phase of $G(\omega)$, $\phi\{G(\omega)\}$, is

$$\phi\{G(\omega)\} = -\tan^{-1}(\omega/\alpha) - \tan^{-1}(\omega/\beta) \quad (\text{Eq. 3-107})$$

A plot of Equation 3-107 versus $\log(\omega)$ is shown in Figure 3-6. Note that the net phase is the arithmetic sum of the phase of each term comprising Equation 3-112. A term of the form $(1 + j\omega/\omega_0)^{-1}$ has the following phase variation as a function of frequency:

TABLE 3-2
PHASE VARIATION OF THE TERM $(1 + j\omega/\omega_0)^{-1}$

Relative Frequency (ω/ω_0)	.1	.5	1	2	10
Phase (Degrees)	-5.7	-26.6	-45.0	-63.4	-84.3

In the event that one had a transform with a term $(1 + j\omega/\omega_0)$ in the numerator, the sign of the phase terms in Table 3-2 would be positive.

3.3.6.1.3 Summary

Given an experimental waveform that approximates a double exponential, an estimate of its Fourier transform is obtained in the following manner:

- (1) Obtain estimates of the parameters A , α , and β in

$$g(t) = A(e^{-\alpha t} - e^{-\beta t}) \quad (\text{Eq. 3-108})$$

The parameter, α , is determined from the late-time behavior of the waveform. If t_D is the time from the beginning of the waveform until it equals 10 percent of its peak, then

$$\alpha = 2.3/t_D \quad (\text{Eq. 3-109})$$

The parameter, β , is determined from the early-time behavior of $g(t)$. If t_R equals the 10 to 90 percent risetime of the waveform, then

$$\beta = 2.2/t_R \quad (\text{Eq. 3-110})$$

The parameter, A , is equal to the product of the normalizing factor, N , given by Figure 3-5 and the peak amplitude of the experimental waveform, P . Thus

$$A = PN \quad (\text{Eq. 3-111})$$

(2) Plot the logarithmic magnitude of

$$G(\omega) = \left(A \frac{\beta - \alpha}{\beta \alpha} \right) \frac{1}{(1 + j\omega/\alpha)(1 + j\omega/\beta)} \quad (\text{Eq. 3-112})$$

For frequencies in the range, $\omega < \alpha$, $\log_{10}|G(\omega)|$ is

$$\log_{10}|G(\omega)| \approx \log_{10} \left(A \frac{\beta - \alpha}{\beta \alpha} \right), \quad \omega < \alpha \quad (\text{Eq. 3-112a})$$

If $\beta \gg \alpha$, then

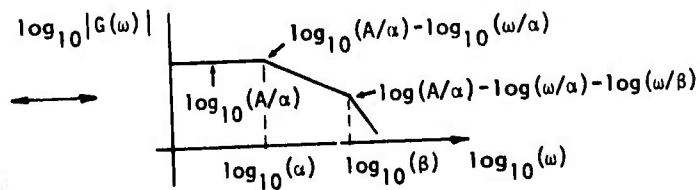
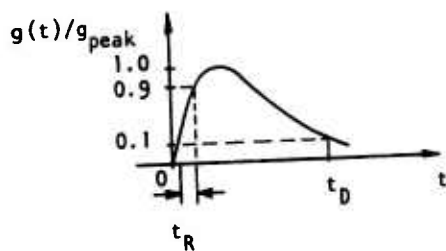
$$\log_{10}|G(\omega)| \approx \log_{10}(A/\alpha), \quad \omega < \alpha, \alpha \ll \beta \quad (\text{Eq. 3-112b})$$

For frequencies in the range, $\alpha < \omega < \beta$,

$$\log_{10}|G(\omega)| \approx \log_{10}(A/\alpha) - \log_{10}(\omega/\alpha), \quad \alpha < \omega < \beta \quad (\text{Eq. 3-112c})$$

For frequencies in the range, $\omega > \beta$

$$\log_{10}|G(\omega)| \approx \log(A/\alpha) - \log_{10}(\omega/\alpha) - \log_{10}(\omega/\beta), \quad \omega > \beta \quad (\text{Eq. 3-112d})$$

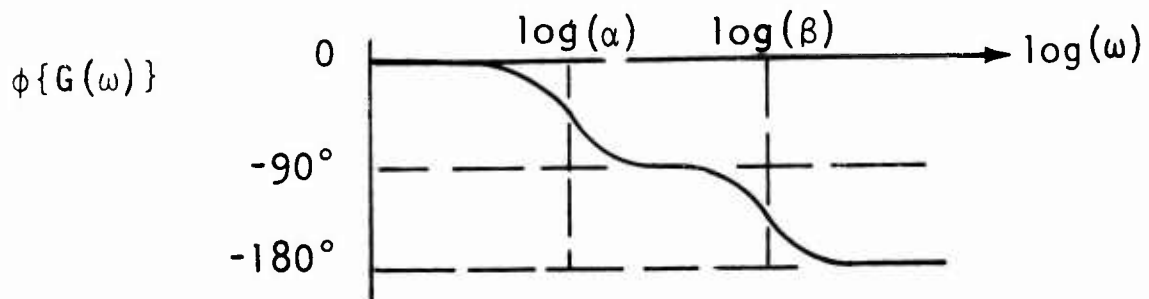


Corrections for the error in the asymptotic magnitude values are given in Table 3-1.

(3) Obtain the phase variation of $G(\omega)$

$$\phi\{G(\omega)\} = -\tan^{-1}(\omega/\alpha) - \tan^{-1}(\omega/\beta) \quad (\text{Eq. 3-107})$$

Table 3-2 gives the phase variation of each term in Equation 3-107.



Note that for a double exponential, the phase varies between $0 > \phi > -180^\circ$ as the frequency varies between $0 < \omega < \infty$.

3.3.6.2 Damped Sinusoid

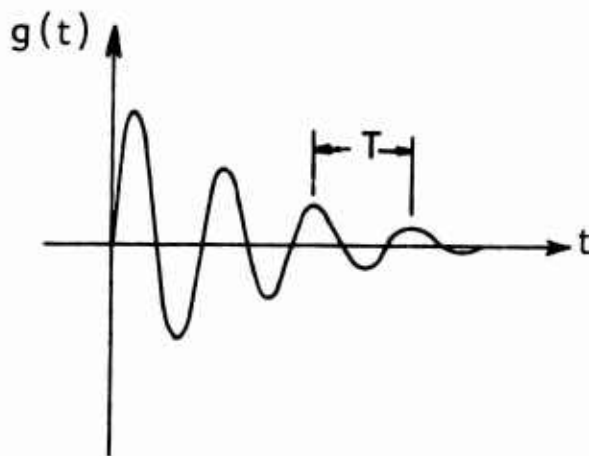
3.3.6.2.1 Parameter Estimation

Assume you have an experimental data record that resembles a damped sinusoid and you want to obtain an estimate of its Fourier transform. The first step is to estimate the parameters, A , α , and β , in

$$g(t) = Ae^{-\alpha t} \sin(\beta t) \quad (\text{Eq. 3-113})$$

The parameter, β , is related to the oscillation period, T , of the experimental data record

$$\beta = 2\pi/T \quad (\text{Eq. 3-114})$$



The parameter, α , is related to the rate of decay of the oscillation. However, the most meaningful way of characterizing α is in terms of Q , the usual radio engineering measure of the "sharpness" of the resonance of a system. In terms of Q , the relation between α and β is

$$\alpha = \beta/2Q \quad (\text{Eq. 3-115})$$

A convenient way of determining Q from an experimental data record is presented in Figure 3-8. In this figure, Q is related to the ratio of the peak amplitudes of adjacent half cycles of the oscillatory waveform. Once β and Q are determined from the data record, α is computed from Equation 3-115.

The parameter, A , is not equal to the experimentally determined peak, P , of the data record since the peak of

$$f(t) = e^{-\alpha t} \sin(\beta t) \quad (\text{Eq. 3-116})$$

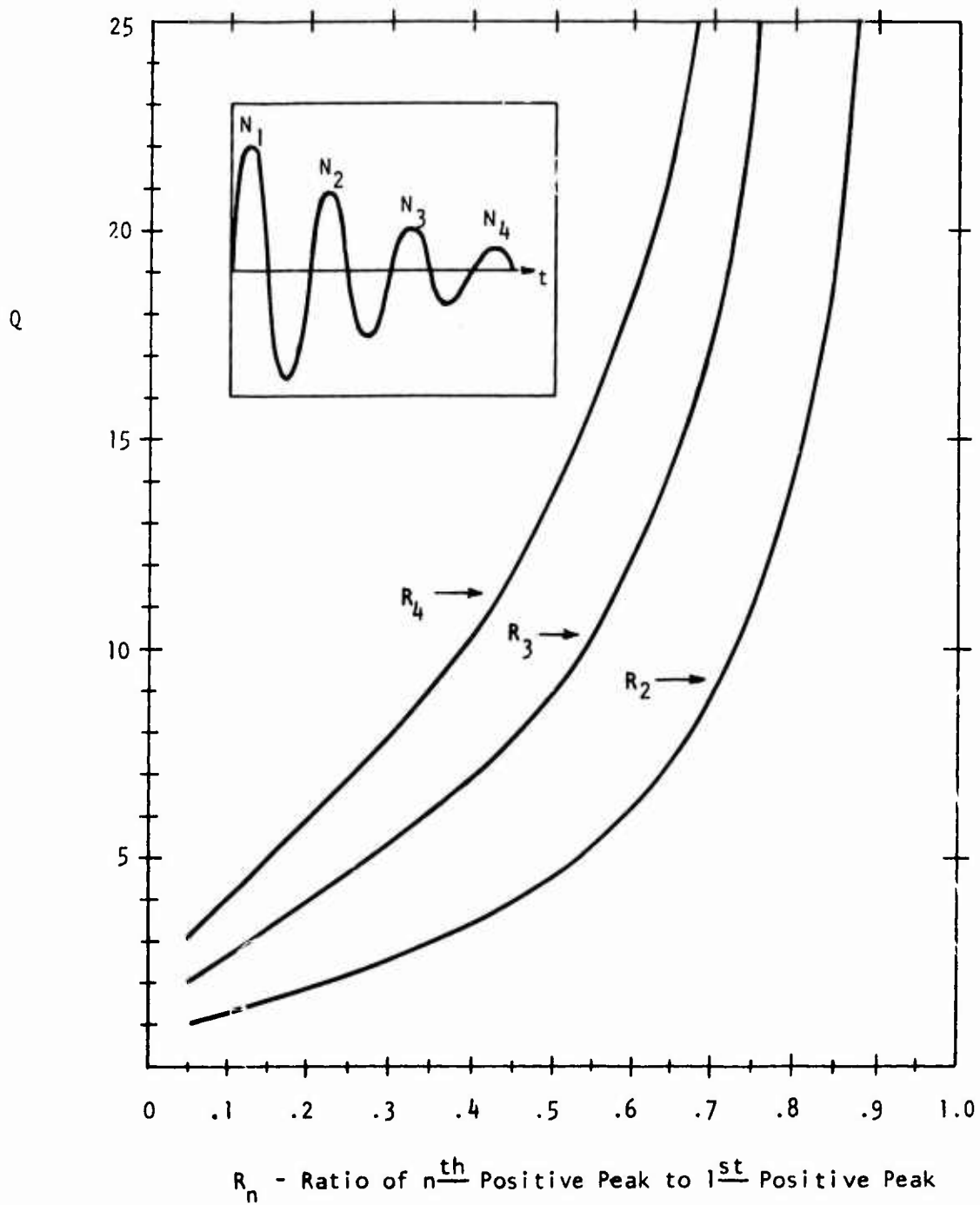


Figure 3-8. Q Versus Damping Rate for a Damped Sinusoid

is not, in general, equal to unity. The multiplicative factor, N , causing the peak of Equation 3-116 to have a value of unity is given in Figure 3-9. In this figure, N is plotted as a function of Q . Once the normalizing factor, N , and the experimentally determined peak amplitude, P , are determined, the parameter, A , is given by

$$A = PN \quad (\text{Eq. 3-117})$$

3.3.6.2.2 Fourier Transform

The Fourier transform of a damped sinusoid, without the multiplicative constant A , is given by Equation 3-76. Once again, the transform data are generally displayed on a log-log plot. When obtaining the logarithm of $|G(\omega)|$, it is best to write Equation 3-76, with the scaling factor A , as

$$\begin{aligned} G(\omega) &= \frac{A}{\beta} \frac{1}{1 + \left(\frac{\alpha}{\beta} + j\frac{\omega}{\beta}\right)^2} \\ &= \frac{A}{\beta} \frac{1}{1 + \left(\frac{1}{2Q} + j\frac{\omega}{\beta}\right)^2} \end{aligned} \quad (\text{Eq. 3-118})$$

Obtaining the logarithm of both sides of this equation, one finds

$$\log_{10}|G(\omega)| = \log_{10}(A/\beta) - \log_{10}\left|1 + \left(\frac{1}{2Q} + j\frac{\omega}{\beta}\right)^2\right| \quad (\text{Eq. 3-119})$$

A plot of Equation 3-119 as a function of $\log_{10}(\omega/\beta)$ is shown in Figure 3-10.

Rules for obtaining estimates of the magnitude of $G(\omega)$ are not as simple to state for a damped sinusoid waveform as compared to a double exponential. However, a few simple asymptotic forms

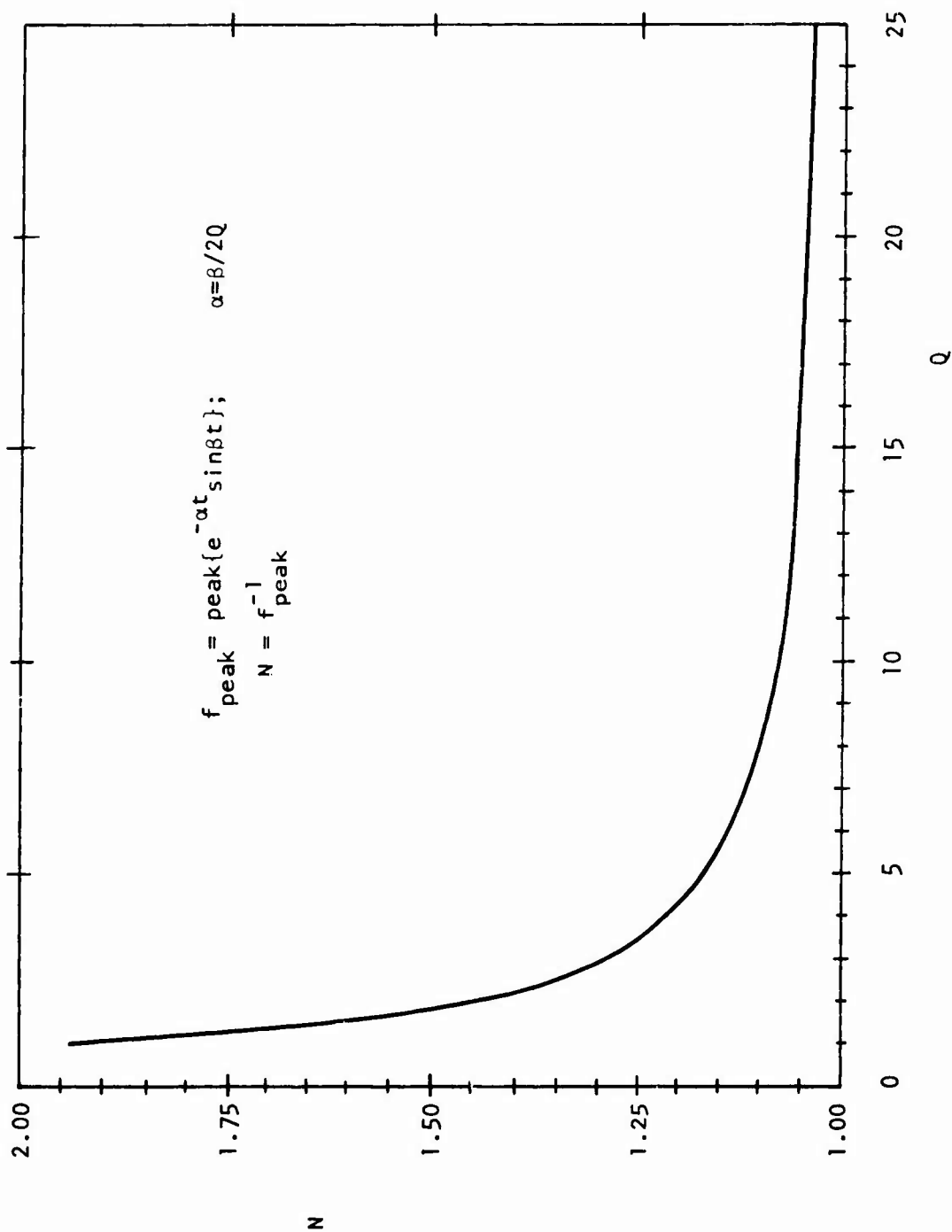


Figure 3-9. Normalization Factor, N, for a Damped Sinusoid

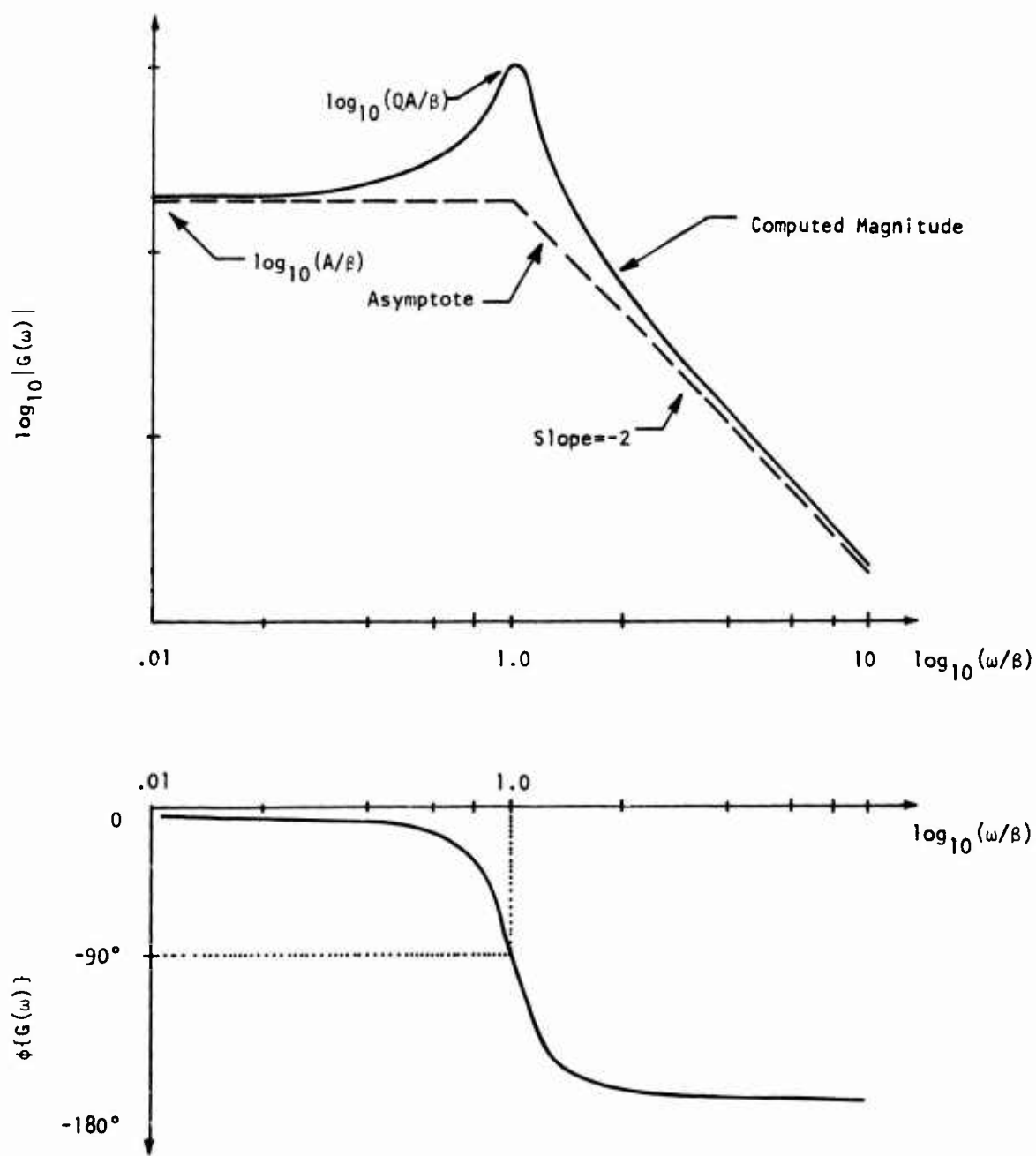


Figure 3-10. Transform Magnitude and Phase for a Damped Sinusoid

will be given. At low frequencies, where $\omega \ll \beta$, Equation 3-119 reduces to

$$\log_{10}|G(\omega)| = \log_{10}(A/\beta) - \log_{10}\left(1 + \frac{1}{4Q^2}\right) \quad (\text{Eq. 3-120})$$

$$\simeq \log_{10}(A/\beta), \quad \omega \ll \beta, Q > 2.$$

At high frequencies, where $\omega \gg \beta$, Equation 3-119 reduces to

$$\log_{10}|G(\omega)| \simeq \log_{10}(A/\beta) - 2\log_{10}(\omega/\beta), \quad \omega \gg \beta. \quad (\text{Eq. 3-121})$$

Note that the second term has a slope of -2 or -40 dB/decade if $|G(\omega)|$ is expressed in decibels. Equations 3-120 and 3-121 describe the asymptotic form of $|G(\omega)|$. In this case, the amplitude is constant with a value given by Equation 3-120 until $\omega = \beta$. Then the magnitude decreases with a slope of -2 or -40 dB/decade. These straight line asymptotic forms are indicated with dotted lines in Figure 3-10. Note that there is considerable error in the asymptotic values when $\omega \simeq \beta$. A simple correction to these asymptotic values is obtained by computing $|G(\omega)|$ when $\omega = \beta$.

$$\log_{10}|G(\omega)| = \log_{10}(QA/\beta) - \log_{10}\sqrt{1 + \left(\frac{1}{4Q}\right)^2}$$

$$\simeq \log_{10}(QA/\beta), \quad \omega = \beta, \quad Q > 2. \quad (\text{Eq. 3-122})$$

Note the peak of $|G(\omega)|$ is a factor of Q greater than its low frequency asymptote. An improved estimate of $|G(\omega)|$ is now obtained by drawing a smooth curve between its value at $\omega = \beta$ and its low and high frequency asymptotes.

Additional points to improve the estimate of $|G(\omega)|$ can be obtained by noting the relation between the Q of a system and the bandwidth of the resonant peak at its 3 dB point. Thus

$$Q = \frac{\beta}{\omega_U - \omega_L}$$

and

$$\omega_U' - \omega_L' = \frac{1}{Q}, \quad \omega' = \omega/\beta \quad (\text{Eq. 3-123})$$

where the subscripts, U and L, refer to the frequencies above and below the resonant frequency, β . Equation 3-123 indicates the frequencies where the amplitude is approximately 3 dB below its maximum. Normalized upper and lower frequencies (ω_U' and ω_L') where the amplitude is 3, 6, 12, and 20 dB below the peak are shown in Table 3-3.

The phase variation of the transform of a typical damped sinusoid is shown in Figure 3-10. In general, the phase is a function of Q as well as frequency. However, simple estimates of the phase can be obtained at three points, the low frequency asymptote ($\omega \ll \beta$), the high frequency asymptote ($\omega \gg \beta$), and at resonance ($\omega = \beta$).

3.3.6.2.3 Summary

Given an experimental waveform that approximates a damped sinusoid, an estimate of its Fourier transform can be obtained in the following manner.

- (1) Obtain estimates of A , α , and β for

$$g(t) = Ae^{-\alpha t} \sin(\beta t) \quad (\text{Eq. 3-124})$$

The parameter, β , is related to the period, T , of the oscillation

$$\beta = 2\pi/T \quad (\text{Eq. 3-125})$$

TABLE 3-3

RELATIVE FREQUENCY WHERE $|G(\omega)|$ ATTAINS SPECIFIED RELATIVE MAGNITUDES

Q	3 dB		6 dB		12 dB		20 dB	
	ω'_L	ω'_U	ω'_L	ω'_U	ω'_L	ω'_U	ω'_L	ω'_U
2	.656	1.202	.267	1.347	-	1.700	-	2.440
3	.798	1.144	.626	1.246	-	1.506	-	2.070
4	.856	1.111	.742	1.191	.120	1.398	-	1.860
5	.888	1.091	.802	1.156	.463	1.329	-	1.727
7	.923	1.067	.864	1.115	.664	1.245	-	1.555
10	.947	1.047	.908	1.082	.781	1.177	.040	1.412
20	.974	1.024	.955	1.042	.897	1.092	.708	1.223

$$\begin{aligned}
 \phi\{G(\omega)\} &= 0 & \omega &\ll \beta \\
 &= -90^\circ & \omega &= \beta \\
 &= -180^\circ, & \omega &\gg \beta
 \end{aligned}
 \quad (\text{Eq. 3-126})$$

The magnitude of the phase of $G(\omega)$ as a function of normalized frequency, $\omega' = \omega/\beta$, is given in Table 3-4.

TABLE 3-4

RELATIVE FREQUENCY WHERE $\phi\{G(\omega)\}$ ATTAINS SPECIFIED VALUES

Q	-30°	-60°	-120°	-150°
	ω'	ω'	ω'	ω'
2	.685	.897	1.185	1.551
3	.765	.922	1.115	1.342
4	.814	.938	1.083	1.248
5	.847	.949	1.064	1.193
7	.887	.962	1.044	1.134
10	.915	.973	1.030	1.092
20	.958	.986	1.015	1.045

The parameter, α , is related to the Q of the resonant system. Data indicating Q as a function of the relative amplitudes of adjacent half cycles are given by Figure 3-8. Then

$$\alpha = \beta/2Q \quad (\text{Eq. 3-127})$$

The parameter, A , is equal to the product of the normalizing factor, N , given in Figure 3-9 and the measured peak amplitude, P , of the experimental data record. Thus

$$A = PN \quad (\text{Eq. 3-128})$$

(2) Plot the logarithmic magnitude of

$$G(\omega) = \frac{A}{\beta} \frac{1}{1 + \left(\frac{1}{2Q} + j\frac{\omega}{\beta} \right)^2} \quad (\text{Eq. 3-129})$$

Estimates of $|G(\omega)|$ are obtained by noting its asymptotic values. When $\omega \ll \beta$, Equation 3-128 reduces to

$$\log_{10}|G(\omega)| \simeq \log_{10}(A/\beta), \quad \omega \ll \beta, \quad Q > 2. \quad (\text{Eq. 3-130})$$

When $\omega \gg \beta$, Equation 3-129 is approximately equal to

$$\log_{10}|G(\omega)| \simeq \log_{10}(A/\beta) - 2\log_{10}(\omega/\beta), \quad \omega \gg \beta \quad (\text{Eq. 3-131})$$

The second term in this equation has a slope of -2 or -40 dB/decade when the magnitude is expressed in decibels. At resonance, the magnitude of $G(\omega)$ is

$$\log_{10}|G(\omega)| \simeq \log_{10}(QA/\beta), \quad \omega = \beta, Q > 2 \quad (\text{Eq. 3-132})$$

Note that the amplitude at resonance is a factor of Q higher than its low frequency asymptote. A smooth curve drawn between these three values will yield an estimate of $|G(\omega)|$. Improved estimates are obtained by using additional data given in Table 3-3.

- (3) Plot the phase of $G(\omega)$. Estimates of the phase when $\omega \ll \beta$, and $\omega \gg \beta$ are

$$\begin{aligned} \phi\{G(\omega)\} &= 0 & \omega \ll \beta & \quad (\text{Eq. 3-133}) \\ &= -90^\circ & \omega = \beta & \\ &= -180^\circ, & \omega \gg \beta & \end{aligned}$$

Additional values of phase versus frequency for various values of Q are given by Table 3-4.

- (4) Procedure for composite waveforms. Some experimentally obtained EMP waveforms resemble the sum of two or more damped sinusoids. If the parameters, A , α , and β ,

associated with each component can be estimated, then the resultant transform is the sum of the transforms associated with each damped sinusoid component. The laws of addition of complex numbers must be used in combining transforms since $G(\omega)$ is a complex quantity.

3.3.7 Special Functions

3.3.7.1 Introduction

The waveforms introduced specifically in the previous section were bounded functions that had finite energy. Furthermore, these functions have Fourier transforms and their associated inverse transforms as described by Equations 3-19 and 3-20. In this section, a class of special functions will be introduced that are either not bounded or do not possess finite energy. In addition, the Fourier transform of these functions cannot necessarily be obtained by straightforward application of the defining equations given in Equations 3-19 and 3-20.

A valid question on the part of an EMP data analyst concerning these special functions could be the justification for studying functions that are obviously a mathematical abstraction. After all, EMP testing involves the excitation of real physical systems with physically realizable electromagnetic fields. The resulting data analysis must involve these physically realizable excitation and response waveforms. Thus, there is apparently no direct application for these special functions. However, the EMP analyst will profit in two ways by mastering these functions. One is that the special functions often provide a reasonable approximation to some physical phenomena. In this case, use of special functions will generally simplify the analysis. However, the second and most important reason for using these special functions is that they provide a powerful tool for the derivation and interpretation of transform relations. Derivations that are extremely tedious can be greatly simplified with the aid of these special functions.

This section will begin with a discussion on the delta function, $\delta(t)$. A thorough definition will be presented. Then $\delta(t)$ will be shown to be a limiting form of a simple analytic function. Finally the Fourier transform of the delta function will be presented. A second special function, namely the step function, $U(t)$, will be treated next. A definition and derivation of its Fourier transform will be given. Various applications of these special functions will be given in Section 3.3.11.

3.3.7.2 The Delta Function

3.3.7.2.1 Definition

The delta function, $\delta(t)$, is the most poorly understood of all the special functions. The reason is probably that insufficient emphasis is placed on its definition. One of the common definitions

$$\begin{aligned} \delta(t - t_0) &= \infty & t &= t_0 \\ &= 0 & t &\neq t_0 \end{aligned} \quad (\text{Eq. 3-134})$$

is useful for conceptually visualizing the function and checking that approximations of the delta function approach the properties given by Equation 3-134 in some limiting process. However, any application of the delta function requires use of the following definition

$$\begin{aligned} \int_a^b f(t) \delta(t - t_0) dt &= f(t_0) & a < t_0 < b \\ &= 0 & t_0 < a \text{ or } t_0 > b \end{aligned} \quad (\text{Eq. 3-135})$$

A special form of this equation is

$$\int_a^b \delta(t - t_0) dt = 1 \quad a < t_0 < b$$

$$= 0 \quad t_0 < a \text{ or } t_0 > b$$

(Eq. 3-136)

A qualitative interpretation of Equation 3-136 is that the net area of the delta function is unity. In Equation 3-135, the net area is unity times the weighting factor, the value of $f(t)$ at $t = t_0$.

It must be emphasized strongly that Equation 3-101 is the only valid and basic definition of the delta function. It must be employed in all occasions when using these functions. The delta function is defined only indirectly in terms of an integral. Furthermore, the delta function has absolutely no interpretation except as to its properties upon integration. These concepts may seem strange at first. However, the delta function is no ordinary function. If these concepts are accepted without reservation, then application of the delta function is straightforward. Many simple applications of this function will be seen in subsequent sections.

3.3.7.2.2 Derivation of Delta Function

The delta function can be shown to be a limiting form of several common analytic functions. A demonstration of this correspondence provides a tie to more familiar functions, illustrates the limiting processes used in the application of special functions, and provides an example of a familiar function that can be used to form a delta function. Several familiar functions can be used to provide this demonstration. However, in this section a variation of the Sinc function will be used

$$\frac{\sin(\omega t)}{\pi t} = (\omega/\pi) \text{Sinc}(\omega t/\pi) \quad (\text{Eq. 3-137})$$

The choice of this function was based on the fact that it illustrates the basic properties of the delta function as well as providing a reader with an illustration of one of the most important functions in Fourier transform theory, namely the Fourier kernel.

In this demonstration, it will be shown

$$\lim_{\omega \rightarrow \infty} (\omega/\pi) \text{Sinc}(\omega t/\pi) \rightarrow \delta(t) \quad (\text{Eq. 3-138})$$

The true test of the limit in Equation 3-138 is whether it satisfies the integral definition given by Equation 3-135. In addition, it will be shown that Equation 3-138 qualitatively approaches the definitions given in Equation 3-134.

The function, $\text{Sinc}(\omega t/\pi)$, has its maximum value of unity when the variable, time, approaches zero. Thus the maximum value of Equation 3-138 is given by

$$\lim_{\omega \rightarrow \infty} (\omega/\pi) \text{Sinc}(\omega t/\pi) = \lim_{\omega \rightarrow \infty} (\omega/\pi) \rightarrow \infty, \quad t = 0 \quad (\text{Eq. 3-139})$$

In addition, the function $\text{Sinc}(\omega t/\pi)$ has zeros when

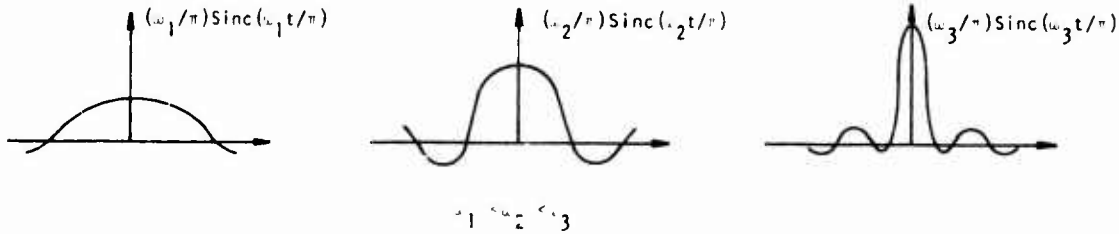
$$\omega t/\pi = \pm n$$

or

$$n \text{ is an integer.} \quad (\text{Eq. 3-140})$$

$$t = \pm \frac{n\pi}{\omega}$$

In the limit where ω approaches infinity, the width of $\text{Sinc}(\omega t/\pi)$ becomes arbitrarily small.



Thus the limiting form of Equation 3-104 exhibits the properties stated by Equation 3-134, namely that the delta function, in the limit, has "infinite amplitude and zero width."

The previous paragraph showed that Equation 3-138 has the qualitative properties of a delta function as stated by Equation 3-134. However, the important and quantitative test is given by Equation 3-135. To verify that Equation 3-104 satisfies Equation 3-135, one forms

$$\begin{aligned} x(t) &= \int_{-\infty}^{\infty} f(t) \frac{\sin(\omega t)}{\pi t} dt \\ &= \int_{-\infty}^{\infty} f(t) (\omega/\pi) \text{Sinc}(\omega t/\pi) dt \end{aligned} \quad (\text{Eq. 3-141})$$

and will show that

$$\lim_{\omega \rightarrow \infty} x(t) = f(0) \quad (\text{Eq. 3-142})$$

the value of $f(t)$ at $t = 0$

Equation 3-142 can be written as the sum of

$$x(t) = \int_{-\infty}^{-\epsilon} f(t) \frac{\sin(\omega t)}{\pi t} dt + \int_{-\epsilon}^{\epsilon} f(t) \frac{\sin(\omega t)}{\pi t} dt + \int_{\epsilon}^{\infty} f(t) \frac{\sin(\omega t)}{\pi t} dt \quad (\text{Eq. 3-143})$$

three integrals where ϵ is an arbitrarily small number. Now it will be shown that the contributions to $x(t)$ from the first and third integral approach zero as ω approaches infinity. To show this fact, evaluate

$$y(t) = \int_a^b \sin(\omega t) \left(\frac{f(t)}{\pi t} \right) dt \quad (\text{Eq. 3-144})$$

in the limit as ω approaches infinity. Integrating Equation 3-144 by parts, one finds

$$y(t) = \frac{1}{\omega} \left[\cos(\omega a) \frac{f(a)}{\pi a} - \cos(\omega b) \frac{f(b)}{\pi b} \right] + \frac{1}{\omega} \int_a^b \cos(\omega t) \left(\frac{f(t)}{\pi t} \right)' dt \quad (\text{Eq. 3-145})$$

where the prime on $(f(t)/\pi t)$ signifies the derivative with respect to time. If $(F(t)/\pi t)$ and $(f(t)/\pi t)'$ have a finite magnitude for every value of t , then

$$\lim_{\omega \rightarrow \infty} y(t) \rightarrow 0 \quad (\text{Eq. 3-146})$$

Therefore the first and third integrals of Equation 3-143 approach zero and

$$x(t) = \int_{-\epsilon}^{\epsilon} f(t) \frac{\sin(\omega t)}{\pi t} dt \quad (\text{Eq. 3-147})$$

Since the limits of this integral are arbitrarily small, $x(t)$ can be approximated as

$$x(t) \simeq f(0) \int_{-\epsilon}^{\epsilon} \frac{\sin(\omega t)}{\pi t} dt \quad (\text{Eq. 3-148})$$

and Equation 3-138 can be shown to satisfy Equation 3-135 by showing

$$\lim_{\omega \rightarrow \infty} \int_{-\epsilon}^{\epsilon} \frac{\sin(\omega t)}{\pi t} dt \rightarrow 1 \quad (\text{Eq. 3-149})$$

If you substitute the variable z for $\omega t/\pi$ in the above equation, you find

$$\lim_{\omega \rightarrow \infty} \int_{-\epsilon}^{\epsilon} \frac{\sin(\omega t)}{\pi t} dt = \lim_{\omega \rightarrow \infty} \int_{-\omega\epsilon/\pi}^{\omega\epsilon/\pi} \text{Sinc}(z) dz \quad (\text{Eq. 3-150})$$

Recall from Equation 3-60 that this last integral approaches unity so that

$$\lim_{\omega \rightarrow \infty} \int_{-\infty}^{\infty} f(t) \frac{\sin(\omega t)}{\pi t} dt = f(0) \quad (\text{Eq. 3-151})$$

Therefore the expression given by Equation 3-138 satisfies the properties of the delta function given by Equation 3-135.

3.3.7.2.3 Transform of a Delta Function

The Fourier transform of the delta function is given straightforwardly by application of Equations 3-1 and 3-101.

$$\begin{aligned}
 F\{\delta(t)\} &= \int_{-\infty}^{\infty} \delta(t) e^{-j\omega t} dt \\
 &= 1
 \end{aligned}
 \tag{Eq. 3-152}$$

Therefore

$$\delta(t) \leftrightarrow 1 \tag{Eq. 3-153}$$

In a similar manner, it can be shown that the inverse Fourier transform of a delta function in the frequency domain is

$$\begin{aligned}
 F^{-1} \delta(\omega) &= \frac{1}{2\pi} \int_{-\infty}^{\infty} \delta(\omega) e^{j\omega t} d\omega \\
 &= \frac{1}{2\pi}
 \end{aligned}
 \tag{Eq. 3-154}$$

Therefore

$$1 \leftrightarrow 2\pi\delta(\omega) \tag{Eq. 3-155}$$

It should be noted that the factor 2π in the above equation signifies the area of this delta function upon integration. For a delta function, the concept of amplitude has no precise meaning.

Equations 3-153 and 3-155 can be generalized for any shift in the argument by use of Equations 3-59 and 3-61. Thus

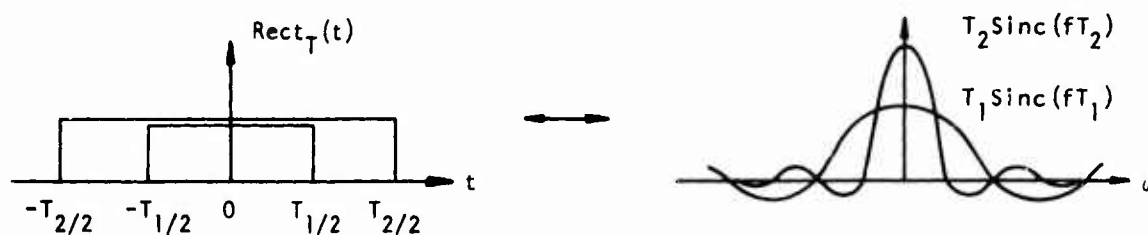
$$\delta(t - t_0) \leftrightarrow e^{-j\omega t_0} \tag{Eq. 3-156}$$

and

$$e^{j\omega_0 t} \leftrightarrow 2\pi\delta(\omega - \omega_0) \quad (\text{Eq. 3-157})$$

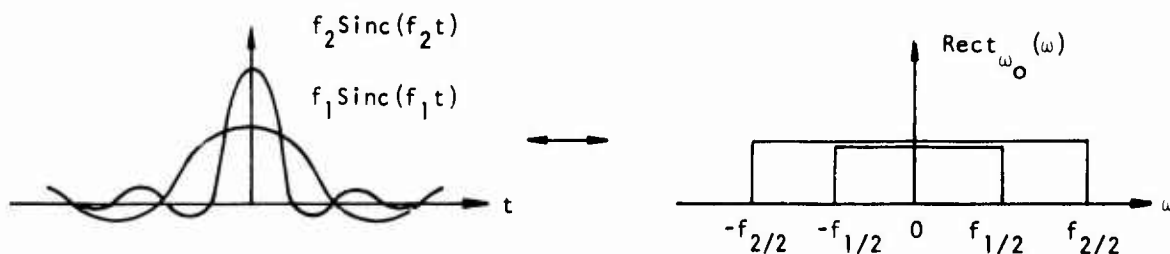
The reader can obtain some feeling for the meaning of the Fourier transform of a delta function by plotting the Fourier transform pairs given by Equations 3-85 and 3-87.

$$\text{Rect}_T(t) \leftrightarrow T \text{Sinc}(fT) \quad (\text{Eq. 3-85})$$



In the limit where the width of $\text{Rect}_T(t)$ becomes large ($T \rightarrow \infty$), the amplitude of $T \text{Sinc}(fT)$ approaches infinity and its width becomes arbitrarily small. In a similar manner examine

$$f_0 \text{Sinc}(f_0 t) \leftrightarrow \text{Rect}_{\omega_0}(\omega) \quad (\text{Eq. 3-87})$$



In the limit where the width of $\text{Rect}_{\omega_0}(\omega)$ becomes large ($\omega_0 \rightarrow \infty$), the amplitude of $f_0 \text{Sinc}(f_0 t)$ approaches infinity and its width becomes arbitrarily small. Note that this last example is similar to the demonstration given by Equations 3-139 to 3-152.

3.3.7.3 Step Function

The step function, $U(t)$, is defined as

$$\begin{aligned} U(t - t_0) &= 1 & t > t_0 \\ &= 0 & t < t_0 \end{aligned} \quad (\text{Eq. 3-158})$$

and is particularly useful in the study of transient phenomena. Multiplication of a bounded function by $U(t - t_0)$ is a means of causing the resultant function to have a definite starting time at $t = t_0$. If $U(t)$ is used in data analysis work, one must know the properties of $U(t)$ as well as its transform. A derivation of the transform of the step function is given below. However, the transform of the "sgn" function will be presented first since it is required in the definition of the transform of $U(t)$.

The sgn function is defined as

$$\begin{aligned} \text{sgn}(t) &= 1 & t > 0 \\ &= -1 & t < 0 \end{aligned} \quad (\text{Eq. 3-159})$$

The derivation of the transform of this function using Equation 3-1 is not straightforward. Therefore the transform of $\text{sgn}(t)$ will be presented without proof

$$F\left\{\text{sgn}(t)\right\} = \frac{2}{j\omega} \quad (\text{Eq. 3-160})$$

and it will be shown that the inverse transform of Equation 3-160 yields $\text{sgn}(t)$. Thus

$$\begin{aligned} F^{-1}\left\{\frac{2}{j\omega}\right\} &= \lim_{\sigma \rightarrow \infty} \frac{1}{2\pi} \int_{-\sigma}^{\sigma} \frac{2}{j\omega} e^{j\omega t} d\omega \\ &= \lim_{\sigma \rightarrow \infty} \frac{1}{\pi} \int_{-\sigma}^{\sigma} \frac{\cos(\omega t) + j \sin(\omega t)}{j\omega} d\omega \quad (\text{Eq. 3-161}) \end{aligned}$$

Noting that $(\cos(\omega t)/j\omega)$ is odd and that there is no contribution to the integral of an odd function between the limits $(-\sigma, \sigma)$, one finds

$$F^{-1}\left\{\frac{2}{j\omega}\right\} = \lim_{\sigma \rightarrow \infty} \frac{1}{\pi} \int_{-\sigma}^{\sigma} \frac{\sin(\omega t)}{\omega} d\omega \quad (\text{Eq. 3-162})$$

This equation can be expressed in terms of the Sinc function by using $\omega = 2\pi f$. Thus

$$F^{-1}\left\{\frac{2}{j\omega}\right\} = \lim_{\sigma \rightarrow \infty} 2t \int_{-\sigma}^{\sigma/2\pi} \text{Sinc}(2ft) df \quad (\text{Eq. 3-163})$$

Now consider the case where t is positive and the substitution, $x = 2\pi ft$, is made in the above equation. Then

$$F^{-1}\left\{\frac{2}{j\omega}\right\} = \lim_{\sigma \rightarrow \infty} \int_{-\sigma t/\pi}^{\sigma t/\pi} \text{Sinc}(x) dx \quad (\text{Eq. 3-164})$$

and

$$\begin{aligned} F^{-1}\left\{\frac{2}{j\omega}\right\} &= \int_{-\infty}^{\infty} \text{Sinc}(x) dx \\ &= 1, \quad t > 0 \end{aligned} \quad (\text{Eq. 3-165})$$

When t is negative, the signs of the limits of the integral in Equation 3-164 change and

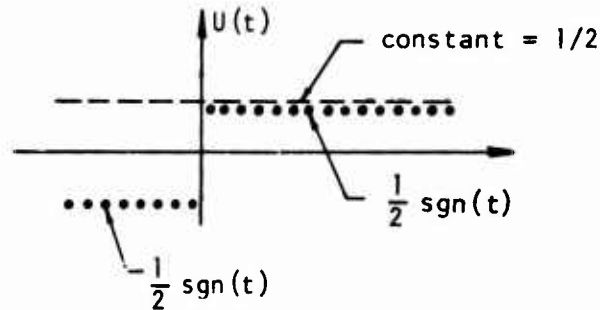
$$\begin{aligned} F^{-1}\left\{\frac{2}{j\omega}\right\} &= \lim_{\sigma \rightarrow \infty} \int_{\sigma/2\pi}^{-\sigma/2\pi} \text{Sinc}(x) dx \\ &= -\lim_{\sigma \rightarrow \infty} \int_{-\sigma/2\pi}^{\sigma/2\pi} \text{Sinc}(x) dx \\ &= -1, \quad t < 0 \end{aligned} \quad (\text{Eq. 3-166})$$

Thus the frequency domain function, $2/j\omega$, has an inverse transform that has the properties of the sgn function as described in Equation 3-159.

The step function, $U(t)$, can be considered as the result of the sum of a constant, independent of time, and the sgn function

$$U(t) = \frac{1}{2} + \frac{1}{2} \text{sgn}(t) \quad (\text{Eq. 3-167})$$

$$U(t) = \frac{1}{2} + \frac{1}{2} \operatorname{sgn}(t)$$



Then the transform of $U(t)$ is given by the sum of the transform of the constant and the sgn function. Using Equations 3-155 and 3-160, one obtains

$$F \{ U(t) \} = \frac{1}{2} (2\pi\delta(t)) + \frac{1}{2} \left(\frac{2}{j\omega} \right) \quad (\text{Eq. 3-168})$$

Thus

$$U(t) \leftrightarrow \pi\delta(\omega) + \frac{1}{j\omega} \quad (\text{Eq. 3-169})$$

3.3.8 Product of Two Functions

3.3.8.1 Introduction

In a previous section, the conceptual experiment of injecting a signal at a given frequency into the input of a system and measuring the magnitude and phase of the output relative to the input was introduced. This experiment can be repeated at every frequency of interest.

If the system is linear and does not change as a function of time (time invariant) then the magnitude of the output is some multiplicative constant, A , times the magnitude of the input. In general, this multiplicative constant will be a function of the frequency used to excite the system. Thus $A = A(\omega)$. One can also designate the phase of the output relative to the input as $\phi(\omega)$. Note that, in general, the phase of the output relative to the input is a function of frequency. The functions, $A(\omega)$ and $\phi(\omega)$, can be combined in a single complex function, $H(\omega)$.

$$A(\omega) = |H(\omega)| \quad (\text{Eq. 3-170})$$

$$\theta(\omega) = \phi\{H(\omega)\}$$

This conceptual experiment can be extended by simultaneously applying signals from two separate generators, $F_1(\omega_1)$ and $F_2(\omega_2)$, operating on different frequencies. Once again, the magnitude and phase of the output, $G(\omega)$, will be measured. If the system is linear and time invariant, then the principle of superposition is valid and the input and output are related as

$$G(\omega) = [F_1(\omega_1) + F_2(\omega_2)] H(\omega) \quad (\text{Eq. 3-171})$$

Now consider extending the conceptual experiment even further by applying a transient time domain signal, $f(t)$, to the input of the system. The Fourier integral transform shows that this transient signal is composed of contributions of an infinite number of frequencies, $F(\omega_i)$, $i = 1, 2, \dots$. Thus a transient signal can be considered, conceptually, as the resultant output of an infinite number of single frequency signal generators applied simultaneously. Once again, if the system is linear and time invariant, the output, $G(\omega)$, of the system is expressed symbolically as

$$G(\omega) = F(\omega) H(\omega) \quad (\text{Eq. 3-172})$$

Equation 3-172 applies, in general, to EMP testing. The transient electromagnetic fields are considered as the input function. The measured response at some point on the test object is considered the output. The test object is considered as the system. In a large percentage of actual cases with EMP testing, the system is sufficiently linear and time invariant so that the relationship given by Equation 3-172 is valid. In the frequency domain, the output simply equals the product of the input or excitation and the system transfer function. On many occasions, it is desired to find the relationship between the input and output in the time domain. Of course, if any two of the functions in Equation 3-172 can be determined, the third can be computed and the inverse Fourier transform will yield the resultant time domain signal. However, there is a strictly time domain procedure of relating the input and output of a system. This procedure is called convolution.

The following paragraphs will discuss the convolution technique. It will be shown that the product of two functions in the frequency domain corresponds to the convolution of the inverse of each function in the time domain. The concept of convolution will be extended to show that the product of two functions in the time domain implies convolution in the frequency domain. Finally some of the concepts and definitions applicable to systems, their inputs, and their outputs will be presented.

The author feels that these concepts relating to linear systems and the product and convolution of two functions to be absolutely indispensable in EMP data analysis. If these concepts are not mastered, then there is hardly any reason for an analyst to invest the effort of obtaining Fourier transforms of transient data in the first place.

3.3.8.2 Convolution

3.3.8.2.1 Time Domain

Given two functions ($f(t)$ and $h(t)$) and their associated transforms ($F(\omega)$ and $H(\omega)$), now the product of the two frequency domain functions will yield

$$G(\omega) = F(\omega) H(\omega) \quad (\text{Eq. 3-173})$$

It will be shown that $G(\omega)$ is the Fourier transform of $g(t)$ which equals the convolution of $f(t)$ with $h(t)$. Noting that

$$F(\omega) = \int_{-\infty}^{\infty} f(t') e^{-j\omega t'} dt', \quad \omega = 2\pi f \quad (\text{Eq. 3-19})$$

one finds Equation 3-173 can be rewritten as

$$G(\omega) = \int_{-\infty}^{\infty} f(t') e^{-j\omega t'} H(\omega) dt' \quad (\text{Eq. 3-174})$$

However, according to Equations 3-58 and 3-59

$$H(\omega) e^{-j\omega t'} = F\{h(t - t')\} \quad (\text{Eq. 3-175})$$

so that

$$G(\omega) = \int_{-\infty}^{\infty} f(t') \left[\int_{-\infty}^{\infty} h(t - t') e^{-j\omega t} dt \right] dt' \quad (\text{Eq. 3-176})$$

If the functions, $f(t)$ and $h(t)$, correspond to finite energy processes, then the order of the integrals in Equation 3-176 can be rearranged to yield

$$G(\omega) = \int_{-\infty}^{\infty} \left[\int_{-\infty}^{\infty} f(t') h(t - t') dt' \right] e^{-j\omega t} dt \quad (\text{Eq. 3-177})$$

However, this equation states that $G(\omega)$ is the Fourier transform of the quantity inside the brackets. Since $G(\omega)$ is the Fourier transform of $g(t)$, then

$$g(t) = \int_{-\infty}^{\infty} f(t') h(t - t') dt' \quad (\text{Eq. 3-178})$$

This equation states that $g(t)$ is the result of convolution of $f(t)$ with $h(t)$.

There are three general comments applicable to convolution. One is that Equation 3-178 is commonly written as

$$g(t) = f(t) * h(t) \quad (\text{Eq. 3-179})$$

where the asterisk indicates the convolution process. A second comment is that it is immaterial which function, $f(t)$ or $h(t)$, has the time shifted argument. Substituting $\tau = t - t'$ in Equation 3-178, one finds

$$\int_{-\infty}^{\infty} f(t') h(t - t') dt' = \int_{-\infty}^{\infty} f(t - \tau) h(\tau) d\tau \quad (\text{Eq. 3-180})$$

Futhermore, inspection of this equation shows that convolution is a commutative process

$$f(t) * h(t) = h(t) * f(t) \quad (\text{Eq. 3-181})$$

The final comment is that the convolution process can be repeated with another function $k(t)$. This implies that

$$F^{-1}\{F(\omega) H(\omega) K(\omega)\} = f(t) * h(t) * k(t) \quad (\text{Eq. 3-182})$$

Furthermore, it is immaterial which two functions are convolved first

$$f(t) * [h(t) * k(t)] = [f(t) * h(t)] * k(t) \quad (\text{Eq. 3-183})$$

This last property implies that convolution is an associative process.

3.3.8.2.2 Frequency Domain

Convolution is not restricted to the time domain. Indeed, given three functions, $p(t)$, $r(t)$, and $s(t)$ related as follows

$$p(t) = r(t) s(t) \quad (\text{Eq. 3-184})$$

Then the Fourier transform of $p(t)$ in terms of the transform of $r(t)$ and $s(t)$ is

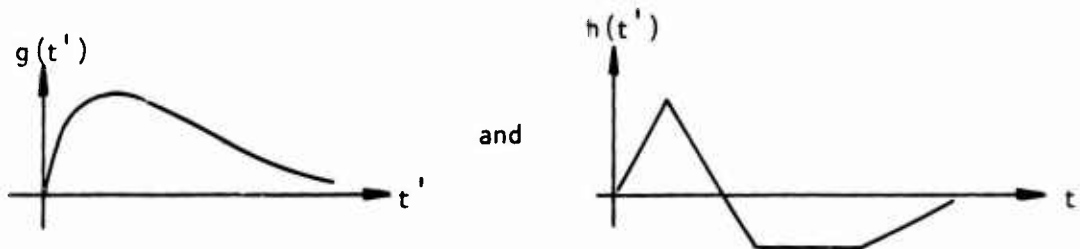
$$P(\omega) = \frac{1}{2\pi} \int_{-\infty}^{\infty} R(\sigma) S(\omega - \sigma) d\sigma \quad (\text{Eq. 3-185})$$

Equation 3-185 can be verified in a manner almost identical to that exhibited by Equations 3-173 to 3-178. Furthermore, the properties given by Equations 3-180 to 3-183 apply to frequency domain convolution also.

3.3.8.2.3 Graphical Interpretation

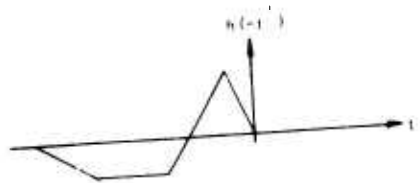
Convolution is basically a simple mathematical function. However, the instructions contained in Equation 3-178 are subtle, and it is highly recommended that the steps involved in computing the convolution integral be sketched in a manner similar to the following. If the reader repeats these symbolic sketches for his particular problem, then there will be no confusion in applying convolution techniques.

Assume one has two functions, $g(t')$ and $h(t')$, such as those illustrated below.

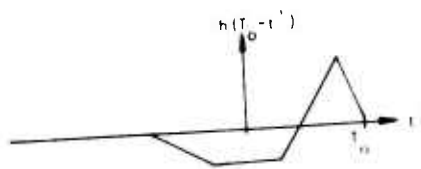


Note in Equation 3-141 that t is a variable and t' is a parameter. To emphasize that t is a parameter, let $t = T_0$. Now one forms the function

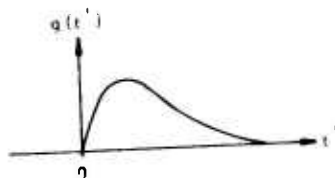
$h(t - t') = h(T_0 - t')$. This function can be derived in two steps. First the axis of $h(t')$ is reversed to yield



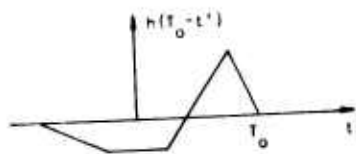
Then the argument is shifted by the amount, T_0 , to form



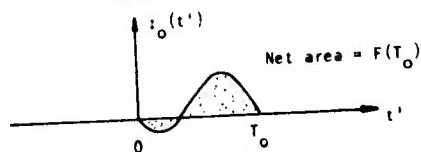
Next $g(t')$ and $h(T_0 - t')$ are multiplied together, point by point, to yield a resultant function which can be given the name, $\phi_0(t')$, if desired.



Multiplied by



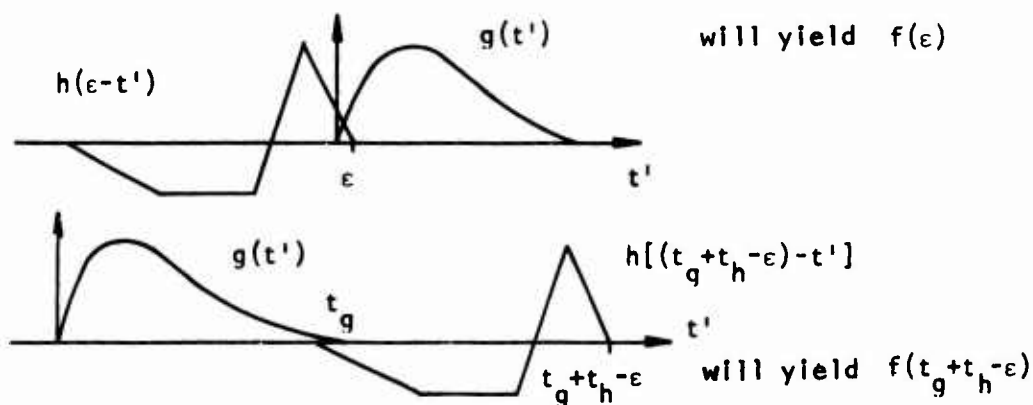
Yields



Then $\phi_0(t')$ is integrated with respect to the variable, t' , to yield $f(T_0)$. It is important to realize that the process of axis reversal, time shifting, multiplying two functions, and integrating the resultant function will yield only one value for $f(t)$ which in this case equals $f(T_0)$. To obtain $f(t)$ at other values of time, T_i , then the whole process must be repeated for each additional value of $f(T_i)$.

Two features of convolution are immediately evident by inspection of these sketches. One is the choice of the proper limits for the integral in Equation 3-178. They are stated, generally, as $(-\infty, \infty)$. However, inspection of the above sketch shows the actual limits need only be $(0, T_0)$ since the product of the two functions is zero outside this interval. A long list of rules could be stated for determining the limits of the integral in the convolution process. However, these rules would probably be poorly understood and promptly forgotten. On the other hand, producing a rough sketch of the product of the two functions being convolved will yield these integral limits by inspection.

Another feature evident from sketches of convolution is that the duration of $f(t)$ is longer than that of either $g(t)$ or $h(t)$. Assume that $g(t)$ and $h(t)$ have non-zero values in the ranges $(0, t_g)$ and $(0, t_h)$. Then $f(t)$ has non-zero values in the range $(0, t_g + t_h)$. Note the two sketches shown below. In these sketches, ϵ is a small positive number.



Graphical techniques can be used to illustrate convolution in the frequency domain also. However, the fact that the frequency domain functions are generally complex tends to obscure the graphical image that is quite obvious with convolution in the time domain. Nevertheless, crude sketches of the function do provide insight in establishing integral limits and distinguishing between parameters and variables of integration.

3.3.8.2.4 Parseval's Theorem

If one has some time domain signal, $g(t)$, that is proportional to either voltage or current (electric or magnetic fields), then the power is proportional to $g^2(t)$. Furthermore, the integral of $g^2(t)$ with respect to time is proportional to the total energy in that signal. Using the convolution theorem, one can find a correspondence between the expression for energy in the time domain and that for energy in the frequency domain.

The integral of $g^2(t)$ with respect to time can be written in terms of Equation 3-19 as ω approaches zero. Denoting the transform of $g^2(t)$ by $S(\omega)$, one finds

$$\lim_{\omega \rightarrow 0} \int_{-\infty}^{\infty} g^2(t) e^{-j\omega t} dt = \lim_{\omega \rightarrow 0} S(\omega)$$

(Eq. 3-186)

$$= S(0)$$

Thus, the energy is proportional to the zero frequency component of the Fourier transform of $g^2(t)$. It has been demonstrated previously that the transform of the product of two functions in the time domain implies convolution of the separate transforms in the frequency domain. Thus

$$\frac{1}{2\pi} \int_{-\infty}^{\infty} G(\omega) G(\sigma - \omega) d\omega = F\{g^2(t)\}$$

(Eq. 3-187)

$$= S(\sigma)$$

Equating the zero frequency component of Equation 3-187 to Equation 3-186, one finds

$$\begin{aligned}\int_{-\infty}^{\infty} g^2(t) dt &= \frac{1}{2\pi} \int_{-\infty}^{\infty} G(\omega) G(-\omega) d\omega \\ &= \frac{1}{2\pi} \int_{-\infty}^{\infty} |G(\omega)|^2 d\omega\end{aligned}\quad (\text{Eq. 3-188})$$

since $G(-\omega) = G^*(\omega)$ and $G(\omega)^* G(\omega) = |G(\omega)|^2$. Note that the superscript asterisk implies the complex conjugate of a complex function.

Equation 3-188 is known as Parseval's Theorem. It shows that the total energy of a function can be computed in either the time or the frequency domain. Furthermore, if one is given a function $g(t)$ and then computes $G(\omega)$, then use of Equation 3-188 serves as a check on the accuracy of the computation of $G(\omega)$.

3.3.8.3 System Definitions

The previous paragraphs describing the relationship between multiplication of two functions and convolution has introduced the concept of a system with an input and an output. In the following paragraphs, system related definitions and notations used elsewhere in this document will be summarized.

(1) Input

The input to a system will be designated by the letter f .

(2) Output

The system output will be signified by use of the letter g .

(3) Frequency Domain

Frequency domain functions will be indicated with capital letters.

(4) Time Domain

Time domain functions will be designated with lower case letters.

(5) Transfer Function

If a system is linear and time invariant, then $H(\omega)$ is called the system transfer function. If $F(\omega)$ and $G(\omega)$ are available, then $H(\omega)$ is computed as $H(\omega) = G(\omega)/F(\omega)$

(Eq. 3-189)

(6) Linear System

If the input is changed from $F(\omega)$ to $AF(\omega)$, then the output is changed from $F(\omega)$ to $AG(\omega)$. A is an arbitrary constant. This same proportionality relationship must also hold for time domain input and output functions.

(7) Time Invariant System

A system is time invariant if $H(\omega)$ is a function of ω only. $H(\omega; \tau)$ is an example of a time varying linear system.

(8) Impulse Response

The function $h(t)$ is called the impulse response of a system. It is equal to the inverse Fourier transform of $H(\omega)$. The name, impulse, refers to the system output when excited by a delta function input. Thus

$$\begin{aligned} g(t) &= \frac{1}{2\pi} \int_{-\infty}^{\infty} H(\omega) F\{\delta(t)\} e^{j\omega t} d\omega \\ &= \frac{1}{2\pi} \int_{-\infty}^{\infty} H(\omega) e^{j\omega t} d\omega \\ &= h(t) \end{aligned} \quad (\text{Eq. 3-190})$$

(9) Causal System

A system is causal if the output follows, in time, the input. All physical systems are causal. If the system input/output relationship is written as

$$g(t) = \int_{-\infty}^{\infty} h(\tau) f(t - \tau) d\tau$$

and $f(t) = 0$ for $t < 0$, then (Eq. 3-191)

$$h(t) \equiv 0 \text{ for } t < 0$$

and

$$g(t) = \int_0^t h(\tau) f(t - \tau) d\tau$$

3.3.9 Transform Theory Summary

A variety of results on Fourier transform theory have been presented in the previous sections. As a matter of convenience, some of the major results will be summarized here.

3.3.9.1 Definition

$$\text{Basic: } G(\omega) = \int_{-\infty}^{\infty} g(t) e^{-j\omega t} dt, \quad \omega = 2\pi f \quad (\text{Eq. 3-19})$$

$$g(t) = \frac{1}{2\pi} \int_{-\infty}^{\infty} G(\omega) e^{j\omega t} d\omega \quad (\text{Eq. 3-20})$$

$$g(t) \text{ real: } g(t) = \frac{1}{\pi} \int_0^{\infty} [R_e\{G\} \cos \omega t - I_m\{G\} \sin(\omega t)] d\omega \quad (\text{Eq. 3-34})$$

$$g(t) \text{ real and: } g(t) = \frac{2}{\pi} \int_0^{\infty} R_e\{G\} \cos(\omega t) d\omega \quad (\text{Eq. 3-38})$$

$$g(t) = 0, \quad t \leq 0$$

$$= -\frac{2}{\pi} \int_0^{\infty} I_m\{G\} \sin(\omega t) d\omega$$

3.3.9.2 Asymptotic Solutions

$$\lim_{t \rightarrow 0} g(t): g(0^+) = \frac{1}{\pi} \int_0^{\infty} R_e\{G\} d\omega \quad \begin{matrix} g(t) \text{ real} \\ g(t) = 0, \quad t \leq 0 \end{matrix} \quad (\text{Eq. 3-41})$$

$$\lim_{\omega \rightarrow 0} G(\omega): G(0^+) = \int_0^{\infty} g(t) dt \quad (\text{Eq. 3-42})$$

$$\lim_{\omega \rightarrow \infty} G(\omega): G(\omega) \approx \frac{\Delta g^{(n)}}{(j\omega)^n + 1} e^{-j\omega t_0} \quad (\text{Eq. 3-50})$$

where the first $n - 1$ derivatives are continuous and n th derivative has a discontinuity at $t = t_0$ equal to $\Delta g^{(n)}$.

3.3.9.3 Waveform Modifications

Assume one has the following transform pair: $g(t) \leftrightarrow G(\omega)$. Then

$$\text{Similarity: } G(t) \leftrightarrow 2\pi g(-\omega) \quad (\text{Eq. 3-53})$$

$$\text{Linearity: } Ag(t) \leftrightarrow AG(\omega); A \text{ is a constant} \quad (\text{Eq. 3-54})$$

$$\text{Ordinate Scaling: } g(at) \leftrightarrow \frac{1}{|a|} G(\omega/a) \quad (\text{Eq. 3-57})$$

$$\text{Time Shift: } g(t - t_0) \leftrightarrow e^{-j\omega t_0} G(\omega) \quad (\text{Eq. 3-59})$$

$$\text{Frequency Shift: } g(t) e^{j\omega t_0} \leftrightarrow G(\omega - \omega_0) \quad (\text{Eq. 3-61})$$

$$\text{Time Differentiation: } g^{(n)}(t) \leftrightarrow (j\omega)^n G(\omega) \quad (\text{Eq. 3-65})$$

$$\text{Frequency Differentiation: } g(t) (-jt)^n \leftrightarrow G^{(n)}(\omega) \quad (\text{Eq. 3-67})$$

3.3.9.4 Simple Transforms

$$\text{Exponential: } e^{-\alpha t} \leftrightarrow \frac{1}{\alpha + j\omega}; \alpha > 0, t \geq 0. \quad (\text{Eq. 3-70})$$

$$\text{Double Exponential: } e^{-\alpha t} - e^{-\beta t} \leftrightarrow \frac{\beta - \alpha}{(\alpha + j\omega)(\beta + j\omega)}; \quad (\text{Eq. 3-73})$$

$$\beta > \alpha > 0, t \geq 0.$$

$$\text{Damped Sinusoid: } e^{-\alpha t} \sin \beta t \leftrightarrow \frac{\beta}{(\alpha + j\omega)^2 + \beta^2};$$

$$\beta > \alpha > 0, t \geq 0 \quad (\text{Eq. 3-76})$$

$$\text{Rect and Sinc: } \text{Rect}_T(x) = 1, \quad |x| < T/2$$

$$(\text{Eq. 3-77})$$

$$= 0 \quad |x| > T/2$$

$$\text{Sinc}(x) = \frac{\sin(\pi x)}{\pi x} \quad (\text{Eq. 3-79})$$

$$\text{Rect}_T(t) \leftrightarrow T \text{Sinc}(fT), \quad f = \omega/2\pi \quad (\text{Eq. 3-85})$$

$$f_0 \text{Sinc}(f_0 t) \leftrightarrow \text{Rect}_{\omega_0}(\omega), \quad \omega_0 = 2\pi f_0 \quad (\text{Eq. 3-87})$$

$$\text{Gaussian: } e^{-\alpha t^2} \leftrightarrow \sqrt{\frac{\pi}{\alpha}} e^{-\left(\frac{\omega^2}{4\alpha}\right)}, \quad \alpha > 0 \quad (\text{Eq. 3-92})$$

3.3.9.5 Special Functions

$$\text{Delta Function: } \int_a^b f(t) \delta(t - t_0) dt = f(t_0) \quad a < t_0 < b$$

$$= 0 \quad t_0 < a \text{ or } t_0 > b$$

$$(\text{Eq. 3-135})$$

$$\delta(t - t_0) = \infty \quad t = t_0$$

$$(\text{Eq. 3-134})$$

$$= 0 \quad t \neq t_0$$

$$\delta(t) \leftrightarrow 1$$

$$(\text{Eq. 3-153})$$

$$1 \leftrightarrow 2\pi\delta(\omega)$$

$$(\text{Eq. 3-155})$$

$$\text{Sgn Function: } \text{sgn}(t) = 1 \quad t > 0 \quad (\text{Eq. 3-159})$$

$$= -1 \quad t < 0$$

$$\text{sgn}(t) \leftrightarrow \frac{2}{j\omega} \quad (\text{Eq. 3-160})$$

$$\text{Step Function: } U(t-t_0) = 1 \quad t > t_0 \quad (\text{Eq. 3-158})$$

$$= 0 \quad t < t_0$$

$$U(t) \leftrightarrow \pi\delta(\omega) + \frac{1}{j\omega} \quad (\text{Eq. 3-169})$$

3.3.9.6 Product of Two Functions

$$\text{Time Domain Convolution: } G(\omega) = F(\omega)H(\omega) \quad (\text{Eq. 3-172})$$

$$g(t) = \int_{-\infty}^{\infty} f(\tau)h(t-\tau)d\tau \quad (\text{Eq. 3-178})$$

$$\text{Frequency Domain Convolution: } p(t) = r(t)s(t) \quad (\text{Eq. 3-184})$$

$$p(\omega) = \frac{1}{2\pi} \int_{-\infty}^{\infty} R(\sigma)S(\omega-\sigma)d\sigma \quad (\text{Eq. 3-185})$$

$$\text{Parseval's Theorem: } \int_{-\infty}^{\infty} g^2(t)dt = \frac{1}{2\pi} \int_{-\infty}^{\infty} |G(\omega)|^2 d\omega \quad (\text{Eq. 3-188})$$

3.3.10 Laplace Transforms

The previous sections have discussed, in some detail, selected topics on the theory of Fourier integral transforms (FIT). It is felt that this attention is justified since the FIT is generally given only cursory treatment in university engineering and physics programs. A transform which is given reasonable attention is the Laplace transform. In order to provide a tie to this existing body of experience, criteria for interchange of Laplace and FIT results are presented below. Also presented is the

rationale on why the FIT is used in preference to the Laplace transform in EMP data analysis.

The Laplace transform of $g(t)$, $L\{g(t)\}$, is defined as

$$L\{g(t)\} = \int_0^{\infty} g(t)e^{-st} dt, \quad s = \sigma + j\omega \quad (\text{Eq. 3-192})$$

There are two major differences between the definition of the Laplace transform and that of the Fourier transform given by Equation 3-19. One is that the limits of the integral are from $(0, \infty)$ instead of $(-\infty, \infty)$. The second is that the function, $g(t)$, is transformed with respect to the complex variable, $s = \sigma + j\omega$, instead of the imaginary variable, $j\omega$, in Equation 3-19.

An important question is when do the results of Laplace transform theory apply to someone using Fourier transforms. The answer is when the two formal differences between Laplace or Fourier transforms indicated above result in no difference in practice. For example, the effect of the difference in the integral limits is immaterial if $g(t)$ is defined only for positive values of time. Since EMP signals are transient in nature with a well-defined starting time, it is always possible to shift the waveform along the time axis until $g(t)$ is defined for positive values of time only. Thus either Fourier or Laplace transforms can be used with transient signals characteristic of EMP data.

Use of the variable s instead of $j\omega$ widens the class of functions where the transform integral converges. Equation 3-155 can be written as

$$\int_0^{\infty} g(t)e^{-st} dt = \int_0^{\infty} [g(t)e^{-\sigma t}]e^{-j\omega t} dt \quad (\text{Eq. 3-193})$$

This equation shows that when $g(t) = 0$ for $t < 0$, the Laplace transform is equivalent to the Fourier transform of $g(t)e^{-\sigma t}$. The primary criteria for either Equation 3-19 or Equation 3-192 to exist is that the integrals converge or that they be absolutely integrable (reference Equation 3-22). It is possible for the integral of $g(t)e^{-\sigma t}$ to converge while that for $g(t)$ does not. However, if σ is set equal to zero and one still has the defining integrals of both the Fourier and the Laplace transforms converge, then the Laplace and Fourier transforms are essentially identical.

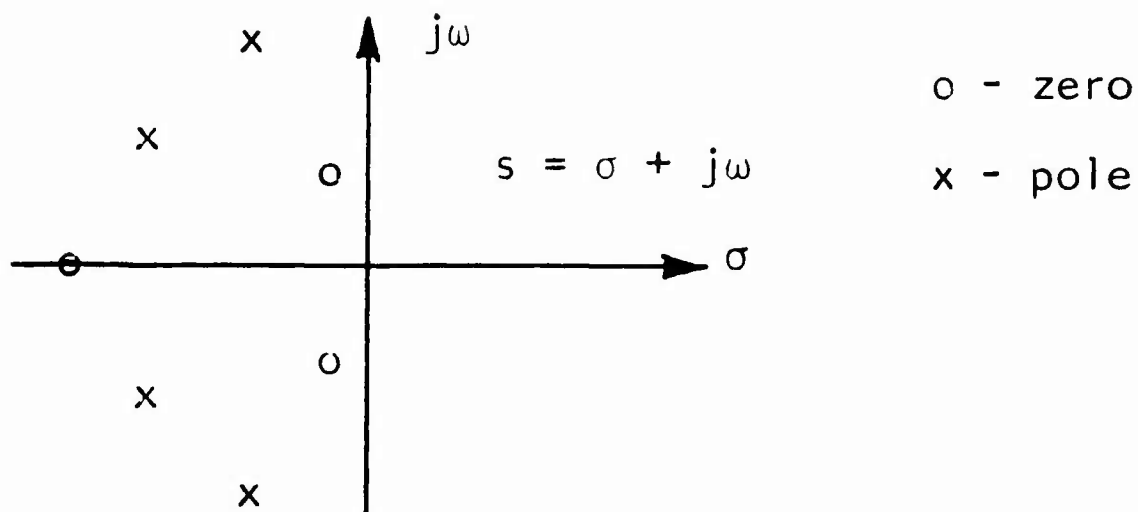
The above discussion indicates the conditions where the Laplace transform is identical in form to the Fourier transform. The two conditions are

$$\begin{aligned} g(t) &= 0, & t < 0 \\ \int_0^{\infty} |g(t)| dt &< \infty \end{aligned} \quad (\text{Eq. 3-194})$$

If these two conditions are valid, then Laplace transforms can be converted to Fourier transforms by the substitution of $j\omega$ for s . Similarly Fourier transforms can be converted to Laplace transforms by the substitution of s for $j\omega$.

The previous paragraph has shown that either Laplace or Fourier transforms can be used with transient signals characteristic of EMP data. However, the Fourier transform is the preferred technique for use with experimental data. The reason for this choice is one of practicality.

Laplace transforms are defined in terms of a complex frequency variable, s . Knowledge of the specific values of s , s_i , where the Laplace transform either goes to zero or to infinity (pole), is all that is required to characterize, except for a scale factor, a Laplace transform.



These poles and zeros can generally be found when using theoretical relations. However, locating these poles and zeros is not straightforward when using experimental data.

Fourier transforms, on the other hand, are defined only on the $j\omega$ axis. The magnitude and phase of the Fourier transform is obtained by straightforward numerical evaluation of Equation 3-19 using an experimental time domain data record. Furthermore, instrumentation calibration data are given in terms of the magnitude and phase of the instrumentation transfer function. This transfer function is measured directly using a tuneable frequency signal generator and a phase and amplitude sensitive detector. Therefore Fourier transform theory is directly compatible with the form of instrumentation calibration data and numerical transforms of experimental transient waveforms.

3.3.11 Examples

3.3.11.1 Introduction

The previous subsections have presented the basic definitions and theorems of Fourier transform theory as well as transforms of simple functions. This material is sufficient to give a reader the basic tools required for the analysis and interpretation of EMP data. However, facility in using transform theory only comes with practice. In order to bridge the gap between theory and practical application, several examples are presented. These examples not only provide demonstrations on the application of Fourier transform theory, but also introduce new results that might be useful to the reader. Many of these examples emphasize use of the delta function and the convolution theorem as facility in using these techniques is mandatory for efficient use of transform theory.

3.3.11.2 Convergence and Gibb's Phenomena

The basic definition of the Fourier transform given by Equations 3-19 and 3-20 implies that if one obtains the transform of $g(t)$ according to Equation 3-19 and then obtains the inverse transform of $G(\omega)$ using Equation 3-20, the resultant function should equal the original.

$$F^{-1}\{F\{g(t)\}\} = g(t) \quad (\text{Eq. 3-195})$$

This result is true if $g(t)$ is continuous. However, the reader may recall from undergraduate electronics, that a Fourier series does not converge at a discontinuity. Indeed there are oscillations in the vicinity of the discontinuity called Gibb's phenomena. The same phenomena occurs with the FIT. The following paragraphs will demonstrate Gibb's phenomena and the convergence of the FIT in the vicinity of a discontinuity.

The simplest function to demonstrate the convergence of the FIT is the unit step function, $U(t)$. The demonstration begins by obtaining the Fourier transform of $U(t)$. Then the inverse transform of the result will be obtained. Thus

$$g(t) = U(t)$$

and

$$G(\omega) = \int_{-\infty}^{\infty} U(\tau) e^{-j\omega\tau} d\tau \quad (\text{Eq. 3-196})$$

Let us first examine the case where only the transform data in the range $(-\omega_0, \omega_0)$ are used to obtain the inverse transform. Then

$$\begin{aligned} F_{\omega_0}^{-1}\{G(\omega)\} &= \frac{1}{2\pi} \int_{-\omega_0}^{\omega_0} \left[\int_{-\infty}^{\infty} U(\tau) e^{-j\omega\tau} d\tau \right] e^{j\omega t} d\omega \\ &= \frac{1}{2\pi} \int_{-\infty}^{\infty} U(\tau) \left[\int_{-\omega_0}^{\omega_0} e^{j\omega(t-\tau)} d\omega \right] d\tau \\ &= \int_{-\infty}^{\infty} U(\tau) \frac{\sin \omega_0(t-\tau)}{\pi(t-\tau)} d\tau \\ &= \int_0^{\infty} \frac{\sin \omega_0(t-\tau)}{\pi(t-\tau)} d\tau \end{aligned} \quad (\text{Eq. 3-197})$$

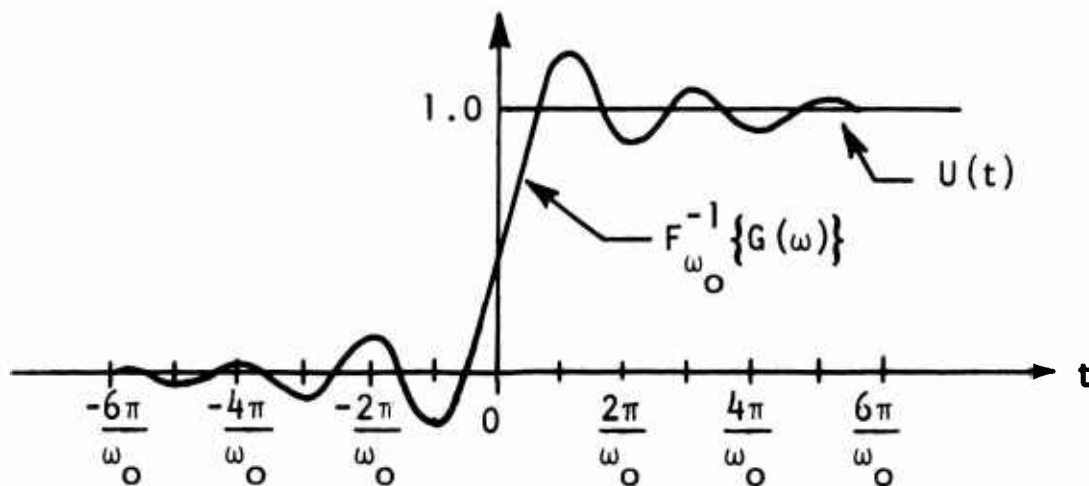
Substituting x for $\omega_o(t-\tau)$, one finds

$$\begin{aligned}
 F_{\omega_o}^{-1}\{G(\omega)\} &= \int_{-\infty}^{\omega_o t} \frac{\sin x}{\pi x} dx \\
 &= \int_{-\infty}^0 \frac{\sin x}{\pi x} dx + \int_0^{\omega_o t} \frac{\sin x}{\pi x} dx \quad (\text{Eq. 3-198}) \\
 &= \int_{-\infty}^0 \text{Sinc}(x) dx + \frac{1}{\pi} \int_0^{\omega_o t} \frac{\sin x}{x} dx
 \end{aligned}$$

Equation 3-80 shows that the first integral equals $1/2$ while Equation 3-81 indicates that the second integral is the Si function. Thus

$$F_{\omega_o}^{-1}\{G(\omega)\} = \frac{1}{2} + \frac{1}{\pi} \text{Si}(\omega_o t) \quad (\text{Eq. 3-199})$$

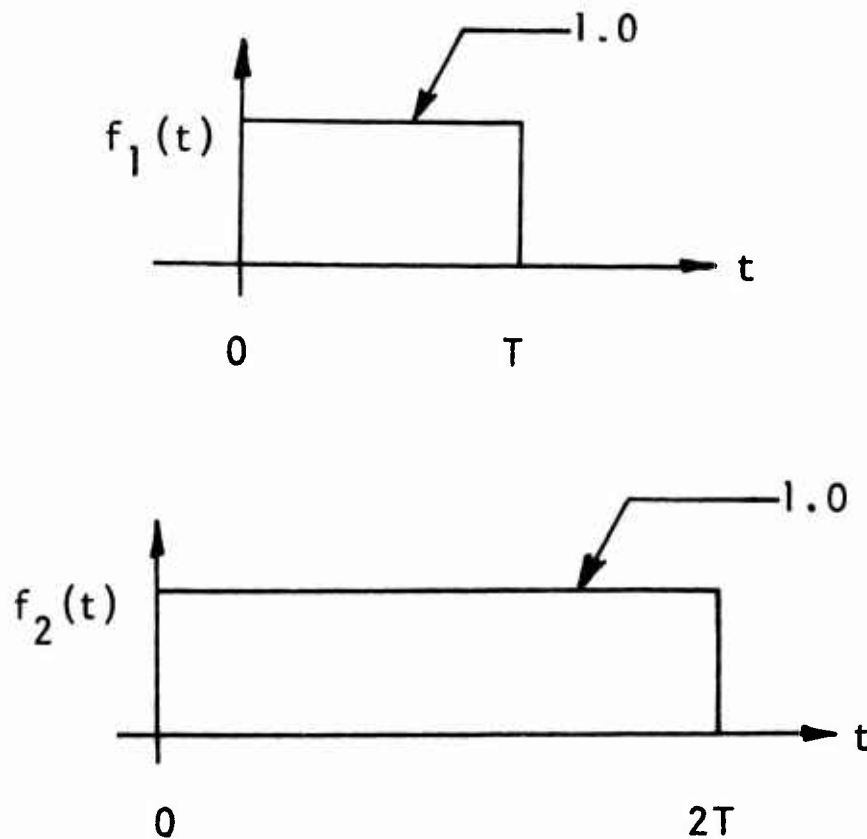
A sketch of this function is shown below.



There are three important points to note about this result. One is that as $t \rightarrow 0$, Equation 3-199 equals $1/2$. Therefore the Fourier transform converges to the mean value of the discontinuity. The second point to note is that as $\omega_0 \rightarrow \infty$, the period of the oscillation decreases but the oscillation magnitude remains constant. The final point is that the maximum overshoot exceeds the desired value by nine percent.

3.3.11.3 Triangular Functions

A triangular function with ramp type increases and decreases from its peak can be constructed from the convolution of two Rect functions. In this example, $f_1(t)$ and $f_2(t)$ are convoluted to obtain $f_3(t)$.



Application of Equation 3-178 yields

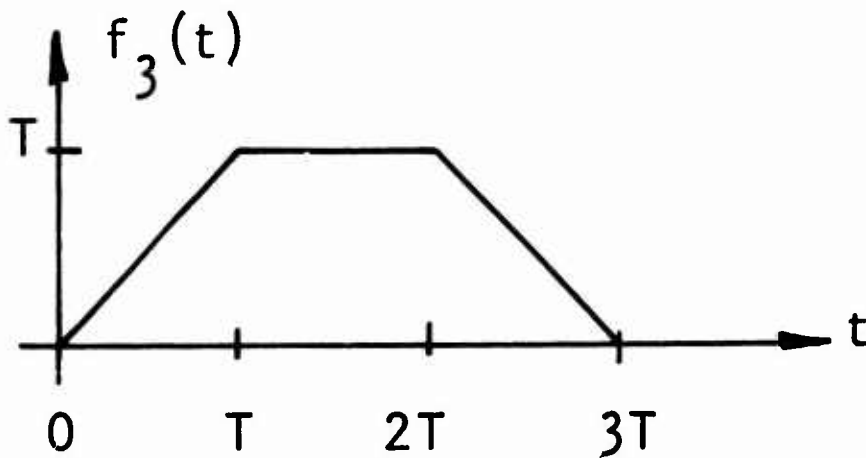
$$f_3(t) = \int_0^t d\tau = t \quad 0 < t < T$$

$$= \int_0^T d\tau = T \quad T < t < 2T$$

(Eq. 3-200)

$$= \int_{t-T}^T d\tau = 2T - t \quad 2T < t < 3T$$

$$= \int_T^T d\tau = 0 \quad 3T < t$$



The reader should graphically construct the convolution process used in this example to verify the limits used in the above equation.

An interesting variation of this example occurs when $f_1(t)$ is convolved with itself to yield $f_4(t)$.

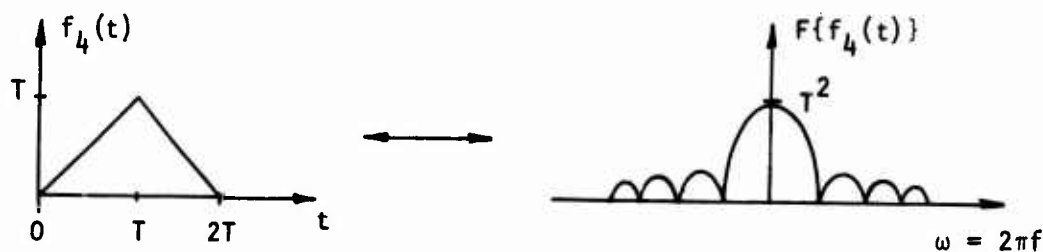
$$\begin{aligned}
 f_4(t) &= \int_0^t d\tau = t & 0 < t < T \\
 &= \int_{T-t}^T d\tau = 2T-t & T < t < 2T \\
 &= \int_T^T d\tau = 0 & 2T < t
 \end{aligned}
 \tag{Eq. 3-201}$$

Now obtain the Fourier transform of $f_4(t)$. This transform can be obtained from the transform of $f_1(t)$. Note that $f_1(t)$ is just $\text{Rect}_T(t)$ shifted by the amount $T/2$. Use of Equations 3-85 and 3-59 provides the transform of $f_1(t)$.

$$F\{f_1(t)\}_f = T \text{Sinc}(fT) e^{-j\omega T/2} \tag{Eq. 3-202}$$

Noting that the convolution of two functions in the time domain implies the product of their transforms in the frequency domain, one finds

$$F\{f_4(t)\} = (T \text{Sinc}(fT))^2 e^{-j\omega T} \tag{Eq. 3-203}$$



3.3.11.4 Delta Functions and Convolution

Delta functions and the convolution theorem, or a combination of both, can be used to provide simple derivations of the Fourier transform of a variety of functions. The following paragraphs present a few examples of this application.

3.3.11.4.1 $\sin(\omega_0 t)$

Equation 3-40 shows that

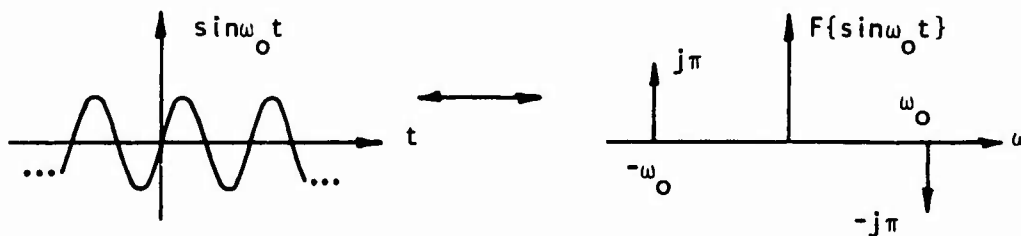
$$\sin \omega_0 t = \frac{1}{2j} \left[e^{j\omega_0 t} - e^{-j\omega_0 t} \right] \quad (\text{Eq. 3-204})$$

However Equation 3-157 indicates

$$e^{j\omega_0 t} \leftrightarrow 2\pi \delta(\omega - \omega_0) \quad (\text{Eq. 3-157})$$

Therefore the Fourier transform of $\sin \omega_0 t$ is

$$\sin(\omega_0 t) \leftrightarrow j\pi \left[\delta(\omega + \omega_0) - \delta(\omega - \omega_0) \right] \quad (\text{Eq. 3-205})$$

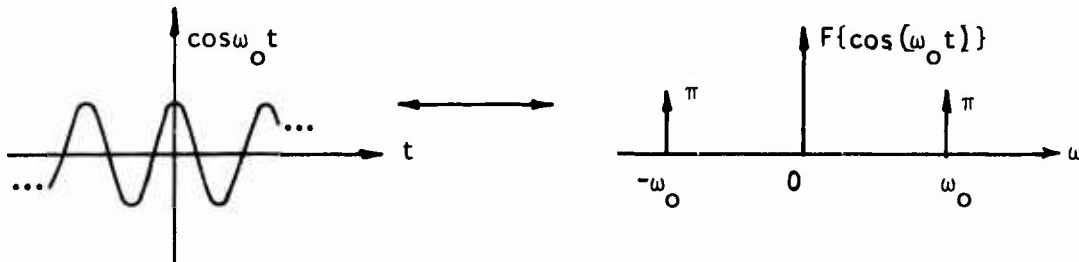


In the previous figure, the arrows located at $\pm\omega_0$ symbolically represent $\delta(\omega \pm \omega_0)$. The factors, $j\pi$, represent the weight of the delta functions.

3.3.11.4.2 $\cos(\omega_0 t)$

The Fourier transform of $\cos(\omega_0 t)$ can be derived by use of Equations 3-40 and 3-157 also. The result is

$$\cos(\omega_0 t) \leftrightarrow \pi \left[\delta(\omega + \omega_0) + \delta(\omega - \omega_0) \right] \quad (\text{Eq. 206})$$



3.3.11.4.3 $e^{-\alpha t} \sin \beta t$

Use of Equation 3-40 shows that

$$e^{-\alpha t} \sin(\beta t) = \frac{1}{2j} \left[e^{-\alpha t} e^{j\beta t} - e^{-\alpha t} e^{-j\beta t} \right]$$

The transform of the product of the two exponentials in this equation can be obtained by the convolution theorem.

$$\begin{aligned}
 F \{ e^{-\alpha t} e^{j\beta t} \} &= F \{ e^{-\alpha t} \} * F \{ e^{j\beta t} \} \\
 &= \frac{1}{\alpha + j\omega} * 2\pi \delta(\omega - \beta) \\
 &= \frac{1}{\alpha + j\omega - j\beta}
 \end{aligned}
 \tag{Eq. 3-207}$$

In a similar manner, one finds

$$F \{ e^{-\alpha t} e^{-j\beta t} \} = \frac{1}{\alpha + j\omega + j\beta} \tag{Eq. 3-208}$$

Combining Equations 3-207 and 3-208 according to Equation 3-205, one finds

$$e^{-\alpha t} \sin(\beta t) \leftrightarrow \frac{\beta}{(\alpha + j\omega)^2 + \beta^2} \tag{Eq. 3-209}$$

This result should be compared to Equation 3-75.

3.3.11.4.4 Burst CW

Given a burst CW waveform, $b(t)$,
defined as follows:

$$\begin{aligned}
 b(t) &= \cos \omega_0 t & |t| < T/2 \\
 &0 & |t| > T/2
 \end{aligned}
 \tag{Eq. 3-210}$$

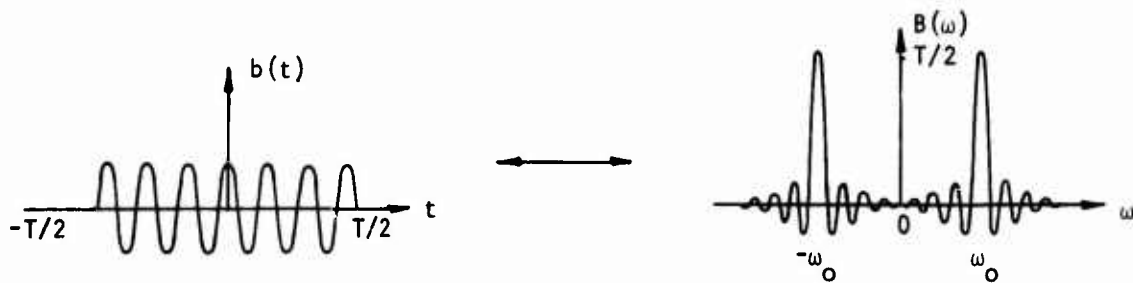
This function is equal to the product of $\text{Rect}_T(t)$ and the sinusoidal function with infinite duration. Thus

$$b(t) = \text{Rect}_T(t) \cos(\omega_0 t) \tag{Eq. 3-211}$$

The transform of $b(t)$ is given by the convolution theorem

$$\begin{aligned}
 B(\omega) &= \pi \left[\delta(\omega + \omega_0) + \delta(\omega - \omega_0) \right] * T \text{Sinc}(fT) \\
 &= \frac{T}{2} \left[\int_{-\infty}^{\infty} \text{Sinc}\left(\frac{\sigma T}{2\pi}\right) \delta(\omega - \sigma + \omega_0) d\sigma + \int_{-\infty}^{\infty} \text{Sinc}\left(\frac{\sigma T}{2\pi}\right) \delta(\omega - \sigma - \omega_0) d\sigma \right] \\
 &= \frac{T}{2} \text{Sinc}[(f + f_0)T] + \frac{T}{2} \text{Sinc}[(f - f_0)T] \quad (\text{Eq. 3-212})
 \end{aligned}$$

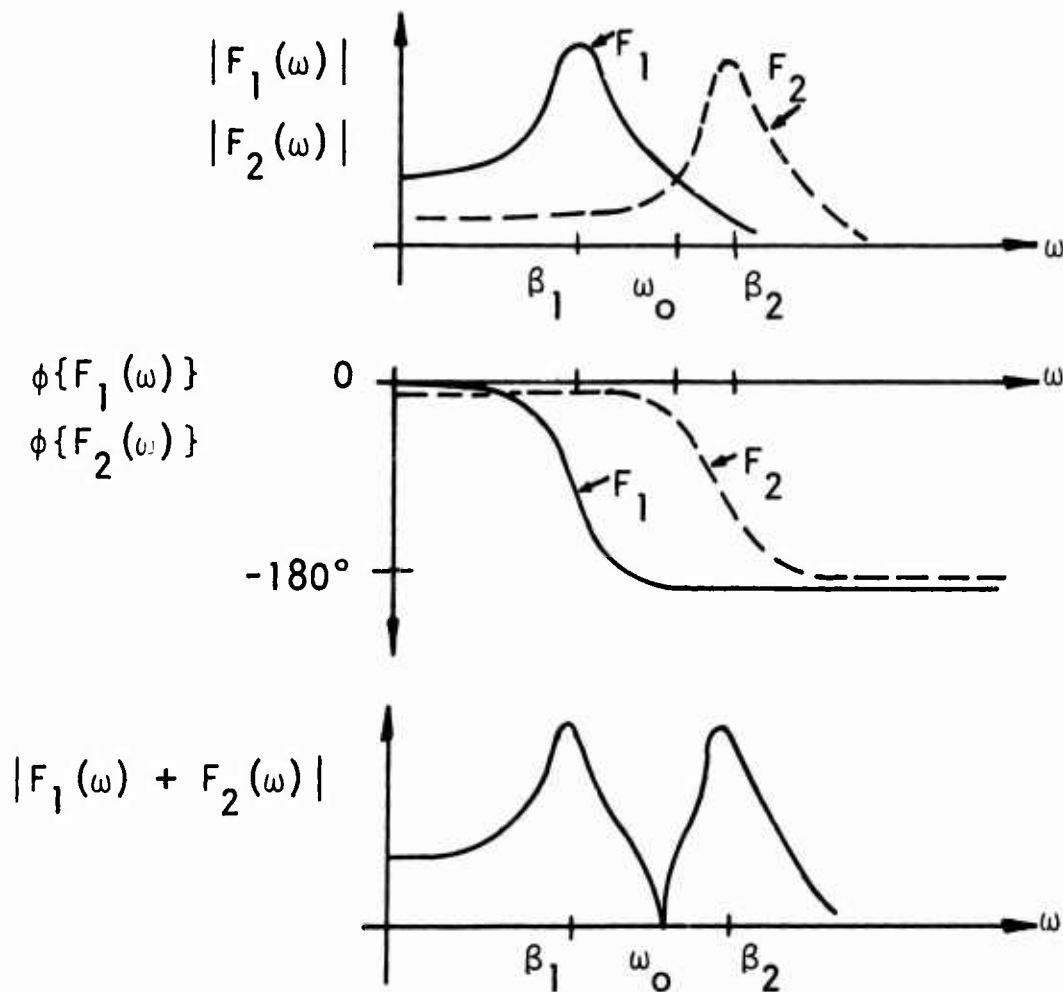
Thus the transform of a burst CW wave is just the Sinc function shifted to $\pm \omega_0$ ($\pm f_0$).



3.3.11.5 Notches

The presence of notches in the magnitude of the Fourier transform sometimes causes concern with EMP data analysis. It is a prominent feature that begs explanation. There are a variety of causes for these notches. For instance, inspection of Equations 3-84 and 3-203 shows that the Rect and the triangular functions have transforms with notches. Another cause is described below.

A spectral notch can occur when two frequency dependent functions interfere destructively. Destructive interference implies the magnitudes of the two functions are equal and the phases differ by 180 degrees. Now consider a specific example of a damped sinusoid. For ω much greater than resonance, the phase is approximately -180 degrees. Now consider a specific example of a damped sinusoid. For ω well below resonance, the phase is close to zero degrees. For ω much greater than resonance, the phase is approximately -180 degrees. If one has two damped sinusoids resonant at β_1 and β_2 , then the phase difference between the Fourier transforms of the two functions is approximately 180 degrees for $\beta_1 < \omega < \beta_2$. If the magnitudes are approximately equal in this range, then there will be a notch or a relative null.



3.3.11.6 Periodicities

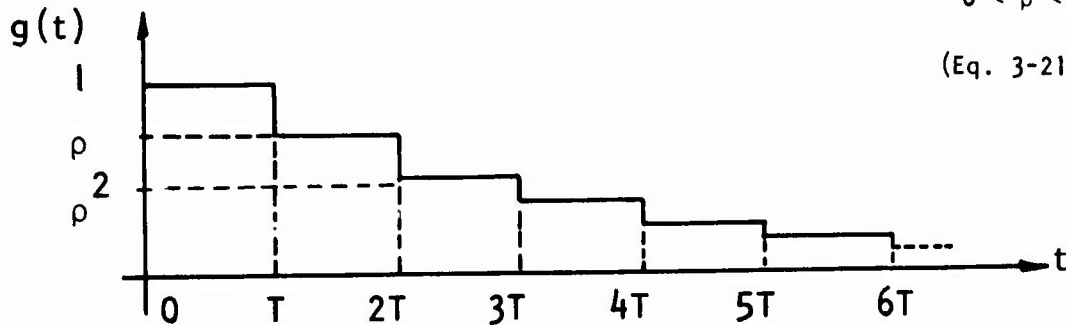
Many signals observed in EMP testing exhibit some type of periodic or repetitive behavior. The periodicity in the time domain waveform results in an interesting periodic behavior in the Fourier transform data. Repetitive nulls or peaks are possible. The following paragraphs present four interesting examples.

Consider a signal of the form

$$g(t) = \text{Rect}_T(t - T/2) + \rho \text{Rect}_T(t - 3T/2) + \rho^2 \text{Rect}_T(t - 5T/2) + \dots$$

$$0 < \rho < 1$$

(Eq. 3-213)

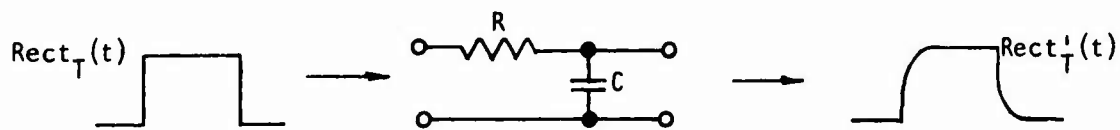


This waveform is characteristic of the ARES electromagnetic field environment in that it has a periodic structure and that it approximates an exponential decay. Using Equations 3-85 and 3-59, one finds the Fourier transform of $g(t)$ equal to

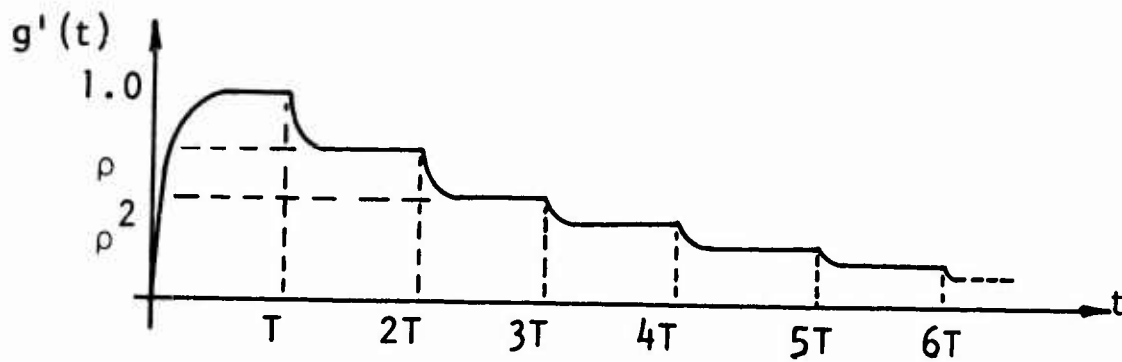
$$\begin{aligned} G(\omega) &= \left[T \text{Sinc}(fT) e^{-j\omega T/2} \right] \left[1 + \rho e^{-j\omega T} + \rho^2 e^{-j\omega 2T} + \dots \right] \\ &= \left[T \text{Sinc}(fT) e^{-j\omega T/2} \right] \left[\frac{1}{1 - \rho e^{-j\omega T}} \right] \end{aligned} \quad (\text{Eq. 3-214})$$

Note that $1 + x + x^2 + \dots = 1/(1 - x)$ where $|x| < 1$. Thus $G(\omega)$ is the product of two functions, one of which ($\text{Sinc}(fT)$) has notches (zeros). Therefore, the resultant function has notches at $f = \pm n/T$ or $\omega = \pm 2\pi n/T$ where n is an integer.

Now consider a waveform similar to the above except that each Rect function is passed through an RC network



The resultant function, $g'(t)$, is sketched below



This waveform is a closer approximation to the ARES environment waveshape than the previous one. The transform of the modified Rect pulse is given by the product of the transform of $\text{Rect}_T(t)$ and the transfer function of the RC network.

$$H_{RC}(\omega) = \frac{1}{RC} \frac{1}{\frac{1}{RC} + j\omega} = \frac{\omega_o}{\omega_o + j\omega} \quad \omega_o = 1/RC \quad (\text{Eq. 3-215})$$

Thus

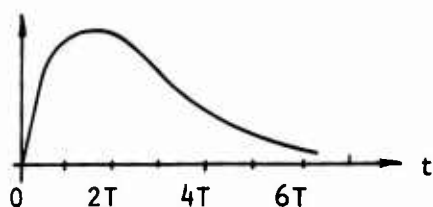
$$F \{ \text{Rect}_T'(t) \} = \left[T \text{Sinc}(fT) \right] \left[\frac{\omega_o}{\omega_o + j\omega} \right] \quad (\text{Eq. 3-216})$$

Finally the Fourier transform of $g'(t)$ is

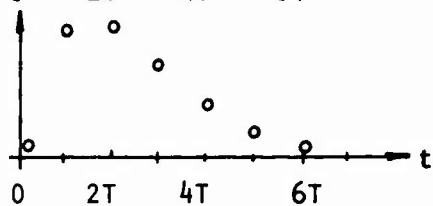
$$G'(\omega) = \left[T \text{Sinc}(fT) e^{-j\omega T/2} \right] \left[\frac{\omega_o}{\omega_o + j\omega} \right] \left[\frac{1}{1 - \rho e^{-j\omega T}} \right] \quad (\text{Eq. 3-217})$$

The general conclusion that can be drawn from this example is that any waveform with notches in the frequency domain that is passed through a linear network still has notches. One can find a more complex network to filter $g(t)$ such that the output very closely resembles the ARES environment. However, as long as $G(\omega)$ has notches and the network is linear, then the resultant output must have notches also.

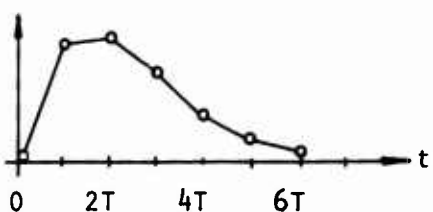
A common occurrence in EMP data analysis is to obtain an experimental data record, digitize it at equally spaced intervals, fit straight line segments between the digitized points, and finally obtain a Fourier transform of the piecewise linear approximation of the experimental data record.



Experimental data record

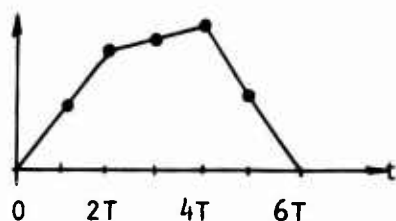


Digitized points

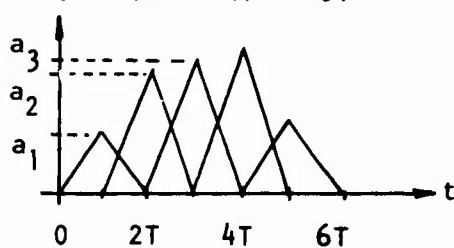


Piecewise linear approximation

The periodicity in the sampling results in notches in the resultant Fourier transform. To see this fact, we will reduce the piecewise linear approximation to a series of triangles.



Piecewise linear approximation



Triangular equivalent

The reader can easily convince himself by either graphical or analytic techniques that the polygon approximation is equivalent to a sum of triangles. Let a triangular function of base with $2T$, centered at $t = 0$, and unity height be designated as $\Delta_{2T}(t)$. Then the triangular representation, $g(t)$, can be written as

$$g(t) = a_1 \Delta_{2T}(t - T) + a_2 \Delta_{2T}(t - 2T) + \dots \quad (\text{Eq. 3-218})$$

The Fourier transform may be obtained by use of Equations 3-203 and 3-59. The result is

$$G(\omega) = \left[T \text{sinc}^2(fT) e^{-j\omega T} \right] \left[a_1 + a_2 e^{-j\omega T} + a_3 e^{-j\omega 2T} + \dots \right] \quad (\text{Eq. 3-219})$$

The first bracketed term has notches at $f = \pm n/T$ where n is an integer. Therefore $G(\omega)$ will have notches at these frequencies independent of the contribution of the second bracket term.

The three previous examples of waveforms with periodic structure show that if the transform of the building block waveform has notches in its spectrum, then so does the complete waveform. In this last example a building block waveform without frequency domain notches is used.

Consider an infinite replication of a waveform without spectral notches

$$g(t) = f_1(t) - \rho f_1(t - T) + \rho^2 f_1(t - 2T) - \rho^3 f_1(t - 3T) + \dots$$

$$0 < \rho < 1$$

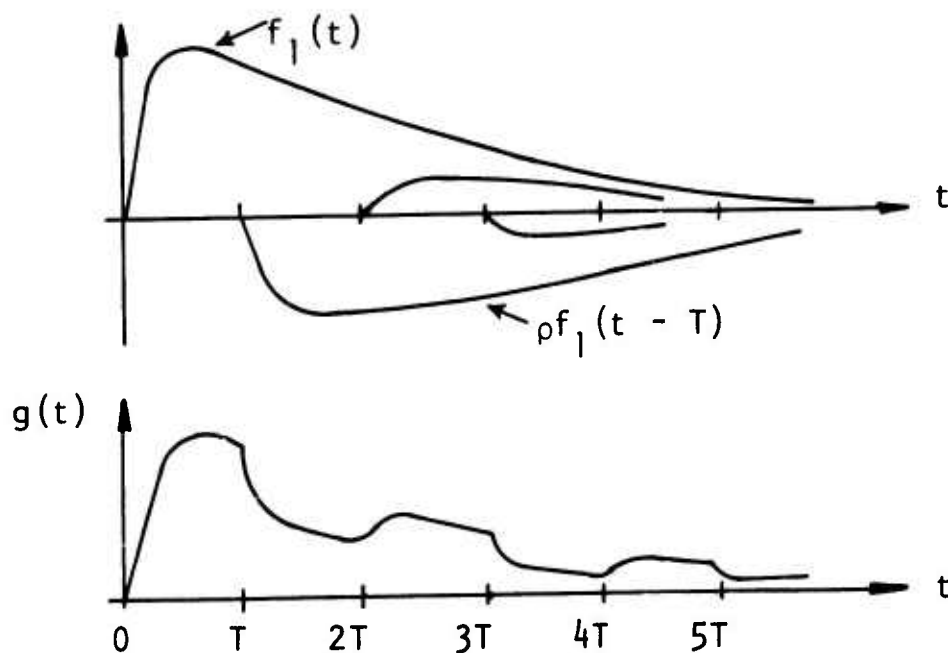
(Eq. 3-220)

This type of signal could be produced by multiple reflections on a cable inside an EMP excited system. Then to consider a specific case, let

$$f_1(t) = e^{-\alpha t} - e^{-\beta t}, \quad t \geq 0$$

$$= 0 \quad t < 0$$

(Eq. 3-221)

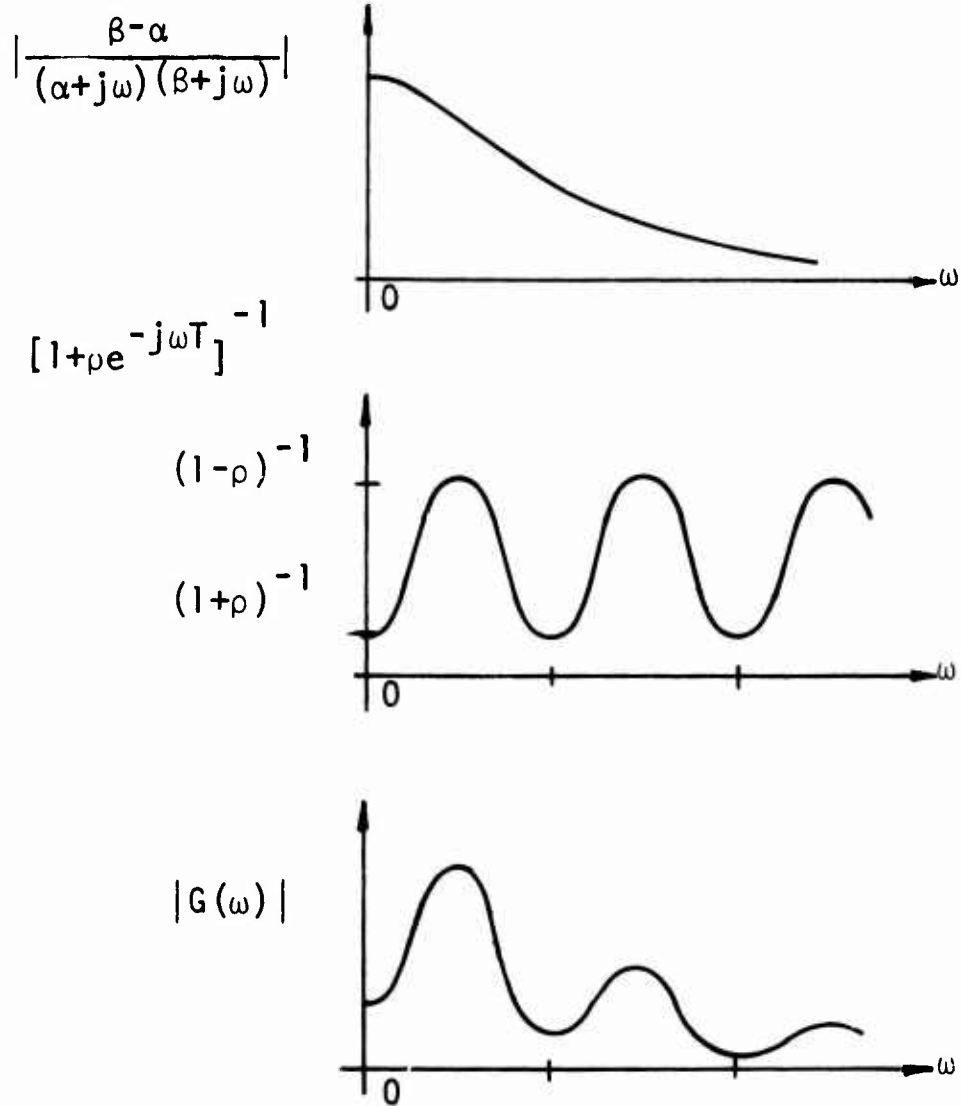


The Fourier transform of $g(t)$ is obtained in a manner similar to the previous examples.

$$G(\omega) = \left[\frac{\beta - \alpha}{(\alpha + j\omega)(\beta + j\omega)} \right] \left[1 - \rho e^{-j\omega T} + \rho^2 e^{-j\omega 2T} - \dots \right] \quad (\text{Eq. 3-222})$$

$$= \left[\frac{\beta - \alpha}{(\alpha + j\omega)(\beta + j\omega)} \right] \left[\frac{1}{1 + \rho e^{-j\omega T}} \right]$$

The second bracketed term has relative minimums located at $f = \pm n/T$ where n is an integer. Peaks are equally spaced between these minimums and can be quite large if ρ is close to unity. Estimates of the resultant spectral magnitude can be obtained by graphical sketches.



Thus the resultant spectral amplitude exhibits periodic peaks and valleys. The structure is determined by the second bracketed term in Equation 3-222. The spectral magnitude of the building block waveform forms the envelope of the resultant amplitude.

3.3.11.7 Integration

Given a waveform $f(t)$ and its transform $F(\omega)$, now obtain the integral of $f(t)$, namely $g(t)$. The integral of $f(t)$ can be written as

$$g(t) = \int_0^t f(\tau) U(t - \tau) d\tau \quad (\text{Eq. 3-223})$$

where $U(t)$ is the step function. Noting the convolution process in this equation, one can write $G(\omega)$ as

$$G(\omega) = F(\omega) \left[\pi \delta(\omega) + 1/j\omega \right] \quad (\text{Eq. 3-224})$$

Finally $g(t)$ can be obtained as the inverse transform of $G(\omega)$. This roundabout procedure is actually convenient, at times, in EMP data analysis. However, in many cases the factor, $\pi \delta(\omega)$, is neglected. The reason is probably that the analyst recalls that the Laplace transform of a step function is $1/s$. Then he substitutes $j\omega$ for s which, in this case, is not valid. In the following paragraphs, the impact of neglecting the delta function term will be investigated.

The contribution to the inverse transform from the factor containing $\delta(\omega)$ will be obtained first.

$$\begin{aligned} F^{-1} \left\{ \pi \delta(\omega) F(\omega) \right\} &= \frac{1}{2\pi} \int_{-\infty}^{\infty} F(\omega) \pi \delta(\omega) e^{j\omega t} d\omega \\ &= \frac{1}{2} F(0) \end{aligned} \quad (\text{Eq. 3-225})$$

From Equation 3-42, one notes that $F(0)$ equals the net area under the curve of $f(t)$. Thus

$$F(0) = \int_{-\infty}^{\infty} f(t) dt \quad (\text{Eq. 3-226})$$

To examine the effect of neglecting the contribution from the delta function, consider a specific example. Let

$$f(t) = e^{-\alpha t}, \quad t \geq 0 \quad (\text{Eq. 3-227})$$

Straightforward integration shows

$$g(t) = \frac{1}{\alpha} [1 - e^{-\alpha t}]$$

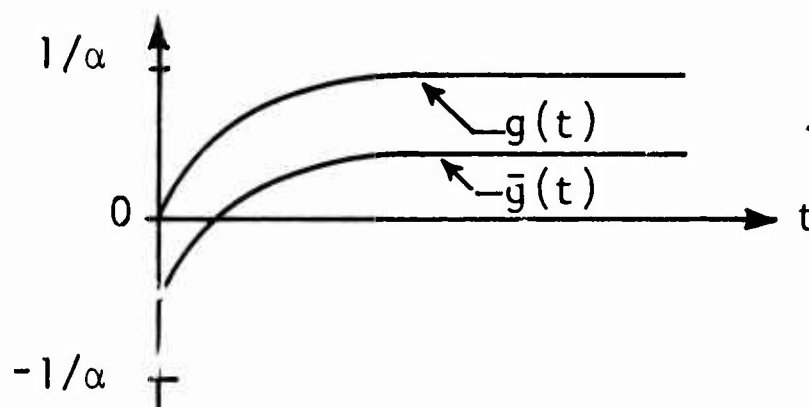
and

(Eq. 3-228)

$$F(0) = \frac{1}{\alpha}$$

If the delta function contribution is neglected, the resultant waveform, $\bar{g}(t)$, is

$$\begin{aligned} \bar{g}(t) &= g(t) - \frac{1}{2} F(0) \\ &= \frac{1}{\alpha} \left[\frac{1}{2} - e^{-\alpha t} \right] \end{aligned} \quad (\text{Eq. 3-229})$$



In this particular case, neglect of the delta function contribution is significant.

Now consider the case where $f(t)$ is the derivation of some function, say $e(t)$. The transform of $f(t)$ is given by Equation 3-65 as

$$F(\omega) = j\omega E(\omega) \quad (\text{Eq. 3-230})$$

When this result is substituted into Equation 3-224, one finds

$$G(\omega) = E(\omega) + j\omega E(\omega) \pi \delta(\omega) \quad (\text{Eq. 3-231})$$

The inverse transform of this equation is

$$\begin{aligned} G(t) &= \frac{1}{2\pi} \int_{-\infty}^{\infty} [E(\omega) + j\omega E(\omega) \pi \delta(\omega)] e^{j\omega t} d\omega \\ &= \frac{1}{2\pi} \int_{-\infty}^{\infty} E(\omega) e^{j\omega t} d\omega \\ &= e(t) \end{aligned} \quad (\text{Eq. 3-232})$$

In this case, there is no contribution from the delta function since the term, $j\omega E(\omega)$, provides zero weight to the delta function upon integration.

The conclusion from this example is that the integral of $f(t)$ equals the inverse transform of $F(\omega)/j\omega$ if and only if $f(t)$ is the derivative of some other function. Otherwise the contribution from the delta function must be included.

3.3.11.8 Filters

Filters are a generic name for a system that selectively transmits or attenuates selected portions of the input signal spectrum. In general, any system can be considered as a filter. However, some systems have a simple form of transfer function that permits simplified analysis of the output. Examples of simple systems are low pass, bandpass, and high pass filters. A brief sample of the use of Fourier transform theory to analyze filter response is presented below. The purpose of these examples is to demonstrate use of convolution, impulse functions, and linear systems concepts in reducing complex problems to several simple exercises. Further examples are given in Papoulis [Reference 23].

3.3.11.8.1 Low Pass

Consider first a low pass filter with a transfer function given in terms of its magnitude, $M(\omega)$, and phase $\phi(\omega)$.

$$H(\omega) = M(\omega) e^{-j\phi(\omega)} \quad (\text{Eq. 3-233})$$

If the filter output is real when the input signal is real, then $M(\omega)$ and $\phi(\omega)$ must be even and odd functions of ω respectively.

$$M(-\omega) = M(\omega) \quad (\text{Eq. 3-234})$$

$$\phi(-\omega) = -\phi(\omega)$$

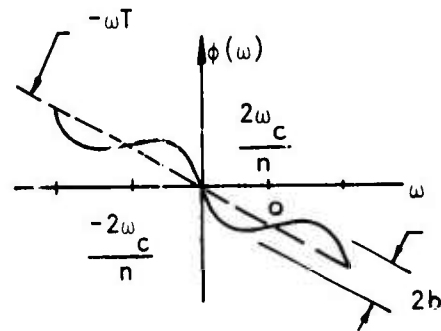
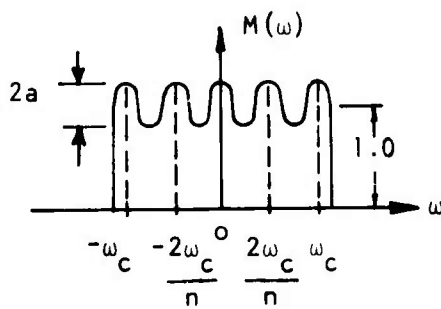
Now consider a specific example where

$$M(\omega) = 1 + a \cos(n\pi\omega/\omega_c) \quad |\omega| < \omega_c$$

$$= 0 \quad |\omega| > \omega_c \quad (\text{Eq. 3-235})$$

$$\phi(\omega) = \omega T + b \sin(m\pi\omega/\omega_c) \quad (\text{Eq. 3-236})$$

where a , b , m , n , and T are constants and ω_c is the cutoff frequency of the low pass filter.

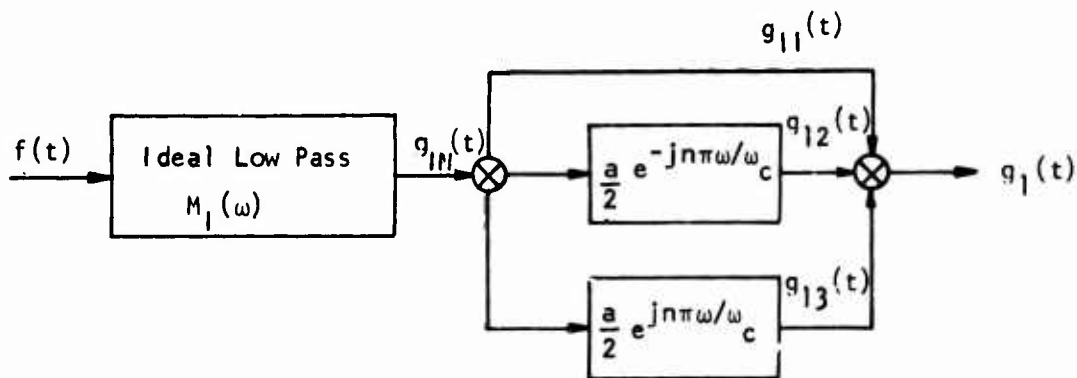


This transfer function is representative of many systems that have a frequency dependent ripple in the magnitude and phase. The output of this filter will be obtained by treating effects of the magnitude and phase separately.

The influence of $M(\omega)$ on the filter output can be examined by reducing Equation 3-235 to an ideal low pass filter. Define the transfer function magnitude of an ideal low pass filter, $M_1(\omega)$, such that

$$\begin{aligned} M_1(\omega) &= 1 & |\omega| < \omega_c \\ &= 0 & |\omega| > \omega_c \end{aligned} \quad (\text{Eq. 3-237})$$

Note that the first term of Equation 3-235 is identical to the definition of $M_1(\omega)$. Furthermore, the second term of Equation 3-235 is equivalent to the sum of two functions of constant magnitude, $a/2$, and a frequency dependent phase equal to $\pm n\pi\omega/\omega_c$. The following flow diagram shows that the steps one should use to compute the output of a filter with a transfer function given by Equation 3-235.



According to Equation 3-87, the impulse response, $h_1(t)$, of $M_1(t)$ is

$$h_1(t) = 2f_c \text{Sinc}(2f_c t), \quad f_c = \omega_c/2\pi \quad (\text{Eq. 3-238})$$

Note that $h_1(t)$ is an even function. This is no coincidence. Since if $M(\omega)$ of a low pass filter is real and even, then its inverse Fourier transform must also be real and even. By the convolution theorem, the output of an ideal low pass filter is

$$g_{111}(t) = f(t) * 2f_c \text{Sinc}(2f_c t)$$

If $f(t)$ is a unit step function, $U(t)$, then $g_{111}(t)$ is given by Equation 3-83.

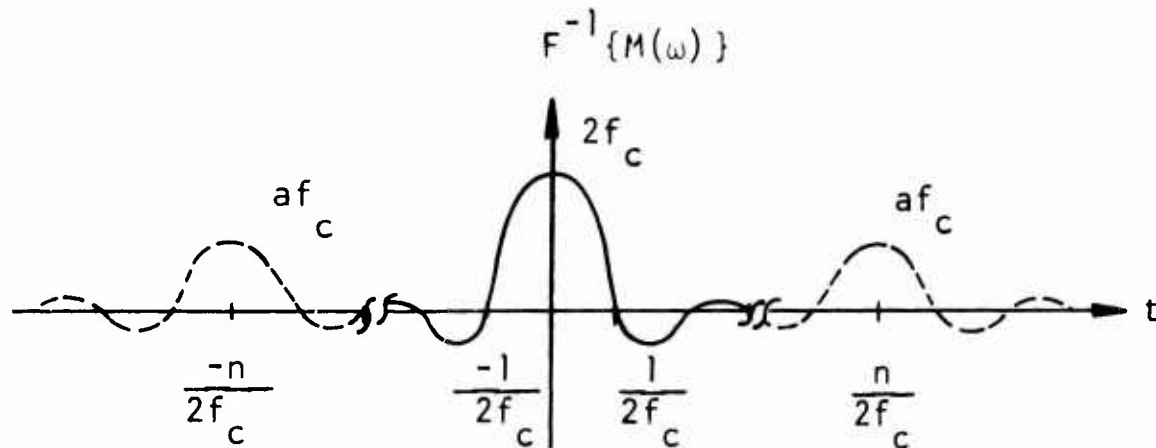
The effects of the terms given by $(a/2)e^{\pm jn\pi\omega/\omega_c}$ are simply determined by referencing Equations 3-54 and 3-59. For example $g_{12}(t)$ in terms of $f(t)$ is

$$g_{12}(t) = f(t) * af_c \text{Sinc}\left[2f_c\left(t - \frac{n}{2f_c}\right)\right] \quad (\text{Eq. 3-239})$$

and $g_1(t)$ is

$$\begin{aligned} g_1(t) = f(t) * 2f_c \left\{ \text{Sinc}[2f_c t] + \frac{a}{2} \right\} & \left\{ \text{Sinc}\left[2f_c\left(t - \frac{n}{2f_c}\right)\right] \right. \\ & \left. + \frac{a}{2} \text{Sinc}\left[2f_c\left(t + \frac{n}{2f_c}\right)\right] \right\} \end{aligned} \quad (\text{Eq. 3-240})$$

The term enclosed in the brackets, $\{ \}$, is the impulse response of Equation 3-235 and is illustrated below.



Note that the term, $(a)\cos(n\pi\omega/\omega_c)$, causes the resultant output to have "echoes" centered at $t = \pm n/2f_c$.

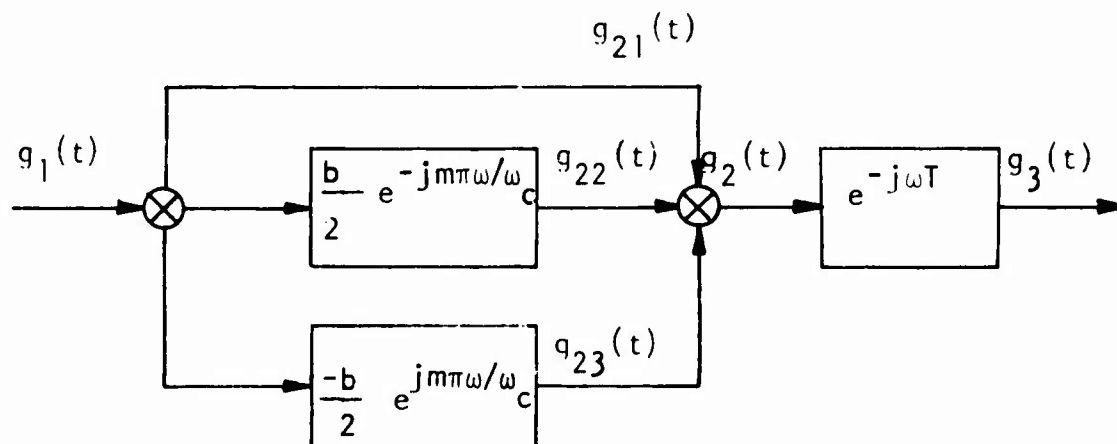
The influence of the phase term, $\phi(\omega)$, can be determined in a similar manner. Consider first, the sinusoidal term in Equation 3-236. When $b \ll 1$, one can approximate the phase as

$$e^{-jb} \sin(n\pi\omega/\omega_c) \approx 1 - jb \sin(n\pi\omega/\omega_c) \quad (\text{Eq. 3-241})$$

Expanding the sin term, one finds

$$e^{-jb} \sin(n\pi\omega/\omega_c) \approx 1 + \frac{b}{2} e^{-jn\pi\omega/\omega_c} - \frac{b}{2} e^{-jn\pi\omega/\omega_c} \quad (\text{Eq. 3-242})$$

Note the similarity of this expansion to that of Equation 3-235. Therefore a flow diagram can be formed similar to the previous one to demonstrate the effects of phase, $\phi(\omega)$, of the overall transfer function, $H(\omega)$.



Note that $g_1(t)$ refers to the output of the previous calculation. Once again, use of Equations 3-54 and 3-59 allows the computation of $g_{22}(t)$ and $g_{23}(t)$ in terms of $g_1(t)$.

$$g_{22}(t) = \frac{b}{2} g_1\left(t - \frac{m}{2f_c}\right)$$

$$g_{23}(t) = -\frac{b}{2} g_1\left(t + \frac{m}{2f_c}\right)$$

(Eq. 3-243)

Furthermore, Equation 3-59 shows that the function, $e^{-j\omega T}$, will contribute an additional time delay equal to T . Therefore, $g_3(t)$ in terms of $g_1(t)$ is

$$g_3(t) = g_1(t - T) + \frac{b}{2} g_1\left(t - \frac{m}{2f_c} - T\right) - \frac{b}{2} g_1\left(t + \frac{m}{2f_c} - T\right) \quad (\text{Eq. 3-244})$$

With sufficient effort, $g_3(t)$ could be formulated in terms of $f(t)$. The resultant expression would have nine terms. In many practical cases, treatment of the largest ripple contributor, either amplitude or phase, is adequate for the required analysis. If consideration of both phase and amplitude ripple is required, then numerical evaluation should be used to obtain quantitative data, and the material in this section will provide quantitative validation of the results.

3.3.11.8.2 High Pass

Discussion of high pass filters will be limited to introducing the complementary principle. Given a high pass filter with a transfer function, $H_H(\omega)$, and normalize the peak amplitude of $H_H(\omega)$ to unity. Define a complementary low pass filter, $H_L(\omega)$, as

$$H_L(\omega) = 1 - H_H(\omega) \quad (\text{Eq. 3-245})$$

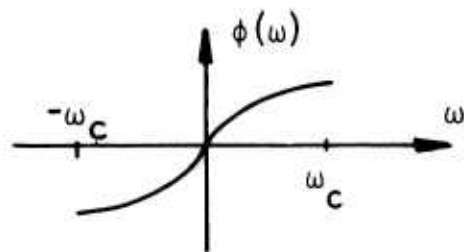
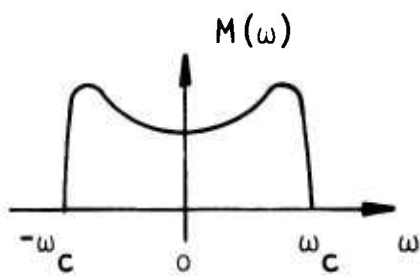
Then the output of a high pass filter is given in terms of the input function and the low pass response to the input function.

$$\begin{aligned} G_H(\omega) &= F(\omega) H_H(\omega) \\ &= F(\omega) - F(\omega) H_L(\omega) \end{aligned} \quad (\text{Eq. 3-246})$$

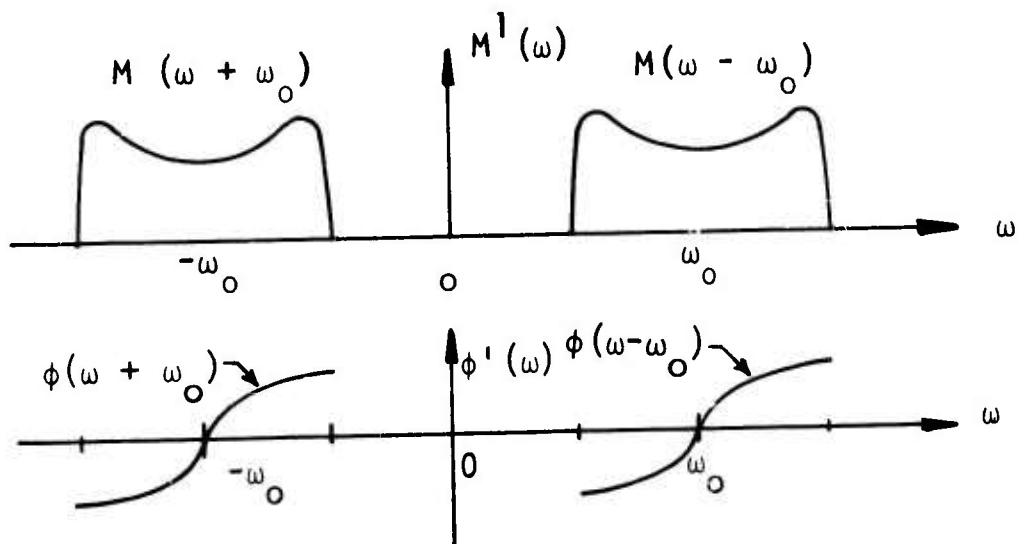
$$g_H(t) = f(t) - f(t) * h_L(t) \quad (\text{Eq. 3-247})$$

3.3.11.8.3 Bandpass

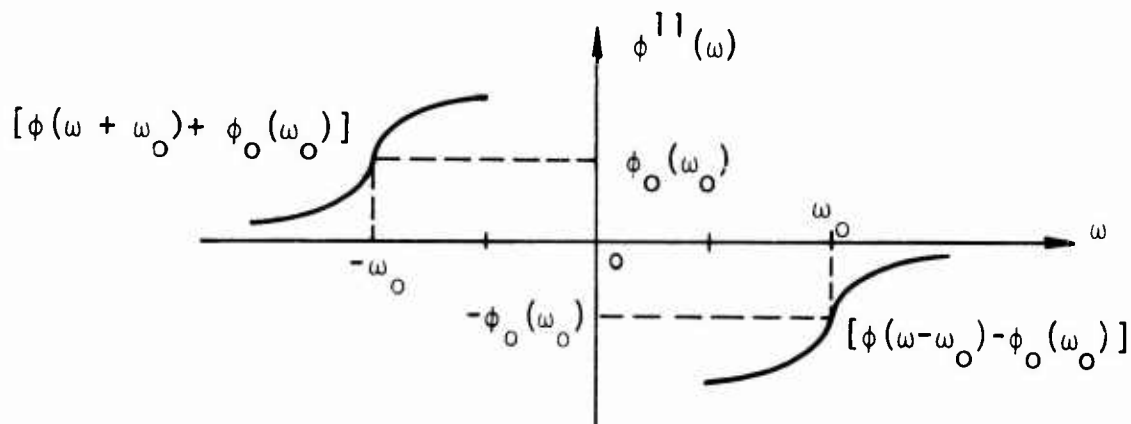
On many occasions, the response of a bandpass filter can be simply described in terms of an equivalent low pass filter. A method of analysis useful in many practical applications is illustrated below. Consider the transfer function of a low pass filter, $H_L(\omega)$, in terms of $M(\omega)$ and $\phi(\omega)$.



Then shift the transfer function to the frequencies $\pm \omega_0$.



Finally shift the magnitude of the phase by $\pm \phi_o(\omega_o)$.



The functions, $M^1(\omega)$ and $\phi^{11}(\omega)$, are characteristic of the magnitude and phase of many practical narrow bandwidth systems.

Now consider the impulse response, $h_B(t)$, of a bandpass system with a transfer function, $H_B(\omega)$, given by

$$H_B(\omega) = M^1(\omega) e^{-j\phi^{11}(\omega)} \quad (\text{Eq. 3-248})$$

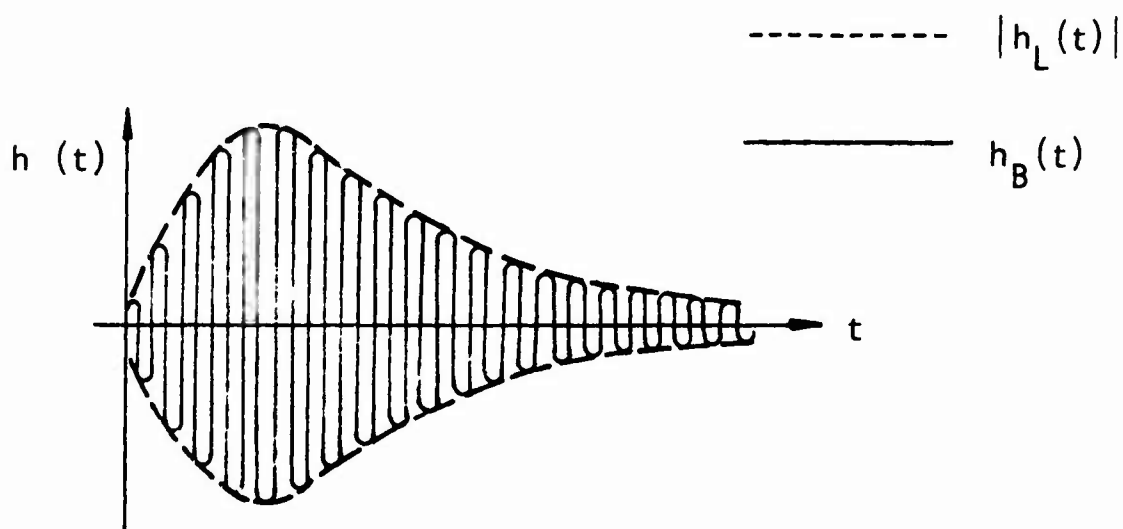
The function, $H_B(\omega)$, can be expressed in terms of $H_L(\omega)$.

$$H_B(\omega) = H_L(\omega + \omega_o) e^{j\phi_o(\omega_o)} + H_L(\omega - \omega_o) e^{-j\phi_o(\omega_o)} \quad (\text{Eq. 3-249})$$

Note that the impulse response of $H_L(\omega)$ is $h_L(t)$ and that according to Equation 3-61, frequency shifting by the amount $\pm \Delta\omega$ implies that the associated time domain function is multiplied by $e^{\pm j\Delta\omega t}$. Thus

$$\begin{aligned} h_B(t) &= h_L(t) e^{-j\omega_o t} e^{j\phi_o(\omega_o)} + h_L(t) e^{j\omega_o t} e^{-j\phi_o(\omega_o)} \\ &= h_L(t) \left[e^{-j(\omega_o t - \phi_o(\omega_o))} + e^{j(\omega_o t - \phi_o(\omega_o))} \right] \\ &= 2 h_L(t) \cos \left[\omega_o t - \phi_o(\omega_o) \right] \quad (\text{Eq. 3-250}) \end{aligned}$$

A typical example of the resultant impulse response, $h_B(t)$, is shown below.



The function, $h_B(t)$, oscillates at a frequency equal to the center frequency of the bandpass system, ω_o . The phase of the oscillating factor,

$\cos(\omega_0 t)$, is shifted by the amount, $\phi_0(\omega_0)$. The envelope of the resultant function is equal to the impulse response, $h_L(t)$, of the equivalent low pass system.

Before one considers this result characteristic of all bandpass systems, two limitations in the development must be emphasized. One limitation is that the transfer function magnitude, $M(\omega \pm \omega_0)$, must be an even function of frequency centered at $\pm \omega_0$. The second limitation is that the phase difference, $\phi^{II}(\omega) \pm \phi_0(\omega_0)$, must be an odd function of frequency centered at $\pm \omega_0$. Expressions for the impulse response when these two assumptions are not valid are available. However, they are generally very complex. Further details are contained in Reference [23].

3.4 SAMPLED FOURIER TRANSFORMS

3.4.1 Introduction

The previous chapter has developed some of the important properties of the Fourier Integral Transform (FIT). In principle, a thorough knowledge of this technique would allow complete analysis of EMP data. However, there are many occasions where it is neither convenient nor practical to use the FIT. Then cousins of the FIT such as the Fourier Series Transform (FST), the Time Sampled Fourier Transform (TSFT), or the Discrete Fourier Transform (DFT) could be employed. It should be noted that the DFT is generally used in the efficient Fast Fourier Transform (FFT) algorithm.

The fundamental difference between the FIT and it's cousin transforms is that the FIT is formulated for use with continuous time and frequency domain functions. Discontinuities are treated as exceptions and do not occur in a regular pattern. On the other hand, transforms such as the FST, the TSFT, and the DFT are fundamentally discontinuous.

Specifically, the time domain, the frequency domain, or both functions are defined only at equally spaced discrete points. For instance, the FST has frequency domain components defined at discrete frequencies. As will be shown later, this discrete frequency domain property is a natural consequence of a repetitive time domain function. The TSFT is a natural analysis technique to employ when the experimental data are available only at equally spaced intervals in the time domain. The DFT has both the time and frequency domain functions defined at equally spaced points. Its principal advantage occurs when it is formulated as an FFT where significant savings of computing time are possible. Any of these transform techniques can be used in the analysis of EMP experimental data. The only implicit requirement is that the user understand the similarities and differences among the various techniques. The final choice of the transform technique will depend on the form of the data, the availability of computer software, and computing time economics.

Casual examination of the various Fourier transform techniques presented in the technical literature shows little commonality. Excluding differences in notation employed by different authors, the primary cause of the apparent differences is that a common method of treating continuous and discrete distributions is rarely presented. Perhaps it is felt that these general techniques might confuse the presentation. However, it is the opinion of the author that the majority of the misunderstanding, mistakes, and misuse of transform theory stems from confusing concepts of continuous and discrete distributions. This confusion is unfortunate since the material presented in the previous section on use of the delta function and the convolution theorem will unify the derivation of the continuous (FIT) and sampled Fourier transforms.

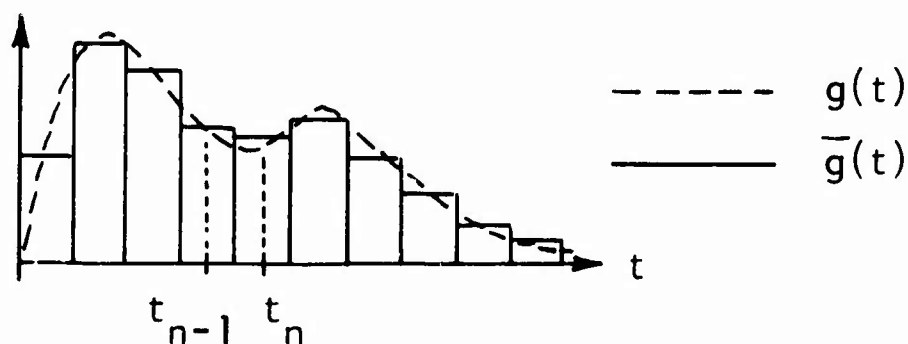
The purpose of this section is to show that the FST, the TSFT, and the DFT are special cases of the FIT. Then, with proper interpretation, all the material presented in the previous section is applicable. The result of employing this approach is that the analyst's mind is not cluttered with a collection of apparently unrelated formulas. All results

necessary for the analysis of EMP data can be derived from a few concepts. The common denominator in these derivations is the use of the delta function and the convolution theorem.

The presentation begins with the development of the Fourier transform of a train of delta functions. This transform pair will allow simple analysis of all sampled transforms. This transform pair will then be extended to define a pair of operators, "Comb and Rep." which will allow efficient manipulation of the mathematical expressions. Finally, specific treatment of the FST, the TSFT and the DFT will be presented.

3.4.2 Sampling Functions

Given a function, $g(t)$, and a pulse approximation of $g(t)$, namely $\bar{g}(t)$, it will be shown that the Fourier transform of $\bar{g}(t)$ is equivalent to the Fourier transform of $g(t)$ sampled at equally spaced intervals. Define a set of equally spaced points, t_n , such that $t_n = n\Delta t$, $n = 0, \pm 1, \pm 2, \dots$. Let each pulse be centered at t_n and define the magnitude of each pulse as $g(t_n)$, $n = 0, \pm 1, \pm 2, \dots$.



The Fourier transform of $\bar{g}(t)$ can be simplified considerably if $e^{-j\omega t}$ is approximately constant over a pulse width. Thus, if $\omega\Delta t \ll 1$

$$\begin{aligned}
 F\{\bar{g}(t)\} &= \int_0^{\infty} \bar{g}(t) e^{-j\omega t} dt \\
 &= \sum_{n=1}^{\infty} \int_{t_n - \Delta t/2}^{t_n + \Delta t/2} \bar{g}(t) e^{-j\omega t} dt \\
 &= \sum_{n=1}^{\infty} g(t_n) e^{-j\omega t_n} \Delta t \\
 &= \Delta t \sum_{n=1}^{\infty} g(t_n) e^{-j\omega t_n}
 \end{aligned}
 \tag{Eq. 3-251}$$

Since the pulse amplitude is determined by the magnitude of $g(t)$ at t_n only, then $g(t)$ is effectively sampled at t_n . Therefore Equation 3-251 gives the Fourier transform of $g(t)$ sampled at equally spaced points, t_n .

Except for the scale factor, Δt , Equation 3-251 can be derived with the aid of delta functions. Define a train of delta functions, $D_{\Delta t}(t)$, as

$$D_{\Delta t}(t) = \sum_{n=-\infty}^{\infty} \delta(t - n\Delta t) \tag{Eq. 3-252}$$

Now obtain the Fourier transform of $g'(t) = g(t) D_{\Delta t}(t)$.

$$F\{g'(t)\} = \int_0^{\infty} g(t) \sum_{n=-\infty}^{\infty} \delta(t - n\Delta t) e^{-j\omega t} dt \tag{Eq. 3-253}$$

Use of Equation 3-134 shows that

$$F\{g'(t)\} = \sum_{n=1}^{\infty} g(t_n) e^{-j\omega t_n} \quad (\text{Eq. 3-254})$$

Equation 3-254 indicates that the Fourier transform of a function, $g(t)$, sampled at $t = t_n$ is equivalent to the Fourier transform of the product of $g(t)$ and $D_{\Delta t}(t)$. From the convolution theorem, one will recall that

$$F\{g(t)D_{\Delta t}(t)\} = F\{g(t)\} * F\{D_{\Delta t}(t)\} \quad (\text{Eq. 3-255})$$

Therefore, determination of the Fourier transform of $D_{\Delta t}(t)$ will provide a convenient means of exploring the properties of sampled Fourier transforms.

In the following material, it will be shown that the Fourier transform of an infinite train of delta functions in the time domain corresponds to an infinite train of delta functions in the frequency domain. In particular

$$D_{\Delta t}(t) \leftrightarrow \Delta\omega D_{\Delta\omega}(\omega), \quad \Delta\omega = 2\pi/\Delta t \quad (\text{Eq. 3-256})$$

and

$$D_{\Delta\omega}(\omega) = \sum_{n=-\infty}^{\infty} \delta(\omega - n\Delta\omega) \quad (\text{Eq. 3-257})$$

To take maximum advantage of existing material (i.e., Equation 3-138), it will be shown that

$$D_{\Delta t}(t) = F^{-1}\{\Delta\omega D_{\Delta\omega}(\omega)\} \quad (\text{Eq. 3-258})$$

Since the Fourier transform is a reversible mathematical operation, verification of Equation 3-258 is equivalent to the proof of Equation 3-256. Verifying Equation 3-258 is somewhat tedious. However, a proof similar to that given in Reference [23] will be presented to provide reader confidence in the result. Once the result is established, it can be used in mathematical derivations rather simply.

Using the basic definition of the inverse Fourier transform, one finds

$$\begin{aligned} F^{-1} \{ \Delta\omega D_{\Delta\omega}(\omega) \} &= \frac{\Delta\omega}{2\pi} \int_{-\infty}^{\infty} \sum_{n=-\infty}^{\infty} \delta(\omega - n\Delta\omega) e^{j\omega t} d\omega \\ &= \frac{1}{\Delta t} \sum_{n=-\infty}^{\infty} \int_{-\infty}^{\infty} \delta(\omega - n\Delta\omega) e^{j\omega t} d\omega \\ &= \frac{1}{\Delta t} \sum_{n=-\infty}^{\infty} e^{jn\Delta\omega t} \end{aligned} \quad (\text{Eq. 3-259})$$

One method of evaluating this infinite series is to form the partial sum, $\sigma_n(t)$,

$$\sigma_n(t) = \frac{1}{\Delta t} \sum_{n=-N}^N e^{jn\Delta\omega t} \quad (\text{Eq. 3-260})$$

and obtain its limit as the integer, N , approaches infinity. Noting the following algebraic identities

$$\begin{aligned} 1 + x + x^2 + \dots + x^N &= \frac{1 - x^{N+1}}{1 - x} \\ x^{-1} + x^{-2} + \dots + x^{-N} &= - \frac{1 - x^{-N}}{1 - x} \end{aligned} \quad |x| < 1 \quad (\text{Eq. 3-261})$$

one finds

$$\begin{aligned}\sigma_N(t) &= \frac{1}{\Delta t} \frac{e^{j(N+1)\Delta\omega t} - e^{-jN\Delta\omega t}}{e^{j\Delta\omega t} - 1} \\ &= \frac{1}{\Delta t} \frac{\sin[(N+1/2)\Delta\omega t]}{\sin[\Delta\omega t/2]}\end{aligned}\quad (\text{Eq. 3-262})$$

The function, $\sigma_N(t)$, can be shown to approach an infinite train of delta functions if one can show it is periodic and it satisfies Equation 3-135, the fundamental definition of a delta function. Periodicity is established by substituting $t + \Delta t$ for t in Equation 3-262 and noting that $\Delta t = 2\pi/\Delta\omega$.

$$\begin{aligned}\sigma_N(t + \Delta t) &= \frac{1}{\Delta t} \frac{\sin[(N+1/2)\Delta\omega(t + \Delta t)]}{\sin[\Delta\omega(t + \Delta t)/2]} \\ &= \frac{1}{\Delta t} \frac{\sin[(N+1/2)\Delta\omega t + (N+1/2)2\pi]}{\sin[\Delta\omega t/2 + \pi]} \\ &= \sigma_N(t)\end{aligned}\quad (\text{Eq. 3-263})$$

Since $\sigma_N(t)$ is periodic, one needs to show only that $\sigma_N(t)$ approaches a delta function in any arbitrary interval. For convenience, choose the interval centered at $t = 0$.

It is instructive to determine the peak amplitude of $\sigma_N(t)$ as N approaches infinity. If this amplitude approaches infinity, then, in the limit, $\sigma_N(t)$ satisfies the minimum requirement for a delta

function described by Equation 3-134. Equation 3-262 can be approximated, for small t , as

$$\sigma_N(t) \approx \frac{1}{\Delta t} \frac{\sin[(N + 1/2)\Delta\omega t]}{\Delta\omega t/2} \quad (\text{Eq. 3-264})$$

$$= \frac{2(N + 1/2)}{\Delta t} \frac{\sin[(N + 1/2)\Delta\omega t]}{(N + 1/2)\Delta\omega t}$$

At $t = 0$

$$\sigma_N(t) = \frac{2N + 1}{\Delta t} \quad (\text{Eq. 3-265})$$

It is clear that $\sigma_N(t)$ satisfies Equation 3-134 as N approaches infinity.

Now determine if $\sigma_N(t)$, in the limit, satisfies Equation 3-135, the strict requirement for a delta function. Write Equation 3-262 as

$$\sigma_N(t) = \frac{\pi}{\Delta t} \left[\frac{\sin[(N + 1/2)\Delta\omega t]}{\pi t} \right] \frac{t}{\sin[\Delta\omega t/2]} \quad (\text{Eq. 3-266})$$

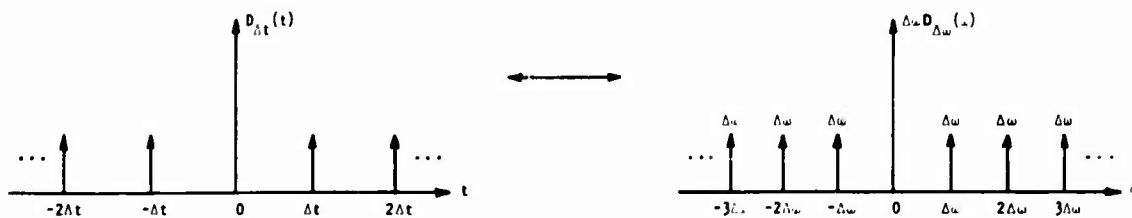
According to Equation 3-138, the bracketed term in this expression approaches $\delta(t)$ as N approaches infinity. Thus

$$\begin{aligned} \lim_{N \rightarrow \infty} \sigma_N(t) &= \left[\frac{\pi}{\Delta t} \frac{t}{\sin[\Delta\omega t/2]} \right] \delta(t) \\ &= \left[\frac{\Delta\omega}{2} \frac{t}{\sin[\Delta\omega t/2]} \right] \delta(t) \end{aligned} \quad (\text{Eq. 3-267})$$

Since this function is defined only at $t = 0$, one has the bracketed term equal to unity (see Equation 3-80) and

$$\lim_{N \rightarrow \infty} \sigma_N(0) = \delta(t) \quad (\text{Eq. 3-268})$$

Therefore Equation 3-256 is verified and one has



where the arrows symbolically represent delta functions and the factor, $\Delta\omega$, over the delta functions in the frequency domain represent the "weight" of the delta function. Note that as Δt is increased, $\Delta\omega$ is decreased and vice versa. Thus, the spacing of the delta functions in one domain (time or frequency) is inversely proportional to its spacing in the opposite domain.

3.4.3 Comb and Rep*

Equation 3-256 can be used to derive most of the properties of sampled Fourier transforms. Indeed direct use of the infinite train of delta functions, $D(t)$ or $D(\omega)$, is a common way of treating the TSFT or the FST. However, a more powerful means of treating sampled Fourier transforms can be obtained by generalizing the application of $D(t)$ or $D(\omega)$ into a pair of operators called "Comb and Rep." Use of these operators will permit one to obtain the relationship between sampled functions and their Fourier transforms by inspection. The resulting simplification will allow the reader to easily derive all necessary results and gain insight into sampled Fourier transforms without getting trapped in the intricate details of a straightforward mathematical derivation.

Prior to presenting the operators, Comb and Rep, it is useful to review the application of $D(t)$ or $D(\omega)$ in sampled Fourier transforms. Suppose one has a function, $g(t)$, with a continuous variable, t . Let $g(t)$ be sampled at equally spaced time intervals, Δt , to obtain $\bar{g}(n\Delta t)$. Then obtain the Fourier transform of $\bar{g}(n\Delta t)$. Equation 3-254 shows that the Fourier transform of the sampled function is equivalent to the Fourier transform of the product of $g(t)$ and $D(t)$.

$$F \left\{ \bar{g}(n\Delta t) \right\} = F \left\{ g(t) D_{\Delta t}(t) \right\} \quad (\text{Eq. 3-254})$$

* These operators were first introduced by Woodward in Reference [24]. Although the terms are not widely used, it is felt that the descriptive form of their names provides a simple means of remembering the important results.

Use of the convolution theorem shows that the Fourier transform of the product is equivalent to the convolution of the transforms of the individual functions. Thus

$$F\{\bar{g}(n\Delta t)\} = F\{g(t)\} * F\{D_{\Delta t}(t)\} \quad (\text{Eq. 3-255})$$

$$= G(\omega) * \Delta\omega D_{\Delta\omega}(\omega), \quad \Delta\omega = 2\pi/\Delta t$$

Substituting the expression for $D_{\Delta\omega}(\omega)$ into the above equation, one finds

$$F\{\bar{g}(n\Delta t)\} = G(\omega) * \Delta\omega \sum_{n=-\infty}^{\infty} \delta(\omega - n\Delta\omega) \quad (\text{Eq. 3-269})$$

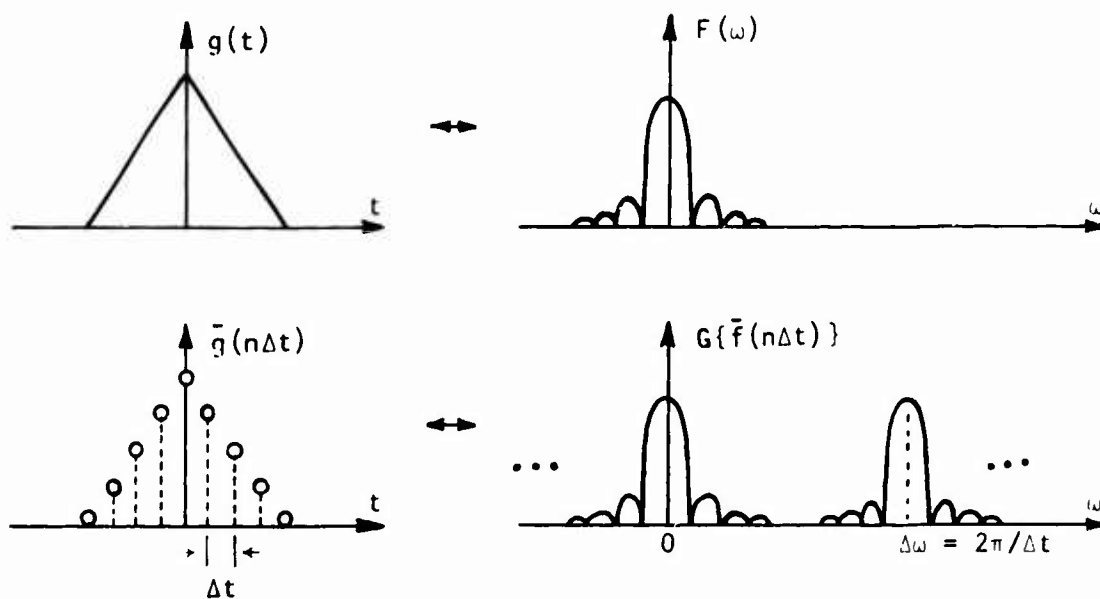
Now note that any function, $g(x)$, convolved with a shifted delta function, $\delta(x-\theta)$, equals the original function shifted by θ . Thus

$$\begin{aligned} g(x) * \delta(x-\theta) &= \int_{-\infty}^{\infty} g(y) \delta(y-(x-\theta)) dy \\ &= g(x-\theta) \end{aligned} \quad (\text{Eq. 3-270})$$

Therefore Equation 3-269 can be written as

$$F\{\bar{g}(n\Delta t)\} = \Delta\omega \sum_{n=-\infty}^{\infty} G(\omega - n\Delta\omega), \quad \Delta\omega = 2\pi/\Delta t \quad (\text{Eq. 3-271})$$

Note that this result is merely an infinite repetition of the original function, $G(\omega)$, shifted to frequencies equal to $\pm n\Delta\omega$.



The process of repeating a Fourier transform, $G(\omega)$, to obtain the transform of a sampled function, $\bar{g}(n\Delta t)$, can be generalized. Given a function, $g(t)$, with its associated Fourier transform, $G(\omega)$. Then define $g(t)$ sampled every Δt seconds as

$$\text{Comb}_{\Delta t}\{g(t)\} = \bar{g}(n\Delta t), \quad n = 0, \pm 1, \pm 2, \dots \quad (\text{Eq. 3-272})$$

The Comb operation must be interpreted carefully. For the time domain, it says that $g(t)$ is defined at discrete points, $n\Delta t$, with a resulting magnitude

of $g(n\Delta t)$. When considering a transform of sampled data, it implies the product of $g(t)$ and $D_{\Delta t}(t)$. The term, $g(n\Delta t)$, in this case, is merely the weight of each delta function component. Furthermore, define an infinite repetition of $G(\omega)$ centered at frequencies equal to $\pm n\Delta\omega$ as

$$\text{Rep}_{\Delta\omega}\{G(\omega)\} = \sum_{n=-\infty}^{\infty} G(\omega - n\Delta\omega), \quad \Delta\omega = 2\pi/\Delta t \quad (\text{Eq. 3-273})$$

Then, one has the following Fourier transform pair

$$\text{Comb}_{\Delta t}\{g(t)\} \leftrightarrow (\Delta\omega)\text{Rep}_{\Delta\omega}\{G(\omega)\}, \quad \Delta\omega = 2\pi/\Delta t \quad (\text{Eq. 3-274})$$

A similar relationship is obtained if $G(\omega)$ is sampled rather than $g(t)$. In this case

$$(\Delta\omega)\text{Comb}_{\Delta\omega}\{G(\omega)\} \leftrightarrow \text{Rep}_{\Delta t}[g(t)], \quad \Delta\omega = 2\pi/\Delta t \quad (\text{Eq. 3-275})$$

where

$$\text{Comb}_{\Delta\omega}\{G(\omega)\} = \bar{G}(n\Delta\omega), \quad n = 0, \pm 1, \pm 2, \dots \quad (\text{Eq. 3-276})$$

and

$$\text{Rep}_{\Delta t}\{g(t)\} = \sum_{n=-\infty}^{\infty} g(t - n\Delta t) \quad (\text{Eq. 3-277})$$

Sometimes one might let $f = \omega/2\pi$ instead of ω . In this case, $\Delta\omega$ in Equations 3-274 and 3-275 is replaced by $\Delta f = 1/\Delta t$.

Equations 3-274 and 3-275 will be used in the subsequent sections to derive results for the sampled Fourier transforms. These operators provide a particularly simple means of obtaining results on sampled functions and their corresponding transforms. Furthermore, the names, Comb and Rep, provide a picturesque means of describing the mathematical processes such that the results are easily remembered.

3.4.4 The Fourier Series Transform

3.4.4.1 Definition

The Fourier Series Transform (FST) can be defined as follows

$$c_n = \frac{1}{\Delta t} \int_{-\Delta t/2}^{\Delta t/2} g(t) e^{-jn\Delta\omega t} dt \quad (\text{Eq. 3-278})$$

$$g(t) = \sum_{n=-\infty}^{\infty} c_n e^{-jn\Delta\omega t}, \quad \Delta\omega = 2\pi/\Delta t$$

These equations can be written in a more conventional form by noting that $g(t)$ is real which implies that the complex coefficient, c_n , must have the following form.

$$c_n = A_n + jB_n$$

(Eq. 3-279)

$$c_{-n} = A_n - jB_n$$

Then Equation 3-278 can be written as

$$g(t) = A_0 + 2 \sum_{n=1}^{\infty} \sqrt{A_n^2 + B_n^2} \cos[n\Delta\omega t - \phi(n\Delta\omega)]$$

$$\phi(n\Delta\omega) = \tan^{-1}(B_n/A_n) \quad (\text{Eq. 3-280})$$

$$A_n = \frac{1}{\Delta t} \int_{-\Delta t/2}^{\Delta t/2} g(t) \cos(n\Delta\omega t) dt$$

$$B_n = \frac{1}{\Delta t} \int_{-\Delta t/2}^{\Delta t/2} g(t) \sin(n\Delta\omega t) dt$$

This transform is probably more widely known than any other. The reason is that many practical waveforms used in the analysis of electronics and communication systems are approximated rather well by summing only the first few terms of the series. Thus this form of the Fourier transform is suitable for hand analysis. The FST can be used for the analysis of transient waveforms characteristic of EMP data. To do so, one must understand the similarities and differences between the FST and the more basic FIT.

3.4.4.2 Relation to the FIT

Consider a function, $h(t)$, composed of an element, $g(t)$, repeated every Δt seconds such that

$$h(t) = \sum_{n=-\infty}^{\infty} g(t-n\Delta t) \quad (\text{Eq. 3-281})$$

Use of Equation 3-275 shows that $h(t)$ has the Fourier transform

$$\text{Rep}_{\Delta t}\{g(t)\} \leftrightarrow (\Delta\omega) \text{Comb}_{\Delta\omega}\{G(\omega)\} \quad (\text{Eq. 3-282})$$

The frequency domain portion of this relation consists of $G(\omega)$ the Fourier transform of $g(t)$, sampled at $\Delta\omega$ intervals. Thus the n^{th} frequency domain component, d_n , equals

$$d_n = \Delta\omega G(n\Delta\omega) \quad (\text{Eq. 3-283})$$

$$= \frac{2\pi}{\Delta t} \int_{-\Delta t/2}^{\Delta t/2} g(t) e^{-jn\Delta\omega t} dt, \quad \Delta\omega = 2\pi/\Delta t$$

Note that this equation differs from the term, C_n , given by Equation 3-278 by the factor 2π . Now expand the frequency domain portion of Equation 3-282 into an infinite train of delta functions and obtain its inverse Fourier transform.

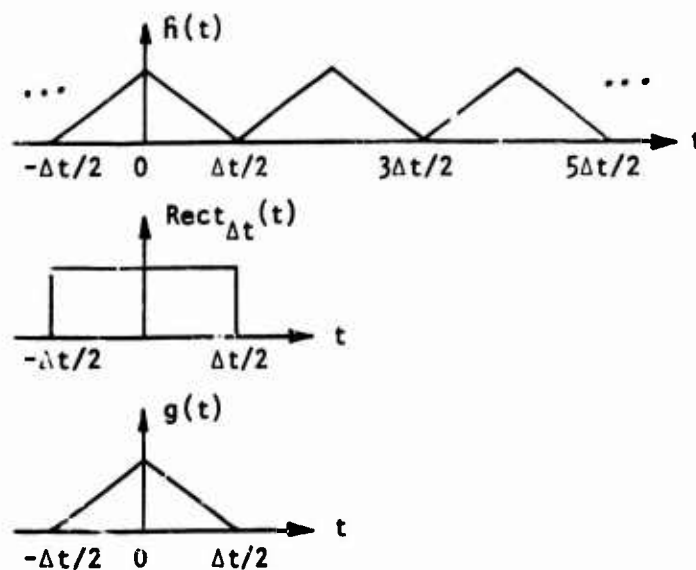
$$\begin{aligned} h(t) &= \frac{1}{2\pi} \int_{-\infty}^{\infty} [(\Delta\omega) \text{Comb}_{\Delta\omega}\{G(\omega)\}] e^{j\omega t} d\omega \\ &= \frac{1}{\Delta t} \int_{-\infty}^{\infty} \sum_{n=-\infty}^{\infty} \delta(\omega - n\Delta\omega) G(\omega) e^{j\omega t} d\omega \\ &= \frac{1}{\Delta t} \sum_{n=-\infty}^{\infty} G(n\Delta\omega) e^{jn\Delta\omega t} \\ &= \sum_{n=-\infty}^{\infty} (d_n/2\pi) e^{jn\Delta\omega t}, \quad \Delta t = \frac{2\pi}{\Delta\omega} \end{aligned} \quad (\text{Eq. 3-284})$$

This demonstration has shown that the FIT of a repetitive function has frequency components defined only where $\omega = n\Delta\omega$.

EMP time domain data are usually not repetitive. Therefore one could ask if the FST can be used and what are its advantages. The answer is that the FST can be used with nonrepetitive data if interpreted properly. In particular, note the following section on nonrepetitive waveforms. One apparent advantage of using the FST is that frequency domain components are required only at discrete points instead of a continuous range. This fact could potentially reduce the computing load. Another possible advantage is software availability. Almost any computer center has software to compute the FST. The following paragraphs will illustrate the use of the FST with EMP data.

3.4.4.3 Nonrepetitive Waveforms

Given a repetitive waveform, $h(t)$, with a period Δt , multiplication of $h(t)$ by $\text{Rect}_{\Delta t}(t)$ will yield the transient nonrepetitive waveform $g(t)$.



Note that the $g(t)$ illustrated above is centered at the origin. This centering was done for the mathematical convenience of the analysis to follow and in no way affects the generability of the results. Most transient data have the beginning of the waveform at the origin. If one wants to move the beginning from $-\Delta t/2$ to zero, then all frequency domain results should be multiplied by the factor $e^{-j\omega\Delta t/2}$.

The Fourier transform pair associated with this non-repetitive waveform can be symbolically written as

$$\text{Rect}_{\Delta t}\{\text{Rep}_{\Delta t}\{g(t)\}\} \leftrightarrow \Delta t \text{Sinc}(f\Delta t) * \Delta\omega \text{Comb}_{\Delta\omega}\{G(\omega)\} \quad (\text{Eq. 3-285})$$

Note that the convolution theorem was used where the product of two functions in the time domain implies the convolution of the transforms of the two functions in the frequency domain. Now note that the Comb operation implies the following when dealing with a Fourier transform

$$\Delta\omega \text{Comb}_{\Delta\omega}\{G(\omega)\} = \Delta\omega \sum_{n=-\infty}^{\infty} G(n\Delta\omega) \delta(\omega - n\Delta\omega) \quad (\text{Eq. 3-286})$$

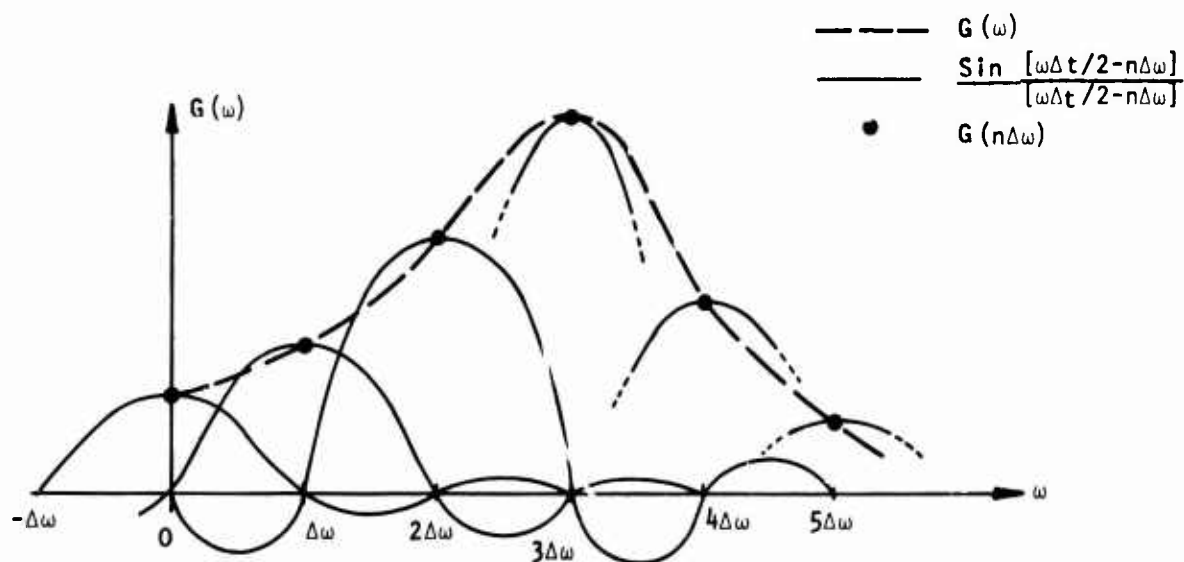
Therefore, the frequency domain portion of Equation 3-285 can be written as

$$(\Delta t) \text{Sinc}(f\Delta t) * \Delta\omega \text{Comb}_{\Delta\omega}\{G(\omega)\} = 2\pi \text{Sinc}(f\Delta t) * \sum_{n=-\infty}^{\infty} G(n\Delta\omega) \delta(\omega - n\Delta\omega) \quad (\text{Eq. 3-287})$$

Writing the Sinc function in terms of $\sin(\omega\Delta t/2)$ and noting Equation 3-270 and 3-185, one finds the Fourier transform of $g(t)$ equal to

$$F\{g(t)\} = \sum_{n=-\infty}^{\infty} G(n\Delta\omega) \left[\frac{\sin[(\omega-n\Delta\omega)\Delta t/2]}{[(\omega-n\Delta\omega)\Delta t/2]} \right] \quad (\text{Eq. 3-288})$$

There are three very important facts given by this equation. One is that $g(t)$ is nonrepetitive. Therefore, its transform must be a function of a continuous variable, ω . Reference to the above equation verifies this statement. A second fact is that the transform of $g(t)$ is uniquely specified by its values at $n\Delta\omega$, namely $G(n\Delta\omega)$, where $\Delta\omega = 2\pi/\Delta t$. The third fact is that the value of the transform of $g(t)$ at frequencies not equal to $n\Delta\omega$ and the $\sin(x)/x$ interpolation formula. The following sketch indicates the interpolation process.



Equation 3-288 shows that the FST can be used to compute the Fourier transform of a transient waveform characteristic of EMP data. One computes the Fourier series coefficients at frequencies equal to $n\Delta\omega$. Then one uses the $\sin(x)/x$ interpolation formula to obtain the frequency domain function at other frequencies. A very common mistake in the use of the FST is to use linear interpolation between the discrete frequency points. Linear interpolation is convenient, but reference to Equation 3-288 shows that it is totally wrong. A suitable compromise between the convenience of linear interpolation and the proper formulation is to decrease the $\Delta\omega$ spacing. Then the error in using linear interpolation can be reduced to an acceptable level.

3.4.4.4 Time Domain Aliasing

An interesting feature of sampled Fourier transforms can be illustrated by the following example. Consider a triangular function of unit height and a base width equal to $2T$. Equations 3-201 and 3-203 state that this function and its associated Fourier transform are

$$\begin{aligned} g(t) &= (t/T) & 0 \leq t < T \\ &= (2T-t)/T & T \leq t < 2T \\ &= 0 & 2T \leq t \end{aligned} \quad (\text{Eq. 3-289})$$

and

$$F\{g(t)\} = T \text{Sinc}^2(fT) e^{-j2\pi fT} \quad (\text{Eq. 3-290})$$

Now suppose one scales Equation 3-290 by Δf and evaluates it at $f = \pm n\Delta f$. Finally suppose Equation 3-284 is used to compute the time domain function associated with these previously computed frequency domain samples. Thus

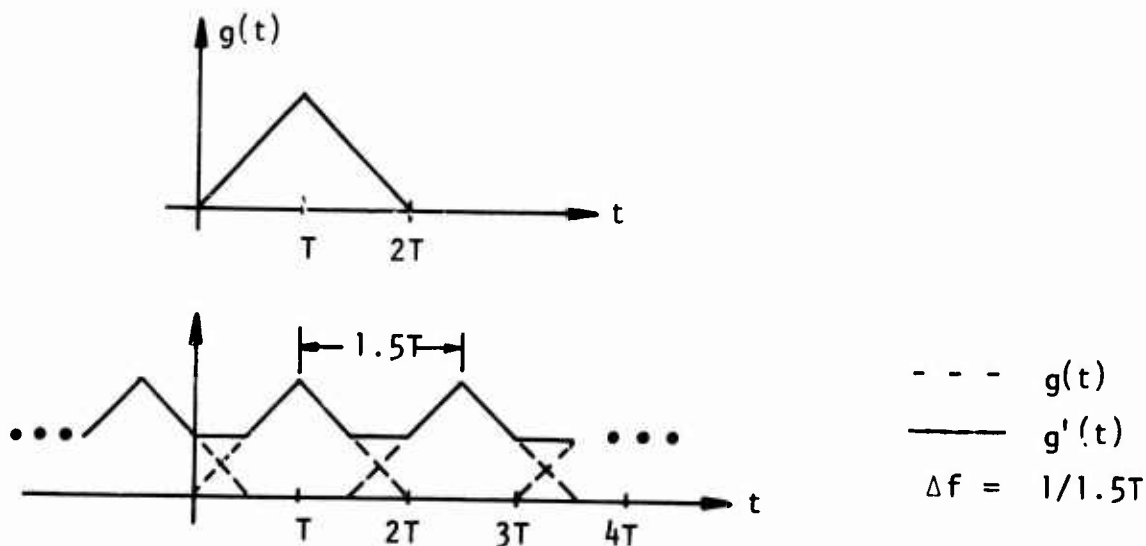
$$g'(t) = \Delta f T \sum_{n=-\infty}^{\infty} \text{Sinc}^2(n\Delta f T) e^{-j2\pi n\Delta f t} e^{j2\pi n\Delta f t} \quad (\text{Eq. 3-291})$$

where $g'(t)$ indicates the time aliased waveform.

Now consider a specific example where $\Delta f = 1/1.5T$. The expression for the resulting time domain function becomes

$$g'(t) = 2/3 + 4/3 \sum_{n=1}^{\infty} \text{Sinc}^2\left(\frac{n}{1.5}\right) \cos\left[\frac{2\pi n}{1.5} (t/T - 1)\right] \quad (\text{Eq. 3-292})$$

Plots of the original function $g(t)$, and the resultant function due to sampling in the frequency domain, $g'(t)$, are shown below.



There are three important facts illustrated by these plots and by Equation 3-292. The first two facts are a verification of features of the FST stated previously. One is that obtaining an inverse Fourier transform (i.e., $g'(t)$) using only sampled frequency domain data yields a repetitive time domain function. The second is that the time domain waveform has a period equal to $1/\Delta f$. In the case illustrated above, the period was forced to be $1.5T$.

The third and most interesting fact about this example is that the time domain data are aliased. That is, the repetitive functions, $g(t)$, overlap to form $g'(t)$. Thus, at a given time t , the resultant function equals the sum of the basic repetitive function, $g(t)$, and portions of $g(t)$ shifted by the repetition period. Note that in this example, the sampling frequency, Δf , was greater than the inverse of the duration of $g(t)$ or $\Delta f > 1/2T$. In order to avoid time domain aliasing, one must use a sampling frequency that is less than the inverse of the duration of the time domain function. Thus

$$\Delta f \leq 1/D \quad (\text{Eq. 3-293})$$

where D is the waveform duration.

3.4.4.5 Convolution

An interesting example of potential time domain aliasing occurs when one samples the product of two functions in the time domain and obtains the inverse transform by FST techniques using Equation 3-284. This problem may be stated in two ways. The first is to assume one has two frequency domain functions, $F(\omega)$ and $H(\omega)$, of a continuous variable, ω . Then one forms the product of these two functions, $G(\omega) = F(\omega)H(\omega)$, samples the resultant function at $\Delta\omega$ intervals, and obtains the inverse

transform. The second way of stating the problem is to assume that one has the FST of a nonrepetitive function. By nonrepetitive, it is meant that the actual signal is nonrepetitive. Use of FST techniques, however, makes the time domain mathematically repetitive. Now assume one passes this signal through a linear system with a transfer function, $H(\omega)$, and computes the resultant output function in the time domain. Except for amplitude scale factors, both problems are mathematically identical.

The convolution theorem and Equation 3-275 will be used to predict the resultant time domain output. Designate the FIT transform pairs of the functions as

$$f(t) \leftrightarrow F(\omega)$$

$$g(t) \leftrightarrow G(\omega) \quad (\text{Eq. 3-294})$$

$$h(t) \leftrightarrow H(\omega)$$

The convolution theorem shows that if $G(\omega) = F(\omega)H(\omega)$, then

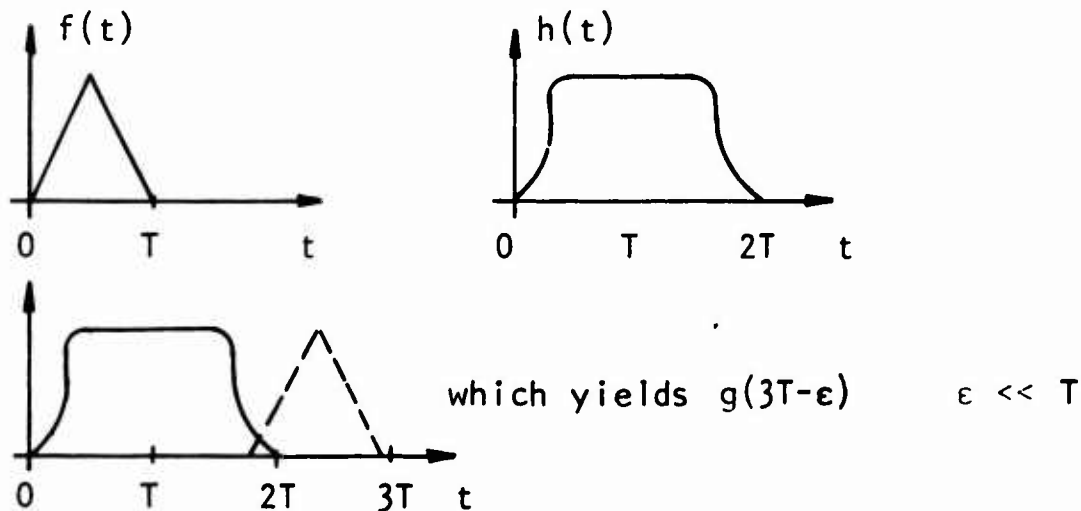
$$g(t) = f(t) * h(t)$$

Finally Equation 3-275 indicates

$$(\Delta\omega)\text{Comb}_{\Delta\omega}\{F(\omega)H(\omega)\} = \text{Rep}_{\Delta t}\{f(t) * h(t)\} \quad (\text{Eq. 3-295})$$

The essential features of this equation can be determined by the following sketches. Let $f(t)$ and $h(t)$ have durations

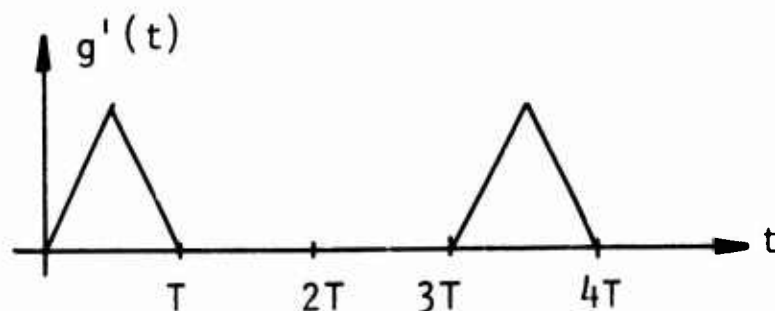
of T and $2T$ respectively. Then the convolution of these two functions yields $g(t)$ which has a duration equal to the sum of the durations of $f(t)$ and $h(t)$ which, in this case, equals $3T$.



In order to avoid time domain aliasing, the repetition period must be $\Delta t \geq 3T$. Therefore, the frequency domain data must be sampled at intervals $\Delta \omega \geq 2\pi/3T$.

Now consider how this situation might occur in practice. Suppose one has an experimental data record given by the $f(t)$ illustrated above. The natural tendency in this case would be to compute the FST coefficients based on $\Delta \omega = 2\pi/T$. However, time domain aliasing would occur when computing a resultant $g(t)$ using $H(\omega)$ corresponding to the $h(t)$ illustrated above. If, however, one artificially extends the repetition period to $3T$ when computing the FST coefficients or,

equivalently reduces the frequency sampling interval, then aliasing will be avoided. The equivalent mathematically repetitive input signal produced by FST techniques, that is minimally acceptable for this example, is shown below.



It is clear that convolution of this signal with $h(t)$ will avoid time domain aliasing. Therefore, if $g(t)$ is computed using FST techniques, the frequency sampling interval for $G(\omega)$ must satisfy $\Delta\omega \leq 2\pi/3T$.

The previous example has used functions that were strictly time limited. However, many functions used in EMP data analysis extend indefinitely. A good example is $e^{-\alpha t}$. When using these functions, the reader must use some criteria to select a maximum time duration, T_0 , such that errors due to time domain aliasing are reduced to an acceptable level.

3.4.5 The Time Sampled Fourier Transform (TSFT)

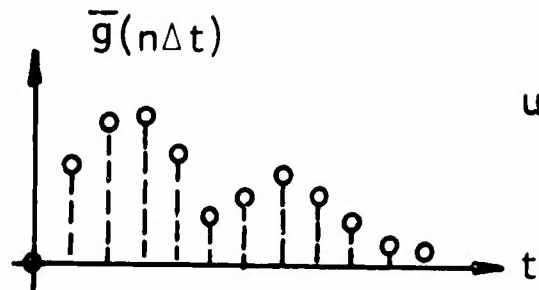
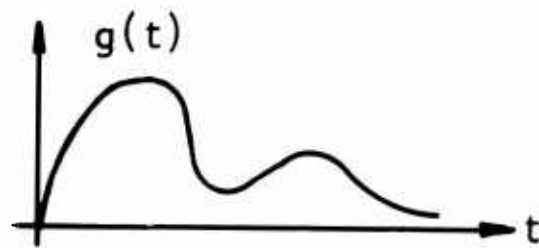
3.4.5.1 Definition

Assume a time domain signal $g(t)$ with its associated transform $G(\omega)$, and assume that $g(t)$ is sampled every Δt seconds to produce $\tilde{f}(n\Delta t)$. Then according to Equation 3-274, the Fourier transform of the sampled data is

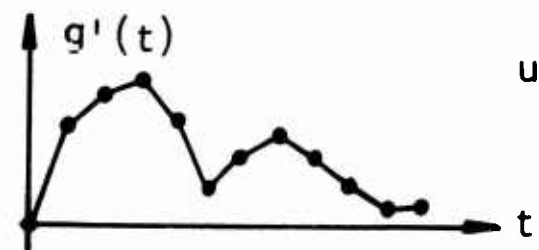
$$\text{Comb}_{\Delta t}\{g(t)\} \leftrightarrow (\Delta\omega)\text{Rep}_{\Delta\omega}\{G(\omega)\}, \quad \Delta\omega = 2\pi/\Delta t \quad (\text{Eq. 3-296})$$

Note that sampling a function in the time domain results in a repetition of the spectrum of the original continuous function in the frequency domain. The transform associated with time domain sampling will be designated as the TSFT.

There is often confusion as to when to apply the results of the TSFT. Many modern digitizers that convert a representation of an analog signal into digital coordinate pairs are capable of producing data at constant intervals along the time axis. Thus the signal is effectively sampled at Δt intervals. Now if the transform of this set of points produced by sampling $g(t)$ at Δt intervals is desired, then Equation 3-296 is applicable. If, however, this set of points is fitted with line segments to produce a continuous function $f'(t)$, that approximates $g(t)$, then FIT techniques are applicable.



use the TSFT

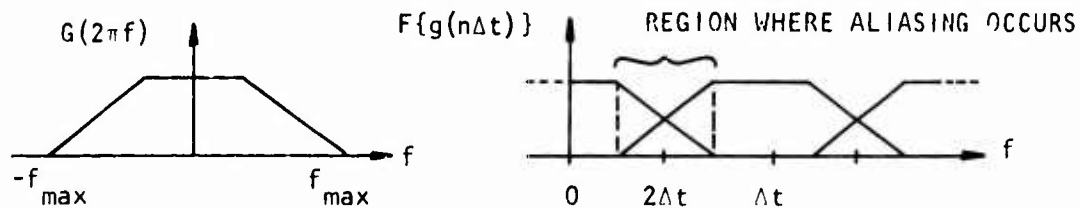


use the FIT

For example, it is common practice in EMP data reduction to fit a set of points with linear segments and obtain the FIT of this approximation of $g(t)$.

3.4.5.2 Aliasing and the Nyquist Frequency

The primary consideration in using the TSFT is that of aliasing. Note that time domain sampling results in a repetition of the transform of the original waveform. If the sampling interval, Δt , is improperly chosen, then the repetitive frequency domain functions will overlap.



In the frequency range where this overlap occurs, the resultant frequency domain data will be in error. This overlap is a clear illustration of the effect of frequency domain aliasing.

Aliasing is avoided by choosing Δt such that

$$1/2\Delta t < f_{\max} \quad (\text{Eq. 3-297})$$

where f_{\max} is the highest frequency component of $G(2\pi f)$ associated with the unsampled time waveform. The frequency equal to $1/2\Delta t$ is called the Nyquist frequency, f_N . Note that f_N is a function of the sampling rate and is independent of the data. Successful application of TSFT techniques requires that f_N be adjusted such that it is greater than f_{\max} .

Definition of f_{\max} is sometimes difficult. For example, the transforms of common waveforms such as $e^{-\alpha t}$ and $e^{-\alpha t} \sin(\beta t)$ have frequency domain components at all frequencies. Therefore, the

analyst has two options; one is to select an f_{\max} such that the aliasing error is reduced to some acceptable level; and the second is to pass the original function, $g(t)$, through a low pass filter before it is sampled. The cutoff frequency of the filter establishes f_{\max} . Then the sampling interval is chosen such that $f_N > f_{\max}$. It is important to note that filtering must be done before sampling occurs. Aliased data cannot be unscrambled without prior knowledge of $G(\omega)$. If this knowledge existed, then there would be no point in computing the TSFT.

3.4.5.3 Computation of Transforms

Equation 3-296 presents the basic features of the transform pair associated with the TSFT. The specific computational formulae for the transforms are implied but not stated explicitly. In this section, the specific transform relations will be given. These transform relations are formulated in a manner analogous to the FIT. The variable, f , will be used instead of ω . This change of variable will simplify the notation somewhat and help familiarize the reader with the variety of notation used in the literature.

Reference to Equation 3-288 shows that the transform of a sampled time domain function is given by

$$G_A(2\pi f) = \sum_{n=-\infty}^{\infty} g(n\Delta t) e^{-j2\pi n f / F}, \quad F = 1/\Delta t \quad (\text{Eq. 3-298})$$

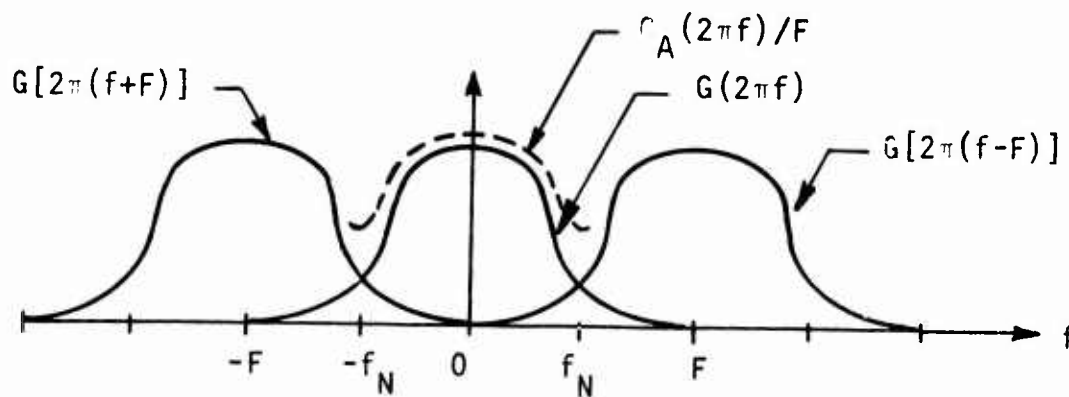
The significance of the subscript, A , will be developed later. The frequency to time transform is similar to the time to frequency transform used in the FIT. In both of these cases, the transform is given by the integration of the basic element of a repetitive function over its period. Then the integration is divided by the period. For the TSFT, the inverse transform is given by

$$g(n\Delta t) = \frac{1}{F} \int_{-F/2}^{F/2} G_A(2\pi f) e^{j2\pi n f / F} df \quad (\text{Eq. 3-299})$$

The significance of $G_A(2\pi f)$ will be explained now. Note that Equation 3-296 indicates that the transform of a time sampled function is equal to an infinite repetition of the transform of the unsampled function, $G(2\pi f)$, times the repetition period, F . Therefore

$$G_A(2\pi f) = F \sum_{p=-\infty}^{\infty} G[2\pi(f-pF)] \quad (\text{Eq. 3-300})$$

In the frequency range $(-F/2, F/2)$, $G_A(2\pi f)$ consists of the basic function, $G(2\pi f)$, centered at $f = 0$ plus the overlap of all repetitions of $G(2\pi f)$ centered at multiples of F .



Thus $G_A(2\pi f)$ is an aliased version of $G(2\pi f)$, and the inverse transform requires integration of $G_A(2\pi f)$ between the Nyquist frequencies, $\pm f_N$. In most cases, the difference between $G_A(2\pi f)$ and $G(2\pi f)$ is due to the two adjacent repetitions of $G(2\pi f)$ centered at $\pm f_N$. Thus

$$\frac{1}{F} G_A(2\pi f) - G(2\pi f) \approx G[2\pi(f - f_N)] + G[2\pi(f + f_N)] \quad (\text{Eq. 3-301})$$

and if the sampling rate is properly chosen, this difference can be made arbitrarily small.

It should be apparent now that the frequency domain function obtained from a time sampled function is not equal to that from the FIT. The transforms from the TSFT and the FIT can be compared in the range $(-f_N, f_N)$ if the transform given by the TSFT is multiplied by $\Delta t = 1/F$. Any remaining difference in the range $(-f_N, f_N)$ is then due to aliasing.

3.4.5.4 Frequency Limited Signals

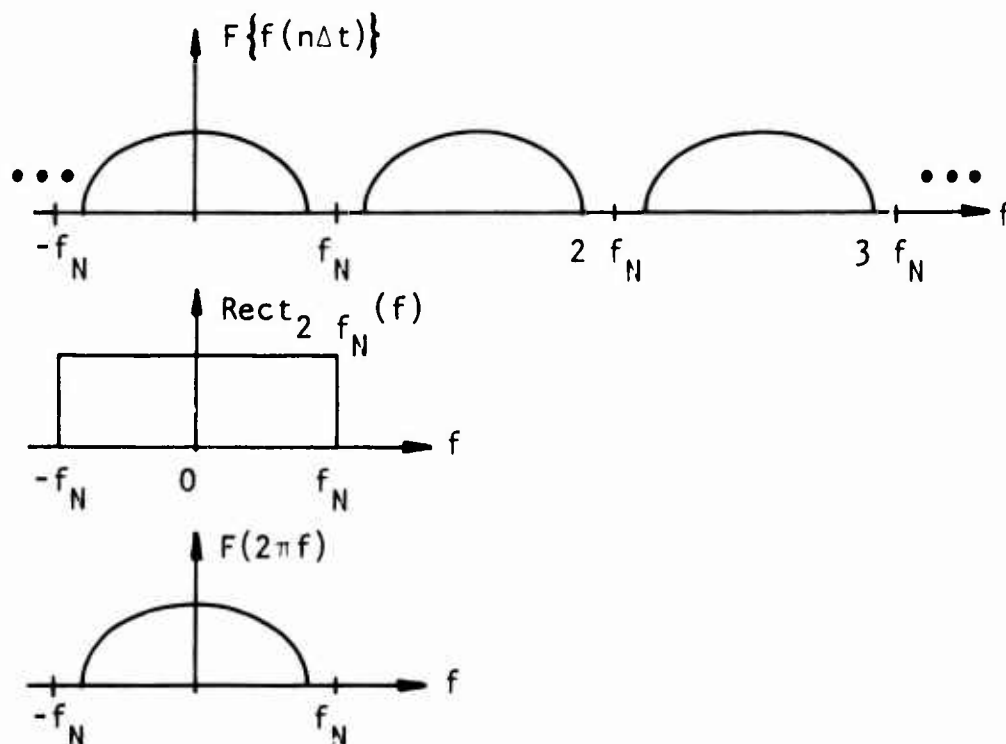
Assume one has a function, $g(t)$, and its associated FIT of $G(2\pi f)$. If $g(t)$ is sampled at Δt intervals, its TSFT is given by Equation 3-296. Furthermore, if

$$G(2\pi f) = 0 \text{ for } f > 1/2\Delta t = f_N \quad (\text{Eq. 3-302})$$

then $g(t)$ can be completely reconstructed at every value of time by use of the values of $g(t)$ at the sample points (i.e., $g(n\Delta t)$).

This reconstruction can be demonstrated by the following argument. By definition, the inverse Fourier transform of $G(2\pi f)$ is equal

to $g(t)$. Now note that if Equation 3-302 is true, then the transform of $g(t)$ is equal to the transform of the sampled function, $g(n\Delta t)$, in the frequency range where $|f| < f_N$. Therefore, obtaining the inverse transform of the sampled spectrum using only the data where $|f| < f_N$ will produce $g(t)$. It will now be shown that $g(t)$ can be constructed from the values of $g(n\Delta t)$.



Multiplication of $F\{g(n\Delta t)\}$ by $\text{Rect}_{2f_N}(f)$ will yield $(2f_N) G(2\pi f)$. The transform of this resultant function is given by use of Equation 3-262, the convolution theorem and Equation 3-87. Thus

$$(2f_N) \text{Sinc}(2f_N t) * \text{Comb}_{\Delta t}\{g(t)\} \leftrightarrow \text{Rect}_{2f_N}(f) (2f_N) \text{Rep}_{2f_N}\{G(2\pi f)\} \quad (\text{Eq. 3-303})$$

Again note that the Comb operation implies

$$\text{Comb}_{\Delta t}\{g(t)\} = \sum_{n=-\infty}^{\infty} g(n\Delta t) \delta(t-n\Delta t) \quad (\text{Eq. 3-304})$$

Therefore, the time domain portion of Equation 3-303 can be written as

$$(2f_N) \text{Sinc}(2f_N t) * \text{Comb}_{\Delta t}\{g(t)\} = (2f_N) \text{Sinc}(2f_N t) * \sum_{n=-\infty}^{\infty} g(n\Delta t) \delta(t-n\Delta t) \quad (\text{Eq. 3-305})$$

Writing the Sinc function in terms of $\sin(2\pi f_N t)$, cancelling the term, $2f_N$, on both sides of Equation 3-303 and noting Equation 3-270, one finds

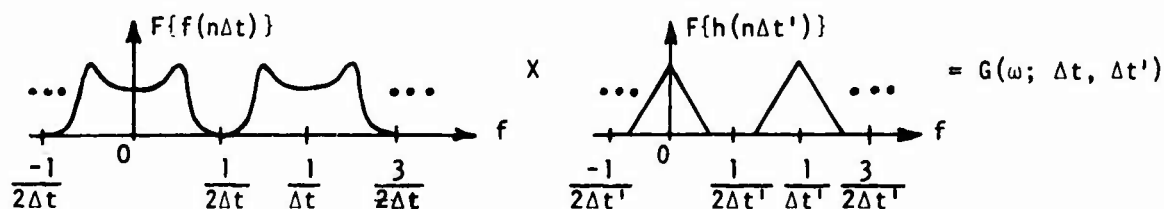
$$g(t) = \sum_{n=-\infty}^{\infty} g(n\Delta t) \left[\frac{\sin[2\pi f_N(t-n\Delta t)]}{2\pi f_N(t-n\Delta t)} \right] \quad (\text{Eq. 3-306})$$

The comments on this interpolation function that were given under the previous section on the FST apply here also.

3.4.5.5 Product of Two Functions

There are many occasions when one desires to multiply the TSFT of a function, $F\{f(n\Delta t)\}$, by some other frequency domain function and obtain the inverse transform of the resultant. The considerations involved in this operation are outlined below.

The important criteria in forming the product of two TSFT functions are to avoid aliasing. Given the functions $f(t)$ and $h(t)$ with TSFT's of $F\{f(n\Delta t)\}$ and $F\{h(n\Delta t')\}$, then define the product of these two frequency domain functions as $G(2\pi f; \Delta t, \Delta t')$.



Assume that neither $F\{f(n\Delta t)\}$ nor $F\{h(n\Delta t')\}$ are aliased. Then the product, $G(2\pi f; \Delta t, \Delta t')$ will not be aliased if both functions, $f(t)$ and $h(t)$, are sampled at the same interval, $\Delta t''$, and $\Delta t''$ is selected to be the smaller of Δt and $\Delta t'$. The common sampling interval will now be written as Δt for convenience.

The inverse transform of $G(2\pi f; \Delta t)$ is computed in a manner similar but not identical to Equation 3-299. Let the transforms of $f(n\Delta t)$ and $h(n\Delta t)$ be given by $(F)\text{Rep}_F\{F(2\pi f)\}$ and $(F)\text{Rep}_F\{H(2\pi f)\}$. Furthermore let $F = 1/\Delta t$ be chosen to avoid aliasing of either function. Then the inverse transform is given by

$$\begin{aligned}
 g(n\Delta t) &= \frac{1}{F^2} \int_{-F/2}^{F/2} [(F)\text{Rep}_F\{F(\omega)\} (F)\text{Rep}_F\{H(\omega)\}] e^{j2\pi n f / F} df \\
 &= \int_{-F/2}^{F/2} F(\omega) H(\omega) e^{j2\pi n f / F} df
 \end{aligned}
 \tag{Eq. 3-307}$$

Note that the scaling factor, F^{-2} , was required in the above equation. If F^{-1} had been used in a manner similar to Equation 3-299, the resultant time domain function would be $(F)g(n\Delta t)$.

The resultant time domain function, $g(n\Delta t)$, may also be obtained from the convolution of $f(n\Delta t)$ and $h(n\Delta t)$. The relation is best derived by starting with functions of the continuous variable, t . Then the time sampled version is obtained in a pulse approximation to the integrand. Let

$$g(n\Delta t) = \int_0^{n\Delta t} f(\tau)h(n\Delta t - \tau)d\tau \quad (\text{Eq. 3-308})$$

Then let the function, $r(\tau) = f(\tau)h(n\Delta t - \tau)$, be approximated in a small interval of width Δt , by its value at the center of the interval. Thus

$$\begin{aligned} g(n\Delta t) &= \sum_{m=0}^n r(m\Delta t)\Delta t \\ &= \Delta t \sum_{m=0}^n f(m\Delta t)h(n\Delta t - m\Delta t) \end{aligned} \quad (\text{Eq. 3-309})$$

Finally the resultant time domain function is expressed as the convolution of two time domain functions

$$g(n\Delta t) = (\Delta t)f(n\Delta t) * h(n\Delta t) \quad (\text{Eq. 3-310})$$

Note that scaling is an important issue and a common pitfall when using sampled Fourier transforms. Equations 3-307 and 3-310 were scaled such that $g(n\Delta t)$ would have identical amplitudes. Furthermore $g(n\Delta t)$ has the same amplitude as $g(t)$ in Equation 3-308 when $t = n\Delta t$.

The convolution of two time sampled functions can be interpreted simply. Let the functions, $f(n\Delta t)$, be written as sequences on strips of paper

$$\begin{array}{l} f(n\Delta t): \\ h(n\Delta t): \end{array} \quad \begin{array}{|c|c|c|c|c|} \hline f_1 & f_2 & f_3 & f_4 & f_5 \\ \hline \end{array} \dots \dots$$

$$\begin{array}{|c|c|c|c|c|} \hline h_1 & h_2 & h_3 & h_4 & h_5 \\ \hline \end{array} \dots \dots$$

where f_n and h_n signify the value of $f(t)$ and $h(t)$ at times equal to $n\Delta t$. The convolution of the sequences, f_n and h_n , is equal to the summation

$$f_n * h_n = \sum_{m=0}^n f_m h_{n-m} \quad (\text{Eq. 3-311})$$

and can be computed by the following artifice. Let the paper strip representing h_m be reversed and shifted n columns to the right. Then form the product of the sequence values in the same vertical column and sum the results. Finally $g(n\Delta t)$ equals

$$\begin{array}{rcl}
 f_m: & & \boxed{f_1 \quad f_2 \quad f_3 \quad f_4 \quad f_5} \\
 \times & & \\
 h_{4-m}: & & \boxed{h_5 \quad h_4 \quad h_3 \quad h_2 \quad h_1} \\
 = & & \\
 g(4\Delta t): & & f_1 h_4 + f_2 h_3 + f_3 h_2 + f_4 h_1
 \end{array}$$

In this example, $n = 4$. If the preceding sum is scaled by Δt , one obtains Equation 3-309.

3.4.6 Discrete Fourier Transform

3.4.6.1 Introduction

The most popular and least understood Fourier transform is the Discrete Fourier Transform (DFT). The popularity stems from the fact that the DFT has an efficient means of computation called the Fast Fourier Transform (FFT). The FFT offers dramatic computational economies when compared to a conventional DFT or other Fourier transforms. The misunderstanding of the DFT (or the FFT) is directly attributable to the fact that many if not most users do not understand sampled Fourier transforms when confined to either the time or frequency domain (TSFT or FST). Therefore it is no surprise that problems arise when there is sampling in both the time and frequency domain as is the case with the DFT.

The DFT (FFT) can be used profitably in the analysis of EMP data. It is capable of any operation that can be performed with the FIT. Furthermore the FFT offers good computational economy. However, the special properties of the DFT must be thoroughly understood before it can be properly used. The following paragraphs present some of the important properties of the DFT. Fortunately most of the concepts have already been introduced when discussing the FST and the TSFT. Therefore this discussion can be limited to a consolidation of previously introduced properties of sampled transforms.

3.4.6.2 Derivation

The DFT has both time and frequency domain data sampled at equally spaced intervals. Therefore one would anticipate that the data in both domains would exhibit a combination of aliasing and repetition. These properties will be developed in detail in the following paragraphs.

The fundamental properties of the DFT, except for a multiplicative constant, can be determined by use of the Comb and Rep functions. Assume one has an FIT pair given by $g(t)$ and $G(2\pi f)$. Note that the frequency variable, f , is being used instead of ω in order to conform with the notation used in the majority of the technical literature on the DFT. Then sampling $g(t)$ at equally spaced intervals, Δt , yields the transform pair

$$\text{Comb}_{\Delta t}\{g(\cdot)\} \xleftrightarrow{\text{proportional}} \text{Rep}_F\{G(2\pi f)\}, \quad F = 1/\Delta t$$

(Eq. 3-312)

The term, proportional, used in the above relation indicates that the two functions differ from being an exact transform pair by a multiplicative constant. Then sampling the repetitive frequency domain function at equally spaced increments, $\Delta f = F/N$ where N is an integer, yields

$$\text{Rep}_T\{\text{Comb}_{\Delta t}\{g(t)\}\} \xleftrightarrow{\text{proportional}} \text{Comb}_{\Delta f}\{\text{Rep}_F\{G(2\pi f)\}\}$$

$$\Delta f = 1/T \quad (\text{Eq. 3-313})$$

In words, this equation indicates that a sequence of time domain samples with a spacing of Δt and a period of T has a Fourier transform that consists of a sequence of frequency domain samples with a spacing of $1/T$ and a period of $1/\Delta t$. Also note that there are N samples within each period of both the time and the frequency domain functions.

Formulas for the computation of the DFT are essentially the same as the summations given in Equations 3-278 and 3-298 for the FIT and the TSFT respectively. However, special care must be used in interpreting the resulting summation for the DFT because of aliasing and the choice of origin.

Consider first the transformation from the frequency to the time domain. The frequency domain portion of the DFT is a sampled version of the frequency domain function for a TSFT. Therefore one can define an aliased periodic function over the period, F , in a manner similar to $G_A(2\pi f)$ in Equation 3-300. Thus

$$G_A(2\pi n\Delta f) = \sum_{p=-\infty}^{\infty} G[2\pi(m\Delta f - pF)] \quad (\text{Eq. 3-314})$$

The transform of this aliased periodic function is obtained in a manner analogous to Equation 3-299 where the periodic function is evaluated over the range of one period. Substituting a summation for the sampled data in place of the integral in Equation 3-299 and deleting the scale factor for now, one obtains

$$F^{-1}\{G_A(2\pi n\Delta f)\} = \sum_{m=-N/2}^{(N/2)-1} G_A(2\pi m\Delta f) e^{j2\pi nm\Delta f/F} \quad (\text{Eq. 3-315})$$

Note that the limits of the sum are centered about $m = 0$ and imply the summation of exactly N terms. The range of the index, m , in the above equation is a natural selection since a frequency domain function is an even function with respect to the origin. However, it is convenient in the computation of DFT's to use only a positive index, m . If one notes that $G_A(2\pi m\Delta f)$ is periodic with a period of F , then one finds

$$G_A(2\pi m\Delta f) \equiv G_A(2\pi n\Delta f), \quad -N/2 \geq m < 0 \quad (\text{Eq. 3-316})$$

$$N/2 \geq n < N-1$$

Therefore, Equation 3-315 can be expressed as

$$F^{-1}\{G_A(2\pi n\Delta f)\} = \sum_{m=0}^{N-1} G_A(2\pi m\Delta f) e^{j2\pi mn/N} \quad (\text{Eq. 3-317})$$

where $\Delta f/F = 1/N$.

Now consider the nature of the time domain function given by $F^{-1}\{G_A(2\pi m\Delta f)\}$. According to the time domain portion of Equation 3-313, the transform associated with $G_A(2\pi m\Delta f)$ is a sampled periodic function. The basic time domain function is $g(t)$. A repetitive function is obtained by the summation of all replicas of $g(t)$ displaced by multiples of the period T . Finally a sampled version is obtained by substitution of $n\Delta t$ for t in the repetitive function. Now in a manner similar to Equation 3-314 one can define a sampled aliased time domain function as

$$g_A(n\Delta t) = \sum_{q=-\infty}^{\infty} g(n\Delta t - qT) \quad (\text{Eq. 3-318})$$

Then the inverse transform of $G_A(2\pi m\Delta f)$ is proportional to

$$g_A(n\Delta t) \sim \sum_{m=0}^{N-1} G_A(2\pi m\Delta f) e^{j2\pi mn/N} \quad (\text{Eq. 3-319})$$

The proportionality constant in the above equation can be found in the following manner. Define the time to frequency domain DFT as

$$G_A(2\pi m\Delta f) = \sum_{n=0}^{N-1} g_A(n\Delta t) e^{-j2\pi mn/N} \quad (\text{Eq. 3-320})$$

Substitution of this equation into Equation 3-318 yields

$$g_A(\ell\Delta t) \sim \sum_{m=0}^{N-1} \left\{ \sum_{n=0}^{N-1} g_A(n\Delta t) e^{-j2\pi mn/N} \right\} e^{j2\pi m\ell/N} \quad (\text{Eq. 3-321})$$

$$\sim \sum_{m=0}^{N-1} g_A(n\Delta t) \sum_{m=0}^{N-1} e^{j2\pi m(\ell-n)/N}$$

Now when $\ell = n + pN$, $p = 0, \pm 1, \dots$, then the second sum in the above equation is equal to N and Equation 3-319 yields

$$g_A(\ell\Delta t) \sim Ng_A(n\Delta t) \quad (\text{Eq. 3-322})$$

Thus, successive application of the DFT and its inverse scales the original function by N . Furthermore, a consistent DFT pair is given by

$$G_A(2\pi m\Delta f) = \sum_{n=0}^{N-1} g_A(n\Delta f) e^{-j2\pi mn/N} \quad (\text{Eq. 3-323})$$

$$g_A(n\Delta f) = \frac{1}{N} \sum_{m=0}^{N-1} G_A(2\pi m\Delta f) e^{j2\pi mn/N}$$

The indices in the time and frequency domain functions are often denoted as subscripts to simplify the notation. Using this convention, the DFT pair is given by

$$G_m = \sum_{n=0}^{N-1} g_n e^{-j2\pi mn/N} \quad (\text{Eq. 3-324})$$

$$g_n = \frac{1}{N} \sum_{m=0}^{N-1} G_m e^{j2\pi mn/N}$$

It is understood that G_m and g_n can potentially be aliased.

In many cases one is only interested in analyzing data in the frequency domain. Furthermore if absolute values are required, this transform data should be independent of the sampling interval, Δt , the summation for G_m in Equation 3-324 can be scaled such that it is approximately equal to $G(2\pi f)$, the FIT of $g(t)$, by multiplying G_m by Δt . Care must be used to remove this factor before inverse transforms are used.

3.4.6.3 Aliasing

The DFT can have aliasing in both the time and frequency domains. Special notation, $g_A(n\Delta t)$ and $G_A(2\pi m\Delta f)$, was used to indicate this potential aliasing and to show that the aliased waveforms constitute a transform pair

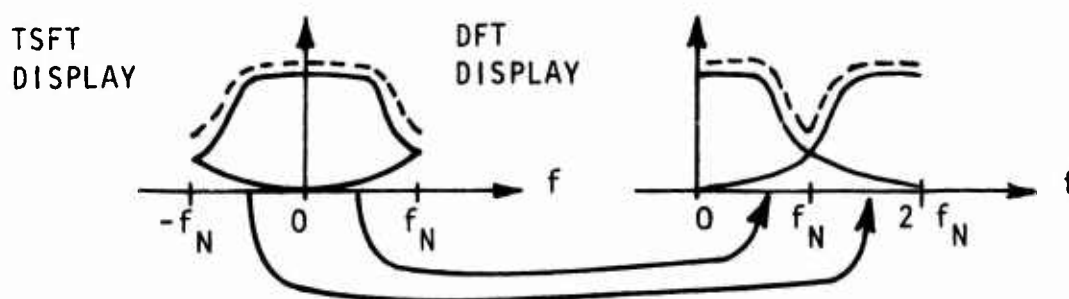
$$g_A(n\Delta t) \leftrightarrow G_A(2\pi m\Delta f) \quad (\text{Eq. 3-325})$$

The above relation shows that the DFT is mathematically valid in the presence of aliasing. However, aliasing can make the data worthless for the user's applications. With proper selection of time and frequency domain sampling intervals, Δt and Δf , aliasing can be minimized or avoided. Except for the obvious differences between sampled data and continuous waveforms, aliasing in the DFT is the same as aliasing in the TSFT or the

FST. Therefore, Subsections 3.4.5.2 and 3.4.5.3 on the TSFT should be consulted for a discussion of frequency domain aliasing, choice of Δt , and the Nyquist frequency. Subsection 3.4.3.4 on the FIT should be referenced for a discussion of time domain aliasing and the choice of Δf .

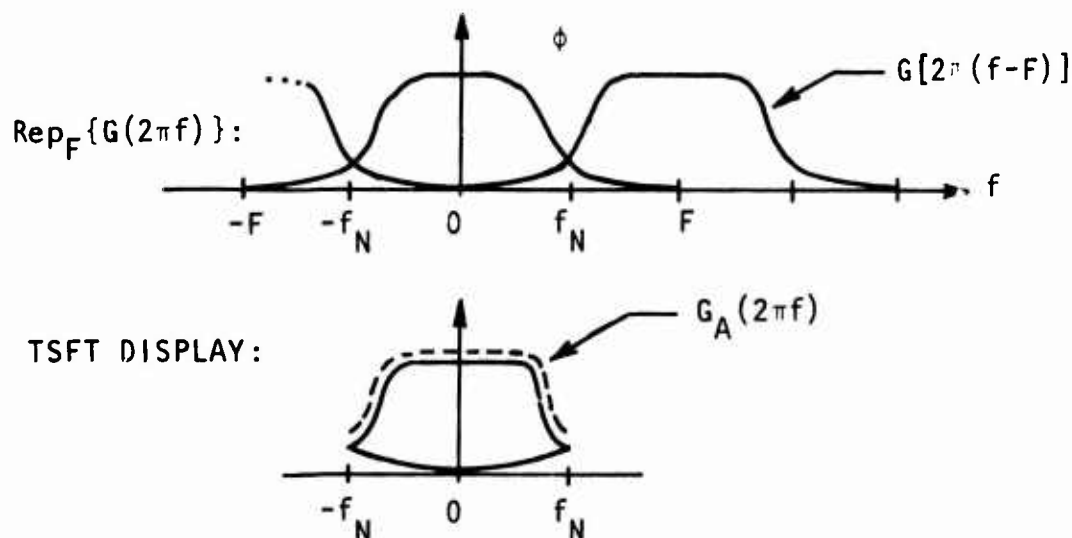
3.4.6.4 Graphical Interpretation

The usual method of displaying data with the DFT is sometimes confusing and needs clarification. Consider first the frequency domain data. Assume one has a waveform, $g(t)$, and its associated FIT of $G(2\pi f)$. Then sampling $g(t)$ at Δt intervals will yield a transform proportional to $\text{Rep}_F\{G(2\pi f)\}$ where $F = 1/\Delta t$. This transform extends over all frequencies. However when using the TSFT, only the data at frequencies less than the Nyquist frequency, $f_N = F/2$, are displayed.



In the case of the DFT, data in the range $(0, F)$ are displayed. There are two ways of interpreting this display. One is that a viewing window, open between $(0, F)$, is placed over the display of $\text{Rep}_F\{G(2\pi f)\}$. Therefore, one views the right half of the basic periodic waveform centered at $f = 0$ and the left half of the basic waveform that is centered at $f = F$. Another interpretation is based on the periodicity of the data. One will note that data in the range $(-f_N, 0)$ are identically equal to that in the range $(f_N, 2f_N)$. Therefore, a display of frequency

domain data can be considered as a decomposition of a similar display for the TSFT. Data in the range $(0, f_N)$ are identical in both displays. However data in the range $(-f_N, 0)$ of the TSFT display are transferred to the range $(f_N, 2f_N)$ to form the DFT display

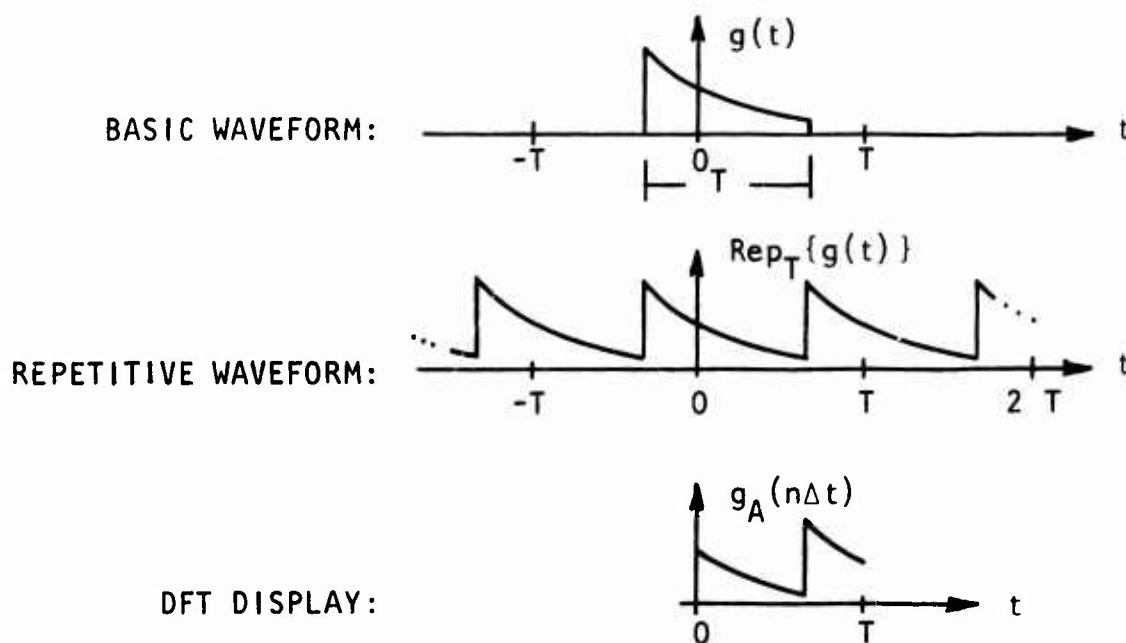


Note that data for the DFT are shown by lines rather than points for graphical clarity.

It is interesting to note that if $g(t)$ is real, then the magnitude of $G(2\pi f)$ is an odd function of frequency. The same symmetry holds for the DFT. Also, the DFT data in the range $(f_N, 2f_N)$ are equal to that in the range $(-f_N, 0)$. However data in the range $(-f_N, 0)$ are the complex conjugate of that in the range $(0, f_N)$. Furthermore, DFT data in the range $(f_N, 2f_N)$ are the complex conjugate of that in the range $(0, f_N)$.

Therefore, one only needs one half the available DFT data, $N/2$ data points, to uniquely specify the frequency domain results.

Time domain data for the DFT are displayed in the range $(0, T)$ where $T = N\Delta t$ regardless of the actual origin of the waveform. Consider a basic waveform that extends over positive and negative time, and is repetitive with a period of T . The basic waveform, the result of its repetition, and the associated DFT display are illustrated below.



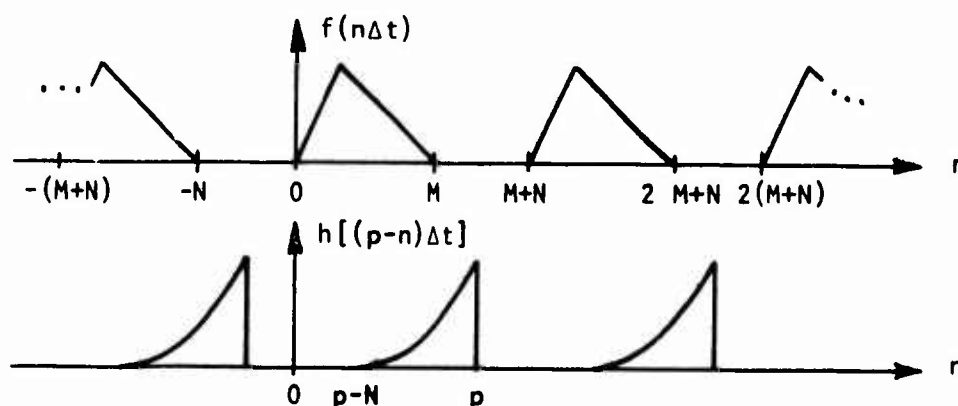
Note that the DFT data are shown by lines rather than points for graphical clarity. Also note that there is no time domain aliasing in this particular example.

3.4.6.5 Convolution

The DFT is often used to obtain the convolution of two functions. The basic procedure is to multiply the transforms of the two functions to be convolved and then obtain the inverse transform of the product. The considerations in using this procedure have been introduced in the section on the FST. These considerations will be applied to the DFT in the following paragraphs.

The basic problem in multiplying two frequency domain functions and obtaining the inverse transform with a DFT is that the convolved product has a length greater than either of the original functions. If one has two functions sampled at equal intervals, Δt , with lengths of $M\Delta t$ and $N\Delta t$, then Equation 3-311 shows that the convolution will have a length of $(M+N-1)\Delta t$. To allow sufficient space to contain the entire convolved function and to avoid overlap problems, each of the original functions must have sufficient zeros appended to the sampled data to increase its length to $(M+N-1)\Delta t$.

Reference to the sketch shown below indicates that the modified sampled data sequences will result in the desired convolution.



The error resulting from the failure to add sufficient zeros can be determined by the following derivation. Assume that one has two time domain functions, $f(t)$ and $h(t)$, that are sampled N times at an increment, Δt , that is chosen to avoid aliasing. Then one has the DFT pairs

$$f(n\Delta t) \leftrightarrow F(2\pi m\Delta f) \quad \Delta f = 1/N\Delta t \quad (\text{Eq. 3-326})$$

$$h(n\Delta t) \leftrightarrow H(2\pi m\Delta f)$$

The inverse transform of the product of these functions is given by

$$\begin{aligned} g(n\Delta t) &= \frac{1}{N} \sum_{m=0}^{N-1} F(2\pi m\Delta f) H(2\pi m\Delta f) e^{j2\pi mn/N} \\ &= \frac{1}{N} \sum_{m=0}^{N-1} \left[\sum_{p=0}^{N-1} f(p\Delta t) e^{-j2\pi pm/N} \right] \left[\sum_{q=0}^{N-1} h(q\Delta t) e^{-j2\pi qm/N} \right] e^{j2\pi mn/N} \\ &= \frac{1}{N} \sum_{p=0}^{N-1} \sum_{q=0}^{N-1} f(p\Delta t) h(q\Delta t) \sum_{m=0}^{N-1} e^{j2\pi m(n-p-q)/N} \\ &= \sum_{p=0}^{N-1} f(p\Delta t) h[(p-q+N)\Delta t] \\ &= \sum_{p=0}^n f(p\Delta t) h[(n-p)\Delta t] + \sum_{p=n+1}^{N-1} f(p\Delta t) h[(N+n-p)\Delta t] \end{aligned} \quad (\text{Eq. 3-327})$$

This complex looking expression has a simple interpretation. The first sum on the last line of Equation 3-327 results in the desired convolution which is similar to Equation 3-311. The second sum is an error

term due to the overlap of $f(n\Delta t)$ and $h[(n+N)\Delta t]$. The second sum will equal zero when sufficient zeros are added.

The sketch on p. 3-192 shows a simple semigraphical method of computing discrete convolutions for the TSFT. The technique is also applicable to convolutions involving the DFT. There are only two modifications required. One is that the sequences must be made periodic. The second is applicable if frequency domain convolution is required. In this case, each sequence location must contain two numbers in order to specify the real and the imaginary parts of the data.

3.5 IMPLEMENTING TRANSFORMS FOR DATA ANALYSIS

3.5.1 Introduction

The previous material contains the theory associated with the transforms used in EMP data reduction. Knowledge of this theory is a prerequisite to the proper use and understanding of the results available from the use of transforms. However, there are a variety of practical details that must be considered in the actual computation of transforms. These details are associated with limitations in the raw data, data handling techniques, and data processing procedures. The effect of these limitations must also be understood before any reduced data can be successfully interpreted.

The following paragraphs present a brief discussion of some of the important considerations involved in implementing transforms and in accounting for limitations in the raw data and data processing techniques. The first topic discussed is data flow analysis. Data flow analysis is a systematic method of tracing the limitations imposed on the information content of data from the point of monitoring all the way to the final computer processed results. The next topic is called transform methodology. Some of the approaches used to compute transforms

are presented. This section also includes a discussion of the proper selection of time and frequency domain sampling intervals and of computer running time economy. The next topic is the influence of noise on Fourier transform data. Then a discussion of truncation of time domain data and its effects on frequency domain transforms is presented. Next a presentation on practical means of numerically integrating EMP test data is given. Finally, methods of computing transfer functions are presented.

3.5.2 Data Flow Analysis

One of the most important tasks in planning an EMP test program is to prepare a data flow analysis. The data flow analysis begins with the induced response signal that one desires to monitor during some test. Then the signal is traced through every stage of monitoring, recording, analog-to-digital conversion, and mathematical data reduction. At each step, the "distortions" of the desired signal are evaluated. Finally, one compares the desired signal to the resultant signal after all stages of instrumentation and data processing. The objective of this analysis is to insure that the desired features of the response signal are preserved during this multistage process. If the distortions are unacceptable, one has two options. One is to improve the instrumentation and/or data processing procedures, if possible. The second is to accept the degraded test data and ask oneself whether there is sufficient information to achieve the test objectives.

An important feature obtained by the preparation of a data flow analysis is that the instrumentation and data processing tasks of a test program will be united. Data processing personnel will get a realistic assessment of the instrumentation imposed limitations on the data with the result that they will not try to derive more information from the raw data than is potentially available. Furthermore, the instrumentation personnel will appreciate the limitations imposed by their instrumentation group as

well as the data processing techniques. Therefore, the instrumentation group should not demand information from the processed data that is not potentially available.

The elements of a data flow analysis are illustrated in the simplified schematic shown in Figure 3-11. The excitation, $f(t)$, induces a response, $g(t)$, into the system under test. The excitation is generally the simulated EMP fields. The response generally constitutes a current flowing on a metal conductor, and it provides information about the system characterized by the impulse response, $h(t)$. Sometimes inspection of $g(t)$ will provide the desired information such as peak amplitude, resonant frequency, or signal duration. On other occasions, a Fourier transform of $g(t)$ may be required to obtain the desired information. Furthermore, one might try to obtain quantitative information about the system impulse response, $h(t)$, or its associated transfer function, $H(\omega)$, by use of $f(t)$, $g(t)$, and transform techniques.

Unfortunately the desired signals, $f(t)$ and $g(t)$, are usually not available. Figure 3-11 shows the sources of distortion associated with $g(t)$. The first source is denoted by the additive term, $n_s(t)$. This term could represent the effect of nonlinearities in the system, the response of the system due to inputs other than $f(t)$, or to system/instrumentation interaction. This term is minimized or accounted for by careful study of the systems composition and electromagnetic coupling modes. Identification and characterization of this term is not the direct responsibility of the data processing personnel. However, all parties should realize it is potentially present. It should be noted that $n_s(t)$ is indicated as an additive term. This designation was done for graphical simplicity. However, this type of error could be related to $g(t)$ or $h(t)$ in almost any manner.

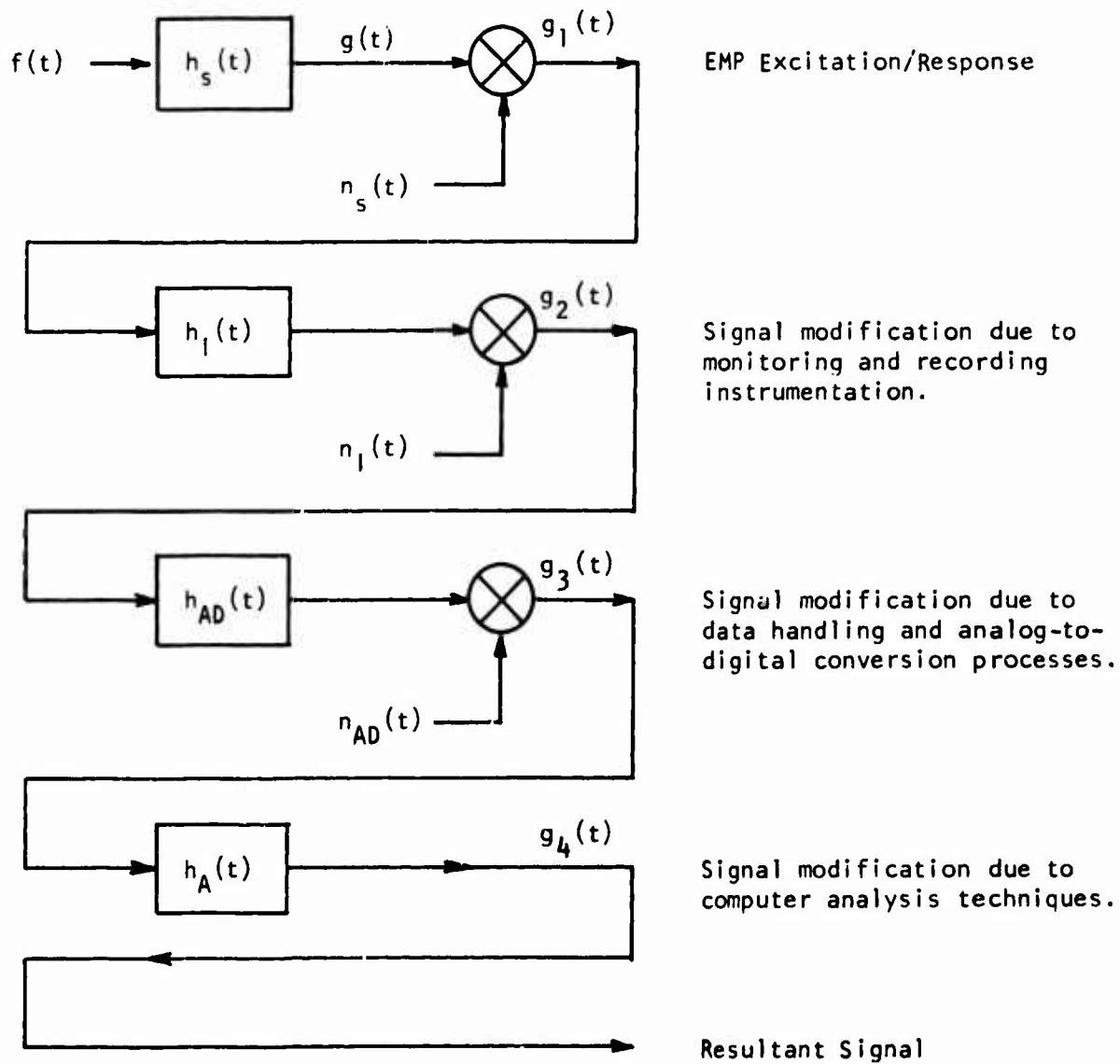


Figure 3-11. Data Flow Analysis

The second and third sources of error are denoted by $h_1(t)$ and $n_1(t)$. These terms represent the combined effects of all instrumentation including sensors, data links, interface electronics, and recording equipment. Ideally the instrumentation would have $h_1(t)$ equal to a delta function so that the output would be identically equal to the input. In practice, the instrumentation generally consists of some sort of low pass filter. Important parameters in specifying the filter characteristics are the bandwidth and deviations from ideal response in the pass band. Bandwidth, in this case, is defined as the frequency range from essentially zero frequency to the cutoff frequency. The cutoff frequency is the highest frequency the instrumentation system will propagate and is usually defined at a point where the output is 3 dB less than its magnitude at lower frequencies. An example of pass band deviations was treated in Section 3.3.8.11 where the effects of amplitude and phase ripple in an ideal low pass filter were evaluated. In most EMP tests, the instrumentation has sufficient bandwidth and fidelity in the pass band that there is only minimal distortion of the data. Nevertheless, the effects of the available instrumentation bandwidth on test data must be evaluated at some stage during a test program.

The additive term, $n_1(t)$, is noise. There are two possible sources of this noise. One is thermal noise, shot noise, etc., associated with the electronics of the instrumentation. The second source is the unwanted response of the instrumentation (rather than the test object) to the exciting fields. Once again, Figure 3-11 displays this noise term as an additive function although it is not necessarily of that form.

The noise sets the lower limit of the desired signal that can be detected unambiguously. An upper signal level also exists. This upper limit is the signal level where saturation, voltage breakdown, or other nonlinear effects begin to occur. The ratio between the maximum and minimum signal level is called the dynamic range. A closely related parameter is the signal-to-noise ratio which is defined as the ratio of

signal amplitude to noise amplitude. In practical applications, the signal-to-noise ratio is less than the dynamic range. There are a multitude of precise definitions for the signal and noise amplitudes and their various ratios. Those definitions need not be developed here. The important point is that these parameters establish the amplitude range and the uncertainty of the time domain signal. The effect of a finite signal-to-noise ratio on Fourier transforms is established in a later section.

Another important specification of an instrumentation system is the minimum resolvable time, t_R , and the maximum recording time, t_D . Since oscilloscopes are usually used to record transient EMP data, the specification of the t_R and t_D is especially important. The minimum resolvable time is limited by the trace width displayed on the face of the oscilloscope. A general rule of thumb is that a well focused oscilloscope has a trace width of 0.1 major divisions or squares on an oscilloscope graticule. Therefore, the period of a high frequency oscillation can be distinguished if adjacent nearly vertical trace segments are separated by at least 0.1 divisions. Thus, if a division corresponds to 100 nanoseconds (100 nanoseconds/division), the minimum resolvable time is 10 nanoseconds.

It should be noted that t_R and t_D are analogous to $n_1(t)$ and the maximum signal amplitude discussed previously. Each of these pairs establishes the minimum resolution and the maximum extent of the variable, t and $g(t)$. One can define a time dynamic range as the ratio, t_D/t_R . For an oscilloscope, the time dynamic range is equal to 100 or 40 dB if one uses the definition of the dB loosely. In many cases the time dynamic range can be extended by using two or more oscilloscopes with differing sweep speeds to record the data. Finally, it should be noted that the finite time dynamic range places constraints on the use of transform data just as the finite signal-to-noise ratio. A further discussion of these transform limitations will be presented in a later subsection.

The fourth and fifth source of error or distortion are the data handling and the analog-to-digital conversion processes. These sources are denoted as $h_{AD}(t)$ and $n_{AD}(t)$. The system function, $h_{AD}(t)$, is used to signify any systematic error that could occur in the data at this stage. Typical systematic errors are optical distortion when photographing the data and errors in locating the origin, baseline, and rotation angle when digitizing an oscillograph or its analog facsimile. In some cases, small systematic errors introduced by data handling or digitization result in large errors in the transform data. The term, $n_{AD}(t)$, signifies noise resulting from loss of resolution in a photographic copying process or the small random errors in time and amplitude introduced by digitization. It should be noted that the digitization noise is not totally independent of the instrumentation noise. The finite trace width present on an oscillograph and caused by instrumentation noise accentuates the noise introduced by digitization. Needless to say, these systematic and random errors affect the resulting transform data. Some of these error effects will be discussed in a later subsection.

The final source of error or distortion in the processed data, $h_A(t)$, is attributable to the Fourier transform algorithms. It should be mentioned that algorithm type errors are usually not associated with any lack of accuracy or precision in the numerics. The actual problem lies in the misuse or misapplication of the particular algorithm. These type errors can either be eliminated or accounted for by a thorough understanding of the material presented in Subsections 3.3 and 3.4. Additional material on the use of Fourier transforms is also presented in the following subsection.

3.5.3 Transform Methodology

3.5.3.1 Introduction

The Fourier transform is the basic analysis tool used in the study of EMP test data. Previous sections have presented the basic

theory on these transforms. In this subsection some practical features of implementing and using transforms are given. The discussion will be limited to the FIT and the FFT as these are the most common types of transforms used for EMP data analysis. The first two topics presented are a brief discussion of the algorithms used to compute the FIT and the FFT. The next two topics are selected guidelines for using the FIT and the FFT. Finally a discussion of the relative advantages of the FIT versus the FFT is given.

3.5.3.2 FIT Algorithm

The defining equations for the FIT are

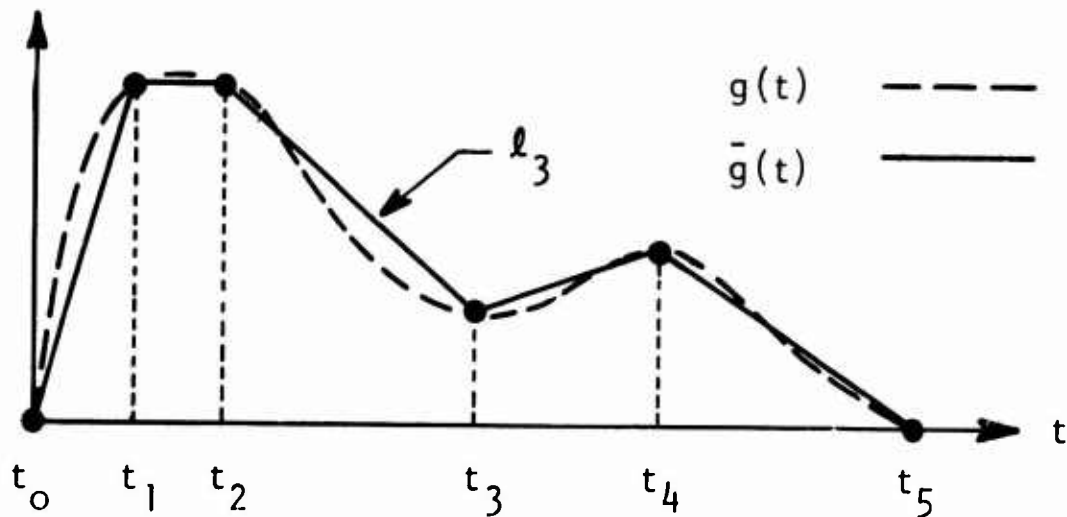
$$G(\omega) = \int_{-\infty}^{\infty} g(t) e^{-j\omega t} dt$$

$$g(t) = \frac{1}{2\pi} \int_{-\infty}^{\infty} G(\omega) e^{j\omega t} d\omega \quad (\text{Eq. 3-328})$$

In practice, the integrals in the above equations are evaluated by some approximate technique to obtain numbers instead of functional relationships. A large variety of approximate techniques have been used in the past to approximate these integrals. One specific technique, called the piecewise linear approximation, will be presented here. This technique illustrates the basic approach for obtaining a numerical algorithm for computing an FIT. Furthermore, this technique is the most commonly used approach for computing the FIT of EMP test data.

Assure one has a function, $g(t)$, available in some form such as an analog trace on an oscillograph or an analytic expression.

The piecewise linear approach is to approximate $g(t)$ with a finite number of linear line segments to yield $\bar{g}(t)$. Then an analytic transform of $\bar{g}(t)$ is obtained.



Note that the spacing between points on the time axis need not be equal. Also note that the waveform is approximated over a finite length interval, $t_N - t_0$, where N is the total number of segments used.

The formulation of the algorithm begins by forming the equation for each of the segments, l_n .

$$l_n = a_n t + b_n \quad (\text{Eq. 3-329})$$

$$a_n = \frac{g(t_n) - g(t_{n-1})}{t_n - t_{n-1}}$$

$$b_n = \frac{t_n g(t_{n-1}) - t_{n-1} g(t_n)}{t_n - t_{n-1}} \quad (\text{Eq. 3-330})$$

Then the resulting FIT at a given frequency, ω_o , is expressed as

$$G(\omega_o) = \sum_{n=1}^N \int_{t_{n-1}}^{t_n} (a_n t + b_n) e^{-j\omega_o t} dt \quad (\text{Eq. 3-331})$$

where N is the total number of line segments used to approximate g(t).

After integrating the above equation, one obtains

$$R_e\{G(\omega_o)\} = \sum_{n=1}^N \frac{1}{\omega_o} \left\{ (a_n t_n + b_n) \sin(\omega_o t_n) - (a_n t_{n-1} + b_n) \sin(\omega_o t_{n-1}) \right. \\ \left. + a_n [\cos(\omega_o t_n) - \cos(\omega_o t_{n-1})] / \omega_o \right\}$$

$$I_m\{G(\omega_o)\} = \sum_{n=1}^N \frac{1}{\omega_o} \left\{ (a_n t_n + b_n) \cos(\omega_o t_n) - (a_n t_{n-1} + b_n) \cos(\omega_o t_{n-1}) \right. \\ \left. - a_n [\sin(\omega_o t_n) - \sin(\omega_o t_{n-1})] / \omega_o \right\}$$

$$\omega_o \neq 0$$

$$(\text{Eq. 3-332})$$

When $\omega_0 = 0$, the transform is equal to

$$G(0) = \sum_{n=1}^N \int_{t_{n-1}}^{t_n} (a_n t + b_n) dt, \quad \omega_0 = 0 \quad (\text{Eq. 3-333})$$

Finally the magnitude and phase of the transform are given by

$$|G(\omega_0)| = \sqrt{R_e^2\{G(\omega_0)\} + I_m^2\{G(\omega_0)\}}$$

$$\phi\{G(\omega_0)\} = \tan^{-1} \left\{ I_m\{G(\omega_0)\} / R_e\{G(\omega_0)\} \right\} \quad (\text{Eq. 3-334})$$

These equations are evaluated for each value of ω_0 desired.

The inverse transform is obtained by a similar procedure. Assuming that $g(t)$ is real, then the inverse transform is given by Equation 3-34

$$g(t) = \frac{1}{\pi} \int_0^{\infty} [R_e\{G(\omega)\} \cos(\omega t) - I_m\{G(\omega)\} \sin(\omega t)] d\omega \quad (\text{Eq. 3-34})$$

Considerable simplification is obtained if it is assumed that $g(t)$ is causal as well as real. In this context, causal means that $g(t) = 0$ for $t < 0$. Then the inverse transform is given by Equation 3-38.

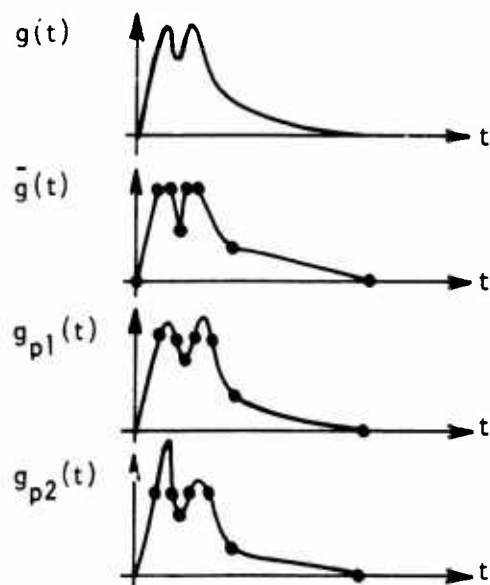
$$g(t) = \frac{2}{\pi} \int_0^{\infty} R_e\{G(\omega)\} \cos(\omega t) d\omega \quad (\text{Eq. 3-38})$$

This equation is the one most commonly used. The algorithm uses linear segments, $m_n = c_n \omega + d_n$, to approximate $R_e\{G(\omega)\}$. Then the inverse transform is expressed as

$$g(t_0) = \frac{2}{\pi} \sum_{n=1}^N \int_{\omega_{n-1}}^{\omega_n} (c_n \omega + d_n) \cos(\omega t_0) d\omega \quad (\text{Eq. 3-335})$$

Once again, note that the spacing between points on the frequency axis need not be equal and that $R_e\{G(\omega)\}$ is approximated over a finite interval, $\omega_N - \omega_0$. Further details on this procedure are given in Reference [25]. A formulation for the inverse transform based on Equation 3-34 when $g(t)$ is not causal is given by Reference [26].

There are other methods of approximating the integrals in the FIT. For instance, some parties approximate the function, $g(t)$, by a finite number of triangles. Then the resulting transform is the sum of the analytic transforms of the individual triangles. However, Equation 3-218 shows that a triangular approximation is identical to a piecewise linear fit. Therefore, there is no fundamental difference in the two approaches. Other methods of approximating the integral are based on fitting the coordinates of the waveform, t_n and $g(t_n)$ to a polynomial. One would think that this "smoother" fit would provide more accurate transform results. However, Reference [27] shows these higher order approximations actually provide poorer results.



Original Function

Piecewise Linear Fit

Polynomial Fit No. 1

Polynomial Fit No. 2

The reason is that polynomial fits are sometimes unstable to small errors in the coordinate points. For instance, the sketch above shows $g_{p1}(t)$ to be a well behaved fit to $g(t)$. However, a slight change in the coordinates (near the first peak in this example) to yield $t_n + \epsilon$ and $g(t_n + \epsilon)$ is arbitrarily small, can produce the polynomial fit indicated as $g_{p2}(t)$. Note the large error in $g_{p2}(t)$. A similar change in coordinates when using a piecewise linear fit would result in a very small change in $\bar{g}(t)$.

3.5.3.3 FFT Algorithm

It was mentioned previously that the FFT was an efficient means of computing a DFT. A short and admittedly incomplete introduction to the method used to compute the FFT will be presented in the following paragraphs. It is hoped that this material will give those who use the FFT a small understanding of the method, and stimulate those who want to write their version of the algorithm to refer to the many good references available [28, 29, 30].

If one has an N point time domain sequence, g_n , then its DFT is given by Equation 3-324.

$$G_m = \sum_{n=0}^{N-1} g_n e^{-j2\pi mn/N} \quad (\text{Eq. 3-324})$$

It is convenient as well as conventional to write the exponential as

$$W^{mn} = (e^{-j2\pi/N})^{mn} = e^{-j2\pi mn/N} \quad (\text{Eq. 3-336})$$

Then Equation 3-324 becomes

$$G_m = \sum_{n=0}^{N-1} g_n W^{mn} \quad (\text{Eq. 3-337})$$

The FFT is derived from the DFT by noting the symmetry in W^{mn} . One approach used in this derivation is indicated below.

A concept called "decimation in time" can be used to obtain the FFT. Suppose that the N point sequence introduced above, g_n , is divided into two sequences. Let one of the sequences, k_n , consist of the even numbered points of g_n and the other sequence, ℓ_n , consist of the odd numbered points. Thus

$$k_n = g_{2n}$$

$$\ell_n = g_{2n+1} \quad n=0, 1, 2, \dots, N/2-1 \quad (\text{Eq. 3-338})$$

The transform of these two $N/2$ point sequences is given by

$$\begin{aligned} K_m &= \sum_{n=0}^{N/2-1} k_n W^{2nm} \\ L_m &= \sum_{n=0}^{N/2-1} \ell_n W^{(2n+1)m}, \quad m=0, 1, 2, \dots, N/2-1 \end{aligned} \quad (\text{Eq. 3-339})$$

Since a Fourier transform is a linear process where superposition is valid, one can express G_m in terms of K_m and L_m . Thus

$$\begin{aligned} G_m &= \sum_{n=0}^{N/2-1} [k_n + W^{2m} \ell_n] W^{2nm} \\ &= K_m + W^m L_m, \quad m=0, 1, 2, \dots, N/2-1 \quad (\text{Eq. 3-340}) \end{aligned}$$

where

$$W^{1m} = W^m = e^{-j2\pi m/N} \quad (\text{Eq. 3-341})$$

Equation 3-340 is defined for frequencies less than $N/2-1$. The frequency components in the range between $N/2-1$ and $N-1$ are determined in the following manner. First note that K_m and L_m were derived from $N/2$ point sequences. Therefore, they are periodic with a period of $N/2$. Thus

$$\begin{aligned} K_{m+N/2} &= K_m \\ L_{m+N/2} &= L_m, \quad m=0, 1, 2, \dots, N/2-1 \end{aligned} \quad (\text{Eq. 3-342})$$

Also note that

$$\begin{aligned} W^{m+N/2} &= e^{-j2\pi(m+N/2)/N} \\ &= -W^m, \quad m=0, 1, 2, \dots, N/2-1 \end{aligned} \quad (\text{Eq. 3-343})$$

Therefore

$$G_{m+N/2} = K_m - W^m L_m, \quad m=0, 1, 2, \dots, N/2-1 \quad (\text{Eq. 3-344})$$

Thus, Equations 3-340 and 3-344 yield the transform of an N point sequence in the range $(0, N-1)$.

The significant feature of this development is that the number of computations is reduced. Inspection of Equation 3-324 shows that N multiplications are required at each frequency. Since there are N frequency components, a total of N^2 multiplications are required. However, Equations 3-340 and 3-344 state that G_m can be obtained from two $N/2$ point sequences. Therefore, $N^2/2$ multiplications are required. The development of the FFT algorithm continues to extend this principle. The two $N/2$ point sequences are divided into four $N/4$ point sequences and transform relations are established similar to Equations 3-340 and 3-344. In this case $N^2/4$ multiplications are required. The process is continued until each sequence has one point. Then the number of multiplications is equal to $N \log_2 N$. The number of points, N , does not have to be very large before the number of multiplications required for the FFT is significantly less than those associated with the DFT. Therefore, the FFT will require much less computer time than the DFT for the same number of points. It should be noted that approximations to the FIT require approximately the same number of multiplications as the DFT when the number of points are the same. Therefore, the FFT has the same speed advantage over the approximations to the FIT as it has over the DFT. One final point must be made. The number of points must be a power of two in order to achieve the maximum speed advantage. There are FFT algorithms that can process any number of points. However, if N is not highly composite in factors of two, then the running time approaches that of a DFT. Obtaining N points that are exactly some power of two is no problem in practice. All one needs to do is add zeros to the original sequence until the sum of the number of original points and the number of zeros equals some power of two.

3.5.3.4 Use of the FIT

3.5.3.4.1 Introduction

Successful use of the FIT requires a thorough knowledge of its basic properties as described in Section 3.3.

However, there are additional considerations when using the FIT with experimental data. These include the selection of raw data and the choice of time and frequency arrays. Some of the important considerations are described in the following paragraphs.

Perhaps the most important decision in the use of the FIT to help analyze experimental data is whether to use it at all. Too many low quality experimental data have been transformed in past EMP test programs. These transform data are incapable of yielding the desired information. Furthermore, they often provide misleading results to the unwary. Therefore, the user must ask himself exactly what information he wants to obtain from a transform. Then he must examine each particular data record to see if it can potentially yield that information. If the data record is incapable of yielding the desired information, then the user must either do without or request that the experiment be repeated such that adequate data are obtained. This last option points out the advantage of performing the data processing and analysis concurrent with the test. If some of the data is inadequate for the analysis objectives, then there is the option of repeating the experiment. After the test is over, the option usually doesn't exist.

3.5.3.4.2 Methodology

There are several features of the raw data that the user should examine before requesting a transform. These include the contrast, signal-to-noise ratio, minimum resolution time, and maximum time duration. A data record with poor contrast, improperly focused trace, or writing dropouts will be impossible to digitize accurately, and the resulting transform will be meaningless. The Fourier transform is a linear mathematical operation. Therefore, additive noise in the time domain will transform to additive noise in the frequency domain. This noise can obliterate the desired information in both the time and frequency domains. More will be said about noise in Subsection 3.5.4. The minimum time resolution

establishes a bound on the highest frequency data that can be obtained. If a high frequency component with a very short time period cannot be resolved in the time domain, then it certainly cannot be computed accurately in the frequency domain. The maximum time duration of the data record must be compared to the signal duration. If the time duration of the data record is much less than the signal duration, there will be two penalties. One is that there is insufficient information to characterize low frequency components with their corresponding long time periods. The second is that the so called truncation error will be introduced (see Subsection 3.5.5). This type of error affects the transform data at all frequencies.

After selecting suitable data for transform analysis, the user should personally familiarize himself with the computer algorithms that will be used to perform the calculations. The detailed coding is not important. However, what is significant is that the user thoroughly understand the capabilities of the particular algorithm to be used. The best way to obtain this familiarity is to utilize simple analytic functions with known characteristics. Typical functions that could be used are $e^{-\alpha t}$ and $e^{-\alpha t} \sin(\beta t)$. The user should first examine the numerical transform of the function used. The most important feature to examine is the scaling. The user should note whether the data are being plotted as functions of f or of $\omega = 2\pi f$. He should also note the amplitude and ask whether it corresponds to the known analytic results. If the amplitude is off by a factor equal to the inverse of the data record duration, then the particular algorithm is probably based on the FST. Also note whether the amplitude is off by a factor of 2π . The natural units for transform quantities is $[]/(\text{radian/second})$ where $[]$ signifies the units of the time domain function. If the time domain data have units of amps, then their transform will have units of $\text{amps}/(\text{radian/second})$. Sometimes the amplitude is multiplied by a factor of 2π to yield data in terms of $[]/(\text{cycle/second})$ or $[]/\text{Hz}$. If the amplitude is off by a factor of 10^3 or 10^6 , then the user should determine whether the algorithm is interpreting the amplitude data in terms of milli $[]$ or kilo $[]$ or the time in

terms of milliseconds or microseconds. After this examination is complete, the user should obtain an inverse transform to verify if the original waveform is obtained. Finally, he should multiply the transforms of two known functions and obtain the inverse of the product. If the user is confident that he understands the idiosyncrasies of the particular algorithm he is using, then he is ready to process test data.

Once the user obtains his processed transform data, he should immediately examine some of its features. For instance, he should check to see if known resonances are occurring at the proper frequency. The resonant frequency of a time domain oscillation can be estimated by noting the period of the oscillation. If there is not a prominent peak at this frequency in the transform data, then the scaling procedures employed during the digitization process are probably in error. The user should also check the amplitude of the transform data at prominent locations such as at a resonant peak. Estimates of the amplitude can be obtained by comparing the transform of the experimental data to that of some simple function that closely resembles it. Other features that the user should check are the low and high frequency regions. Excess amplitude at low frequencies could mean that there was baseline offset or baseline rotation error introduced during digitization (see Subsection 3.5.6). Excess amplitude at high frequencies could be due to noise (see Subsection 3.5.4) or truncation error (see Subsection 3.5.5). If the transform data have periodic oscillations with a period equal to the inverse of the data record duration, then this is a system of truncation error (see Subsection 3.5.5). If the data have notches, that could imply that the original data record consisted of the superposition of two or more signals (see Subsection 3.3.11.5). If the transform data have periodic notches or peaks, then the original data record was produced by a multiple reflection process (see Subsection 3.3.11.6). The notches in the ARES environment spectrum are due to multiple reflections inside the pulser.

3.5.3.4.3 Time Domain Sampling

The sampling used to characterize an experimental time domain record is an important consideration in the use of the FIT. Common sense says that there should be a sufficient density of samples such that a piecewise linear fit closely approximates the original data. However, the minimum spacing between samples is determined from two criteria. One is that the highest frequency component that one might have confidence in is inversely proportional to the minimum distance between samples of the time domain record.

$$f_{\max} = \frac{1}{\Delta t_{\min}} \quad (\text{Eq. 3-345})$$

This criterion is not as precise as the Nyquist criteria used with the TSFT or the DFT(FFT) since samples for the FIT usually don't have constant spacing. However, it does constitute an engineering guide to the highest possible credible frequency. The second criterion is the minimum time resolution available from an oscillograph. The minimum time resolution, (t_R), fixes the minimum sample interval and, hence, the maximum frequency for the transform data.

$$t_R = \Delta t_{\min} = \frac{1}{f_{\max}} \quad (\text{Eq. 3-346})$$

If one has an oscillograph recorded at 100 nanoseconds/division, then the minimum time resolution will be about 10 nanoseconds and the maximum frequency will be about 100 MHz.

A damped sinusoid is characteristic of most EMP response data. Therefore it is interesting to investigate the effect

of sampling rate on the resultant transform data. Figure 3-12 shows the waveform that will be used for this example. Figures 3-13 and 3-14 show the transform of this function when it is sampled at equal increments at a rate of four and eight samples per cycle. The transform was calculated by evaluating the analytic form of the time domain function at the desired values of time. Then a FIT algorithm was used to compute the transform using the values of the sampled analytic function. Inspection of Figures 3-13 and 3-14 shows large errors occurring at multiples of the inverse of the sampling interval. In this example, a period is equal to 0.1 seconds. A sampling rate of four samples per cycle implies $\Delta t = 0.025$ seconds. The largest error occurs at a frequency equal to $1/0.025 = 40$ Hz and its harmonics in Figure 3-13. The large error is centered at 80 Hz in the example shown in Figure 3-14. These errors are due to use of equally spaced samples and are predicted by use of Equation 3-218.

Three conclusions can be obtained by inspecting Figures 3-13 and 3-14. One is that the error at every frequency is greater when using a smaller number of samples. Another is that the error becomes quite large at a frequency approximately equal to one half of the inverse of the sampling interval. However, this frequency is the same as the Nyquist frequency. Therefore, the Nyquist criteria is a useful guide in choosing sampling rates to use with the FIT. The final conclusion is that the waveform should be sampled from eight to 10 times per cycle. Then the "Nyquist frequency" will be four to five times higher than the center frequency of the resonant peak. In this case, the Q of the resonance can be determined accurately. Higher sampling rates would be desirable, but they would be impractical to achieve in most cases.

Although the FIT usually does not employ equally spaced data, these examples illustrate limitations that are partially true when using unequally spaced data. This fact is demonstrated in Figure 3-15 which shows the transform of the same time domain function when using unequally spaced intervals typical of those produced by most

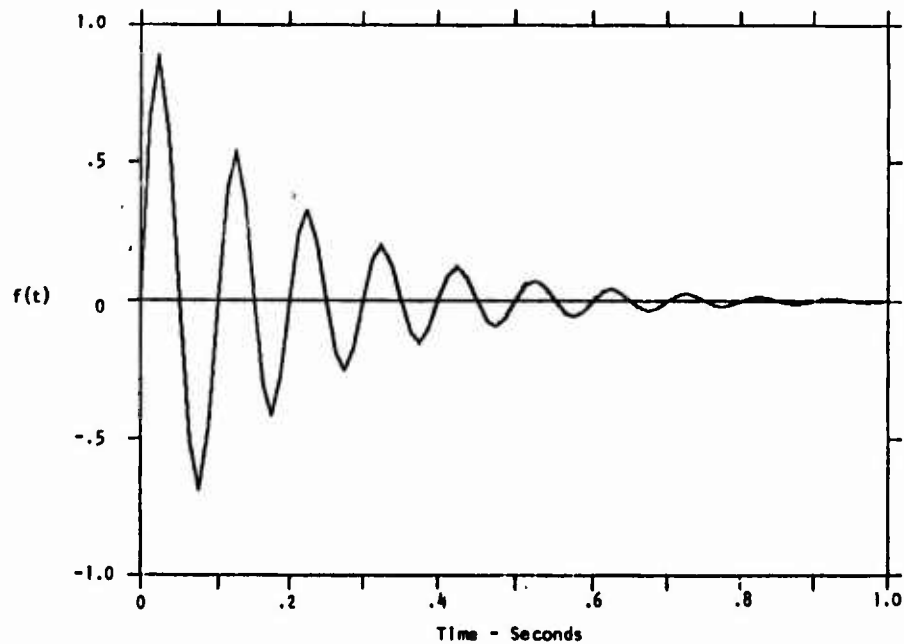


Figure 3-12. Time Domain Function Used for Sampling Study - $f(t)$

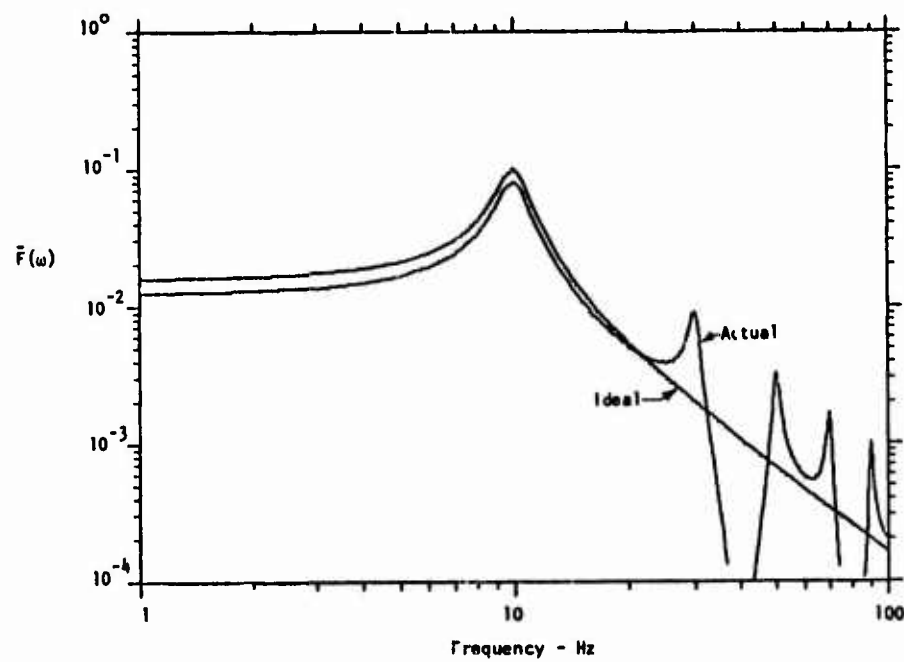


Figure 3-13. Transform of $f(t)$, $\bar{F}(\omega)$, When $f(t)$ is Sampled 4 Times Per Cycle

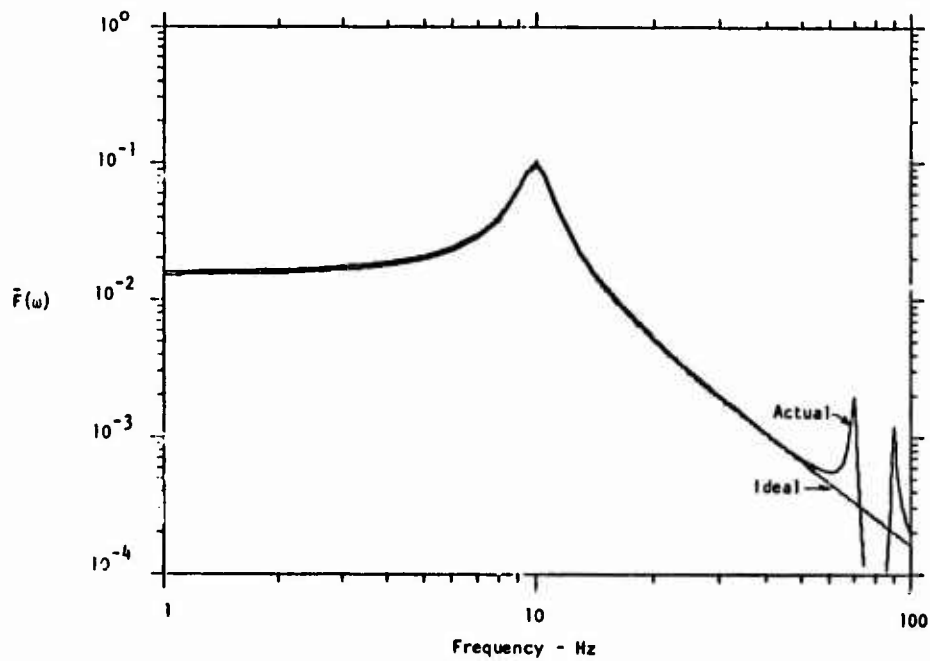


Figure 3-14. Transform of $f(t)$, $\bar{F}(\omega)$, When $f(t)$ is Sampled 8 Times Per Cycle

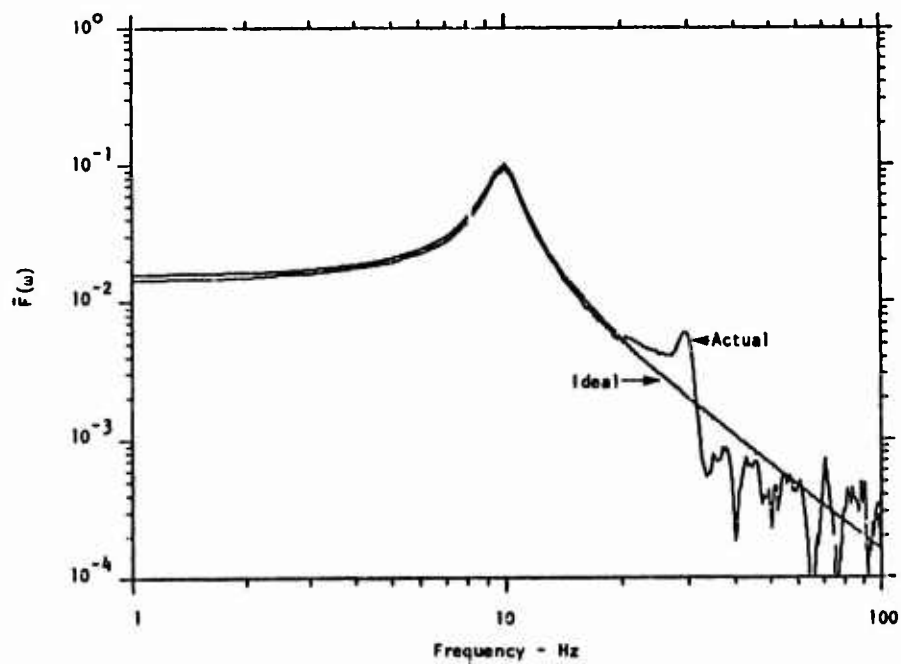


Figure 3-15. Transform of $f(t)$, $\bar{F}(\omega)$, With Random Time Sampling Averaging 8 Samples Per Cycle

digitizer systems. The time increments were generated in the following way. A copy of Figure 3-12 was placed on the digitizer surface and the waveform was digitized in a standard manner. That is, points were obtained at peaks, zero crossings, and regions of high curvature. An average of eight samples per cycle was obtained. Then these values of time obtained by the digitizing process were used to evaluate the analytic function. Finally the FIT algorithm was used to calculate the transform using the unequally sampled data from the analytic function.

Inspection of Figure 3-15 shows two interesting features. One is the large error in the vicinity of 20-25 Hz which is similar to that in Figure 3-13. This error is due to the nearly periodic sampling at the peaks and zero crossings. The second feature is that the transform has a noise-like appearance and large fluctuating errors at frequencies greater than the "Nyquist frequency." In this case, the "Nyquist frequency" is equal to one half the inverse of the average sample interval. Therefore, the conclusions presented above for equally spaced sampling are valid for unequally spaced sampling. Two additional conclusions are also evident. One is that equally spaced sampling should be used, if practical, with the FIT since the errors are more predictable. The second conclusion is that Equation 3-345 presents an overly optimistic measure of the highest credible frequency. A more useful definition is given by

$$\frac{1}{4\Delta t_{\text{ave}}} < f_{\text{max}} < \frac{1}{2\Delta t_{\text{ave}}} \quad (\text{Eq. 3-347})$$

where Δt_{ave} is the average sampling interval when using unequally spaced samples.

When using the FIT, the choice of frequencies to be computed are left to the discretion of the user. The previous discussion shows that it is meaningful to restrict the frequency range to $(0, f_{\max})$. Then the only decision is the choice of the frequency increments. Reference to the FST or DFT would indicate that the frequency increments should be equally spaced with a value equal to the inverse of the data record length. However, one rarely has a data record length that spans the entire duration of the signal. Therefore, use of the criteria could provide poor resolution, especially for narrow resonant peaks. A more useful criterion that is a compromise between resolution and running time economy is the following

$$\Delta f = 1/3T \quad (\text{Eq. 3-348})$$

This is the criterion that has been used at ARES.

3.5.3.4.4 Inverse Transforms

When computing inverse transforms, the criteria for specifying a frequency array are slightly different than those presented previously. An FIT of a time domain function has frequency domain components at all frequencies regardless of whether they are accurate or erroneous. Furthermore, all of these components are required to exactly reproduce the original function when an inverse transform is calculated. The practical problem is to obtain some useful criteria for defining an upper frequency such that the error in performing an inverse transform is minimized. One will note that truncating a frequency domain function above some frequency, f_{\max} , yields a resultant function, $\bar{G}(2\pi f)$, equal to $G(2\pi f) \text{ Rect}_{2f_{\max}}(f)$. Reference to Equation 3-67 shows the transform of $\bar{G}(2\pi f)$ is equal to

$$F^{-1}\{\bar{G}(2\pi f)\} = g(t) * 2f_{\max} \text{Sinc}(2f_{\max}t) \quad (\text{Eq. 3-349})$$

The effect of this convolution is to reduce the time resolution of $g(t)$ to a time approximately equal to the width of the central peak of the Sinc function. Thus the minimum time resolution, t_{\min} , would equal f_{\max}^{-1} . Now one defines the upper cutoff frequency by specifying the desired value of t_{\min} . Then

$$f_{\max} = 1/t_{\min} \quad (\text{Eq. 3-350})$$

Now one must choose a sampling interval, Δf , for the frequency domain function. Common sense says that the frequency domain function must be sampled sufficiently to produce a good piecewise linear fit to the original function. In most cases the Δf defined by Equation 3-348 will suffice. However, one must note that $G(2\pi f)$ is a complex quantity that is specified in terms of its magnitude and phase. Adequate sampling of the magnitude is not sufficient. The phase must also be considered. One will note that any trigonometric function is periodic with a period of 2π radians. Therefore, the phase difference, $\Delta\phi(2\pi f)$, between adjacent sample points must be less than 2π to avoid ambiguity.

$$\Delta\phi(2\pi f) < 2\pi \quad (\text{Eq. 3-351})$$

Once again Equation 3-348 provides useful criteria in most cases. However, if the time domain function is shifted from the origin by an amount, t_0 , then the phase of the transform will contain an additive term equal to $2\pi f t_0$. When obtaining an inverse transform, the total phase change,

including this additive term, must be less than 2π . Figure 3-16 shows an example where these phase sampling criteria are violated.

3.5.3.5 Use of the FFT

Most of the material presented in Subsection 3.5.3.4 on the FIT is applicable to the FFT. That is, one must use high quality experimental data, evaluate whether the raw data have the potential information content desired, familiarize oneself with the particular algorithm being used, and perform spot checks on the processed results. The rationale in setting Δt , Δf , etc. is essentially the same for the FFT as for the FIT. The only major difference is the aliasing criteria and the fact that Δt , Δf , f_{\max} , and t_{\max} are not independent of each other. Subsection 3.4.6 on the DFT should be consulted for the details on aliasing and the interrelationship of the time and frequency domain parameters. In fact, all the material in Subsection 3.4.6 is applicable to the FFT. There is, however, one major difference between the DFT and some particular algorithms for the FFT. This difference involves the method of displaying inverse transform data and emphasizes the importance of familiarizing oneself with the specific algorithm being used.

The following example shows some typical results that can be obtained from some FFT algorithms. The user must be alert for those characteristics so that he can choose the number of sample points, N , properly. Assume one has two time domain functions, $g_1(n\Delta)$ and $g_2(n\Delta t)$. Then obtain the FFT of these two functions. Finally, obtain the inverse of the two frequency domain functions to yield $\bar{g}_1(n\Delta t)$ and $\bar{g}_2(n\Delta t)$.

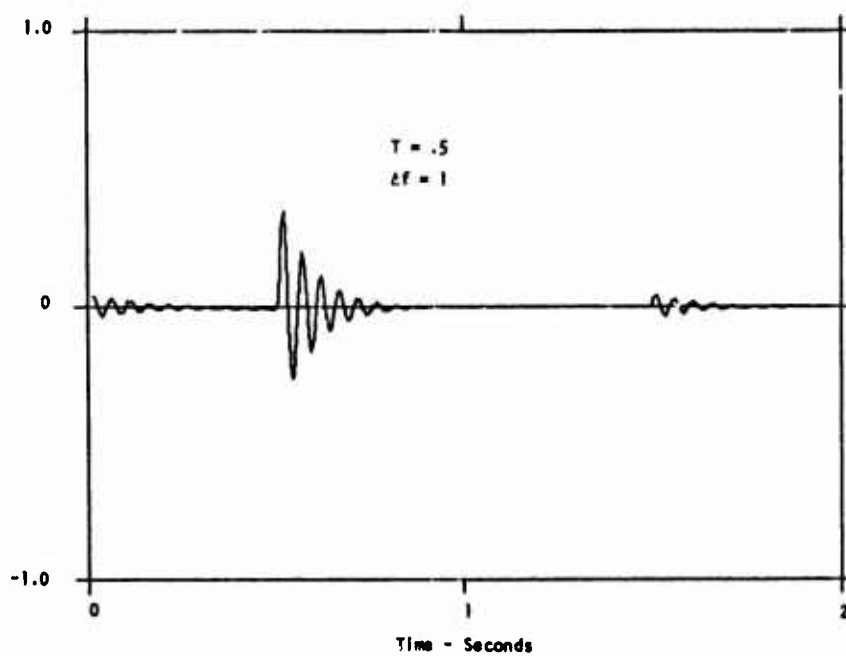
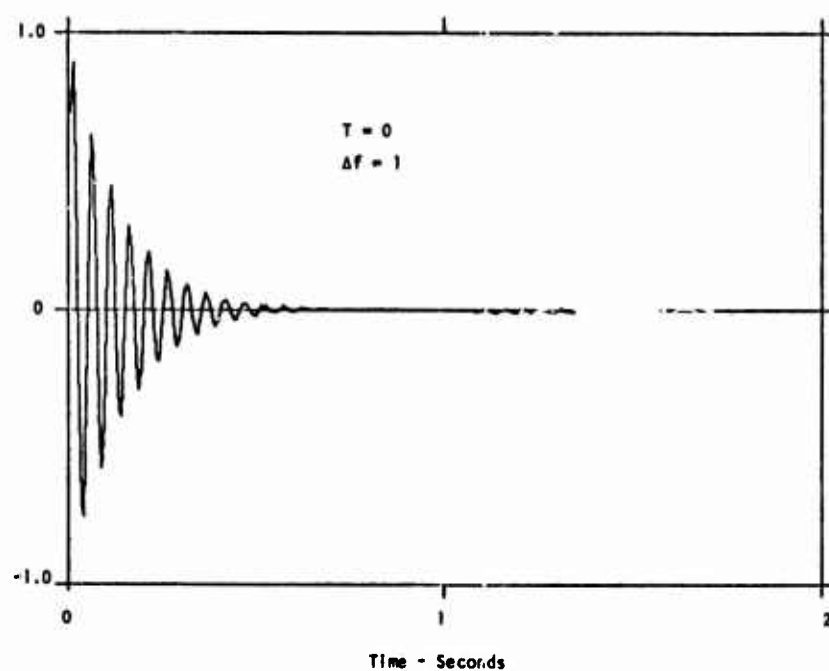
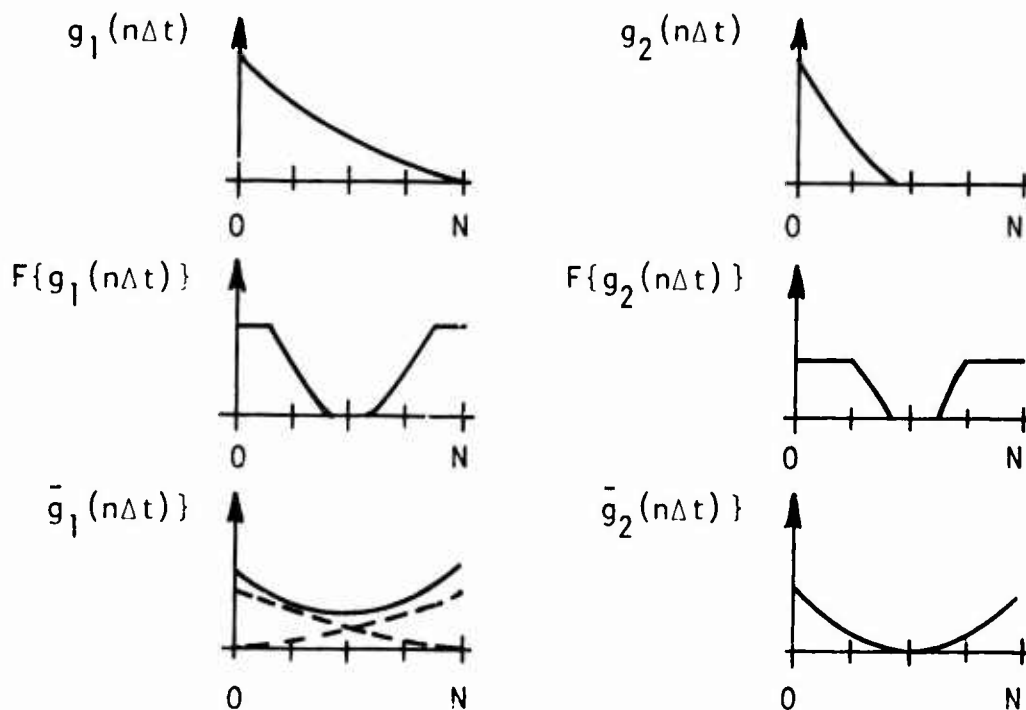
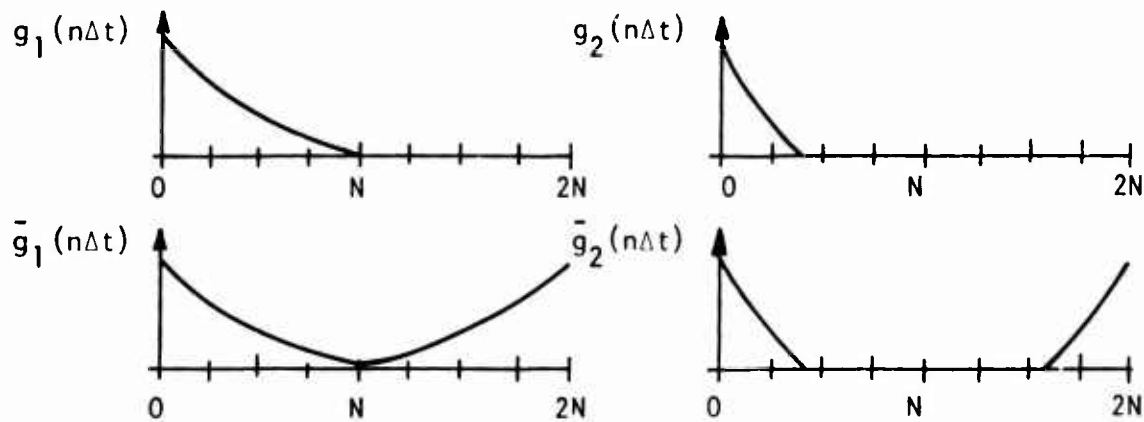


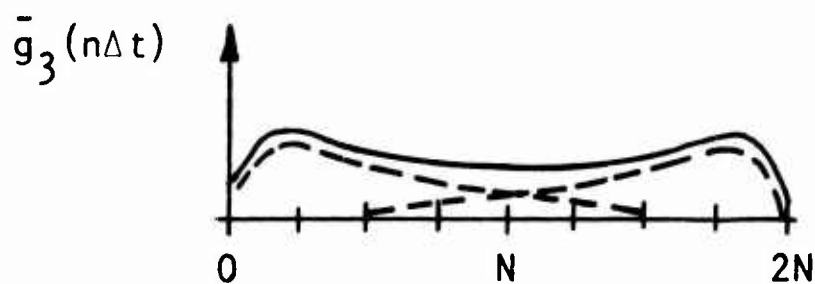
Figure 3-16. Inverse Fourier Transform of a Damped Sinusoid With an Additive Phase Shift - $\phi(f) = 2\pi fT$



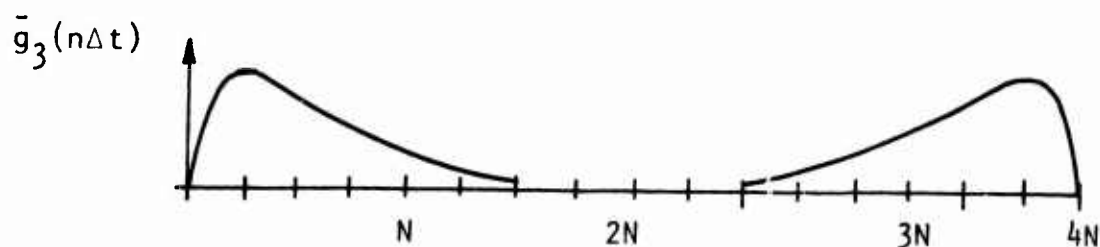
Note that the resultant time domain data are symmetric about the midpoint of the interval in a manner similar to the frequency domain data. Also note that the resultant time domain data are one half the magnitude of the original function and that $\bar{g}_1(n\Delta t)$ is aliased in the time domain. Now assume one adds N zeros to the two original functions and repeats the transform and its inverse. The resulting waveforms are sketched below.



In this case, aliasing of $\bar{g}_1(n\Delta t)$ is eliminated and the amplitudes are correct. Now assume one multiplies the transforms $\bar{g}_1(n\Delta t)$ and $\bar{g}_2(n\Delta t)$ defined over an interval $2N$ and then computes the inverse transform of the product. This procedure is equivalent to convolving $g_1(t)$ and $g_2(t)$ to yield $g_3(t)$. The result obtained by the above procedure, $\bar{g}_3(n\Delta t)$, is sketched below.



Note that the resultant convolution is aliased. Now assume one adds sufficient zeros to $g_1(n\Delta t)$ and $g_2(n\Delta t)$ such that these functions are defined over an interval of size $4N$. Then repeating the transform, product, and inverse transform process as described above, one obtains the convolution sketched below.



In this case, the resultant time domain data are not aliased. However, the amplitude is a factor of two too large. The above example can be generalized. Assume one has two time domain sequences of length M and N and one wants to affect their convolution using the FFT. To avoid aliasing, one must first add sufficient zeros to each sequence such that the total length is $2(M+N)$. Then the transform, product, and inverse transform procedure is performed. If the resulting function is divided by two, then the correct result will be obtained.

3.5.3.6 Comparison of the FIT and the FFT

The FFT and the FIT are both acceptable transforms to use for the analysis of EMP data. The choice of one transform versus another depends on three factors which the user must evaluate for his particular case. One factor is availability. It is expedient to use existing computer codes rather than write new software. The second factor is ease of understanding. Most engineers find the FIT easier to understand than the FFT. Therefore, there is a higher probability that the FIT will be used properly. The final factor is economy. The FFT runs considerably faster than the DFT for the same number of samples. The following table compares central processor running time on a CDC 6600 for the two transforms.

TABLE 3-5
COMPARISON OF RUNNING TIME OF THE FIT AND THE FFT

NUMBER OF POINTS	RUNNING TIME (SECONDS)	
	FIT	FFT
256	7.778	0.040
512	30.965	0.085
1024	122.966	0.176

It should be noted that in practical applications, the running time advantage of the FFT over the FIT is not likely to be as great as that shown above. The reason is that fewer points are required to characterize a waveform with unequally spaced points. Therefore, the FIT will use, in general, fewer points than the FFT which requires equally spaced points.

3.5.4 Truncation Errors

3.5.4.1 Introduction

So called truncation error results in a Fourier transform whenever an incomplete or truncated time function is used in the transform. As discussed in Paragraph 3.2.3 (Time Tying), truncated EMP transient waveforms result when only the early portion of a total response waveform is recorded on the oscillograph. This partial recording technique is necessary to expand the early portion of the response to obtain sufficient oscillograph resolution of high frequency data which often occur in the initial portion of the response.

As indicated in Paragraph 3.2.3, time tying of waveforms is the ideal method of eliminating undesired truncation effects in transforms. However, it was also indicated that time tying techniques are not widely used because of apparent implementation difficulties. Therefore, truncated time waveforms are often used in EMP data analysis.

3.5.4.2 Manifestation of Error in the Frequency Domain

In the material that follows, the effect of truncation on transforms will be considered in some detail and techniques to minimize the effects without using time tying will also be considered.

For casual time functions, the FIT has been defined as (Equation 3-19)

$$G(\omega) = \int_0^{\infty} g(t)e^{-j\omega t} dt \quad (\text{Eq. 3-352})$$

If $g(t)$ is truncated, then Equation 3-352 becomes

$$\bar{G}(\omega) = \int_0^T g(t) e^{-j\omega t} dt \quad (\text{Eq. 3-353})$$

where truncation of $g(t)$ is assumed to occur at $t = T$. The effect of truncation on a Fourier transform can be conveniently analyzed by recognizing that truncation of $g(t)$ is mathematically equivalent to multiplying $g(t)$ by a rectangular function of unit amplitude and range $t = 0$ to $t = T$. A function which closely resembles this rectangular function has been previously defined in Equation 3-77 as

$$\begin{aligned} \text{Rect}_T(t) &= 1, & |t| < T/2 \\ &= 0, & |t| > T/2 \end{aligned} \quad (\text{Eq. 3-354})$$

Note that $\text{Rect}_T(t)$ is not exactly what is needed since it is centered on the origin. However, it can be conveniently shifted to the right by $T/2$,

$$\begin{aligned} \text{Rect}_T(t - T/2) &= 1, & 0 < t < T \\ &= 0, & t < 0 \text{ and } t > T \end{aligned} \quad (\text{Eq. 3-355})$$

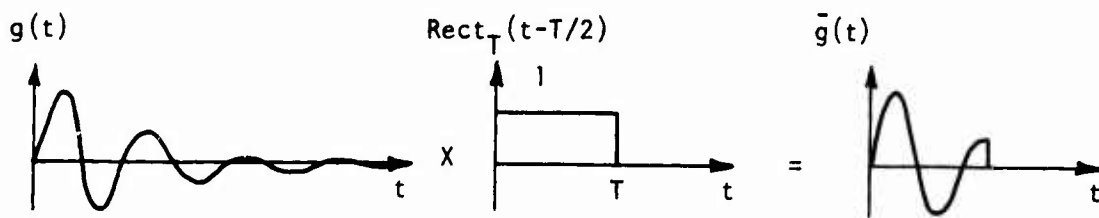
The transform pair for $\text{Rect}_T(t)$ is given in Equation 3-85 as

$$\text{Rect}_T(t) \leftrightarrow T \text{ Sinc}(fT) \quad (\text{Eq. 3-356})$$

The shift to the right of $T/2$ modifies the transform pair as follows.

$$\text{Rect}_T(t - T/2) \leftrightarrow e^{-j\omega T/2} T \text{ Sinc}(fT) \quad (\text{Eq. 3-357})$$

The effect of multiplying $g(t)$ and $\text{Rect}_T(t - T/2)$ is shown below.



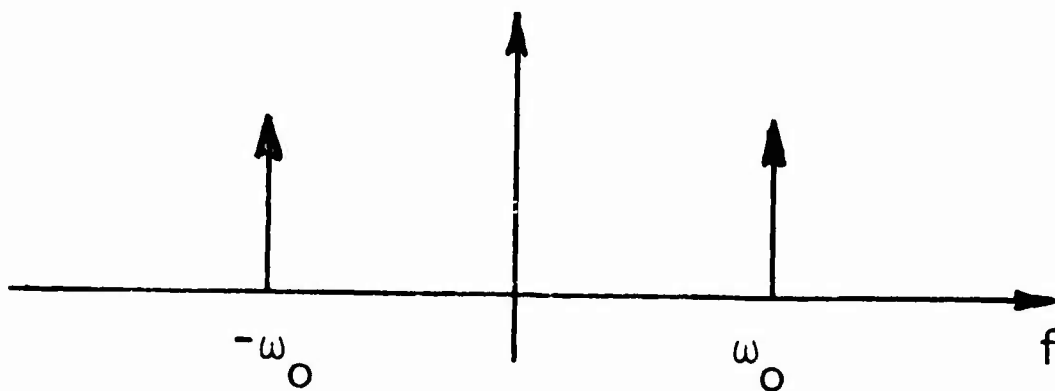
Next, if one recognizes that multiplication of two functions in the time domain results in the convolution of the transforms in the frequency (see Equation 3-184 and 3-185), the following relationship can be written

$$g(t) \cdot \text{Rect}_T(t - T/2) \leftrightarrow G(\omega) * e^{-j\omega T/2} T \text{ Sinc}(fT) \quad (\text{Eq. 3-358})$$

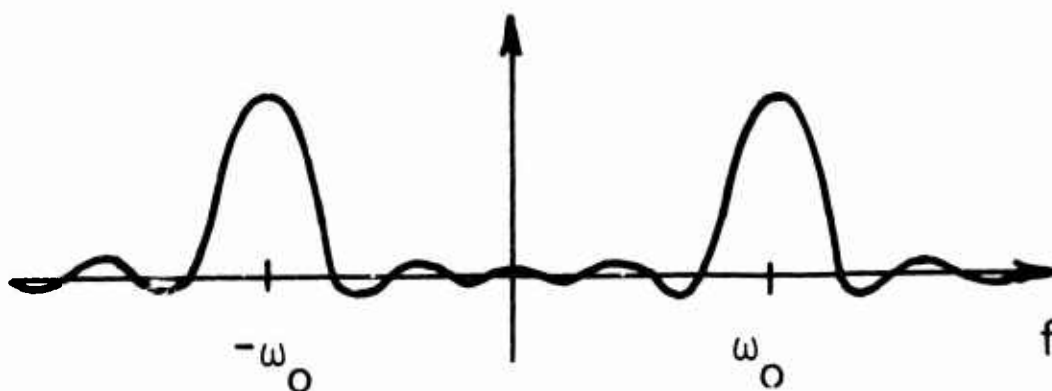
Therefore, any time a time function is truncated, its transform is convolved with a Sinc function.

At this point in the analysis difficulties arise. Unless $g(t)$ (and hence $G(\omega)$) is known in closed form, the convolution cannot be computed. Also if $G(\omega)$ is mathematically complicated, the convolution may be very difficult to perform. One can, however, analyze the general effects of the truncation by considering certain properties of convolution and the Sinc function.

First, the convolution of any two functions tends to have a smearing effect on the result. As a very simple example, assume $G(\omega)$ is the transform of a pure sinusoid (i.e., two impulses).



Then convolving $G(\omega)$ with $T \text{Sinc}(fT)$ results in



Thus, if $G(\omega)$ has resonant peaks, which is characteristic of EMP response data, these peaks will be smeared or broadened if $g(t)$ is truncated.

The amount of smearing or broadening is a function of how severely $g(t)$ is truncated. For example, as $T \rightarrow \infty$ in $\text{Rect}_T(t)$, then $\text{Sinc}(fT)$ approaches a delta function, and there is no error in $G(\omega)$. This is, of course, expected since $T \rightarrow \infty$ implies no truncation. On the other hand, as $T \rightarrow 0$ in $\text{Rect}_T(t)$, then $T \text{Sinc}(fT)$ broadens with its first zeros approaching infinity, and severe smearing occurs.

A second viewpoint for considering the effects of truncation is to look at a specific function such as the double exponential, which is characteristic of the EMP simulator forcing function.

$$g(t) = e^{-\alpha t} - e^{-\beta t}, \quad t \geq 0 \quad (\text{Eq. 3-359})$$

Rather than performing the frequency domain convolution of $G(\omega)$ and $T e^{-j\omega T/2} \text{Sinc}(fT)$, the effects of truncation can be more conveniently handled by evaluating the Fourier integral between limits of $t = 0$ and $t = T$ (see Equation 3-353). First, the transform of the double exponential is repeated (see Equations 3-72 and 3-73) so that it can be used for comparison.

$$\begin{aligned} e^{-\alpha t} - e^{-\beta t} &\leftrightarrow \frac{1}{\alpha + j\omega} - \frac{1}{\beta + j\omega} \\ &\leftrightarrow \frac{\beta - \alpha}{(\alpha + j\omega)(\beta + j\omega)} \end{aligned} \quad (\text{Eq. 3-360})$$

Now the truncated function is evaluated as,

$$\int_0^T (e^{-\alpha t} - e^{-\beta t}) e^{-j\omega t} dt = \frac{1}{\alpha + j\omega} e^{-(\alpha + j\omega)t} \Big|_0^T - \frac{1}{\beta + j\omega} e^{-(\beta + j\omega)t} \Big|_0^T$$

$$= \frac{1}{\alpha + j\omega} - \frac{1}{\beta + j\omega} - \frac{e^{-(\alpha + j\omega)T}}{\alpha + j\omega} + \frac{e^{-(\beta + j\omega)T}}{\beta + j\omega}$$

(Eq. 3-361)

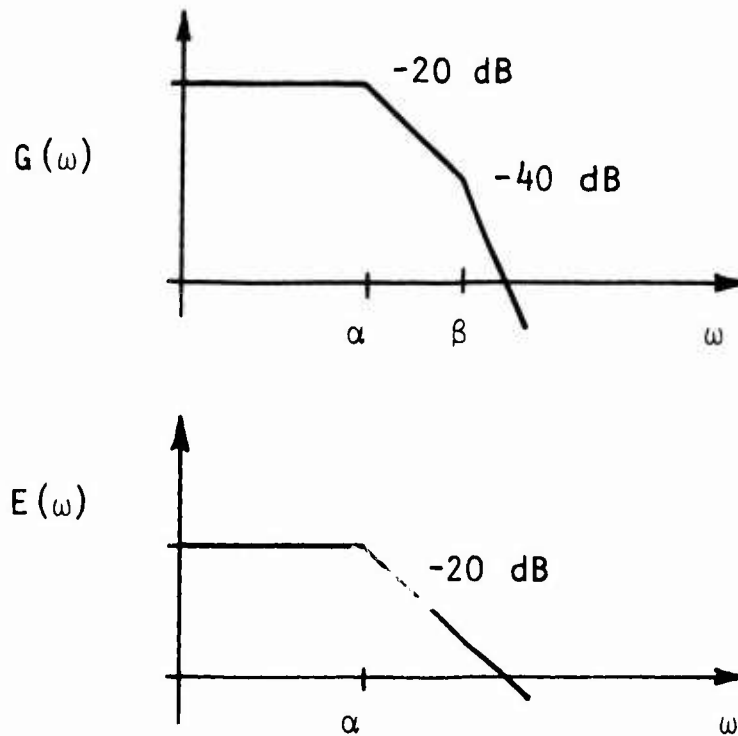
As is common in EMP functions, $\beta \gg \alpha$. Therefore, Equation 3-361 can be simplified to

$$\bar{G}(\omega) = \frac{\beta - \alpha}{(\alpha + j\omega)(\beta + j\omega)} - \frac{e^{-(\alpha + j\omega)T}}{(\alpha + j\omega)}, \quad (\text{Eq. 3-362})$$

where: $\frac{\beta - \alpha}{(\alpha + j\omega)(\beta + j\omega)} = G(\omega)$, the untruncated function

$$\frac{e^{-(\alpha + j\omega)T}}{(\alpha + j\omega)} = E(\omega), \text{ the truncation error function.}$$

It can be seen that the untruncated function $G(\omega)$ rolls off at 40 dB/decade, whereas the error term, $E(\omega)$ rolls off at only 20 dB/decade.



The effect of the error term $E(\omega)$ is to cause $G(\omega)$ to roll off at -20 dB/decade instead of -40 dB/decade. This can be seen by modifying Equation 3-362 as follows

$$\bar{G}(\omega) = \frac{1}{\alpha + j\omega} \left\{ \frac{\beta - \alpha}{\beta + j\omega} - e^{-\alpha T} e^{-j\omega T} \right\} \quad (\text{Eq. 3-363})$$

The $\frac{1}{\alpha + j\omega}$ term causes a -20 dB/decade roll-off. The first term in the brackets would tend to cause $\bar{G}(\omega)$ to roll off at -40 dB/decade after $\omega > \beta$. However, the second term in the brackets becomes predominant for large values of ω and causes the total expression to roll off at -20 dB/decade. The exact point at which this occurs is dependent on the values of α , β , and T .

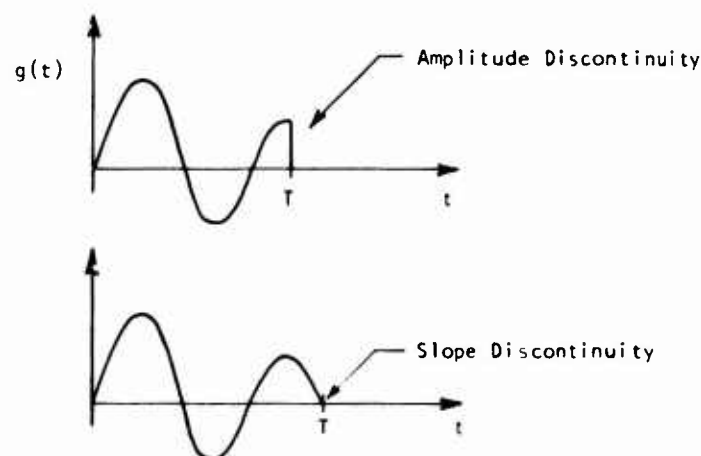
This decrease in roll-off rate by -20 dB/decade is characteristic of truncation which causes amplitude discontinuity* in

* See Paragraph 3.3.3.5 for a thorough discussion of discontinuities on transforms.

$g(t)$ which is the case for the double exponential function. Now consider a function which can be truncated such that there is either an amplitude discontinuity or slope discontinuity when truncated. Such a function is the damped sinusoid,

$$g(t) = e^{-\alpha t} \sin \beta t \quad (\text{Eq. 3-364})$$

The following two plots illustrate first how amplitude discontinuity and slope discontinuity occur depending on the truncation point.



The Fourier transforms for the amplitude and slope discontinuous damped sinusoid are shown in Figures 3-17 and 3-18 respectively. Each overlays the transform of the untruncated function. Note that in the case of the amplitude discontinuous function, the transform rolls off at a slower rate (-20 dB/decade as opposed to -40 dB/decade) than the true transform. In the case of slope discontinuity, the roll-off rate is unaffected. This suggests that if truncation must occur, less error will result in the transform if the truncation causes only slope discontinuity in the time function.

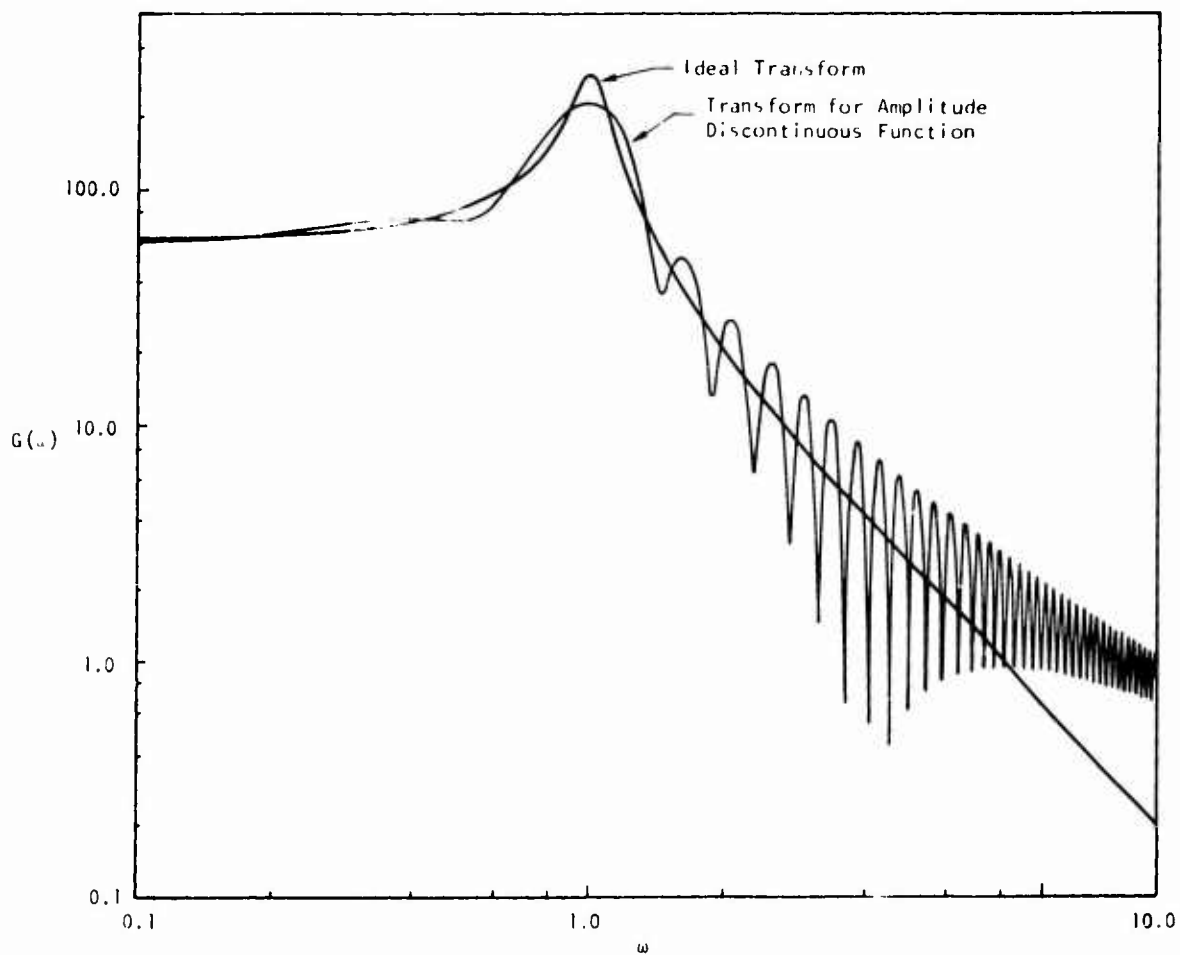


Figure 3-17. Fourier Transforms for Ideal $g(t)$ and Amplitude Truncated $g(t)$

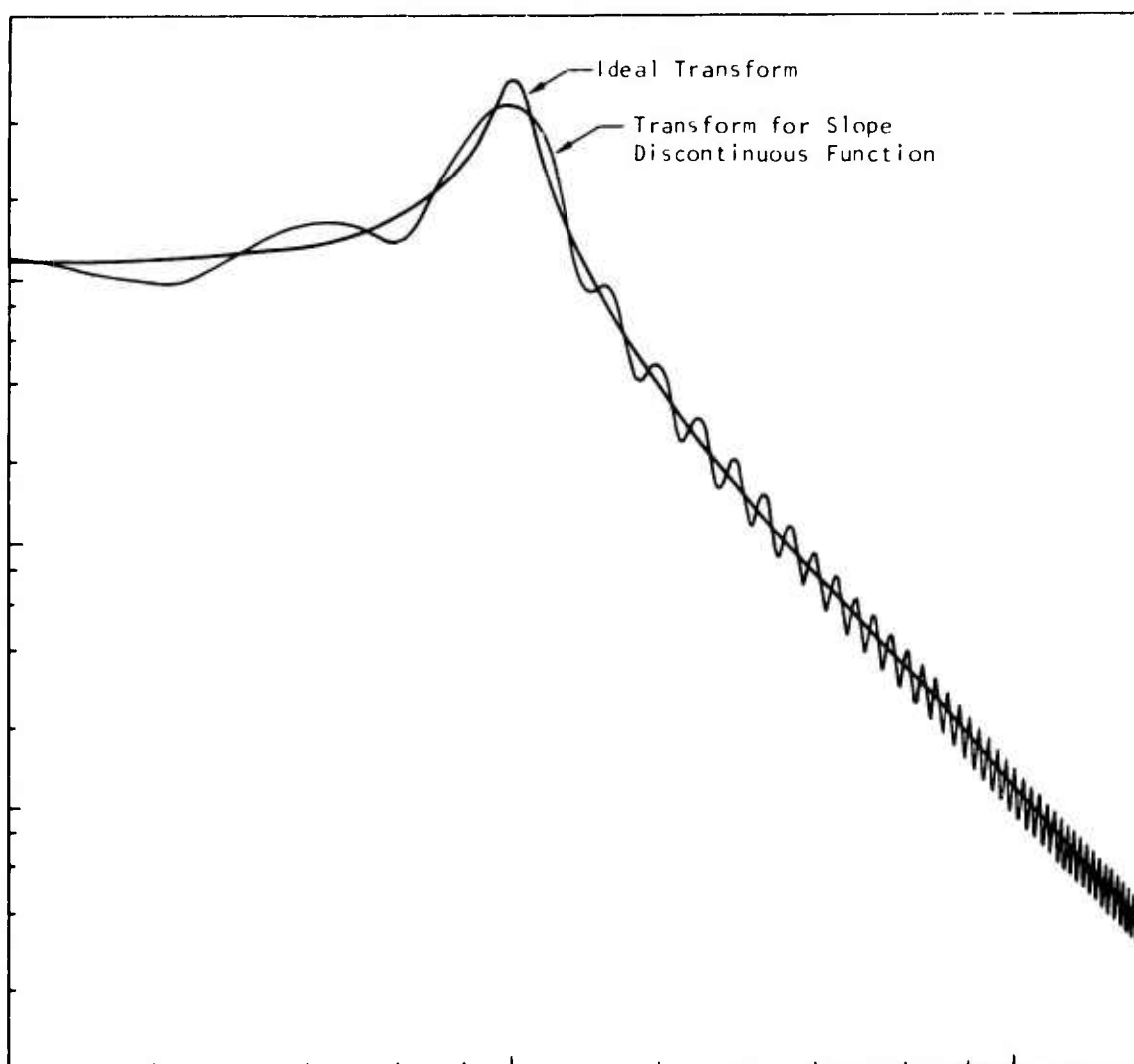


Figure 3-18. Fourier Transforms for Ideal $g(t)$ and Slope Discontinuous $g(t)$

Note also the ripple in the transforms. This is characteristic in transforms of truncated functions. Referring back to Equation 3-363, one can see how ripple would result in the transform of the truncated double exponential function. The second term in the brackets contains a multiplicative factor of $e^{-j\omega T}$. This factor can be expressed as

$$e^{-j\omega T} = \cos\omega T + j \sin\omega T \quad (\text{Eq. 3-365})$$

which explains the oscillatory nature of the transform.

The characteristic ripple in the transforms of Figures 3-17 and 3-18 is caused by the same type of terms in the transform equation of the truncated damped sinusoid. This equation is given below without derivation.

$$\bar{G}(\omega) = \frac{\beta}{(\alpha + j\omega)^2 + \beta^2} \left\{ 1 + \left(\frac{\alpha e^{-\alpha T} \sin\beta T}{\beta} \right) e^{-j\omega T} + \right. \\ \left. \left(\frac{j e^{-\alpha T} \sin\beta T}{\beta} \right) e^{-j\omega T} - \left(j e^{-\alpha T} \cos\beta T \right) e^{-j\omega T} \right\} \quad (\text{Eq. 3-366})$$

Note also from Figures 3-17 and 3-18 that the ripple is much less severe for slope discontinuity. This further suggests that if truncation must occur, slope discontinuity causes less error in the transform than amplitude discontinuity. The point at which truncation occurs can be controlled in the digitizing process.

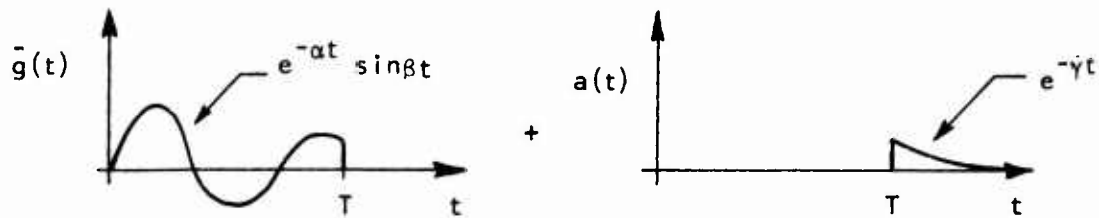
3.5.4.3 Methods for Minimizing Errors

Now, what can be done to minimize truncation effects beyond time tying or selection of the truncation point to force only slope discontinuity? Two techniques have been tried with some success. The first technique amounts to artificially extending the truncated time function $\bar{g}(t)$. The second amounts to passing $\bar{g}(t)$ through a window or filter. Note that the general effect of truncation is to create a time function with higher frequency information than the untruncated time function. The effect of a given type of truncation (amplitude, slope, second derivative) can be formally stated as follows: If the M th derivative of $g(t)$ is impulsive, then its transform $G(\omega)$ dies away as f^{-M} . In the case of amplitude discontinuity, the first derivative of $\bar{g}(t)$ is impulsive and therefore $\bar{G}(\omega)$ dies away as $1/f$. For slope discontinuity, the second derivative is impulse, and thus $\bar{G}(\omega)$ dies away as $1/f^2$.

The first technique for reducing truncation effects, artificial extension of $\bar{g}(t)$, works only for amplitude discontinuities. It is typical to assume that $g(t)$, the EMP response waveform, has the form of the sum of damped sinusoids

$$g(t) = \sum_{i=0}^n e^{-\alpha_i t} \sin(\beta_i + \phi_i)t \quad (\text{Eq. 3-367})$$

One could attempt to somehow estimate the values of α_i , β_i , and ϕ_i and extend the truncated function based on these parameters. However, such estimation tends to be a very complex and time consuming problem. The most common approach to artificial extension is to use an exponential function which will be denoted $a(t)$.



Extending $\bar{g}(t)$ with the exponential eliminates the amplitude discontinuity. However, a slope discontinuity can result. The slope discontinuity can also be eliminated if the slope of $a(t)$ is forced to equal that of $\bar{g}(t)$ at the tie point. The slope of $a(t)$ at its initial value is

$$\left. \frac{da(t)}{dt} \right|_{t=0} = \left. \frac{d e^{-\gamma t}}{dt} \right|_{t=0} = -\gamma \quad (\text{Eq. 3-368})$$

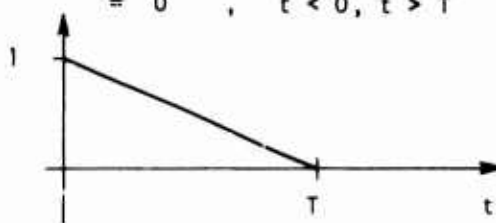
If $\bar{g}(t)$ is truncated so that its slope at $t = T$ is close to zero, then γ for $a(t)$ must be chosen very near zero to effect a slope match. However, when γ is close to zero, the exponential decays very slowly and $\bar{g}(t) + a(t)$ must be allowed to extend a significant length beyond $t = T$ if truncation is not to occur again. Therefore, it is desirable to have the slope of $\bar{g}(t)$ at $t = T$ somewhere on the order of -1 which should keep the artificial extension from becoming too long.

One must keep in mind that any type of artificial extension of $\bar{g}(t)$ adds information to $\bar{g}(t)$ which may be quite different from the information in $g(t)$ which has been lost. Therefore, artificial extension does not in any way guarantee that $\bar{g}(t)$ extended is closer to $g(t)$ than $\bar{g}(t)$. The only guarantee is that extension will help minimize truncation effects.

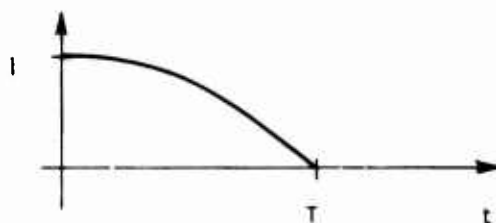
The second technique for minimizing truncation errors is to pass the truncated time function through a special window. By

passing $\bar{g}(t)$ through a special window, it is meant that $\bar{g}(t)$ is multiplied by a function ($W(t)$) which tends to minimize the truncation effects in the transform. Several such functions have been evaluated. Each function has the same general characteristics (i.e., at $t = 0$, $W(t) = 1$, and at $t = T$, $W(t) = 0$). Examples of such functions are:

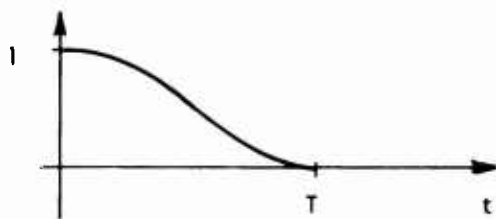
$$(1) \quad W(t) = 1 - t/T, \quad 0 \leq t \leq T \\ = 0, \quad t < 0, t > T$$



$$(2) \quad W(t) = \cos\left(\frac{\pi t}{2T}\right), \quad 0 \leq t \leq T \\ = 0, \quad t < 0, t > T$$



$$(3) \quad W(t) = \frac{1}{2} \left[1 + \cos\left(\frac{\pi t}{T}\right) \right], \quad 0 \leq t \leq T \\ = 0, \quad t < 0, t > T$$



Experimental results for the application of windows (1) and (3) are shown in Figures 3-19 and 3-20 respectively. For each case, the upper curves show the window shape and $\bar{g}(t)$ after it was passed through the window. The lower curves show the resulting transform compared with the transform of $g(t)$, the untruncated function. Of all windows evaluated in this experiment, the window defined in (1) tended to give the best results. "Best" is defined as most closely matching the true transform. All windows tended to decrease the amplitude of the transform at the resonant peak (i.e., $g(t) = e^{-\alpha t} \sin \beta t$). Again, the least decrease in this peak resulted from the use of window (1). The evaluation of such windows is still in the experimental stages. What is needed for their practical use is relationships which predict how much spectral peaks or resonances are decreased when $\bar{g}(t)$ is passed through a given window type. If experimentation continues to show promise, this method of minimizing truncation effects represents a very simple, practical method.

3.5.5 Numerical Integration

There are occasions where derivative type data are recorded directly on an oscilloscope. This direct recording is the only alternative when the signal amplitude is low. Another case occurs when the voltage across a capacitive type element is desired and the current through the element is monitored and recorded. In either case, the derivative data are digitized and integrated by some digital computer technique. A large list of pitfalls exist when using these numerical techniques. The following subsections describe two of the more common errors when using numerical integration techniques.

3.5.5.1 Time Domain Integration

A straightforward means of integrating transient data recorded on Polaroid film records is to digitize the analog trace and operate on the digital coordinate pairs in the time domain with some

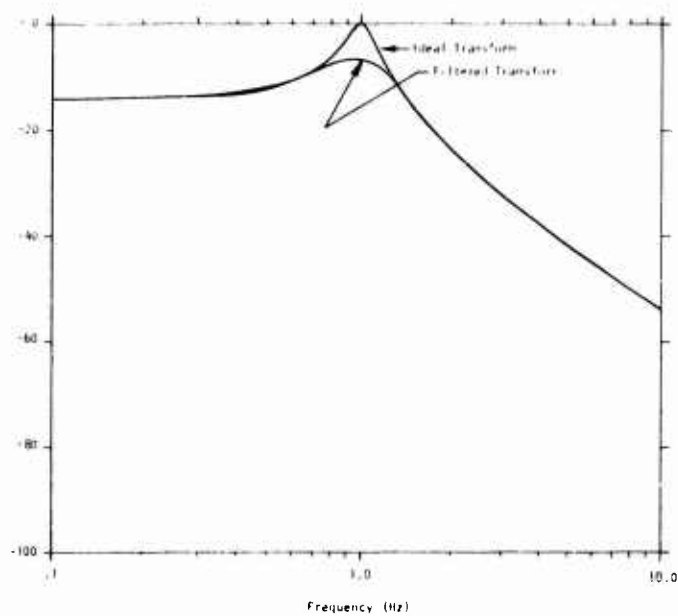
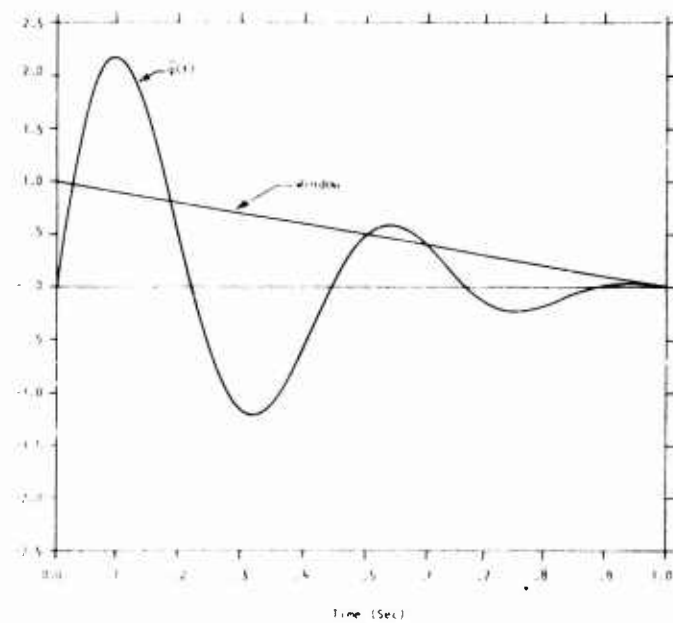


Figure 3-19. Illustration of Time Window Technique for Truncation Error Reduction Using Window Shape (1)

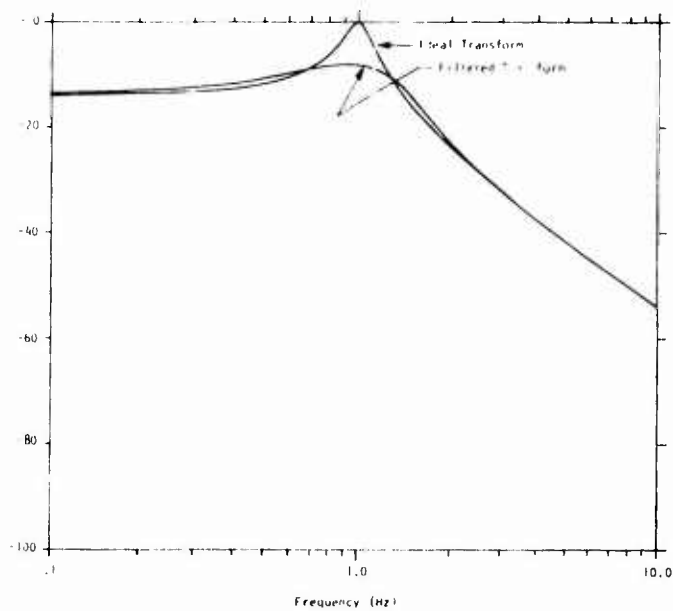
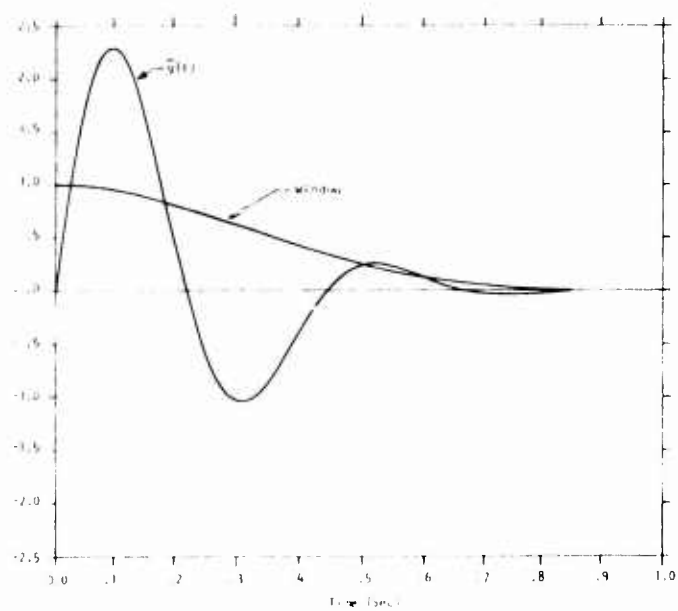


Figure 3-20. Illustration of Time Window Technique for Truncation Error Reduction Using Window Shape (3)

integration algorithm. The resultant accuracy depends on factors such as the particular algorithm employed and the digitizing process. Proper selection of an integration algorithm is widely discussed in standard references on numerical analysis and will not be repeated here. The sensitivity of any integration technique to certain small systematic errors in the digitization process is not widely appreciated, and this topic will be discussed in the following paragraphs. Also discussed is a means of minimizing these error contributions to the integrated data.

Any digitization process converts a recording of the analog waveform into a series of coordinate pairs based on the coordinate system of the instrument. These coordinate pairs are calibrated by digitizing additional points to define the coordinate system of the analog waveform relative to the coordinates of the digitizer. The calibration data are used to scale the amplitude and time axes, to locate the coordinate system origin, and to define the rotation angle of the analog record coordinate system relative to that of the digitizer reference plane or working surface.

Small errors in calibration occur even when using the best procedures and equipment. These errors are primarily due to the limited quality of the analog data record. The finite trace width of both the waveform and the gridlines cause uncertainty in defining the precise coordinates of the data. Additional difficulties in defining precisely the data coordinates are due to the limited writing speed of the oscilloscope, poorly developed film resulting in low or uneven contrast, poor or uneven illumination of the gridlines, and the inability to distinguish waveform, gridline, and calibration pulse data in the neighborhood where these traces intersect.

The impact of these small errors depends on the application of the calibration data. Errors in scaling result in the same relative error for both the original and the integrated waveforms.

On the other hand, small errors in defining the rotation angle or the zero amplitude baseline result in relatively large errors in the integrated waveforms.

The impact of small errors in rotation angle or in the baseline will be demonstrated in the following example. The resultant waveform consisting of a derivative signal, $f'(t)$, with baseline offset and rotation angle errors is expressed as

$$f'_{R}(t) = f'(t) + \epsilon_a + \frac{\epsilon_b}{T} t \quad (\text{Eq. 3-369})$$

where T is the duration of the analog data record. Consider two representative examples of $f'(t)$, namely

$$f'_{I}(t) = \frac{d}{dt} (e^{-\alpha t} - e^{-\beta t}) \quad (\text{Eq. 3-370})$$

$$f'_{II}(t) = \frac{d}{dt} (e^{-\gamma t} \sin \delta t) .$$

It is realistic to assume that the error terms, ϵ_a and ϵ_b , will equal a given percentage of the full scale deflection of the record of Equation . An extremely small estimate for both these error terms is 1/2 percent of the peak deflection. Therefore, the resultant derivative waveform for the two examples becomes

$$f'_{RI}(t) = \frac{d}{dt} (e^{-\alpha t} - e^{-\beta t}) + .005(\beta - \alpha)(1 + t/T) \quad (\text{Eq. 3-371})$$

$$f'_{RII}(t) = \frac{d}{dt} e^{-\gamma t} \sin \delta t + .005 \delta (1 + t/T) .$$

Upon integration, these equations become

$$f_{RI}(t) = (e^{-\alpha t} - e^{-\beta t}) + .005 (\beta - \alpha) (t + t^2/2T)$$

(Eq. 3-372)

$$f_{RII}(t) = e^{-\gamma t} \sin \delta t + .005 \delta (t + t^2/2T)$$

Plots of Equation 3-372 for representative values of α , β , γ , and δ are shown in Figure 3-21. Note the divergent character of the resultant waveform at late times. Also, note that errors in the derivative data equaling 1/2 percent of peak can result in integrated results with error terms exceeding 100 percent of the peak of the true signal.

The detection of these offset and rotation angle errors is a prerequisite to any corrective procedure. The detection is best done by inspecting the integrated time domain waveforms since the presence of the small errors may not be evident in the derivative data record. Transient waveforms encountered in EMP tests eventually decay to zero amplitude at late times. Therefore, the detection of a late time divergent trend in the data is an indication of the existence of baseline offset or rotation angle errors. This observation can be confirmed, at times, by the inspection of a Fourier transform of the derivative data. The Fourier transform of the dc offset and ramp type errors over the time from 0 to T are given by

$$F\{\epsilon_a\} = \epsilon_a T \left[\frac{\sin \omega T/2}{\omega T/2} \right] e^{-j\omega T/2}$$

(Eq. 3-373)

$$F\left\{\frac{\epsilon_b}{T} t\right\} = \frac{\epsilon_b}{\omega} \left[\frac{\sin \omega T/2}{\omega T/2} - e^{-j\omega T/2} \right] e^{-j(\omega T/2 + \pi/2)}$$

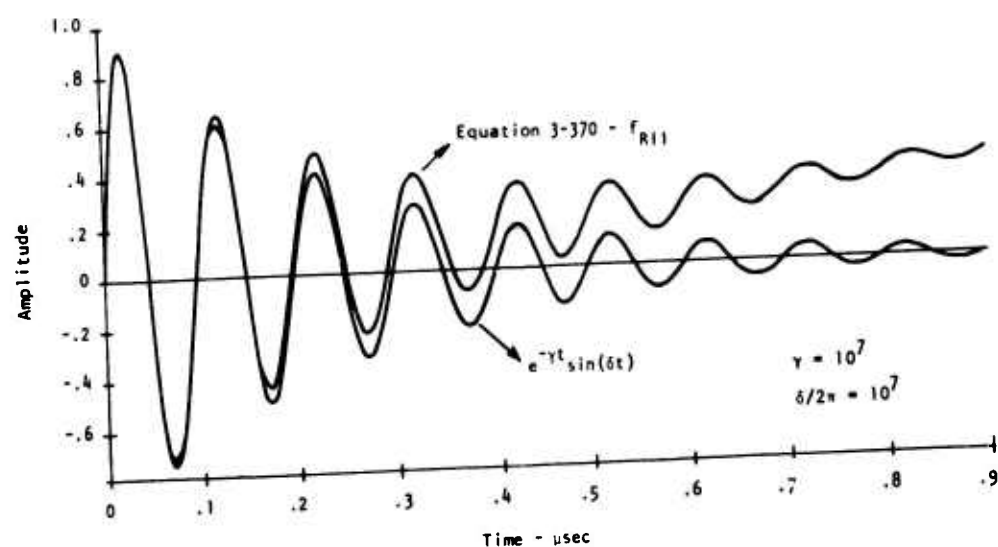
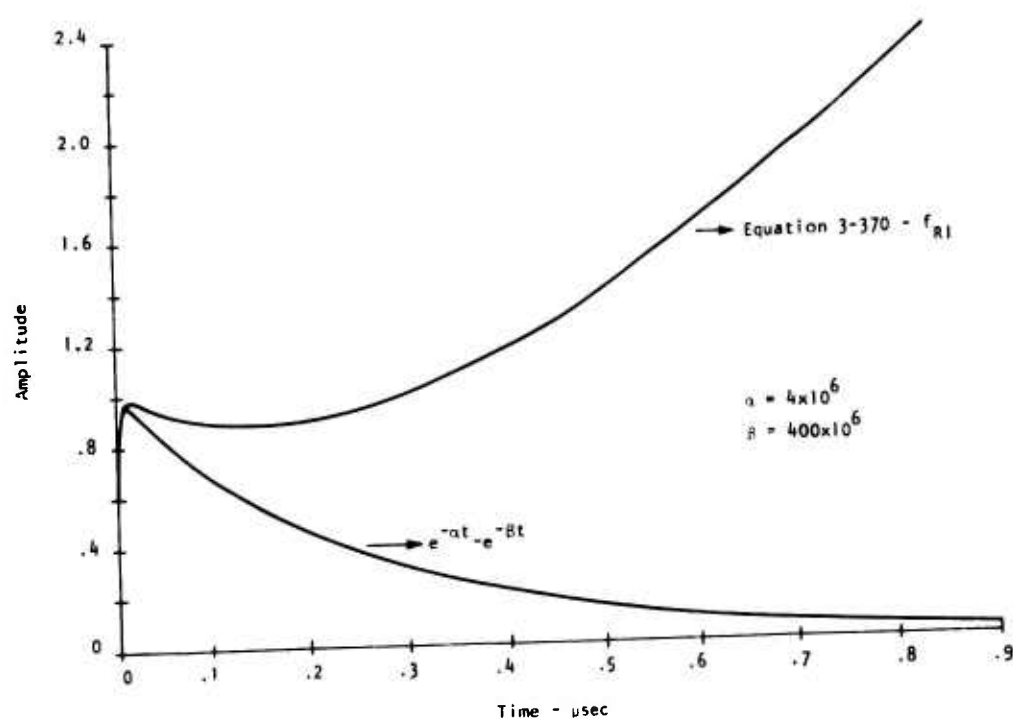


Figure 3-21. Integral of Typical Derivative Waveforms with Ramp and dc Offset Errors

Both of these terms have significant amplitude at low frequencies. Therefore, the existence of excess amplitude or negative slopes in the low frequency portions of a Fourier transform of the derivative data is another indication of these errors. Figures 3-22 and 3-23 show Fourier transforms of the resultant derivative waveforms given by Equation 3-371. Note the excess amplitude and negative slopes at low frequencies as well as the notch and fine structure that almost inevitably accompanies the Fourier transform of the sum of two waveforms (in this case, $f'(t)$ and the error terms).

3.5.5.2 Correction of Time Domain Integration Error

There is no foolproof or complete way of eliminating these error contributions. Therefore, the analyst must use judgment in adjusting and interpreting the data. The first step in a corrective procedure is to redigitize the analog data record if offset or ramp type errors are evident in the digitized derivative data. Since there is a practical limit in the amount this error can be reduced by careful digitization, the analyst must decide whether there are any improvements that can be obtained by this reprocessing. The second step in a corrective procedure is to find some means of treating the digitized data with existing errors.

Simple criteria for correcting the data are based on the observation that the integral of the derivative data record should equal zero at late times. This statement is based on the fact that the physical observable is a transient waveform that decays to zero at late times, and that the recorded data are the derivative of this physical observable. If the integral does not equal zero, then a constant is subtracted from the derivative data such that the integral is identically equal to zero. Let us examine the consequence of applying these criteria to Equation 3-370. The definite integral of Equation 3-369 is

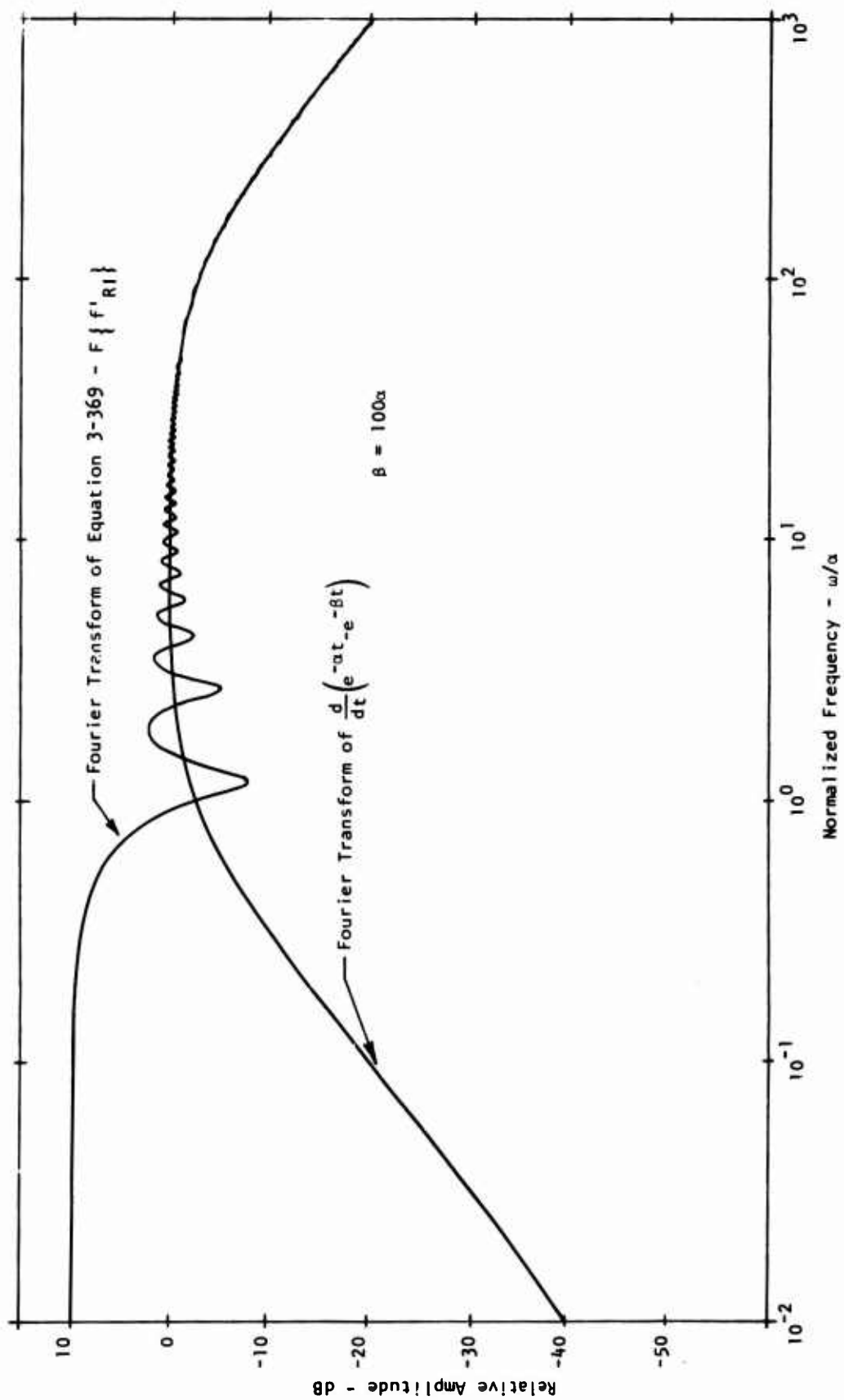


Figure 3-22. Fourier Transform of Derivative of Double Exponential Waveform with Ramp and dc Offset Errors

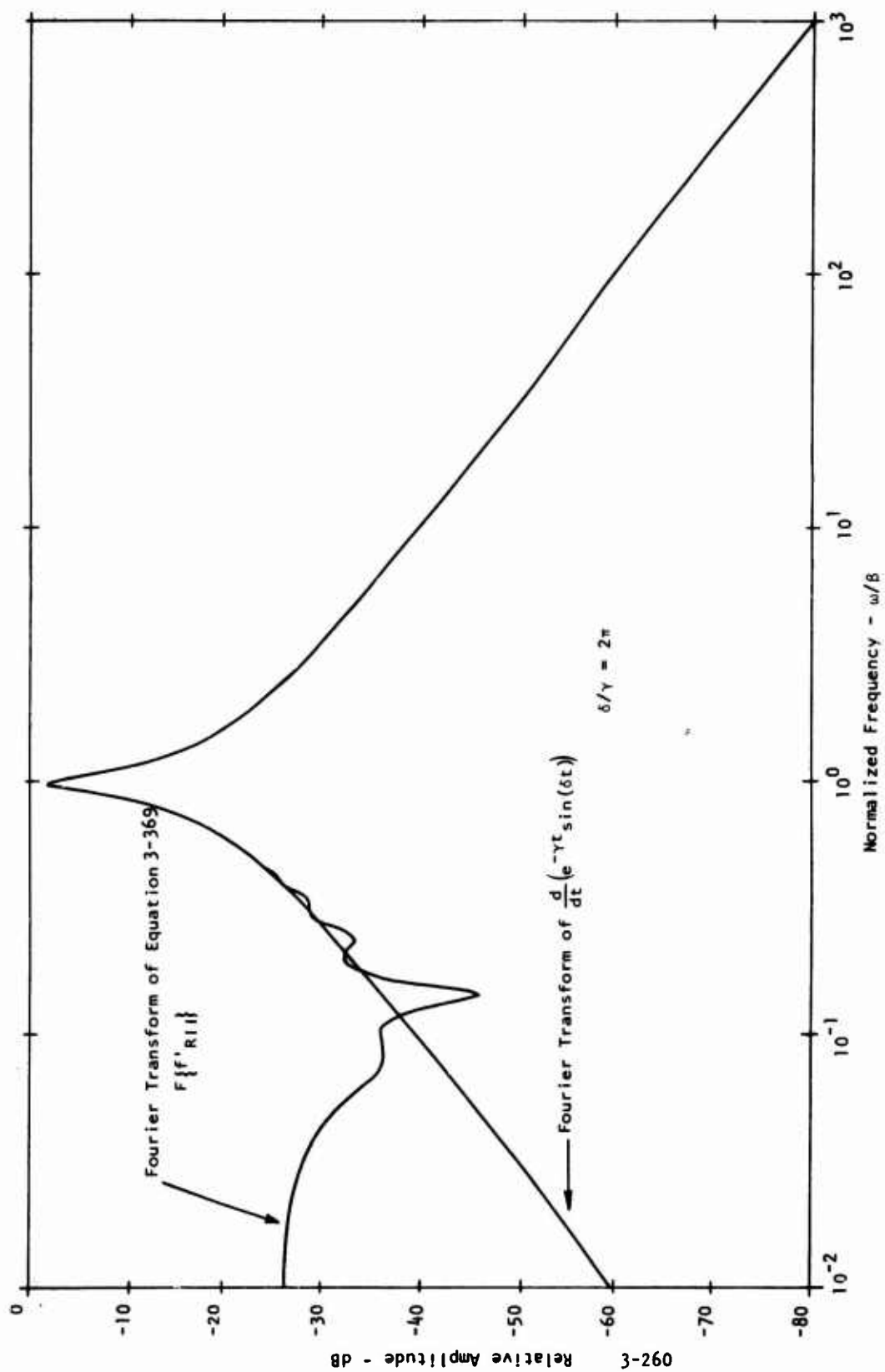


Figure 3-23. Fourier Transform of Derivative of Damped Sinusoid Waveform with Ramp and dc Offset Errors

$$\int_0^T f'_R(t) dt = f(T) - f(0) + (\epsilon_a + \epsilon_b/2)T. \quad (\text{Eq. 3-374})$$

In this case, $f(0) = 0$ since $f'(t)$ has no impulses at the origin. Equating Equation 3-374 to a constant, θ , times the time duration of the data record, we find

$$\theta T = [f(T)/T + \epsilon_a + \epsilon_b/2]T. \quad (\text{Eq. 3-375})$$

If θ is subtracted from Equation 3-369, a corrected data record for the derivative waveform is obtained

$$f'_{RC}(t) = f'(t) - f(T)/T + \epsilon_b (t/T - 1/2) \quad (\text{Eq. 3-376})$$

Integration of Equation 3-374 yields

$$\int_0^T f'_{RC}(t) dt = f(t) - f(T)(t/T) + (\epsilon_b/2) t (t/T - 1). \quad (\text{Eq. 3-377})$$

A plot of Equation 3-377 for the two analytic examples shown in Figure 3-17 is presented in Figure 3-24. Note that the resultant error is reduced considerably, but it is not eliminated. This procedure has been applied to experimental data records. Figure 3-25 shows an example of a numerically integrated waveform before and after applying the correction. Although the true version of this waveform is unknown, the corrected data appear much more credible than the uncorrected version.

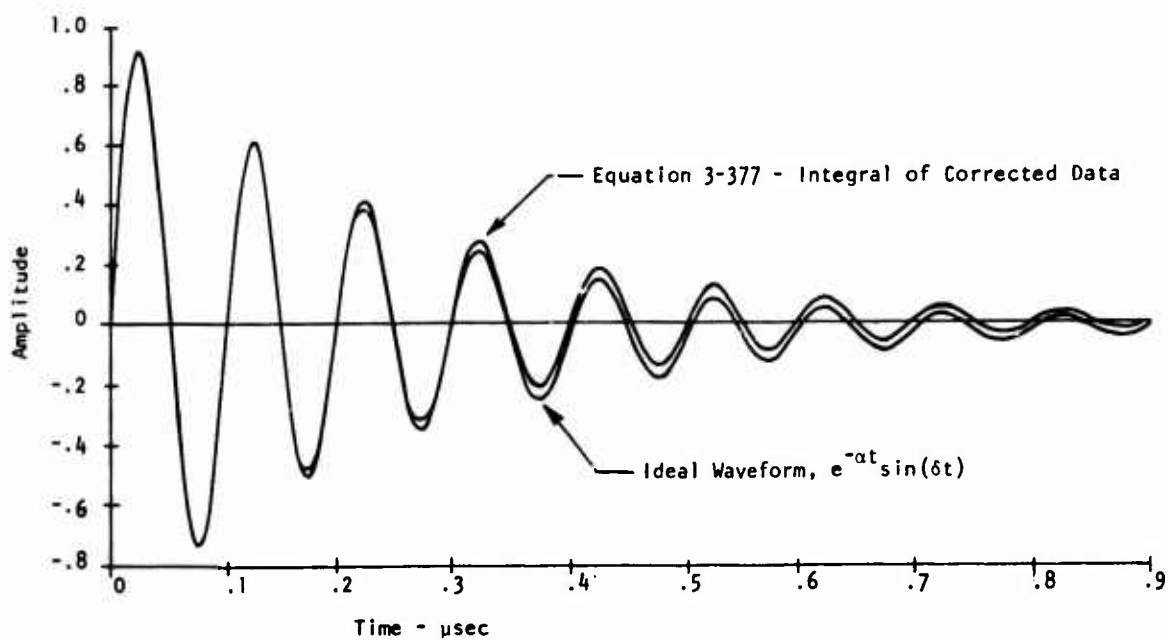
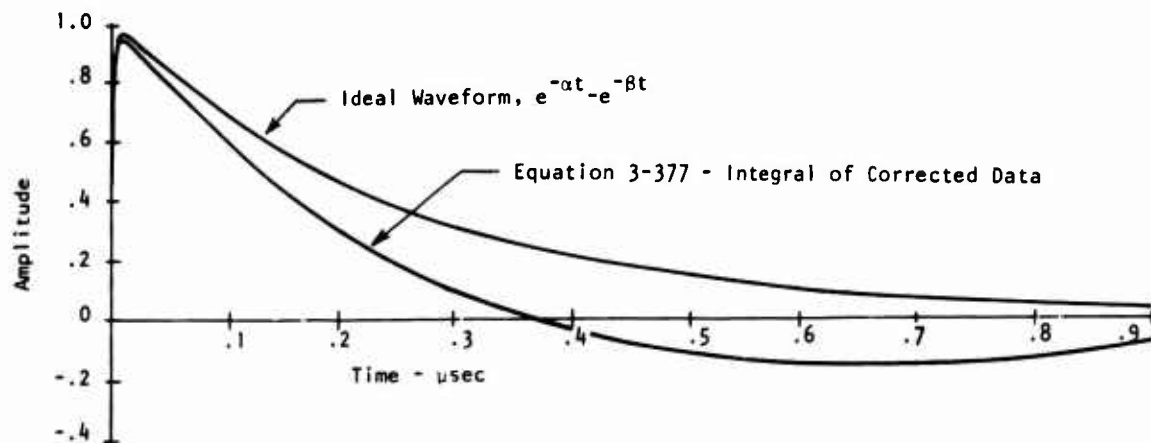


Figure 3-24. Integral of Typical Analytic Derivative Waveforms with Ramp and dc Offset Errors Using Total Area Correction Technique

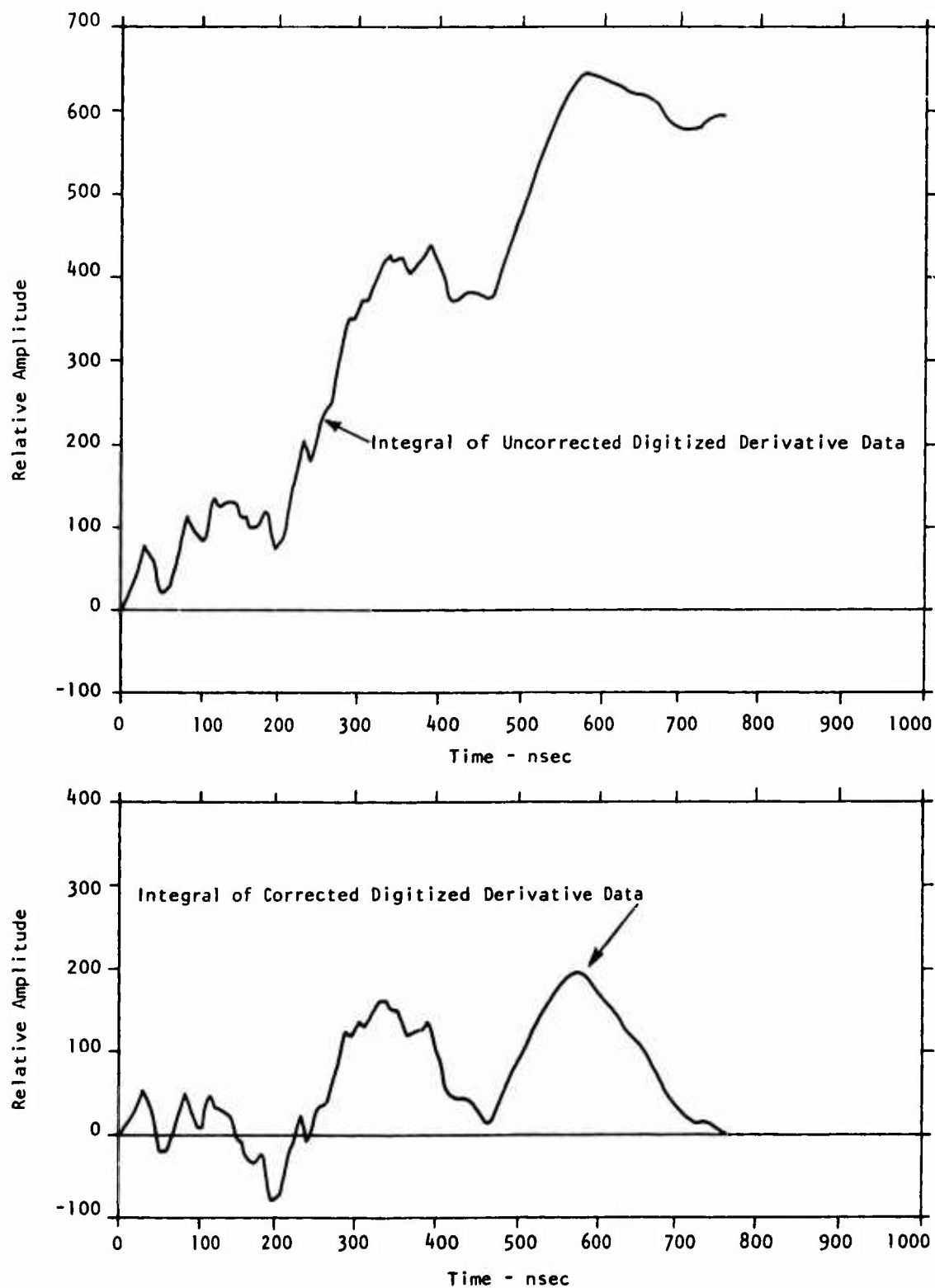


Figure 3-25. Integral of Typical Experimental Derivative Waveform with Ramp and dc Offset Errors With and Without Use of Total Area Correction Technique

There are several observations to be made concerning this error reduction procedure. One is that the contribution of the offset error, ϵ_b , remains. No practical method of eliminating ϵ_b has been demonstrated to date. The second observation is that the data acquisition personnel should strive to record adequate late time data in order to insure that $f(T)$ approaches zero. The term, $f(T)$, is a bias error introduced in the correction procedure. A third observation is that if $f(T)$ is approximately equal to zero, then the maximum error occurs at $T/2$. The error at the beginning and end of the record is zero. The final observation is that the analyst must use some caution and judgment in interpreting the corrected results because of the residual error terms.

3.5.5.3 Frequency Domain Integration

Another method of numerically integrating a derivative data record is by use of Fourier transforms. The common procedure is to obtain a Fourier transform of the derivative data record, multiply this complex array by $(j\omega)^{-1}$, and obtain the inverse transform of the resultant. This procedure is not generally valid. However, use of this invalid procedure can be part of a technique to reduce the effects of offset and ramp type errors previously discussed. The reader is referred to Paragraph 3.3.11.7 for a thorough discussion of the time domain - frequency domain relationships for time domain integration.

3.5.5.4 Correction of Frequency Domain Integration Errors

Now consider the special case where the integral of a derivative is desired

$$f(t) = \int_0^T f'(t) dt \quad (\text{Eq. 3-378})$$

If $f(0+) = 0$, a condition that is always true with practical experimental data, then the Fourier transform of Equation 3-378 is given by

$$F(\omega) = \pi \delta(\omega) j\omega R(0) + j\omega \left[\frac{I(\omega)}{\omega} - j \frac{R(\omega)}{\omega} \right] \quad (\text{Eq. 3-379})$$

$$\equiv F(\omega).$$

The interpretation of this result is that the integral of the derivative response of an experimental transient process can be obtained by dividing the Fourier transform of the derivative data record by $j\omega$ and obtaining the inverse transform. However, if there are error terms corresponding to the Fourier transform of

$$\begin{aligned} E_1(\omega) &= F\left\{\epsilon_a t\right\} \\ E_2(\omega) &= F\left\{\frac{\epsilon_b}{2T} t^2\right\} \end{aligned} \quad (\text{Eq. 3-380})$$

Then their dc contribution to the inverse transform should be considered according to Equation 3-379.

It should be noted that the proper inverse transform of the error terms is not necessarily desired. What is desired is to eliminate all contributions of the error terms to the integrated time domain result. Therefore, elimination of the $R(0)/2$ term in Equation 3-379 will help to reduce the effects of the error since there is no contribution to the separate $R(0)/2$ term from the desired signal. This thinking can be extended by noting that the low frequency portions of Figures 3-22 and 3-23 are primarily the result of the error terms. Therefore, the qualitative conclusion is that the estimate of $f(t)$, $f_e(t)$, would be improved if the low frequency portions of the resultant transform are eliminated. Thus

$$f_e(t) = \frac{1}{\pi} \int_{\omega_c}^{\infty} [F(\omega) + E(\omega)] e^{j\omega t} d\omega \quad (\text{Eq. 3-381})$$

where $E(\omega)$ is the abbreviation for the error terms in Equation 3-379. If the low frequency portions of $F(\omega)$ are small compared to the peak of $F(\omega)$ and negligible compared to $E(\omega)$, then it is possible to select a cutoff frequency, ω_c , such that $f_e(t) \approx f(t)$.

The Fourier transform of the derivative data record used to obtain Figure 3-25 is shown in Figure 3-26. The low frequency error contributions are evident. Choosing $\omega_c/2\pi$ to be 2×10^6 Hz and obtaining the inverse transform results in an estimate of $f(t)$ as shown in Figure 3-27. Compare Figure 3-25 with Figure 3-27. The frequency domain technique results in some improvement over the uncorrected case. Note the frequency domain technique for minimizing errors results in an apparently better looking result in this example. The analyst should consider using both time and frequency domain techniques. Neither is strictly accurate. However, one may be superior to the other in a specific case.

3.5.6 Transfer Function Estimation

3.5.6.1 The Transform Approach

Determination, or more correctly estimation, of transfer functions is a common objective of EMP test data assessment. The use of the transfer function in assessment is covered in general in Subsection 3.1. The material presented in this paragraph covers the subject of how transfer function estimates are made from pulse test data.

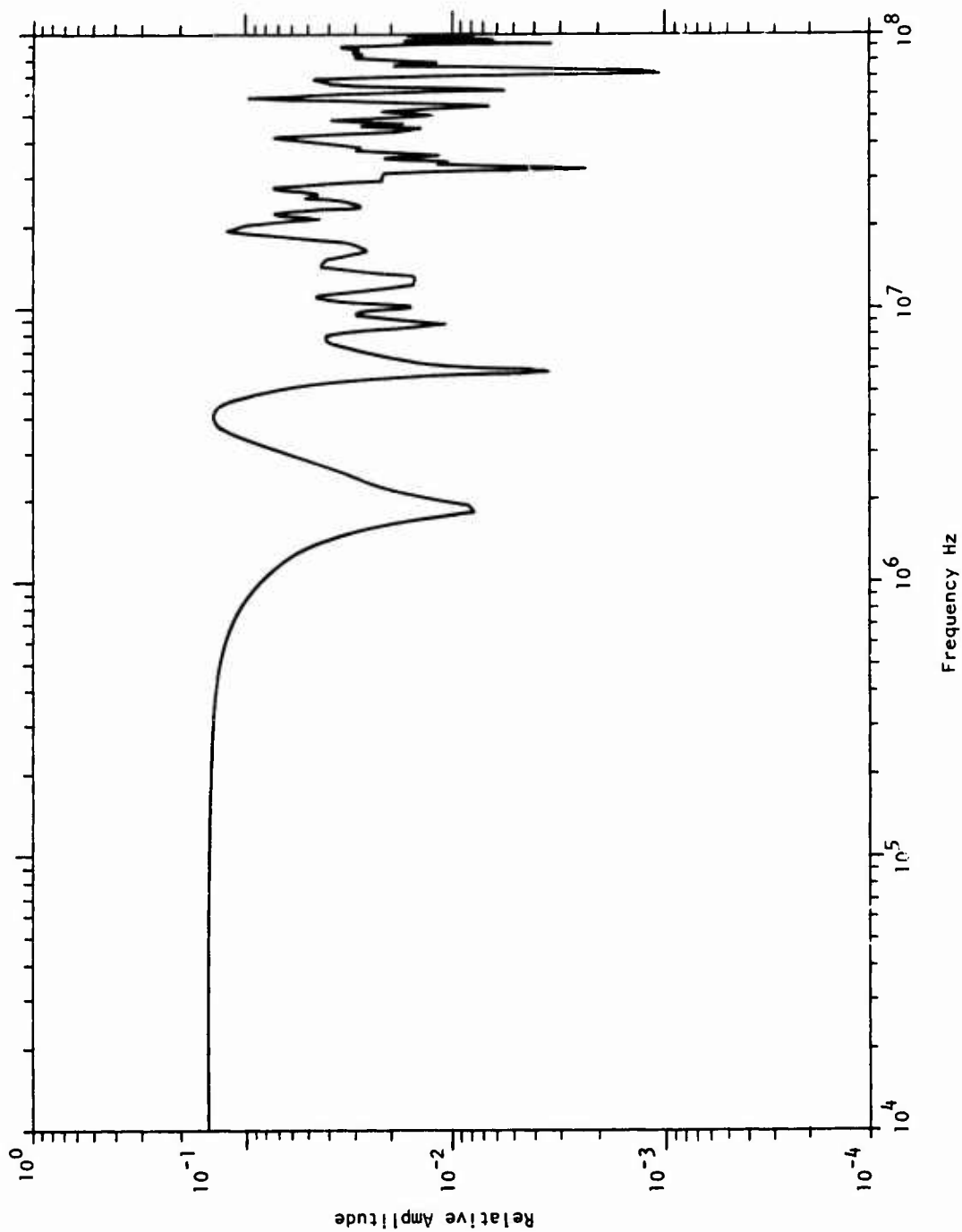


Figure 3-26. Fourier Transform of Typical Experimental Derivative Waveform with Ramp and dc Offset Errors

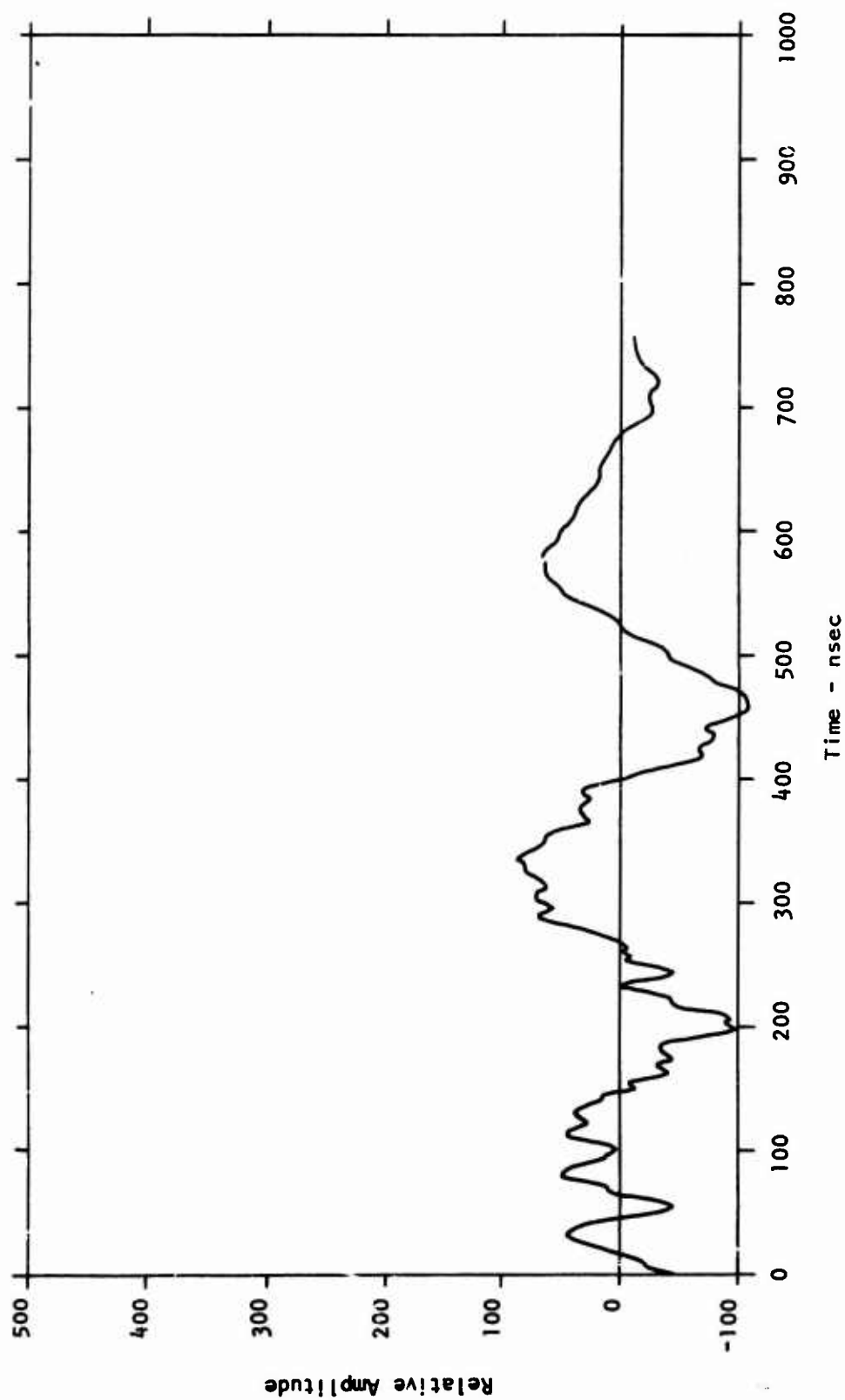
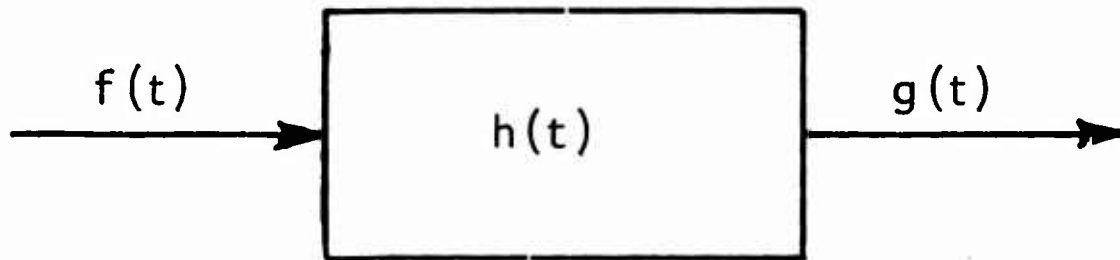


Figure 3-27. Integral of Typical Experimental Derivative Waveform with Ramp and dc Offset Errors Using Fourier Transform Techniques with Low Frequencies Filtered Out

The transfer function is defined in the following way. Assume a linear system with forcing function, $f(t)$, system response function, $g(t)$, and system impulse response, $h(t)$.



The three functions are related by the convolution integral (Equation 3-178) as follows:

$$g(t) = \int_{-\infty}^{\infty} h(t - \tau) f(\tau) d\tau \quad (\text{Eq. 3-382})$$

It has also been shown (Equation 3-173) that the Fourier Transform of $g(t)$ is given by

$$G(\omega) = H(\omega) F(\omega) \quad (\text{Eq. 3-383})$$

In Equation 3-383, the function, $H(\omega)$, is defined as the transfer function of the linear system.

For pulse testing, $f(t)$ and $g(t)$ are often recorded test variables (e.g., $f(t)$ may be induced current at some point on the test object and $g(t)$ is the measured response at another point.) Then $f(t)$ and $g(t)$ are used to estimate $H(\omega)$. Equation 3-383 indicates a very convenient

method to estimate $H(\omega)$. If $F(\omega)$ and $G(\omega)$ are generated from $f(t)$ and $g(t)$, then $H(\omega)$ is computed by,

$$H(\omega) = \frac{G(\omega)}{F(\omega)} \quad (\text{Eq. 3-384})$$

This procedure for computing $H(\omega)$ which amounts to deconvolution in the frequency domain, is deceptively simple. The functions $f(t)$ and $g(t)$ are typically contaminated with noise during the data recording and digitizing processes. Now assume that all the noise contamination occurs in $g(t)$ and the contaminated functions are defined as,

$$d(t) = g(t) + \text{noise}(t) \quad (\text{Eq. 3-385})$$

which implies that,

$$D(\omega) = G(\omega) + \text{NOISE}(\omega). \quad (\text{Eq. 3-386})$$

If the transfer function is now estimated with $D(\omega)$, instead of $G(\omega)$ one has

$$\begin{aligned}
 \hat{H}(\omega) &= \frac{D(\omega)}{F(\omega)} \\
 &= \frac{G(\omega)}{F(\omega)} + \frac{\text{NOISE}(\omega)}{F(\omega)} \\
 &= H(\omega) + \frac{\text{NOISE}(\omega)}{F(\omega)}
 \end{aligned}
 \tag{Eq. 3-387}$$

Inspection of Equation 3-387 shows that the transfer function estimate generated equals the sum of the true transfer function, $H(\omega)$, and an error term. Now consider the behavior of this error term. $F(\omega)$ is typically a band limited function and tends to zero at high frequencies (e.g., $F(\omega)$ often approximates the transform of a double exponential function). The noise term, $\text{NOISE}(\omega)$, on the other hand, can exhibit considerable spectral energy in the region where $F(\omega)$ is very small. Thus, the division of $\text{NOISE}(\omega)$ by $F(\omega)$ in this region can cause large spectral noise spikes in $\hat{H}(\omega)$.

One can also consider what happens when the noise is assumed to occur only in $F(\omega)$. The estimate, $\hat{H}(\omega)$, is given by

$$\hat{H}(\omega) = \frac{G(\omega)}{F(\omega) + \text{NOISE}(\omega)}
 \tag{Eq. 3-388}$$

Now again assume that $F(\omega)$ approximates the transform of a double exponential forcing function (i.e., $F(\omega)$ is positive over most of its range of interest). $\text{NOISE}(\omega)$ is the transform of a random noise signal, and, therefore, can be expected to have random phase, as well as random amplitude. If $\text{NOISE}(\omega)$ is approximately equal in magnitude but opposite in phase to $F(\omega)$, the denominator of Equation 3-388 can approach zero and $\hat{H}(\omega)$ approaches infinity. In practice, very large noise spikes can occur in $\hat{H}(\omega)$. The same sort of arguments can be made if noise is assumed to contaminate both $f(t)$ and $g(t)$.

Thus, one can see that the simple estimation method of Equation 3-384 can produce very unreliable transfer function estimates. Figure 3-28 illustrates the effects of noise contamination on spectral estimates. The system transfer function shown has resonant peaks at 1, 5, and 25 MHz. A continuous wave (CW) transfer function estimate (assumed to be very close to the true transfer function) is shown for comparison. The curve labeled "unfiltered" was generated by the technique of Equation 3-330 (the curve labeled "filtered" will be discussed in a subsequent paragraph). Note the noise spikes beyond 25 MHz. With no a priori knowledge of $H(\omega)$ before the unfiltered estimate was generated, the analyst may be very tempted to assume that these noise spikes are real system resonances in addition to those at 1, 5, and 25 MHz.

3.5.6.2 Methods for Improving Transfer Function Estimates

Referring again to Figure 3-28, one can see that the noise in the unfiltered transfer function estimates is concentrated in the high frequency portion of the displayed spectra. The complete reason for this behavior is not entirely understood. But it is strongly believed that the contaminating noise in $f(t)$ and $g(t)$ was caused mainly in the digitizing process and this noise tends to be high frequency relative to the sampling rate for $f(t)$ and $g(t)$. Thus, if one has some idea at what frequencies the significant spectra energy in $H(\omega)$ will occur, he can sample $f(t)$ and $g(t)$ so that the significant spectra energy is in the lower portion of the total generated spectrum. The high frequency portion of the spectra would be ignored as noise contaminated and thus useless, but it would presumably contain no useful information anyway.

A second method, which has been evaluated with reasonable success, is the Hunt Algorithm³⁴. The Hunt Algorithm is a frequency domain implementation of a time domain deconvolution algorithm developed by Phillips and Twomey for application to numerical data. Hunt's

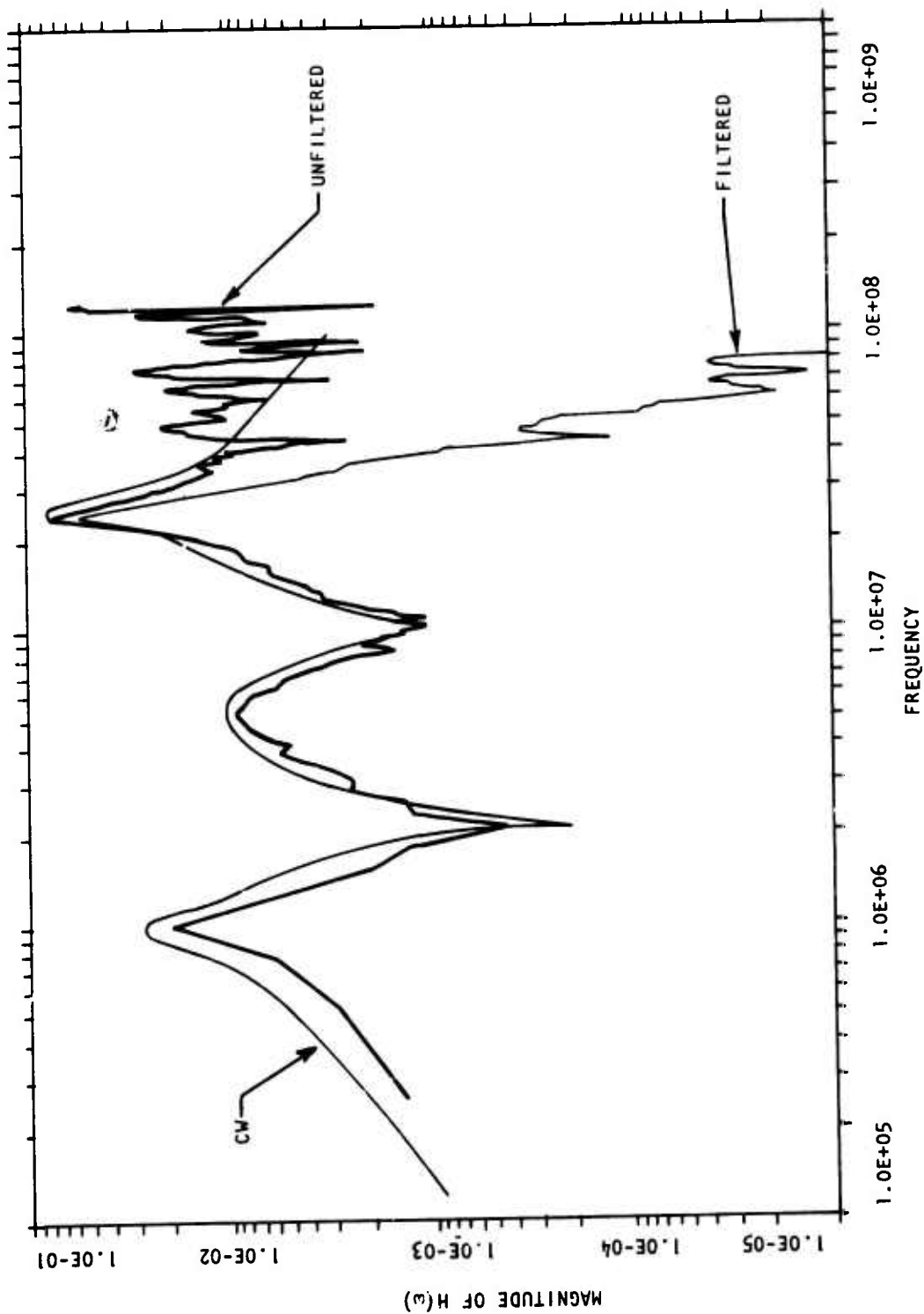


Figure 3-28. Unfiltered and Filtered Transfer Function Estimates Illustrating Noise Contamination Problems and Fixes

algorithm is basically a digital filter method for generating smoothed estimates of $H(\omega)$ based on constrained regression. The constraint is to pick the solution for $h(t)$ (thus, $H(\omega)$) which minimizes the second derivative of $h(t)$ (or second differences of $h(t)$ in the case of sampled data)). The result of applying the algorithm to an estimation problem is shown in Figure 3-28 as the filtered curve. Note that the algorithm acts to low-pass filter $H(\omega)$. Note also, that the algorithm has caused the filtering action to occur just beyond the 25 MHz peak, which is where the noise problems begin.

So far, the Hunt Algorithm technique has only been evaluated on somewhat idealized test data and must be extended to more realistic test data before it is considered a proven technique. It is also somewhat time consuming in the preparation of test data required and in computer time for execution. However, it appears to be the most promising technique so far available.

The final technique which is discussed is the coherence function approach. Reliable transfer function estimates can be generated if the time domain data are statistically stationary. This approach has been extended to nonstationary data (note that EMP transient test waveforms are nonstationary) with only very limited success. Thus; the only remark that can be made about the technique is that the utility of the technique for transient data is still in its very early stages of evaluation.

REFERENCES

1. Dyche, James W. and Richard A. Kitter, Facility Description Volume III Data Processing System, BDM/A-87-72-TR, 30 June 1972, pg. 11-11.
2. Dyche, Kitter, op. cit., pg. 11-15.
3. Dyche, Kitter, op. cit., pg. 111-15.
4. Dyche, Kitter, op. cit., pg. 111-3.
5. Dyche, Kitter, op. cit., pg. V-10 to V-28.
6. Dyche, Kitter, op. cit., pg. V-29 to V-37.
7. Dyche, Kitter, op. cit., pg. 111-11 to 111-15.
8. Dyche, Kitter, op. cit., pg. 111-16 to 111-18.
9. Marce Eleccion, A/D and D/A Converters, IEEE Spectrum, July 1972.
10. Schmid, Hermann, An Electronic Design Practical Guide to A/D Conversion, Electronic Design No. 25, 5 December 1968.
11. Datagrid Digitizer Operating and Service Manual, Bendix Corporation, Computer Graphics, Farmington, Michigan, November 1970.
12. Felty, Darrell W., Photo-Optical Data Processing, Air Force Weapons Laboratory, Computational Services Division, Preprocessing Branch, Photo Reduction Section, December 1971, pg. 29.
13. Felty, Darrell W., op. cit., pg. 26 to 28.
14. Digitizer Unplot Data, The Hewlett-Packard Keyboard, Vol. 4, No. 2, pg. 5.
15. Felty, Darrell W., op. cit., pg. 18 to 25.
16. Cover, R. K., SID, A Fast Low Cost Graphic Scanner, Sandia Laboratories, Albuquerque, New Mexico.
17. Transient Recorder Model 8100, Technical Data Sheet Biomation, 1070 East Meadow Circle, Palo Alto, California 94303, June 1972.
18. Dyche, James W., Feasibility Study - ARES Autonomous Computer Facility, BDM/A-76-72-TR, 25 April 1972.

REFERENCES (Continued)

19. Dyche, Kitter, op, cit., pg. IV-2 to IV-8.
20. Memorandum, R. L. Hutchins to J. C. Wirth, Integration, BDM/AR-RLH-1155-72, 16 October 1972.
21. Garner, J. W., Program TTCAL, DC-TN-12092-1, Dikewood Corporation, 1970.
22. Boyd Boitnott to James W. Dyche, conversation on time tying methods, 15 January 1973.
23. Papoulis, Athanasios, The Fourier Integral And Its Applications, McGraw Hill, 1962.
24. Woodward, P. M., Probability And Information Theory With Applications To Radar, 2nd Edition, Pergamon Press, Oxford, 1964.
25. Penick, C. A., "Subroutines FTF and FFT", DC-TN-2099-6, Prepared under Contract No. F29601-69-C-0093, 4 August 1969.
26. Kitter, R. A., "Modified Inverse Fourier Transform Method and Frequency Step Size Specification For Calculating Fourier Transforms," BDM Memo No. BDM/ARES-TR-0035, 22 May 1972.
27. "Data Reduction, Planning and Coordination," EG&G Report No. AL-648, 31 August 1972.
28. Cochran et. al., "What is the Fast Fourier Transform?", IEEE Transactions on Audio and Electroacoustics, Vol. AV 15, No. 2, June 1967.
29. Cooley, J. W., Lewis, P. A., and Welch, P. D., "Application of the Fast Fourier Transform to Computation of Fourier Integrals, Fourier Series and Convolution Integrals," IEEE Transactions on Audio and Electroacoustics, Vol. AV-15, No. 2, June 1967.
30. Brenner, N. M., "Three Fortran Programs that Perform the Cooley-Tukey Fourier Transform," MIT Lincoln Laboratory Technical Note 1967-Z, 28 July 1967.
31. McEwen, A. J., "Transfer Function Error Analysis," EG&G Albuquerque Division, No. AL-413, 11 May 1970.
32. Locasso, J. V., "In-Place EMP-Confidence Limits on F Domain Transfer Functions," North American Rockwell internal letter No. 71-31-243-023-EMP-036, 9 March 1971.
33. Doran, L. L., and L. C. Nielsen, "A Study of Errors in the Manual Digitization of Oscilloscope Trace Photographs," EG&G Albuquerque Division, No. ASD 70-213, June 1970.

REFERENCES (Concluded)

34. Dyche, J. W. and H. J. Wagon, "The Hunt Algorithm Filter Technique Applied to EMP Transfer Function Estimation," Braddock, Dunn and McDonald, Inc. for Air Force Weapons Laboratory, Technical Report No. AFWL-TR-72-34, Sept. 1972.